Responses of bovine and human neutrophils to members of the *Mycobacterium tuberculosis* complex

Inauguraldissertation

zur

Erlangung des akademischen Grades eines

Doktors der Naturwissenschaften

(Dr. rer. nat)

der

Mathematisch-Naturwissenschaftlichen Fakultät

der

Universität Greifswald

Vorgelegt von

Rachana Borkute

Greifswald, 20.07.2022

Dekan: Prof. Dr. Gerald Kerth

1. Gutachter: Prof. Dr. Anca Dorhoi

2. Gutachter: Prof. Dr. Jonathan Jantsch

Tag der Promotion: 25.01.2023

कर्मण्येवाधिकारस्ते मा फलेषु कदाचन।
मा कर्मफलहेतुर्भूर्मा ते सङ्गोऽस्त्वकर्मणि॥

Meaning of the verse is:

You have a right to perform your prescribed duties, but you are not entitled to the fruits of your actions. Never consider yourself to be the cause of the results of your activities, nor be attached to inaction.

Bhagavad Gita, Chapter 2, Verse: 47

Dedicated to my beloved family

Table of Contents

List of Abbreviations

2ME	2-Mercaptoethanol
2NBDG	2-(N-(7-Nitrobenz-2-oxa-1,3-diazol-4-yl) Amino)-2-Deoxyglucose)
ABB	Annexin binding buffer
ADC	Albumin dextrose catalase
AG	Arabinogalactan
AIM2	Absent in Melanoma 2
ALRs	AIM2 like receptors
AMP	Adenosine monophosphate
AMΦ	Alveolar macrophage
ATP	Adenosine triphosphate
ATPase	Adenosine triphosphatase
BCG	Bacillus Calmette–Guérin
BSA	Albumin fraction V
bTB	Bovine tuberculosis
Ca^{2+}	Calcium bivalent cations
CaM	Calmodulin
CARD9	Caspase recruitment domain family member 9
CD	Cluster of differentiation
CFP-10	10 kDa culture filtrate protein
CFU	Colony forming unit
cGAS	Cyclic guanosine adenosine monophosphate synthase
CGD	Chronic granulomatous disease
CLPs	Common lymphocyte progenitors
CLRs	C-type lectin receptors
CMPs	Common myeloid progenitors
CPT	Camptothecin
CR3	Complement receptor 3
DAT	Diacyltrehalose
DCs	Dendritic cells
DC-SIGN	Dendritic cell-specific intracellular adhesion molecule-3 grabbing non-integrin
DIM	Dimycocerosate
DMSO	Dimethyl sulfoxide
DNA	Deoxyribonucleic acid
E. coli	*Escherichia coli*
EA	Early apoptotic
EDTA	Ethylenediaminetetraacetic acid
ESAT-6	Early secreted antigenic target-6
ESX-1	ESAT-6 secretion system 1
FACS	Fluorescence-activated cell sorting
Fc	Fragment crystallizable
FCS	Fetal calf serum

FLI	Friedrich-Loeffler-Institut
fMLP	Formyl-methionyl-leucyl-phenylalanine
FPRs	Formyl-peptide receptors
G-	Gram negative
G+	Gram positive
GFP	Green fluorescent protein
gMFI	Geometric mean fluorescence intensity
GPI	Glycophosphatidylinositol
GTP	Guanosine triphosphate
GTPase	Guanosine triphosphatase
H	Hour
H_2O_2	Hydrogen peroxide
H_2SO_4	Sulphuric acid
HBSS	Hanks balanced salt solution
HEPES	4-(2-hydroxyethyl)-1-piperazineethanesulfonic acid
HNP-1	Human neutrophil peptide-1
HOCl	Hypochlorous acid
HRP	Horse radish peroxidase
HSCs	Hematopoietic stem cells
IFN-β	Interferon beta
IFN-γ	Interferon gamma
IL-1R	Interleukin-1 receptor
IL-1β	Interleukin-1 beta
ITAMs	Immunoreceptor tyrosine-based activation motifs
kDa	Kilo Dalton
LA	Late apoptotic
LAM	Lipoarabinomannan
LM	Lipomannan
LL-37	Active form of the cathelicidin antimicrobial peptide (CAMP)
LPS	Lipopolysaccharide
LT-HSCs	Long-term hematopoietic stem cells
MΦ	Macrophage
M. bovis	*Mycobacterium bovis*
M. caprae	*Mycobacterium caprae*
M. tb	*Mycobacterium tuberculosis*
MA	Mycolic acid
Mac-1	Macrophage-1 antigen
MACS	Magnetic-activated cell sorting
ManLAM	Mannosylated lipoarabinomannan
MAPK	Mitogen-activated protein kinases
MARCO	Macrophage receptors with collagenous structure
Mbp	Mega base pair
MCL	Macrophage C-type lectin

MDSCs	Myeloid-derived suppressor cells
MHC	Major histocompatibility complex
Min	Minute
mL	Millilitre
mM	Millimolar
MMPs	Matrix metalloproteinases
MPO	Myeloperoxidase
MR	Mannose receptor
Ms	Millisecond
MTBC	*Mycobacterium tuberculosis* complex
MyD88	Myeloid differentiation primary response 88
MβCD	Methyl β-Cyclodextrin
NADG	N-acetyl D-Glucosamine
NADPH	Nicotinamide adenine dinucleotide phosphate
$NaHCO_3$	Sodium bicarbonate
NE	Neutrophil elastase
NeP	Early-stage neutrophil progenitor
NETs	Neutrophil extracellular traps
NF-κB	Nuclear factor kappa-light-chain-enhancer of activated B cells
NH_4Cl	Ammonium chloride
NK	Natural killer cells
NOD	Nucleotide-binding oligomerization domain
O_2	Molecular oxygen
O_2^-	Superoxide
OADC	Oleic albumin dextrose catalase
OD	Optical density
OIE	World Organization for Animal Health
Ops	Serum opsonized
OsO_4	Osmium tetroxide
PAF	Platelet activating factor
PBMCs	Peripheral blood mononuclear cells
PBS	Phosphate buffer saline
PDIM	Phthiocerol dimycocerosate
PFA	Paraformaldehyde
PG	Peptidoglycan
PI	Propidium iodide
PI3k	Phosphatidylinositol-3 kinase
PI3P	Phosphatidylinositol-3-phosphate
PIMs	phosphatidyl-myoinositol mannosides
PKC	Protein kinase C
PMA	Phorbol myristate acetate
PMN	Polymorphonuclear leukocytes/Neutrophils
PMs	Promyeloblasts

pncA	Gene encoding pyrazinamidase/nicotinamidase
PPD	Purified protein derivative
PRRs	Pattern recognition receptors
Ptp	Protein-tyrosine phosphatase
RBCs	Red blood cells
RD	Region of difference
RIG-I	Retinoic acid inducible gene I
RIPK	Receptor interacting protein kinase
ROS	Reactive oxygen species
rpm	Rounds per minute
RPMI	Rosewell Park Memorial Institute
rRNA	Ribosomal ribonucleic acid
RT	Room temperature
SD	Standard deviation
Sec	Second
SL	Sulfolipids
SLAMF1	Signaling lymphocytic activation molecule family member 1
SNP	Single nucleotide polymorphism
SRs	Scavenger receptors
ST-HSCs	Short-term hematopoietic stem cells
STING	Stimulator of interferon genes
SVs	Secretory vesicles
T	Time
TACO	Tryptophan-aspartate containing coat protein
TB	Tuberculosis
TBK1	Serine threonine protein kinase
TDM	Trehalose dimycolate
TEM	Transmission electron microscopy
Th1	T-helper 1 cell
TLRs	Toll-like receptors
TMB	3,3′,5,5′-Tetramethylbenzidine
TNF-α	Tumor necrosis factor alpha
TREM2	Triggering receptor expressed on myeloid cells 2
TRIF	Toll/IL-1R domain-containing adapter-inducing interferon beta
TST	Tuberculin skin test
v/v	volume/volume
v-ATPase	vacuolar-Adenosine triphosphatase
w/v	weight/volume
WHO	World Health Organization
WT	Wildtype
x g	Times gravity
α	Alpha
β	Beta
β_2-m	Beta-2-microglobulin

γ	Gamma
µL	Microlitre
µM	Micromolar
%	Percentage

1 Introduction

1.1 Bovine tuberculosis

Tuberculosis (TB) remains a global health threat for humans worldwide ranking above HIV and malaria, and emerging as a deadly infectious disease caused by a single infectious agent, *Mycobacterium tuberculosis* (*M. tb*) (WHO 2019). Bovine tuberculosis (bTB) is a chronic infectious disease which is found mainly in cattle and is caused by the members of *M. tb* complex (MTBC) (Vordermeier, Jones et al. 2016). The most common causative agent of bTB in cattle is *Mycobacterium bovis* (*M. bovis*) and to a lesser extent *Mycobacterium caprae* (*M. caprae*) (Domingo, Vidal et al. 2014). *M. bovis* being an animal adapted strain is not only causing TB in cattle but it has the ability to infect a wide variety of mammals including humans (Renwick, White et al. 2007, Waters, Palmer et al. 2012). *M. bovis* severely impacts the livestock farming which relies on bovids for meat and milk production (WHO 2017). It has also decreased international trade of animals and their products as well as increased censure of carcasses and infected parts, which cannot be consumed (WHO 2017).

During 2017 and 2018, 188 countries and territories have reported the status of bTB to the World Organization for Animal Health (OIE) with 82 countries reporting the presence of the disease in livestock and wildlife (OIE 2019). The global distribution of bTB is shown in Figure 1.1. Out of the 82 countries, 29 countries reported the presence of bTB in wildlife as well as farm animals, 51 countries reported the presence in livestock and 2 countries reported the presence of bTB only in wildlife (OIE 2019). Eurasian badger in United Kingdom (UK) and Ireland is considered as a reservoir host of *M. bovis* facilitating spread in cattle (Murphy, Gormley et al. 2010). Likewise, wild boars in Spain (Naranjo, Gortazar et al. 2008), the brushtail possum in New Zealand, the white-tailed deer in Michigan are the main reservoir hosts of *M. bovis* in wildlife in various regions (Palmer, Thacker et al. 2012).

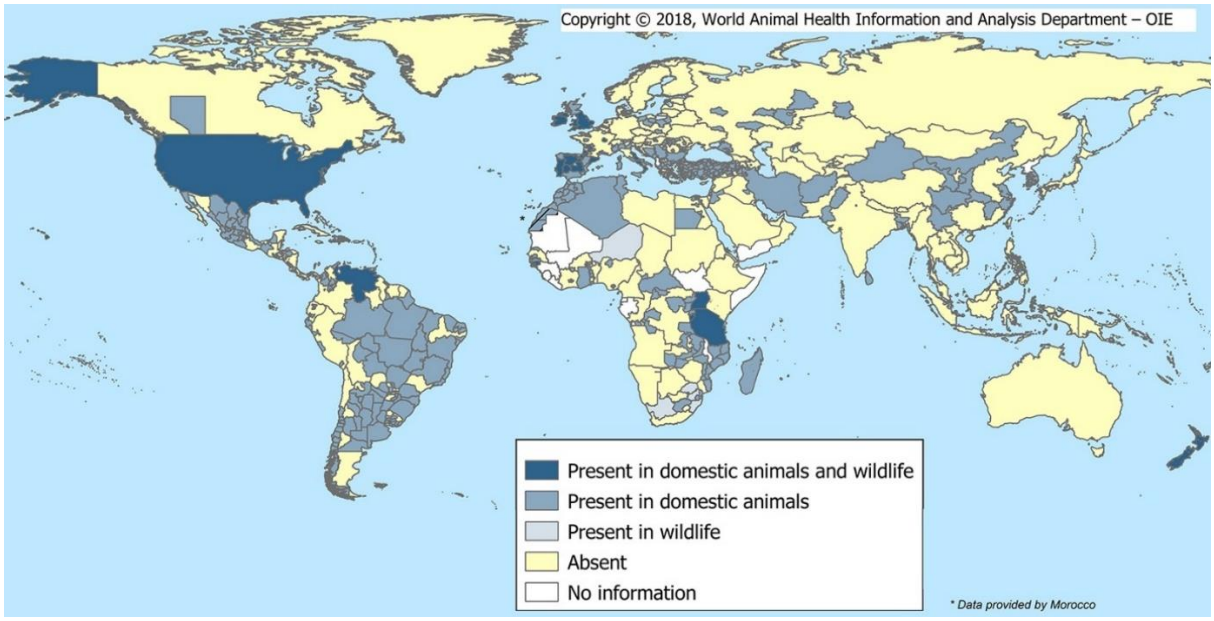

Figure 1.1: Global distribution of bTB in 2017 and first half of 2018. Image taken from OIE Panorama Bulletin, 2019.

Transmission of *M. bovis* depends on a number of factors, which includes the intrinsic characteristics of the bacterium and the potential host, persistence of bacterium in different environments, probability of exposure to infected animals and the effectiveness of control strategies such as removal of infected animals (Broughan, Judge et al. 2016). Ethiopia which is the second most populated country in Africa has over 85% population living in the rural areas and 80% of them rely on the livestock for food and survival (Areda, Muwonge et al. 2019). A study conducted in central Ethiopia and meta-analysis in India reveal that 90% of the herd population and 21.8 million cattle, tested positive for bTB (Areda, Muwonge et al. 2019) with a prevalence of 50% in some of the large dairy herds (Firdessa, Tschopp et al. 2012, Srinivasan, Easterling et al. 2018). Despite this high prevalence in domestic animals, control and preventive measures are largely absent in these countries (Areda, Muwonge et al. 2019, Chauhan, George et al. 2019, Refaya, Bhargavi et al. 2020). However, many other countries with bTB eradication or control programs identify the affected herds and remove the infected animals or clear off the entire herd (Waters, Maggioli et al. 2014). Nevertheless, high-income and industrialized countries like Germany, China and Uruguay with high developed animal traceability systems and national animal health surveillance programs control bTB, however disease incidences in cattle and pigs have been found (Probst, Freuling et al. 2011, Eisenberg, Nesseler et al. 2016, Picasso, Alvarez et al. 2017, Gong, Chen et al. 2021). All these data point towards an urgent need to implement strict routine surveillance strategies all over the world to control global bTB spread.

There are a number of ways by which cattle can be infected with *M. bovis*. Routine farm practices, age, behavior, environment conditions and the climate influence the infection

outcome (Pollock and Neill 2002). The most common route of entry is inhalation of the bacteria excreted from infected animals, or indirectly from contaminated pastures, water or fomites (Neill, Pollock et al. 1994). Exposure results in formation of lesions in the nasopharynx, lower respiratory tract, lungs and its associated lymph nodes (Domingo, Vidal et al. 2014). Experimental studies on *M. bovis* infection in cattle have suggested a profound role of the infective dose on the severity of the infection and the resulting disease (Dean, Rhodes et al. 2005). Intranasal infection of young calves with colony forming unit (CFU) ranging between 10^4 and 10^7 *M. bovis*, led to higher severity of bTB compared to naturally infected cattle (Cassidy, Bryson et al. 1998). The lesions were observed on the mucosa linings the upper respiratory tract, nasal mucosa, turbinate, and nasopharynx (Neill, Bryson et al. 2001). Intratracheal delivery of 5×10^5 *M. bovis* CFU resulted in gross granulomatous pathology in lung and associated lymph nodes with moderate calcification of the lesions and granuloma specific giant cells, and many caseous foci were observed (Buddle, Aldwell et al. 1994). A follow up study indicated that a CFU as low as 1 is sufficient to cause tuberculous induced pathology in cattle (Dean, Rhodes et al. 2005). Cattle may remain asymptomatic after *M. bovis* infection as it takes months for the symptoms to develop (Ramos, Silva et al. 2015) and the latency period is estimated to range between 87 days to 7 years depending on the cattle's immune system (Barlow, Kean et al. 1997). Some cattle appear to be tuberculin test negative, but encapsulated lesions detected upon slaughter confirmed presence of the causative agent *M. bovis* (Good and Duignan 2011). Infected but asymptomatic cattle might transmit the infection to the herd via pasture contaminated with excreted faeces (Phillips, Fosterb et al. 2003). In experimental studies with *M. tb* H37Rv infected animals, no visible pathology was noticed (Whelan, Coad et al. 2010). However, *M. bovis* AF2122/97 or *M. bovis* 10-7428 infected cattle showed pathology indicative of bTB (Whelan, Coad et al. 2010, Palmer, Wiarda et al. 2019). Asymptomatic cattle naturally infected with *M. bovis* may show exacerbated tissue pathology (Menin, Fleith et al. 2013). Reduced or absent gross pathology was repeatedly reported in cattle experimentally infected with *M. tb* compared to *M. bovis* infection (Whelan, Coad et al. 2010, Villarreal-Ramos, Berg et al. 2018). Thus, the fate of infection with various mycobacteria differs in cattle and it is very important to develop advanced techniques to detect and differentiate infection with various virulent mycobacteria in livestock.

Numerous techniques are routinely used for the detection and diagnosis of bTB. The tuberculin skin test (TST), which measures delayed-type hypersensitivity reaction, is a method of bTB detection and surveillance in live cattle. This involves injecting bovine tuberculin, a purified protein extract derived from *M. bovis,* intradermally and measuring the swelling at that site of injection after 72 hours (h) (Awah-Ndukum, Temwa et al. 2016, OIE 2018). However, sensitivity of this test is quite variable (Wood and Rothel 1994). An alternative to TST is the Interferon gamma (IFN-γ) release assay, which is a rapid *in vitro* based detection method using whole blood and is significantly more reliable than the intradermal skin test (Wood and Rothel 1994, Lahuerta-Marin, Gallagher et al. 2015). Single intradermal comparative cervical test has been routinely used for the detection of bTB (Tsairidou,

Brotherstone et al. 2016, Stanski, Lycett et al. 2021). The test comparatively measures skin thickness before and after simultaneous inoculation of *M. bovis* purified protein derivative (PPD) and *Mycobacterium avium* (*M. avium)* PPD antigens (Tsairidou, Brotherstone et al. 2016). The specificity of the test is >99%, however, its sensitivity varies between 55 and 91% (Tsairidou, Brotherstone et al. 2016). Therefore, efforts are being made to develop several peptide cocktails to increase the sensitivity and specificity of the skin test so that the surveillance and diagnosis of bTB is more accurate (Vordermeier, Whelan et al. 2001, Cockle, Gordon et al. 2006, Xin, Jia et al. 2013, Srinivasan, Jones et al. 2019, Bayissa, Sirak et al. 2021).

The zoonotic risk of *M. bovis* infection has been speculated since the early 18th century when bTB was linked to consumption of contaminated milk by children (Grange 2001). Later in 1865, studies by Villemin showed that the disease can be transmitted from animals to humans (Grange 2001, Davies 2006). Zoonotic TB is caused by *M. bovis*, however, other members of MTBC like *M. orygis, M. caprae*, *M. pinnipedii* have also been isolated from humans suffering from TB (WHO 2017, Duffy, Srinivasan et al. 2020). Many investigators have debated about the age distribution of zoonotic TB (Davies 2006). Infants and children are more prone to zoonotic TB (OIE 2017). The disease is often caused by consumption of contaminated food (mainly unprocessed dairy products) or inhalation of aerosol droplets by people in close contact with infected animal including slaughterhouse workers, butchers, veterinarians, and farmers (OIE 2017). In 2016, about 147,000 new cases of zoonotic TB in humans were reported globally, and 12,300 deaths due to this disease were recorded (OIE 2017). Approximately 68,900 cases of zoonotic TB in people were reported in Africa, followed by 43,400 cases in South east-Asia, 18,000 cases in Western Pacific, 8,190 cases in Eastern Mediterranean, and the lowest numbers were reported in the European Union in 2019 (OIE 2017) (Figure 1.2).

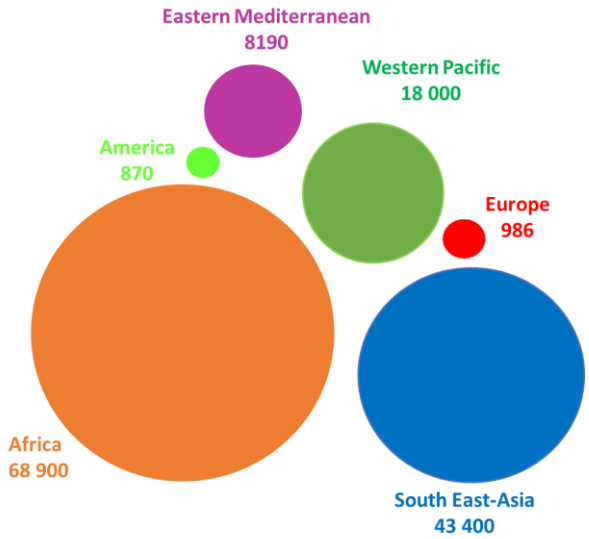

Figure 1.2: Estimated incidences of zoonotic TB for WHO regions and globally 2016. Image modified from zoonotic TB factsheet (OIE 2017).

The number of cases and the true incidences of zoonotic TB remain unclear because of the lack of routine surveillance in low-income and high-burden countries (Olea-Popelka, Muwonge et al. 2016). Zoonotic TB also poses a major challenge to effective treatment of patients due to the resistance of *M. bovis* to pyrazinamide, one of the four medications used in the standard first-line anti-TB treatment regimen (OIE 2017). The resistance to pyrazinamide is due to a point mutation in the *pncA* gene in *M. bovis* (Guimaraes and Zimpel 2020). Currently, treatment and diagnosis of human TB focus on pulmonary disease associated with *M. tb* (Achkar, Lawn et al. 2011), but *M. bovis* infection in cattle and zoonotic TB in humans is frequently associated with extra-pulmonary TB which makes the diagnosis difficult due to complexity in obtaining samples, e.g. lymph node aspirates (Durr, Muller et al. 2013). Therefore, it is critical to evaluate differences in responses of distinct host species to virulent mycobacteria to better understand pathophysiology of TB, including zoonotic infection. Comparative evaluation of bovine host responses to cattle-adapted *M. bovis* and human-adapted *M. tb* may shed light on diverging outcomes regarding development of active TB and inform interventions.

1.2 *Mycobacterium tuberculosis* complex (MTBC)

The mycobacteria grouped in MTBC share more than 99.9% genome sequence similarity and have identical 16s ribosomal ribonucleic acid (rRNA) sequences, however they differ widely in terms of pathogenicity, host tropism and phenotypes (Brosch, Gordon et al. 2002, Jia, Yang et al. 2017). Phylogenetic analysis indicates that human-adapted strains encompass several different lineages (i.e., lineage 1-6 and lineage 7) and are referred to as *M. tb sensu stricto*. Two evolutionarily ancient lineages, which belong to *M. africanum*, are grouped into lineage 5 and 6. These two lineages cause pulmonary TB in West African regions (De Jong, Antonio et al. 2010). Recently, Coscolla *et al*. revealed a new lineage L9 which belongs to the *M. africanum* group, but unlike the lineages L5 and L6, L9 is distributed in the East African regions (Coscolla, Gagneux et al. 2021). A clade-specific deletion in the region of difference (RD) 7, 8, 9 and 10 has led to the emergence of the animal-adapted strains in MTBC and they all share a common ancestor at the branching point (Brosch, Gordon et al. 2002, Brites, Loiseau et al. 2018) (Figure 1.3). The animal-adapted strains comprise of *M. microti* (adapted to wolves), *M. pinnipedii* (adapted to seals and sea lions), *M. orygis* (adapted to antelopes), *M. mungi* (adapted to mongooses) (Alexander, Laver et al. 2010), *M. suricattae* (adapted to meerkats), the “chimpanzee bacillus” (adapted to Chimpanzees), *M. bovis* and *M. caprae* (Brites, Loiseau et al. 2018). For human-adapted mycobacteria no animal reservoirs have so far been reported (Yeboah-Manu, de Jong et al. 2017). *M. bovis* is a successful pathogen and infects more than 40 different species (Rodriguez-Campos, Smith et al. 2014, Spickler 2019).

In the following, a detailed description of *M. bovis* and *M. tb* similarities, as well as major differences between the cell wall and the secretome of these two pathogens are discussed.

Moreover, information about the vaccine strain *M. bovis* Bacillus Calmette-Guérin (BCG) is provided. These bacteria have all been used in this work.

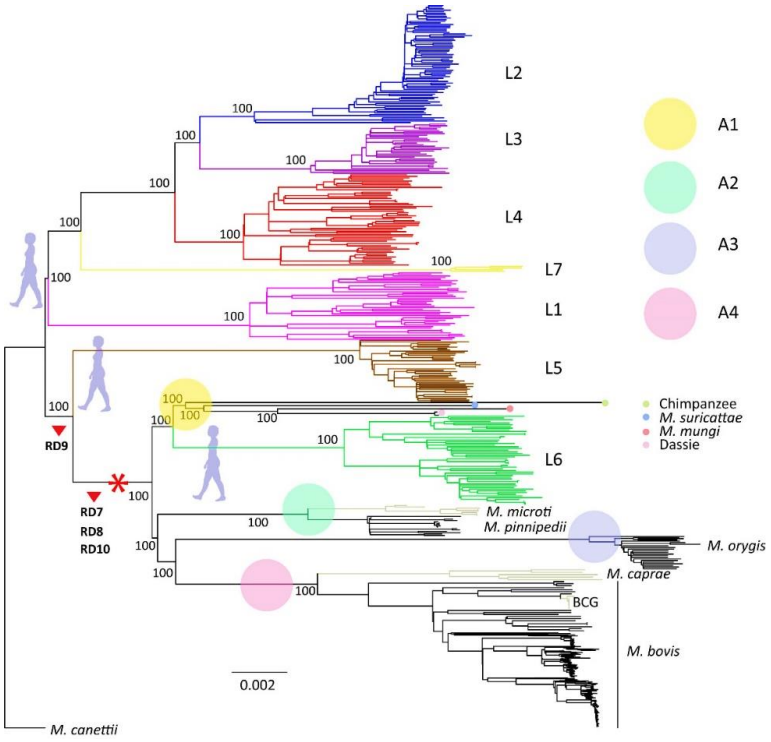

Figure 1.3: Phylogenetic tree of human- and animal-adapted MTBC members. Human-adapted strains are depicted as lineage L1-L7 and animal-adapted strains as A1-A4. Main deletions in animal-adapted strains are denoted by red arrow heads, and red asterisk (*) marks the different host species in the MTBC. Image sourced from (Brites, Loiseau et al. 2018).

1.2.1 *Mycobacterium tuberculosis*

M. tb is taxonomically classified as Gram-positive (G+) pathogen given its rich content in peptidoglycan (PG) and structural similarities to G+ bacteria, however, it does not retain Gram stain (Hett and Rubin 2008). The bacterium retains the acid-fast stain and is identifiable also by Ziehl-Neelsen staining (Hett and Rubin 2008). *M. tb* has a single circular chromosome of approximately 4.4 Mega base pair (Mbp) and drug resistance is associated with chromosomal mutations and rearrangements (Koch and Mizrahi 2018). It grows slowly and has a generation time of approximately 20 h in laboratory media (Cole, Brosch et al. 1998, Koch and Mizrahi 2018). Due to its rich, flexible metabolic repertoire, the bacteria easily adapt to variable environments inside the host (Koch and Mizrahi 2018). The most dominant feature of mycobacteria is the cell envelop which contains a bulk of complex sugars and lipids contributing to 40% of the dry mass of the cell (Jackson 2014).

The insoluble 'core' cell wall of *M. tb* consists of PG, mycolic acid (MA) and arabinogalactan (AG) (Abrahams and Besra 2018). The soluble cell wall entities like lipoarabinomannan (LAM), phosphatidyl-myoinositol mannosides (PIMs), lipomannan (LM), phthiocerol, trehalose containing lipids and other phosphatidylinositol-containing glycolipids are important for the pathogenesis of *M. tb* (Crick, Quadri et al. 2017). The classical ultrastructural features of the cell envelop comprises of four layers: the plasma membrane or inner membrane, the peptidoglycan-arabinogalactan complex, the outer membrane or mycomembrane covalently linked to AGP by MA and the external capsule (Kalscheuer, Palacios et al. 2019). The outer leaflet also contains various glycolipids, including trehalose monomycolate and trehalose dimycolates (TDM), phospholipids and some species-specific lipids such as glycopeptidolipids (GPL), phthiocerol dimycocerosate (PDIM) and sulfolipids (SL) (Zuber, Chami et al. 2008). The polysaccharides are the major components of the capsule in slow growing mycobacteria while the major components in fast growers like *Mycobacterium smegmatis* are proteins (Lemassu, Bardou et al. 1996, Ortalo-Magne, Laneelles et al. 1996). In slow growing, pathogenic mycobacteria the LAM caps are attached to the β-Arabinose residue with mannose residues and are known as Mannosylated lipoarabinomannan (ManLAM) whereas, the fast growing mycobacteria have phosphoinositide capped LAM known as phosphoinositide capped LAM (Hett and Rubin 2008). LAMs in mycobacteria are associated with the virulence properties by impairing the phagosome maturation and may inhibit several steps in the phosphatidylinositol-3-phosphate (PI3P) pathway (Neyrolles and Guilhot 2011). PDIM contributes to phagosomal escape of *M. tb* leading to increased cell necrosis (Quigley, Hughitt et al. 2017). TDM modulates the expression and presentation of surface antigens and interferes with phagosome maturation (Kan-Sutton, Jagannath et al. 2009, Patin, Geffken et al. 2017). MA induces foam cell formation by modulating the cholesterol metabolism and supporting the pathogen replication within the host cell (Vermeulen, Baird et al. 2017). The role of purified SL as a phagosome-lysosome inhibitor has been demonstrated in several studies (Goren, Hart et al. 1976, Brodin, Poquet et al. 2010). Thus, the cell wall components greatly contribute to the virulence of *M. tb*.

1.2.2 *Mycobacterium bovis*

The bovine tubercle bacillus was named *M. bovis* in early 1970 and the strain type was defined as *M. tuberculosis subtype bovis*, referenced in Bergey's Manual of Systematic Bacteriology (Guimaraes and Zimpel 2020). It is 0.5 to 1.5 µm long, usually G+ (Garnier, Eiglmeier et al. 2003), has dysgonic growth and is non-motile, acid-fast rod (Dostal, Richter et al. 2003). *M. bovis* grows in small, round and white colonies with irregular edges and a granular appearance (Dostal, Richter et al. 2003). The bacteria replicate very poorly in medium containing glycerol and require sodium pyruvate (Dostal, Richter et al. 2003, Golby, Hatch et al. 2007), unlike *M. tb* which requires glycerol (Diel, Vandeputte et al. 2014). The genome

sequence of *M. bovis* is approximately 4.4 Mbp long, arranged in a single circular chromosome and the average Guanosine Cytosine content is 65.63% (Garnier, Eiglmeier et al. 2003). Comparison of RNA and protein expression levels between *M. tb* H37Rv and *M. bovis* AF2122/97, a strain isolated from caseous lesions of a diseased cow in Great Britain, has shown a high degree of variation in the secretome (Garnier, Eiglmeier et al. 2003). Of note is the high expression of two genes encoding MPB70, a secreted protein accounting for 10% of *M. bovis* culture filtrate proteins, and MBP83 which is a glycosylated cell wall protein (Garnier, Eiglmeier et al. 2003, Malone, Rue-Albrecht et al. 2018).

PhoPR, a two-component regulatory system plays a major role in conferring virulence phenotype to *M. tb*. PhoPR controls the synthesis and expression of a variety of molecules involved in SL synthesis, production of the lipid species diacyltrehalose (DAT), polyacyltrehalose (PAT) via *pks2* and *pks3* regulon, and the type VII secretion system component early secreted antigenic target-6 secretion system-1 (ESX-1) (Broset, Martin et al. 2015). PhoPR is mutated in *M. bovis* indicating host specific differences in human and bovine-adapted mycobacteria (Malone, Rue-Albrecht et al. 2018). A single nucleotide polymorphism (SNP) in glycine at position 71 and proline-172 in *M. tb* PhoPR, replaced to isoleucine and leucine, respectively, might be one of the reasons for the absence of SL, PAT and lipase F in the cell wall of *M. bovis* (Golby, Hatch et al. 2007). Early secreted antigenic target-6 (ESAT-6), which is a part of the PhoP regulon and requires the *espACD* operon for its production, is well known for providing virulence properties to *M. tb* (Walters, Dubnau et al. 2006, Frigui, Bottai et al. 2008). A specific deletion in RD8 and various SNPs upstream of *espACD* removes the binding sites for EspR and MprAB. The deletion event in RD8 blocks the expression of *espACD* (Figure 1.4). However, the animal-adapted strain *M. bovis* and *M. africanum* L6 lineages have acquired compensatory mechanisms to bypass the regulatory loop controlling espACD expression and hence restore ESAT-6-dependent virulence (Gonzalo-Asensio, Malaga et al. 2014).

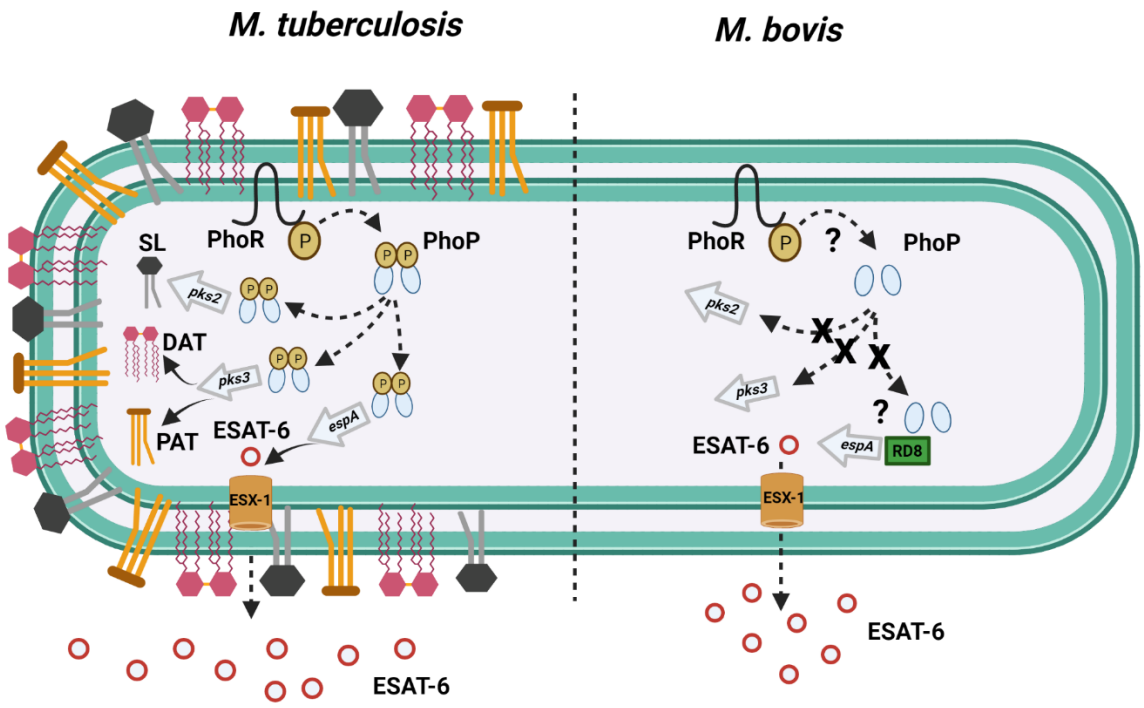

Figure 1.4: Comparative illustration of the cell wall of *M. tb* and *M. bovis*. The functional PhoR in the cell wall of *M. tb* and its phosphorylation via PhoP results in the synthesis of SL, PAT and DAT through the *pks2, pks3* gene expression. The phosphorylation of PhoP also results in the secretion of ESAT-6 via the *espA* gene axis. ESAT-6 is secreted via assembly of the ESX-1. In *M. bovis* defective PhoR limits the phosphorylation of PhoP and the synthesis of SL, PAT and DAT is hampered. However, a compensatory deletion in RD8 results in restoration of ESAT-6 secretion and thereby contributing to the virulence of *M. bovis*. Image modified from (Broset, Martin et al. 2015). *Image created with BioRender.com.*

The vaccine strain Bacillus Calmette–Guérin (BCG), which has been derived by *in vitro* attenuation of *M. bovis,* is the only available vaccine against TB for human use and was first reported in 1921 (Calmette 1931, Oettinger, Jørgensen et al. 1999). Multiple sub strains exist at the moment (Zhang, Ru et al. 2016). BCG provides good protection against TB in newborns, but its efficiency against pulmonary and latent forms of TB in adults is highly variable (Dockrell and Smith 2017). BCG confers immunity against heterologous infections in neonates (Prentice, Nassanga et al. 2021), adults and elderly (Escobar, Molina-Cruz et al. 2020, Giamarellos-Bourboulis, Tsilika et al. 2020, Moorlag, Rodriguez-Rosales et al. 2020), likely by induction of trained immunity. The variable efficacy of this vaccine against TB could be related to the absence of a number of genes, which are present in the virulent strain *M. bovis.* The most important difference which confers BCG attenuation is the absence of the RD1 region. RD1 encodes virulence-associated type VII secretion system molecules, including genes

coding for ESAT-6 and 10 kilo Dalton (kDa) culture filtrate protein (CFP-10) (Mahairas, Sabo et al. 1996).

1.3 Innate immunity to tuberculosis

The immune response to mycobacterial infection requires coordinated efforts of the innate and adaptive immune system. Diverse cells, secreted antibodies and proteins like complement and pentraxins, all contribute to the immune response to the pathogen (Lu, Marjon et al. 2011). The major innate immune cells involved in the defense against mycobacteria are macrophages (MΦ), dendritic cells (DCs), neutrophils (PMN), as well as natural killer (NK) cells (Warrington, Watson et al. 2011), invariant NK T cells (Sada-Ovalle, Chiba et al. 2008) and innate lymphoid cells (Ardain, Domingo-Gonzalez et al. 2019). Their response depends on conserved molecular features present on the pathogen which the phagocytes recognize and respond to (Pai, Behr et al. 2016). The following three subchapters give detailed information about host receptors involved in recognition of mycobacteria, phagocytosis of bacilli, bacterial escape into the cytosol and the cell signaling within phagocytes.

1.3.1 Recognition of mycobacteria by professional phagocytes and phagocytosis

The innate immune cells recognize microbes using several classes of pattern recognition receptors (PRRs) on their cell membrane (Toll like receptors (TLRs), e.g. 2,4,6; C-type lectin receptors (CLRs), e.g. Dectin-1; inside endosomes TLR 3, 7, 8, 9 (Yamashiro, Oliveira et al. 2014) and in the cytosol (Retinoic acid-inducible gene (RIG)-I-like receptors and Nucleotide-binding oligomerization domain (NOD)-like receptors (NLRs), cytosolic deoxyribonucleic acid (DNA) sensor nucleotidyltransferase cyclic guanosine monophosphate-AMP synthase (cGAS) (Collins, Cai et al. 2015). PRR activation initiates production of cytokines and triggers inflammation, which results in attraction of immune cells to the site of infection (Medzhitov 2008, Bertoni, Minuti et al. 2015). Alveolar MΦ (AM) are the first ones to encounter inhaled mycobacteria (Piercy, Werling et al. 2007, Dorhoi and Kaufmann 2014). MΦ, along with PMN and DCs which are also professional phagocytes, express a large variety of PRRs like CLRs which includes mannose receptors (MR) (Rajaram, Arnett et al. 2017), dendritic cell-specific intercellular adhesion molecule-3 grabbing non integrin (DC-SIGN) (Tailleux, Schwartz et al. 2003), Dectin-1, Dectin-2, Mannose binding Lectin and Mincle (Rothfuchs, Bafica et al. 2007, Feinberg, Jegouzo et al. 2013, Bartlomiejczyk, Swierzko et al. 2014, Decout, Silva-Gomes et al. 2018). Surfactant proteins A, Surfactant proteins D, Scavenger receptors (SRs), MΦ receptors with collagenous structure (MARCO) and CD36 interact with mycobacteria as well (Ferguson, Voelker et al. 1999, Lao, Kang et al. 2017). The CLRs like MR, Mincle on MΦ recognize PIMs,

LM and TDM present on the mycobacterial cell wall (Berg, Kaur et al. 2007). ManLAM also binds to DC-SIGN (Tailleux, Schwartz et al. 2003). Depending on the degree of acylation the higher order PIMs bind to MR, whereas lower order PIMs and LM are recognized by DC-SIGN, independent of the degree of acylation (Schlesinger, Azad et al. 2017). Mincle, which is also known as Clec4e or Clecsf9, is a MΦ-inducible CLR. It has a lower expression on non-activated leukocytes (Guirado, Schlesinger et al. 2013). The increased expression due to activation is a result of exposure to different inflammatory stimuli like TLR ligands and cytokines (Guirado, Schlesinger et al. 2013). Another CLR, MΦ C-type lectin (MCL) is a receptor for TDM (Miyake, Toyonaga et al. 2013, Lizasa, Chuma et al. 2021). Recently, DAP12-associated triggering receptor expressed on myeloid cells 2 (TREM2) has been shown to recognize non-glycosylated MA suggesting a critical role in control of host responses to TB (Lizasa, Chuma et al. 2021). TLRs recognize a variety of bacterial products. TLR2 along with TLR1 or TLR6 recognize PIMs, LM, LAM, 38 kDa and 19 kDa glycoprotein (Means, Jones et al. 2001). Triacylated lipoproteins are recognized by TLR2/TLR1 and diacylated glycoproteins are recognized by TLR2/TLR6 (Thoma-Uszynski, Stenger et al. 2001). Naphthoquinone phthiocol produced by *M. tb* is sensed within the host cytosol by the aryl hydrocarbon receptor (Moura-Alves, Fae et al. 2014). Other cytosolic PRRs like cGAS and absent in melanoma 2 (AIM2) are known to recognize mycobacterial DNA (Manzanillo, Shiloh et al. 2012, Collins, Cai et al. 2015, Watson, Bell et al. 2015).

Mycobacteria enter the host cells via receptor-mediated phagocytosis and inside the phagosome are destined to be killed by a plethora of antimicrobial mechanisms (Welin and Lerm 2012). The lectin-like C-domain of the Complement Receptor 3 (CR3) recognizes non-opsonized mycobacteria and the I-domain recognizes complement coated pathogens (Le Cabec, Carreno et al. 2002). Fragment crystallizable (Fc) receptors recognize immunoglobulin G that tags the target pathogen whereas, glycophosphatidylinositol (GPI)-anchored membrane receptors (e.g. CD14) are amongst the most well-known phagocytic receptors (Sia and Rengarajan 2019). *M. tb* possesses a cholesterol-specific sensor denoted as 'C_k' like molecule which utilizes the cholesterol-rich microdomain to enter the MΦ (Kaul, Anand et al. 2004). In addition, coronin-1 also known as Tryptophan-aspartate containing coat protein (TACO) associates with the cholesterol microdomain and facilitates mycobacterial entry into human MΦ (Anand and Kaul 2005).

Recognition and internalization of mycobacteria is not a single-receptor event, but it depends on multiple receptors and therefore, absence of or blocking of one receptor still permits uptake by phagocytes to various extents.

1.3.2 Phagosomal maturation and cytosolic escape

Once bacteria are sensed by phagocytes, a signaling cascade is launched by the phagocytic cell wherein the actin cytoskeleton is remodeled and the membrane protrusions result in the formation of a phagocytic cup surrounding the particle (Pauwels, Trost et al. 2017). Phagosomal maturation processes are initiated by fusion with early endosomes and eventually lysosomes to form phago-lysosomes (Ramachandra, Smialek et al. 2005). The network of Rab Guanosine triphosphatase (GTPase) proteins regulate the dynamics of phagosome maturation, i.e. progression from early to late stages (Queval, Brosch et al. 2017). The presence of Rab GTPases on the phagosomal membrane further recruits vacuolar-ATPases (v-ATPases) to acidify phagosomal contents by inward pumping of protons (Guirado, Schlesinger et al. 2013, Pauwels, Trost et al. 2017).

Multiple virulence factors circumvent *M. tb* killing by MΦ and eventual replication inside these cells (Ehrt and Schnappinger 2009, Cambier, Falkow et al. 2014, Queval, Brosch et al. 2017). The early endosome markers Rab5, Rab22A and Rab14 are retained on the mycobacteria-containing phagosome and the recruitment of late endosomal marker Rab7 and lysosomal marker CD63 is impaired (Clemens and Horwitz 1995, Upadhyay, Mittal et al. 2018). Phosphatidylinositol 3-phosphate (PI3P), which is generated by one of the Rab5 effectors, the type III Phosphatidylinositol-3 kinase (PI3K) hVPS34, is important for phagosomal maturation. However, inhibition of Calcium bivalent cations (Ca^{2+}) flux induced by virulent *M. tb* followed by limited calmodulin (CaM) recruitment at the phagosome membrane and impairment in the $Ca2^{+}$-CaM-hVPS3 complex formation leads to reduced production of PI3P (Vergne, Chua et al. 2003, Schlesinger, Azad et al. 2017). In addition, coronin-1 is usually released from the phagosome for the fusion with lysosomes (Jayachandran, Sundaramurthy et al. 2007). However, virulent live mycobacteria residing in phagosomes manipulate the phagosomal environment by activation of Ca^{2+}-dependent phosphatase calcineurin. TACO is actively retained on the membrane thereby blocking the lysosomal delivery (Ferrari, Langen et al. 1999, Jayachandran, Sundaramurthy et al. 2007). P27 also known as LprG is a secreted surface-expressed glycolipoprotein antigen described in *M. bovis* and conserved in many species belonging to the *Mycobacterium* genus. The gene *p27* together with *p55* also known as *Mb1445c*, are relevant for mycobacterial virulence (Bianco, Blanco et al. 2011). The *p27-p55* operon is critical for phagosomal arrest in mycobacteria-infected bovine MΦ and P27 is essential in this process (Vazquez, Bianco et al. 2017). *M. tb* lipid phosphatases like protein-tyrosine phosphatase A and B (PtpA and PtpB), and the secreted acid phosphatase M disrupt the endocytic pathway leading also to phagosomal arrest (Wong, Li et al. 2018). Out of the 11 serine/threonine protein kinases that the *M. tb* encodes (Prisic, Husson et al. 2014), PknG and PknK have no transmembrane domain. However, only PknG has been shown to be secreted in the cytosol (van der Woude, Stoop et al. 2014, Zulauf, Sullivan et al. 2018). This protein is also secreted by the SecA2 pathway and it is responsible for the inhibition of phagosome maturation (van der Woude, Stoop et al. 2014, Zulauf, Sullivan et al. 2018). Additionally, interaction between MΦ PRRs, i.e., Mincle and TDM delays the phagosome maturation and the acidification process

(Axelrod, Oschkinat et al. 2008). Furthermore, the interaction of ManLAM with the MR plays an important role in the blocking of phagolysosomal maturation (Sweet, Singh et al. 2010).

To escape the early endosomes and access the cytosol virulent mycobacteria employ the ESX-1 system (van der Wel, Hava et al. 2007). The proteins encoded by the RD1 region, CFP-10 and ESAT-6 are key virulence factors in mycobacterial pathogenesis (van der Wel, Hava et al. 2007). However, the precise mechanism of how *M. tb* and *M. bovis* are able to damage the phagosome membrane is still unclear and also the structure of ESX-1 and the stability of damaged phagosomes in the cytosol are not completely understood (Bussi and Gutierrez 2019). Additional factors that contribute to the cytosolic escape of mycobacteria were identified to be the mycobacterial outer membrane lipids dimycocerosate (DIM) and PDIM (Augenstreich, Arbues et al. 2017, Quigley, Hughitt et al. 2017).

1.3.3 Host cell activation and signaling

The presence of *M. tb* or its structural components in the phagosome results in the activation of the endosomal and upon cytosolic escape the cytosolic PRRs (Yamashiro, Oliveira et al. 2014). The stimulation of cell membrane receptors and TLRs by mycobacterial ligands results in initiation of signaling cascade. The recognition by TLR-2 results in the initiation of myeloid differentiation primary response 88 (MyD88), interleukin-1 receptor (IL-1R) associated kinase 4, TNF Receptor Associated Factor 6 and nuclear factor kappa-light-chain-enhancer of activated B cells (NF-κB) signal transduction pathways (Rahman, Sobia et al. 2014). However, *M. tb* downregulates the key genes in the TLR-2/MyD88 pathway to facilitate the escape into the cytosol (Rahman, Sobia et al. 2014). Signaling can occur independent of MyD88 and include the Toll/IL-1R domain-containing adaptor inducing interferon beta (TRIF) pathway (Bulut, Michelsen et al. 2005). Particularly CLRs converge signals to the adaptor molecule caspase recruitment domain family member 9 (CARD9) (Shenderov, Barber et al. 2013). CARD9 contributes to the control of *M. tb,* as demonstrated in a mouse model of pulmonary TB (Dorhoi, Desel et al. 2010).

Cytosolic entry of the bacteria influences the fate of both host cell and bacteria (Queval, Brosch et al. 2017). The interaction between bacterial pathogen associated molecular patterns and the intracellular sensors including NOD like receptor 1 and NOD 2, cGAS, AIM2 like receptors (ALRs) results in activation of these receptors (Nakaya, Lilue et al. 2017). Several studies demonstrate that the mycobacterial DNA is sensed by the cytosolic DNA sensor cGAS (Collins, Cai et al. 2015, Watson, Bell et al. 2015) although the precise mechanism of how the mycobacterial DNA gets into the cytosol remains unknown (Groschel, Sayes et al. 2016). cGAS utilizes Adenosine triphosphate (ATP) and Guanosine triphosphate (GTP) and synthesizes a second messenger cyclic guanosine adenosine monophosphate, which binds and activates stimulator of interferon genes (STING) leading to the production of interferon through serine/threonine-protein kinase (TBK1)-interferon regulatory factor 3 and Type-I Interferon

(Wassermann, Gulen et al. 2015, Watson, Bell et al. 2015). Virulent mycobacteria and mycobacterial DNA is sensed by AIM2 inflammasome in turn activating caspase-1 (Majlessi and Brosch 2015). The activated caspase-1 contributes to the secretion of protective cytokine Interleukin-1β (IL-1β) and IL-18 (Saiga, Kitada et al. 2012, Majlessi and Brosch 2015, Groschel, Sayes et al. 2016). *M. tb* and *M. bovis* activate NOD-like receptor family pyrin domain containing 3 inflammasome in ESX-1 dependent manner and potassium efflux is the key determinant of the inflammasome activation (Dorhoi, Nouailles et al. 2012, Beckwith, Beckwith et al. 2020). Mycobacterial RNA accesses the cytosol through the SecA2/ESX-1 mechanism and the activation of retinoic acid inducible gene (RIG-I) mitochondrial antiviral signaling protein-TBK-1 pathway results in the production of interferon beta (IFN-β) synergistic to the DNA sensing pathway (Cheng and Schorey 2018). Mycobacterial ESX-1-TBK-1 triggers the cytosolic surveillance pathway, including STING/TBK1 activation, which further mediates delivery of ubiquitin-marked bacilli to autophagosome (Watson, Manzanillo et al. 2012). However, *M. tb* subverts the autophagic flux (Romagnoli, Etna et al. 2012). *M. bovis* induces mitophagy to limit host autophagy/xenophagy and facilitate its intracellular growth (Song, Ge et al. 2022). Thus, once the mycobacteria or mycobacterial components are sensed by the host cell, the activation of downstream signaling events still fail to control the bacterial replication and they eventually escape the killing pathways.

1.3.4 Contribution of innate myeloid cells to TB granuloma

Mycobacteria-infected MΦ release cytokines and chemokines, which drive recruitment of T-lymphocytes, blood leukocytes, and tissue MΦ at the infection site (Fitzgerald, Abendano et al. 2014). Within infected tissue, the infected MΦ recruit uninfected MΦ, which surround them and form a compact organized structure called granuloma (Clay, Davis et al. 2007, Davis and Ramakrishnan 2009). The rapid and continuous migration of MΦ to the nascent granuloma is dictated by the RD1 locus in virulent mycobacteria, suggesting that the presence of RD1 is advantageous for the bacteria (Davis and Ramakrishnan 2009). In zebra fish studies, it has been shown that animals infected with mycobacteria deficient in RD1 failed to induce granuloma formation and loose MΦ aggregates were seen (Swaim, Connolly et al. 2006, Volkman, Pozos et al. 2010). Infection with RD1-deleted mycobacteria resulted in attenuation of virulence in mice (Lewis, Liao et al. 2003). Murine studies with *M. tb* and BCG infection suggest that during early infection there is accumulation of alveolar MΦ, PMN and DCs in the granulomatous lesions (Tsai, Chakravarty et al. 2006). DCs infected with BCG are associated with mycobacteria-specific T cells and induce a new multi-foci lesion demonstrating their role in the granuloma reformation (Harding, Rayasam et al. 2015). PMN either confer host protection by driving T cell response and granuloma formation, or increase disease severity (Seiler, Aichele et al. 2003, Keller, Hoffmann et al. 2006). In experimental *M. tb* infection in mice, the myeloid derived suppressor cells (MDSCs) accumulate at the infection site and restrict the T cell response (Knaul, Jorg et al. 2014). These studies suggest that the early innate

immune response to *M. tb* infection fail to kill the pathogen or restrict interaction and early granuloma formation may rather facilitate bacterial replication and *M. tb* spread.

The classic human tuberculous granuloma is caseous with epithelioid MΦ surrounding the necrotic region and present at the periphery is a cuff of lymphocyte consisting of B and T cells (Flynn, Chan et al. 2011). Recent studies using the zebra-fish model and *M. tb* infected macaques have revealed that along with a robust T-helper 1 (Th1) response Th2 signals are also important for MΦ epithelialization (Cronan, Hughes et al. 2021). *Stat6* signaling is involved in the epithelization of granuloma, already at early stages (Cronan, Hughes et al. 2021). Foamy MΦ may be elicited by *M. tb* oxygenated MA, as observed for human monocyte-derived MΦ (Peyron, Vaubourgeix et al. 2008). Metabolic factors, such as activation of ketone pathway or lipid metabolic genes, promote development of foamy MΦ (Singh, Jamwal et al. 2012). Of note, the pulmonary lesions observed in TB patients are highly heterogeneous even within the same host. Starting with a fully cellular granuloma to necrotic or fibrous lesions, the granuloma evolves and can form large open cavities when in direct contact with an airway (Lenaerts, Barry et al. 2015). PMN are found in the caseous granuloma in *M. tb*-infected macaques (Mattila, Maiello et al. 2015) and TB patients (Kim, Wainwright et al. 2010), and have been associated with granuloma caseation and cavitation (Ong, Elkington et al. 2015). Therefore, their role in TB cannot be neglected. The primary lesion which contain the bacteria may develop into calcified granuloma which is relatively stable compared to other lesion types (Ulrichs and Kaufmann 2006).

Recent data by Palmer *et al.* demonstrated that within the bovine host, the bacterial burdens and cytokine expression in individual granuloma was highly heterogeneous (Palmer, Thacker et al. 2021). Also, animals inoculated with *M. bovis* intranasally developed granulomas which were abundant in PMN (Cassidy, Bryson et al. 1998). Lesions represented by caseonecrotic core surrounded by epithelial MΦ, T cells, B cells, multinucleated giant cells, and fibroblasts were observed in four different stages (Carrisoza-Urbina, Morales-Salinas et al. 2019). The initial “stage I” granuloma consisted of aggregation of epithelioid MΦ, lymphocytes and giant cells. No necrosis was observed even though PMN infiltration was seen. The “stage II” granuloma appeared to be a solid aggregation of epithelioid MΦ, with a higher number of multinucleated giant cells than in stage I. Lymphocytes were also seen in the periphery and caseous necrotic center was also observed. In “stage III” the granuloma was completely surrounded by a connective tissue capsule and mineralized caseous necrotic granuloma was observed. The last and final “stage IV” was found to have a completely compact arrangement of cells with connective tissue capsule, epithelioid MΦ, foam cells, and multinucleated giant cells surrounded by lymphocytes and a highly caseous necrotic granuloma (Carrisoza-Urbina, Morales-Salinas et al. 2019) (Figure 1.5).

Granuloma formation poses dual functionality, it restricts the spread of infection to surrounding tissue yet allows the mycobacteria to gain access to permissive cells thereby conferring an environment for replication and eventually persistence (Volkman, Clay et al. 2004, Volkman, Pozos et al. 2010).

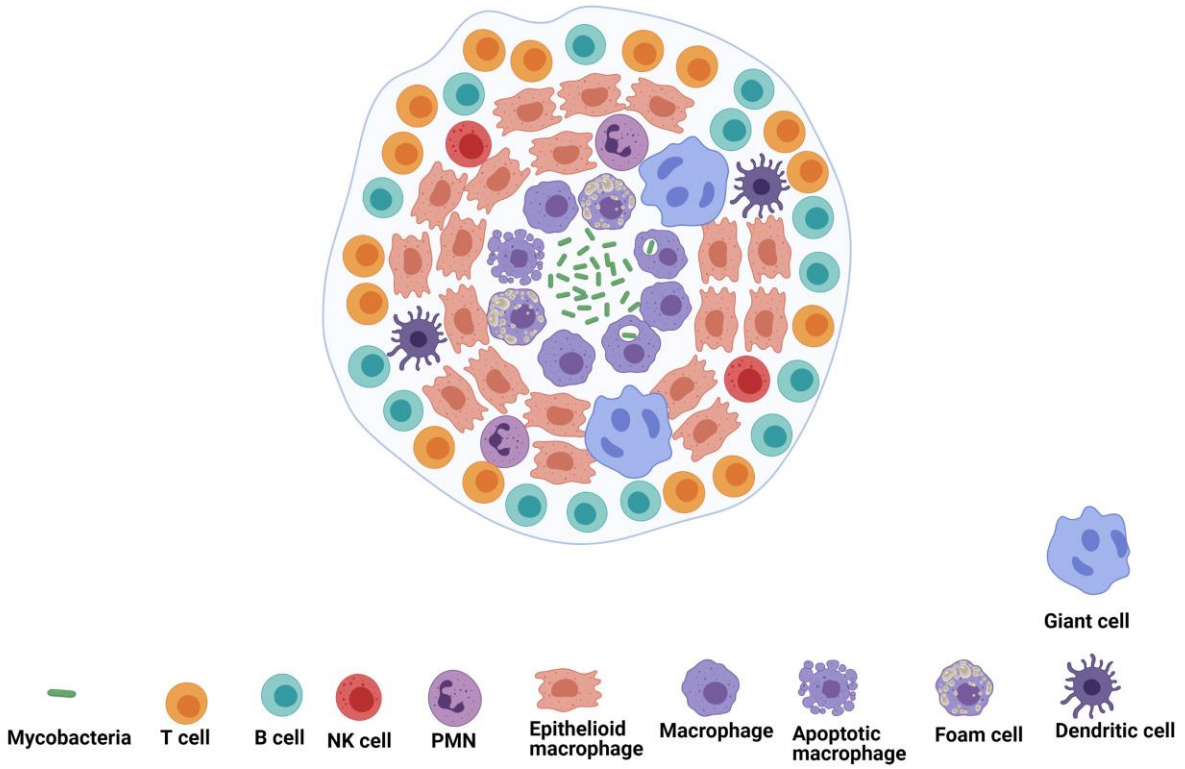

Figure 1.5: Granuloma structure. A typical necrotic tuberculous granuloma consists of a central necrotic area with presence of numerous free mycobacteria. These bacilli are surrounded by MΦ and PMN, some of which contain the pathogen. MΦ reprogramming events result in the epithelialization of the MΦ (epithelioid MΦ) and genesis of foamy and giant cells. The outer layer contains primary lymphocytes, T cells, B cells, scattered NK cells and DCs. *Image created with BioRender.com.*

1.4 Neutrophils

PMN are indispensable for clearing invading bacterial pathogens (Strydom and Rankin 2013) and are the predominant leukocyte subset in circulation in humans, but not in all mammals (Paape, Bannerman et al. 2003, Fingerhut, Dolz et al. 2020). Human blood comprises 50 - 70% PMN whereas in bovine blood PMN contribute only 25% to total leukocyte count (Paape, Bannerman et al. 2003, Strydom and Rankin 2013, Lawrence, Corriden et al. 2018, Mortaz, Alipoor et al. 2018). PMN harbor an arsenal of antimicrobial molecules for clearing the infection (Mortaz, Alipoor et al. 2018). Upon activation, these cells quickly leave the circulation and transmigrate to the tissues through a process known as PMN extravasation (Park and Hyun 2016), and accumulate at the site of infection (Mortaz, Alipoor et al. 2018). To balance the amount of extravasated PMN, a large number of PMN are mobilized from the bone marrow and the marginal pools in the circulation (Christoffersson and Phillipson 2018).

After reaching the infection site PMN engulf the invading pathogen using several phagocytic receptors and release reactive oxygen species (ROS), granular contents, antimicrobial peptides and or carry out a rather passive killing mechanism by releasing neutrophil extracellular traps (NETs) (Perobelli, Galvani et al. 2015). Following successful disposal of the pathogen, under physiological conditions PMN undergo apoptosis, a process by which the plasma membrane of the PMN undergo blebbing and released apoptotic bodies are cleared by locally residing phagocytes (Kennedy and DeLeo 2009). However, PMN may also contribute to tissue damage by excessive inflammation due to released ROS and proteases (Kruger, Saffarzadeh et al. 2015).

The following chapters focus on bovine and human neutrophils and give an overview on their genesis, granule formation, cell surface receptors, microbial-induced activation, and antimicrobial functions.

1.4.1 Genesis and maturation

PMN genesis is a hierarchical process in which a lineage committed multipotent hematopoietic stem cell (HSCs) has a potential to differentiate and give rise to a unipotent PMN progenitor (Mortaz, Alipoor et al. 2018, Yvan-Charvet and Ng 2019). During the developmental process, the HSCs gradually divide into long term (LT-HSCs) and short term (ST-HSCs) (Kondo 2010). The LT-HSCs have self-renewal ability thereby contributing to lineage reconstitution of irradiated host upon transplantation (Kondo 2010). ST-HSCs have a very limited self-renewal ability and differentiate into a multipotent progenitor cell which further differentiates into common lymphoid progenitors (CLPs) or common myeloid progenitors (CMPs) (Mortaz, Alipoor et al. 2018). CLPs give rise to T cells, B cells or NK cells (Bonilla and Oettgen 2010), whereas CMPs give rise to erythrocytes, platelets, monocytes, dendritic cells and granulocytes (Bonsall 2013). Zhu *et al*. identified a committed unipotent early-stage PMN progenitor (NeP) in adult mouse bone marrow and a similar unipotent PMN progenitor in human bone marrow which has pro-tumoral activity (Zhu, Padgett et al. 2018). Thus, lineage differentiation contributes to the development of individual cell types.

Granulocyte colony-stimulating factor is essential for the production of PMN at steady state and during infection (Yvan-Charvet and Ng 2019). NeP give rise to myeloblasts which further differentiate into promyeloblasts (PMs). PMs progress to myelocyte and at this step, the cell division stops. Myelocytes differentiate into metamyelocytes followed by band cell formation. At this step, the nucleus starts segmenting and the mature PMN showing segmentation of the nucleus is ready to be released from the bone marrow (Bainton, Ullyot et al. 1971, Yin and Heit 2018). Bovine PMN have a lower myeloid to erythroid ratio in comparison to humans and rodents (Bassel and Caswell 2018).

1.4.2 Granules and secretory vesicles

The beginning of granule formation starts in the first stages of PMN formation, i.e. MB and the PM stage, and it continues for 4 to 6 days (Lawrence, Corriden et al. 2018). PMN granules can be divided into three types based on their contents; i) the primary or azurophilic granules or peroxidase positive granules which are first detected in PM stage (Fingerhut, Dolz et al. 2020), ii) specific or secondary granules and iii) the tertiary granules which are also called large dense granules in case of bovine PMN. The last ones are formed in the later stages of PMN maturation (myelocyte and metamyelocyte stage) (Paape, Bannerman et al. 2003, Bassel and Caswell 2018) .

Primary granules are rich in myeloperoxidase (MPO) in human PMN. This enzyme is yet found in lower amounts in bovine counterparts (Bassel and Caswell 2018, Fingerhut, Dolz et al. 2020). Proteases in the azurophilic granules such as neutrophil elastase (NE) and membrane permeabilizing proteins like acid hydrolases, which play a role in microbicidal activity, are also detected in very low amounts in bovine PMN (Gennaro, Dewald et al. 1983, Styrt 1989, Bassel and Caswell 2018, Yin and Heit 2018, Fingerhut, Dolz et al. 2020). Contrary to human PMN, bovine cells lack α-defensins. However, β-defensins which are mostly produced by epithelial cells, are found in bovine PMN (Selsted, Tang et al. 1996, Fingerhut, Dolz et al. 2020). Whereas human PMN store defensin in azurophilic granules, in cattle the defensins are found in a novel class of granules termed peroxidase negative granules (Bassel and Caswell 2018). PMN also contain cathelicidins, antimicrobial peptides that act on both G+ and Gram negative (G-) bacteria (Agier, Efenberger et al. 2015). Out of the several classes of cathelicidins, only a single class known as LL-37, an active form of the cathelicidin antimicrobial peptide (CAMP) is expressed in humans (Agier, Efenberger et al. 2015). However, bovine PMN contain several classes of cathelicidins (bactenecins-5, 7, cyclic dodecapeptide, indolicidin, BMAP-27, 28, 34) (Bassel and Caswell 2018, Fingerhut, Dolz et al. 2020). Azurophilic granules also contain hydrolases such as β-glucuronidase, cathepsins, aryl sulphatases (Borregaard, Sehested et al. 1995).

The secondary or specific granules are rich in lactoferrin and contain low levels of gelatinase. These granules are peroxidase negative (Borregaard and Cowland 1997) and store microbicidal proteins like lysozyme which is also found in the azurophilic granules (Borregaard and Cowland 1997). Bovine PMN contain a relatively low or negligible amount of lysozyme compared to human PMN (Styrt 1989, Bassel and Caswell 2018).

Tertiary or gelatinase granules contain, high amounts of gelatinase (Yin and Heit 2018). The novel large peroxidase-negative granules present in bovine PMN contain O_2 (molecular oxygen), independent bactericidal agents (Gennaro, Dewald et al. 1983) and a highly cationic peptide called bactenectin with two isoforms called Bac7 and Bac5 (Paape, Bannerman et al. 2003). The main content of these granules are the β-defensins which target both G+ and G- bacteria (Paape, Bannerman et al. 2003).

Human PMN contain granules which are enriched in ficolin-1 and exocytosed in response to formyl-methionyl-leucyl-phenylalanine (fMLP). Detailed information about their contents, synthesis and function is still missing (Yin and Heit 2018). The secretory vesicles (SVs) contain various transmembrane proteins and receptors required for the phagocytosis and early inflammatory response (Faurschou and Borregaard 2003). These vesicles are formed through the endocytosis of the cell surface proteins and the endocytosed proteins are not degraded in the vesicles, but are stored for subsequent release (Nordenfelt and Tapper 2011, Yin and Heit 2018). PMN also store pre-formed cytokines like transforming growth factor-α (TGF-α) and TNF-α in the SVs (Sheshachalam, Srivastava et al. 2014). All the granules are released in a sequential manner depending on the type of immune response required (Fingerhut, Dolz et al. 2020). Similarities and differences between the human and bovine PMN thus span from surface receptors to the cellular content (Figure 1.6).

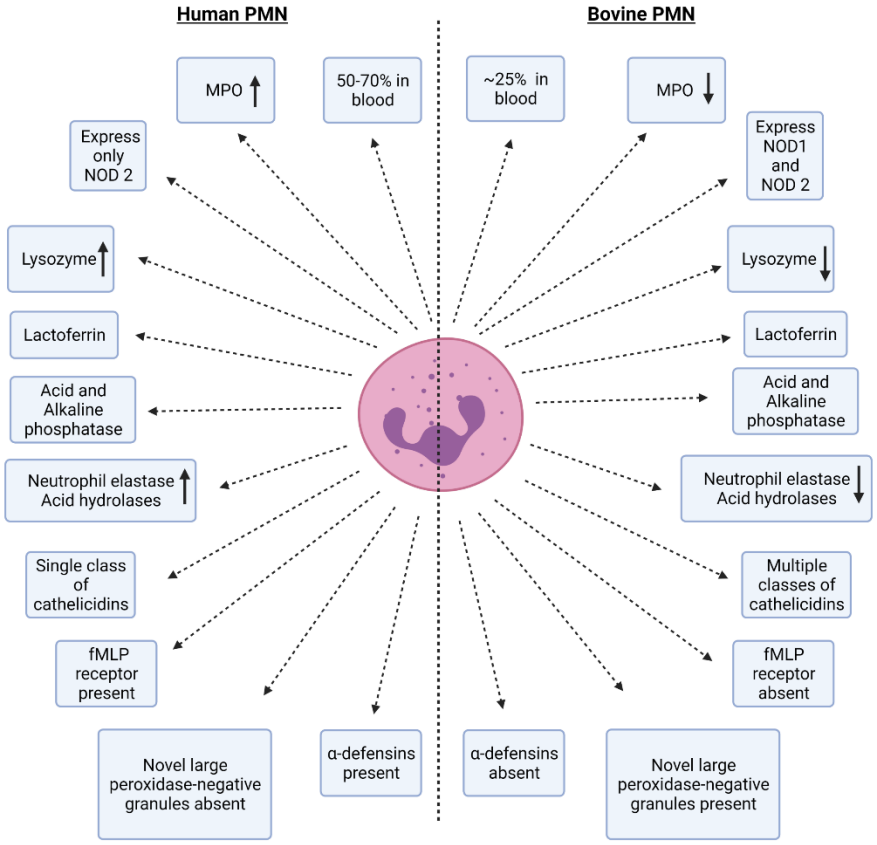

Figure 1.6: Intrinsic differences between human and bovine PMN. Abbreviations: MPO, myeloperoxidase; fMLP, N-formyl-methionyl-leucyl-phenylalanine; NOD 2, nucleotide-binding oligomerization domain-containing protein 2. *Image created with BioRender.com.*

1.4.3 Cell surface receptors

PMN express a large variety of cell surface receptors including Fc receptors FcγRIIA (CD32) and FcγRIIIb (CD16), SRs, G-protein coupled receptors like Formyl-peptide receptors (FPRs), chemoattractant receptors, chemokine receptors and PRRs such as TLR 1, 2, 4, 5, 6 (Futosi, Fodor et al. 2013). From the various PRRs, NOD1 and NOD2 are the receptors present in the cytosol for the recognition of bacterial peptidoglycan (NOD1, γ-D-glutamyl-meso-diaminopimelic acid (iEDAP); NOD2, Muramyl Dipeptide (MDP)), however human PMN express only NOD2 unlike the bovine PMN which express both NOD1 and NOD2 (Ekman and Cardell 2010, Bassel and Caswell 2018). They also express certain CLRs like dectin-1 which recognizes fungal β-glucans, Mincle which recognizes TDM and also fungi and many other receptors like MCL which recognizes TDM (Futosi, Fodor et al. 2013, Miyake, Toyonaga et al. 2013). Furthermore, PMN express chemotactic receptors for platelet activating factor (PAF) and leukotriene B-4 (Dale, Boxer et al. 2008). Integrins belonging to the adhesion superfamily, for instance αMβ2 integrins or Mac-1 (MΦ-1 antigen) or CD11b/CD18 or CR3, are expressed on the PMN surface (Dupuy and Caron 2008). These receptors are regarded as bonafide receptors for complement opsonized particles or bacteria (Dupuy and Caron 2008) and they bind to the iC3b fragment of the opsonic molecule (Lim, Grinstein et al. 2017). Unlike human PMN which express FcγRI and FcγRII for recognition of immunoglobulins, bovine PMN lack those receptors (Paape, Bannerman et al. 2003). However, cattle have a unique receptor known as Fcγ2 which binds IgG2 molecules (Bassel and Caswell 2018). FcR mediated phagocytosis depends on the phosphorylation of the immunoreceptor tyrosine-based activation motifs (ITAMs) in the cytoplasmic tail of the receptor, which occurs upon recruitment of activated Src-family kinases (Lee, Harrison et al. 2003). The phosphorylated ITAMs serve as binding sites for SH2 domain proteins specifically the tyrosine kinase Syk (Lee, Harrison et al. 2003). The involvement of Syk and the stimulation and activation of Phosphatidylinositol 3-kinase (PI3K) and Protein kinase C (PKC) is followed by actin remodeling, endosome formation and thereby the phagosome is sealed (Lee, Harrison et al. 2003). Comparative analysis of human and bovine PMN indicate that bovine PMN are unresponsive to fMLP, which suggests that they lack FPRs which are important chemotactic receptor in humans (Styrt 1989, Brown and Roth 1991, Fingerhut, Dolz et al. 2020). An overview of various phagocytosis and PRRs is depicted in (Figure 1.7).

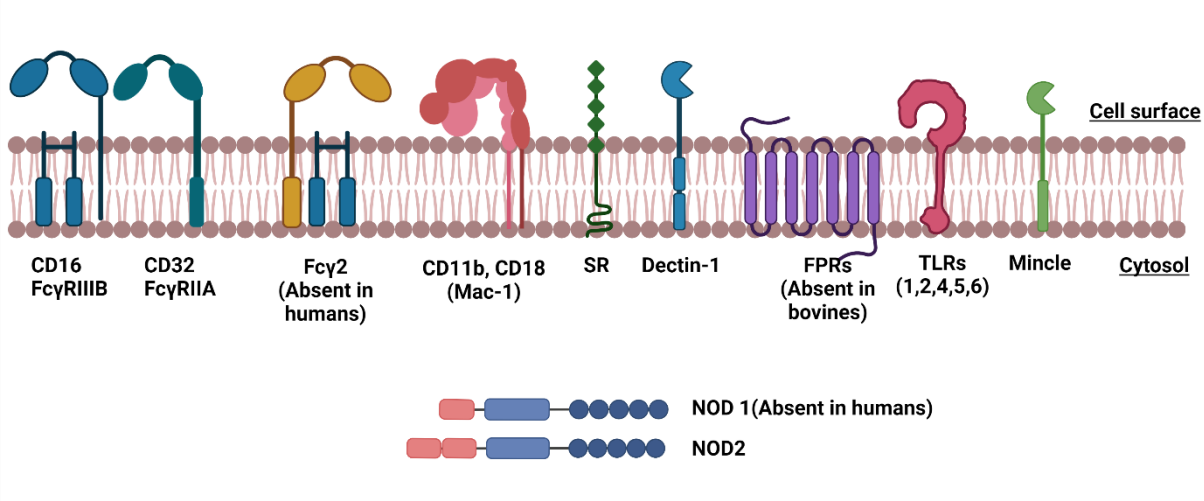

Figure 1.7: Neutrophil cell surface receptors involved in phagocytosis and bacterial recognition. Abbreviations: FcγRIIA (CD32) and FcγRIIIB (CD16), Fc receptors; CD11b, CD18 (Mac-1, or CR3), complement receptors; SR, scavenger receptors; FPRs, formyl peptide receptors; TLRs, toll like receptors; NOD, nucleotide-binding oligomerization domain-containing protein. *Image created with BioRender.com.*

1.4.4 Antimicrobial mechanisms

1.4.4.1 Oxidative killing

MPO and nicotinamide adenine dinucleotide phosphate (NADPH) oxidase are the two most powerful weapons of PMN which results in generation of oxidants, i.e. ROS and hypochlorous acid, and subsequently fungal or bacterial killing (Kato 2016). Phagocytosis of the microbes initiates the assembly of the cytosolic subunits ($p47^{phox}$, $p67^{phox}$ and $p40^{phox}$) and phagosomal membrane subunits ($gp91^{phox}$ and $p22^{phox}$, cytb) at the phagosome (Sheppard, Kelher et al. 2005). After complete assembly of the NADPH oxidase complex the active enzyme generates electrons and converts O_2 into O_2^- (Babior, Kipnes et al. 1973). The GTPase Rac-2 is essential for the activation of the NADPH oxidase (Rosen and Klebanoff 1979, Kim and Dinauer 2001). The enzyme superoxide dismutase converts the generated O_2^- into hydrogen peroxide (H_2O_2) by utilizing the protons pumped by the v-ATPases. MPO is released from the granules into the phagosome and it catalyzes the conversion of H_2O_2 into hypochlorous acid (HOCl) resulting in killing of the encountered pathogen (Segal 2005).

Defects in the NADPH oxidase machinery results in a primary immunodeficiency disorder known as chronic granulomatous disease (CGD) (Quie, White et al. 1967, Anjani, Vignesh et al. 2020). In CGD patients, pathogen clearance is impaired due to limited ROS production (Quie, White et al. 1967, Anjani, Vignesh et al. 2020). Also, deficiency of MPO in certain

patients with type 2- diabetes mellitus leads to increased susceptibility to various fungal infections (Yin and Heit 2018).

1.4.4.2 Neutrophil extracellular traps

NETs are a meshwork of chromatin fibers released by the PMN which contain antimicrobial peptides, cathepsin G, MPO and NE (Brinkmann, Reichard et al. 2004). DNA, histones, and chromatin fibers constitute the major components of NETs (Kaplan and Radic 2012). Upon cell activation, PMN release NE from the azurophilic granules into the cytosol and are then translocated into the nucleus and histone cleavage results in decondensation of chromatin (Branzk, Lubojemska et al. 2014). During chromatin decondensation, levels of intracellular Ca^{2+} rise thereby activating peptidyl arginine deaminase 4 which converts arginine in the histones to citrulline and positive charge on the proteins is reduced (Neeli, Khan et al. 2008). MPO is required for NE entry into the nucleus (Metzler, Goosmann et al. 2014). NE binds to F-actin and degrades it thereby entering the nucleus (Metzler, Goosmann et al. 2014). Stimulants like Phorbol myristate acetate (PMA), lipopolysaccharide (LPS) and IL-8, and also G+ and G- bacteria can induce NET formation *in vitro* (Brinkmann, Reichard et al. 2004). The rupture of nuclear and granular membrane releases the decondensed chromatin and granule contents into the cytoplasm and these components are then released outside the cell (Kroon, Coussens et al. 2018). The size of the microbe could determine whether it will proceed along with microbial killing or PMN will elicit NET formation for disposal of the microbe (Kroon, Coussens et al. 2018). NETs are released when the microbe size is too large to be phagocytosed (Ley, Hoffman et al. 2018). NETs bind to the bacteria, virus, fungi or parasite through electrostatic forces and prevents their spread to surrounding tissue (Ley, Hoffman et al. 2018). However, it remains unclear how much they contribute to the killing of specific microbes by PMN.

1.4.4.3 Release of granule contents and antimicrobial peptides

During infection, the granule cargoes are released in the phagosome containing the entrapped pathogen for killing. The process of controlled mobilization and release of the PMN granules during inflammation and infection is termed degranulation (Witko-Sarsat, Rieu et al. 2000). The secretory vesicles have the highest propensity for release at inflammatory sites (Faurschou and Borregaard 2003). With possessing a strong antimicrobial activity, the granule contents are also highly cytotoxic and therefore, their release is tightly regulated (Sheshachalam, Srivastava et al. 2014). Increase in intracellular Ca^{2+} levels along with the hydrolysis of ATP and GTP are important for the mobilization, exocytosis and fusion of granules to the target membrane (Theander, Lew et al. 2002, Lacy 2006). Small GTPases like

Rab27a regulate the vesicular trafficking and exocytosis of a subpopulation of azurophilic granules, tertiary granules and specific granules (Herrero-Turrion, Calafat et al. 2008, Johnson, Brzezinska et al. 2010). Munc 13-4, a Rab 27a effector induces priming of PMN for a positive interaction with receptors on the plasma membrane (Pivot-Pajot, Varoqueaux et al. 2008, Elstak, Neeft et al. 2011). Interaction of Munc 13-4 with the Soluble N-ethylmaleimide-sensitive factor activating protein receptor proteins facilitates the fusion of the granules to the membrane of the cell thereby releasing the granule content in the extracellular space for ROS production (Ley, Hoffman et al. 2018).

Human neutrophil peptide-1 (HNP-1), one of the defensins released by PMN inhibits protein translation to ensure inflammation due to MΦ is minimized (Brook, Tomlinson et al. 2016). LL-37 which belongs to the cathelicidin family is present in high abundance in NETs (Neumann, Vollger et al. 2014). This peptide protects PMN DNA from nuclease degradation (Neumann, Vollger et al. 2014) and requires the proteolytic cleavage of the inactive form of human cathelicidin into active LL-37 (Durr, Sudheendra et al. 2006). PMN azurophilic granules which are rich in the three serine proteases, NE, proteinase 3 and Cathepsin G have direct anti-bacterial activity (Cole, Shi et al. 2001, Kobayashi, Voyich et al. 2005). For instance, NE is involved in the direct killing of *Klebsiella pneumoniae* and *Escherichia coli* (*E. coli*) (Belaaouaj, McCarthy et al. 1998, Belaaouaj, Kim et al. 2000). Matrix metalloproteinases (MMPs) remodel tissue, modulate local inflammation site and also angiogenesis (Xu, Webb et al. 2018). Out of the family of MMPs, MMP-2 (72 kDa type IV collagenase) and MMP-9 (gelatinase B) are the two major gelatinases extensively studied owing their association with tumor invasion and metastasis (Aparna, Rao et al. 2015, Kunz, Sahr et al. 2016). The release of MMP-9 in response to endotoxin and proinflammatory mediators has been identified as early marker for cell activation during inflammation and sepsis (Pugin, Widmer et al. 1999).

1.4.5 Life span and cell death

PMN cell death is an indispensable event during infection and inflammation. During homeostasis approximately 10^{11} PMN are generated per day to replace the aging ones (Savill, Wyllie et al. 1989, Simon 2003). The notion that circulating PMN have a life span of 7-12 h *in vivo* (Fox, Leitch et al. 2010) has been challenged during the last decade. Using deuterium labelling PMN viability in circulation for approximately 5.4 days has been demonstrated (Pillay, den Braber et al. 2010, Lahoz-Beneytez, Elemans et al. 2016). Aging PMN are destroyed in spleen or liver. In mice, aged PMN are $CD62L^{low}$ and $CXCR4^{high}$ PMN and are eliminated from the circulation (Casanova-Acebes, Pitaval et al. 2013). However, during inflammation and infection, the PMN infiltrate the tissues to perform their antimicrobial function as shown in murine models (Kim, Liu et al. 2008, Bian, Guo et al. 2012). Also, growth factors and cytokines increase the lifespan of PMN (Aga, Mukherjee et al. 2018). For instance, the Type-1 IFNs like

IFN-α, IFN-β, IFN-ω interfere with the apoptotic pathway thereby delaying this form of cell death (Aga, Mukherjee et al. 2018).

Several PMN cell death pathways such as apoptosis, necrosis, pyroptosis, necroptosis and NETosis have been described (Dąbrowska, Jabłońska et al. 2019). Mac-1 mediated phagocytosis promotes PMN cell death via the caspase 8/3 pathway resulting in apoptotic cell death (Zhang, Hirahashi et al. 2003). Mitogen-activated protein kinases (MAPK) extracellular signal-regulated kinases downregulates the caspase 8/3 activation resulting in increased survival of PMN (Le'Negrate, Rostagno et al. 2003, Alvarado-Kristensson, Melander et al. 2004). TNF, Granulocyte-monocyte-colony stimulating factor encountered by the PMN exploits the anti-apoptotic and ROS signal resulting in increased survival of PMN at inflammatory sites (Zhang, Hirahashi et al. 2003). Several pathogens including *Streptococcus pneumoniae*, *Shigella flexneri* and *M. tb* cause PMN necrosis (Francois, Le Cabec et al. 2000, Zysk, Bejo et al. 2000, Dallenga, Repnik et al. 2017). Absence of NADPH oxidase NOX2 results in *Pseudomonas aeruginosa* flagellin mediated PMN pyroptosis depending on CARD domain-containing 4 (NLRC4) and TLR5 (Ryu, Kim et al. 2017). Another way of PMN cell death involves receptor interacting protein kinases 1 and 3 (RIPK1 and RIPK3) and mixed lineage kinase domain-like (MLKL). This type of cell death is mediated by inhibition of caspase 8, facilitates killing of *Leishmania infantum* and it is termed necroptosis (Barbosa, Fiuza et al. 2018).

1.5 Neutrophils in tuberculosis

PMN are amongst the first innate immune cells to interact with *M. tb*. They are promptly recruited at the infection site, as demonstrated in mice after intranasal infection with *M. tb* or BCG (Lombard, Doz et al. 2016). They are the most abundant cells in the sputum of TB patients and at an early infection stage in non-human primates (Eum, Kong et al. 2010, Phuah, Junecko et al. 2018). PMN are found in the earliest stage of lesions after *M. bovis* infection in cattle (Cassidy, Bryson et al. 1998, Palmer, Wiarda et al. 2019). In human patients suffering of pulmonary TB a massive influx of PMN in the lungs and an increased expression of IL-8 has been observed (Pokkali and Das 2009).

The following chapters give detailed insights into interaction of PMN with mycobacteria, including the cell surface receptors involved in recognition, and how mycobacteria escape PMN killing. The roles of PMN in inflammation and tissue damage along with their utility as biomarkers are also presented.

1.5.1 Mycobacterial recognition, phagocytosis and signaling

The recognition of *M. tb* by PMN plays a major role in the immune response to TB (Blomgran and Ernst 2011, Hilda, Selvaraj et al. 2012). However, there is scant information about interaction of bovine PMN with *M. bovis*. The cell wall of *M. tb* has unique structures which are recognized by PMN. *M. tb* SL, LM, LAM, ManLAM, PDIM, TDM and MA are recognized by human PMN (Stamm, Collins et al. 2015). The I-domain of CR3 recognizes the C3bi fragment of the complement system whereas the lectin like C-domain recognizes and bind the LAM (Peyron, Bordier et al. 2000). TLR-2 recognizes 19 kDa lipoprotein, LM, LAM and PIM (Jones, Means et al. 2001, Neufert, Pai et al. 2001, Quesniaux, Nicolle et al. 2004). Mycobacterial LAM is recognized by lactosyl-ceramide enriched lipid rafts present on PMN membrane (Nakayama, Kurihara et al. 2016).

Out of the various phagocytic receptors present in PMN, the opsonic receptors CR3, Fc receptors and non-opsonic receptors CR3 are predominantly involved in the uptake of mycobacteria (Futosi, Fodor et al. 2013). *M. kansasii* binds to the CR3 via the GPI-anchored proteins and the binding and phagocytosis is also dependent on cholesterol-rich microdomains in human PMN (Peyron, Bordier et al. 2000). Phenolic glycolipid expressed by *M. leprae* is involved in the engagement with the CR3 increasing phagocytosis by murine lung PMN (Doz-Deblauwe, Carreras et al. 2019).

Selected CLR mediate phagocytosis of mycobacteria by PMN. For instance, MCL couples with FcRγ and binds to *M. tb* TDM thus resulting in bacilli uptake (Miyake, Toyonaga et al. 2013). Other CLR members are primarily involved in signaling and subsequent recognition of mycobacteria. Virulent mycobacteria contain ManLAM which binds to lactosyl-ceramide via the α1,2-mannose residues resulting in signaling rather than bacterial engulfment (Nakayama, Kurihara et al. 2016). TLR-2 senses LAM and activates the MAPK signaling pathway resulting in the release of pro- and anti-inflammatory cytokines (Hook, Cao et al. 2020). Dectin-1 is involved in cytokine release by PMN however, the exact ligand remains undefined (Dorhoi, Desel et al. 2010). In murine PMN *M. tb* triggers CLR/Dap-12/Syk/Card9 induced signaling pathway and release of IL-10 (Dorhoi, Desel et al. 2010). Similarly, TDM administration in mice resulted in TDM mediated inflammation via Mincle dependent manner and recruitment of PMN. The TDM induced Mincle signaling is reliant on MAPK kinase, syk and src (Lee, Kang et al. 2012).

MΦ studies demonstrated that the nascent phagosome containing *M. tb* fuses with early endosomes (Kelley and Schorey 2003). However, there is no phagolysosome fusion as the early endosomal marker Rab5 is retained in the phagosome membrane and Rab7 recruitment is halted. As a consequence, the phagosome maturation is impaired (Kelley and Schorey 2003). Similarly, in *M. tb* infected human PMN Rab5a in a GTP-bound form and Syntaxin-4 are retained on the phagosome membrane suggesting Rab5a as a regulator of granule fusion with the nascent phagosome (Perskvist, Roberg et al. 2002). ROS is generated upon infection albeit with limited impact on killing of *M. tb* within PMN. In murine *M. tb* infection, KatG detoxifies ROS and Lsr2, a histone-like protein that inhibits phagosome maturation and ROS generation by binding to *M. tb* DNA (Ng, Cox et al. 2004, Colangeli, Haq et al. 2009). Excessive ROS

released by PMN causes necrotic cell death and bacteria remain viable. PMN necrotic cell death is dependent on mycobacterial ESX-1 secretion system (Corleis, Korbel et al. 2012, Dallenga, Repnik et al. 2017). Virulent mycobacteria escape the killing mechanism of PMN (Keane, Remold et al. 2000) possibly also by inhibition of TNF-α and induction of IL-10 (Flynn, Goldstein et al. 1995).

Attenuated mycobacteria induce apoptotic cell death in infected phagocytes (Keane, Remold et al. 2000). PMN infection with virulent mycobacteria has been linked to necrosis (Keane, Remold et al. 2000), as mentioned above. However, a recent *in vivo* study in mice revealed that BAX/BAK activation and apoptosis via the intrinsic pathway occur in PMN within the infected tissue. BCL-2 regulated apoptosis pathways are protective in TB by eliminating PMN and restricting pulmonary inflammation (Stutz, Allison et al. 2021). Interference with apoptosis and autophagy have been reported in PMN during murine TB and in TB patients (Blomgran, Desvignes et al. 2012). Infection of mice with nuoG mutant *M. tb* revealed that myeloid cells, including PMN, undergo accelerated apoptosis and activate the adaptive immune system thereby leading to proliferation of Ag85B-specific CD4 T cells (Blomgran, Desvignes et al. 2012). In patients, reduced expression of signaling lymphocytic activation molecule family member (SLAMF1) on PMN subverts autophagy (Pellegrini, Sabbione et al. 2020).

In vitro studies reveal on the other hand that PMN are able to kill *M. tb* by non-oxidative killing thereby rendering resistance to infection (Martineau, Newton et al. 2007). PMN from patients with CGD are able to kill *M. tb* in a ROS independent manner (Jones, Amirault et al. 1990). In line with this, α-defensins are involved in *M. tb* killing by human PMN and TNF-α is involved in the stimulation of the process (Kisich, Higgins et al. 2002). Another study reports that PMN kill *M. tb* H37Ra, an attenuated strain of *M. tb,* in a Ca^{2+}-dependent manner (Majeed, Perskvist et al. 1998). Additionally, LL-37 and HNP-1-3 at higher concentrations display a strong anti-tubercular activity (Martineau, Newton et al. 2007). However, several recent studies have reported contradictory results. *M. tb* can induce MPO mediated DNA release in the form of NETs in PMN, nevertheless the PMN fail to kill the pathogen (Ramos-Kichik, Mondragón-Flores et al. 2009). Also, *in vivo* infection of *M. tb* in guinea pigs suggest the failure of *M. tb* killing by PMN (Filio-Rodriguez, Estrada-Garcia et al. 2017). However, such information about bovine PMN is largely missing. One *ex vivo* study demonstrated that the PMN infected with *M. bovis* underwent necrotic cell death similar to human PMN and failed to eliminate the pathogen unless starved or stimulated with TLR ligands (Wang, Zhou et al. 2013). Thus, it is important to investigate cell biology of bovine PMN upon infection with virulent mycobacteria. This knowledge will contribute to a better understanding about roles of PMN in bTB. Figure 1.8 summarizes the events within mycobacteria-infected PMN, starting from mycobacterial recognition, phagosome formation, signaling, escape from killing and various ways in which an infected PMN die following infection.

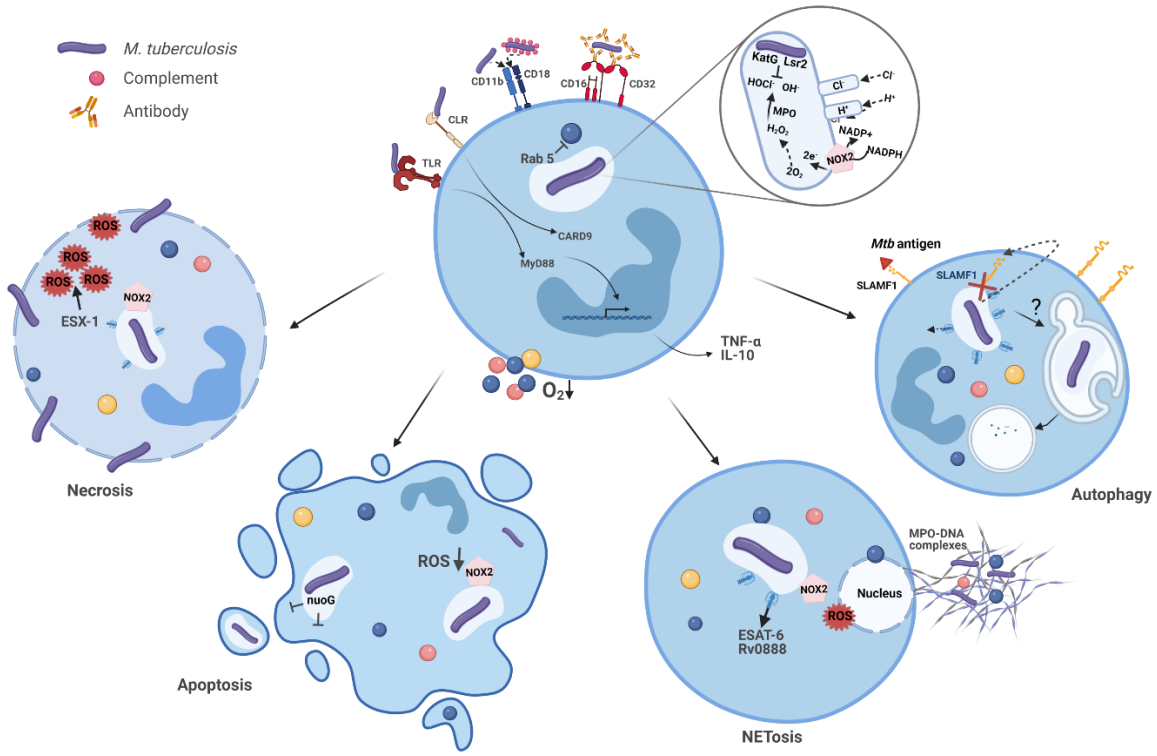

Figure 1.8: Overview of PMN events and fate after mycobacterial infection. Recognition and phagocytosis of mycobacteria is controlled by complement receptor (CR3, CD11b/CD18), Fc receptor (CD16/CD32), Toll like receptors (TLRs) and C-type lectin receptors (CLRs). NADPH oxidase NOX2 recruited at the phagosomal membrane activates PMN however, reactive oxygen species (ROS) do not kill the bacteria. Autophagy and apoptosis are regulated by mycobacteria whereas excess ROS results in PMN death by necrosis and NETosis. Abbreviations: nuoG, operon in *M. tb*; MyD88, myeloid differentiation primary response 88; CARD 9, caspase recruitment domain-containing protein 9; MPO, myeloperoxidase; KatG, catalase-peroxidase; Lsr2, nucleoid-associated protein of *M. tb*; ESAT-6, 6 kDa early secreted antigenic target; SLAMF1, signaling lymphocytic activation molecule family member 1, ESX-1,6 kDa early secreted antigenic target secretion system 1; O_2, molecular oxygen; IL, interleukin. Image modified from (Borkute, Woelke et al. 2021) and created with *Biorender.com*.

1.5.2 Role in inflammation and tissue damage

Inflammation plays a critical role in control of mycobacteria (Piergallini, Scordo et al. 2021). In response to the encountered pathogen PMN activate effector responses including the activation of NADPH complex and generation of ROS (Van Acker and Coenye 2017). During the early stages of systemic mycobacterial infection, subsequent intravenous infection, PMN downregulate inflammation and contribute to mycobacterial clearance (Pedrosa, Saunders et al. 2000). These findings could not yet be replicated in aerogenic models. Depletion of PMN

in TB-prone mice is protective also in early stage, suggesting deleterious roles (Eruslanov, Lyadova et al. 2005, Dorhoi, Yeremeev et al. 2014). During chronic mycobacterial infection PMN primarily foster inflammation (Zhang, Majlessi et al. 2009). Patients with active TB disease have higher level of granulocytes (Kerkhoff, Wood et al. 2013, Panteleev, Nikitina et al. 2017, Ndlovu, Peetluk et al. 2020, Muefong, Owolabi et al. 2021).

There are several pieces of evidence that PMN trigger tissue damage in TB and underlying molecules and processes have been partly unveiled. MMPs are emerging as the key proteases causing TB immunopathology (Belton, Brilha et al. 2016). Pulmonary TB lesions are highly hypoxic and MMP1 drives tissue destruction (Belton, Brilha et al. 2016). PMN are the major cell type found in the pulmonary cavities and PMN driven release of matrix MMP8 through NF-κB signaling is observed in patients with active TB disease (Ong, Elkington et al. 2015). MMP8 driven tissue damage caused in human pulmonary TB infection is via AMP-adenosine protein kinase signaling (Ong, Elkington et al. 2015). Hypoxia augments capacity of PMN to release MMP8 (Ong, Fox et al. 2018). In the guinea pig model, PMN expressing S100A9 marker protein were found in the center of granuloma after BCG challenge, similar to granuloma observed in TB patients, suggesting the roles in lung lesion progression (Yoshioka, Mizutani et al. 2016). In mice genetically susceptible to *M. tb* PMN accumulation is associated with exacerbated tissue injury and inflammation (Eruslanov, Lyadova et al. 2005) and it is dependent on the proinflammatory cytokine IL-17 and the induction of S100A8/A9 proteins (Gopal, Monin et al. 2013). TB susceptible (C3HeB/FeJ) mice infected with *M. tb* generate abundant levels of Type I IFN which triggers NETs formation, promoting bacterial growth and survival along with increased severity of the disease (Moreira-Teixeira, Stimpson et al. 2020).

All these findings suggest that an efficient removal of mycobacteria-infected PMN during pulmonary TB is crucial for the resolution of inflammation and for minimizing organ damage.

1.5.3 Biomarkers for disease severity and therapy outcome

Host biomarkers such as blood RNA signatures (Berry, Graham et al. 2010, Penn-Nicholson, Mbandi et al. 2020), C-reactive protein (Gao, Guo et al. 2019), procalcitonin and soluble triggering receptor expressed on myeloid cells (s-TREM-1) have been studied as a useful tool for distinguishing pulmonary TB infection from community acquired pneumonia (Kang, Kwon et al. 2009, Ugajin, Miwa et al. 2011, Tintinger, van der Merwe et al. 2012). Soluble factors derived from PMN as well as PMN frequencies or phenotype emerge as potential biomarkers for TB severity (Muefong, Owolabi et al. 2021). IL-8 is a major chemokine released during inflammation has been shown to be detected in higher concentration than IFN-γ and could be a promising biomarker for the detection of bTB progression (Gao, Guo et al. 2019). Expression of CD15, a PMN marker could also serve as marker for disease severity. High PMN counts and lower levels of CD15 on cell surface have been associated with high bacterial load in the sputum and severe damage on chest X-ray (Ndlovu and Marakalala 2016, Ndlovu,

Peetluk et al. 2020). A recent study reveals that PMN-derived soluble mediators such as MMP8 and S100A8 correlate with severe lung pathology in TB patients. (Gopal, Monin et al. 2013, Muefong, Owolabi et al. 2021). S100A8/A9 also mediates PMN accumulation via CD11b expression during chronic TB (Scott, Swanson et al. 2020). Targeting these mediators could support development of novel therapies which minimize TB-induced lung pathology and enhance lung recovery (Muefong, Owolabi et al. 2021).

Blood PMN frequencies may predict the therapy outcome in TB patients. A study assessing the possible predictors of radiologic severity during TB therapy has reported that PMN infiltration was the major cause of poor radiologic outcome (Jones, Dabbaj et al. 2021). In an observational study with a cohort of culture-confirmed pulmonary TB patients, increased PMN count in blood before anti-TB treatment indicated unfavorable outcomes such as death, treatment failure or TB recurrence (Carvalho, Amorim et al. 2021). Recently, emerging roles of neutrophilic MDSCs (PMN-MDSCs) as a target for immunotherapy are highlighted for both human and cattle (Cassetta, Baekkevold et al. 2019, Rambault, Doz-Deblauwe et al. 2021). These cells share markers with PMN and accumulate during pathological conditions like TB (El Daker, Sacchi et al. 2015). In TB-resistant and TB-susceptible mice PMN-MDSCs are found in lung parenchyma during *M. tb* infection and they suppress T cell activity (Knaul, Jorg et al. 2014). Additionally, in a non-human primate model of pulmonary TB, PMN-MDSCs were found in a higher proportion in the lungs of animals with active TB compared to those with latent infection, suggestive of their immunosuppressive capabilities (Singh, Singh et al. 2021). Increased frequencies of MDSCs during active TB infection and suppression of T cell function results in reduced mycobacterial containment and disease progression (du Plessis, Loebenberg et al. 2013, Davids, Pooran et al. 2021, Grassi, Vanini et al. 2021). Therapeutic strategies like reversing the suppressive activity of PMN-MDSCs and blocking their activation are emerging as promising targets for host directed therapies for TB (du Plessis, Kotze et al. 2018).

1.6 Objectives

TB is a threat to both human and cattle health. Research focusing on interactions of human PMN with *M. tb* revealed host beneficial but also detrimental role of these phagocytes in TB outcome. There is scant information about the involvement of bovine PMN in *M. bovis* infection in cattle and limited data of their *ex vivo* responses to distinct members of MTBC family. Additionally, it is not understood how *M. tb* infection is cleared by immunocompetent cattle in the absence of tissue lesions. Whether bovine PMN play a role in clearance of *M. tb* is still unknown. Comparative investigations on responses of bovine PMN to *M. tb* and *M. bovis* have not been performed so far. Therefore, this work addresses the following objectives:

- Establishment of a method for isolation of highly pure bovine PMN.
- Comparative functional analysis of bovine and human PMN upon infection with *M. bovis* BCG.
- Comparative functional analysis of bovine PMN infected with *M. bovis* AF2122/97 and *M. tb* H37Rv.

2 Materials and methods

2.1 Ethical statement

This PhD thesis includes work with human peripheral blood samples which was approved by the ethics committee of the University of Greifswald (reference number BB114/19). The bovine blood was collected and handled according to the approvals granted to the Friedrich-Loeffler-Institut (FLI) from the "Landesamt für Landwirtschaft, Lebensmittelsicherheit und Fischerei Mecklenburg-Vorpommern" (LALLF) (reference number LALLF 7221.3-2-041/17).

2.2 Overview of materials

2.2.1 Antibodies and stains

Table 2.1: Overview of antibodies used

Antibody	Clone	Isotype	Reference#	Supplier
Anti-bovine CD11b	CC126	IgG2b	MCA1425GA	Bio-RAD
Anti-human CD11b	ICRF44	IgG1	301302	Biolegend
Anti-bovine CD62L	BAQ92A	IgG1	BOV2046	Monoclonal antibody center Washington
Anti-mouse IgG1 magnetic particles	A85-1	IgG1	557983	BD Biosciences
Fc Receptor block	2.4G2		101301	Biolegend
Fc Receptor block (Human)			130-059-901	Miltenyi Biotec
Anti-mouse Alexa fluor 647	Polyclonal	IgM	1020-31	Southern Biotech
Anti-mouse Dylight 405	Poly24091	IgG1	409109	Biolegend
Goat anti-mouse biotin	Polyclonal	IgM	1020-08	Southern Biotech
Anti-bovine CD11b (Integrin αM)	CC104	IgG2b	SC101829	Santa Cruz Biotechnology
Isotype control mouse IgG1	MG-145	IgG1	401402	Biolegend
Isotype control mouse IgG2b	MPC-11	IgG2b	400302	Biolegend
Isotype control rat IgG2b	RTK4530	IgG2b	400602	Biolegend

Anti-bovine CD11b FITC	CC126	IgG2b	MCA1425F	Bio-RAD
Anti-bovine G1	CH138A	IgM	BOV2067	Monoclonal antibody center Washington
Anti-bovine MHCII	CAT82A	IgG1	BOV-CT2012	Monoclonal antibody center Washington

Table 2.2: Overview of stains used

Stain	**Reference#**	**Supplier**
Annexin V BV421	640924	Biolegend
DAPI Biochemica	A10010010	PanReach Appli chem
Filipin III from *Streptomyces filipinensis*	F4767	Sigma-Aldrich
Kwik Diff stain kit	9990700	Thermo Fisher Scientific
Propidium Iodide	P4864	Sigma-Aldrich

2.2.2 Reagents, buffers and media composition

Table 2.3: Overview of reagents, buffers and media used

Reagent/ buffer and media	**Reference #**	**Supplier**
2 Mercaptoethanol	M6250	Sigma-Aldrich
2-(N-(7-Nitrobenz-2-oxa-1,3-diazol-4-yl) Amino)-2-Deoxyglucose) (2NBDG)	36702	ATT Bioquest
10x Phosphate buffer saline (PBS)	70011-044	Gibco
1-step fix lyse solution	005333-54	Invitrogen
1x PBS	14190-144	Gibco
Agarose low-melting	11408.02	SERVA Electrophoresis
Albumin fraction V (BSA)	8076.4	Carl Roth
Ammonium chloride (NH_4Cl)	k292.2	Carl Roth
BBL Middlebrook (Albumin dextrose catalase) ADC enrichment	212352	BD Biosciences
BBL Middlebrook (Oleic albumin dextrose catalase) OADC enrichment	212240	BD Biosciences
BBL™ Seven H11 Agar base	212203	BD Biosciences
BD Difco Mycobacteria 7H11	283810	BD Biosciences
BD Difco ™ middlebrook 7H9 broth	271310	BD Biosciences
BD Difco™ Aspargine	214410	BD Biosciences
Biocoll 1.077 g/mL	BS.L.6115	Bio & SELL
Camptothecin	C9911	Sigma-Aldrich

Cytochalasin B from *Drechslera dematiodea*	C2743	Sigma-Aldrich
Cytochalasin D	C2618	Sigma-Aldrich
Cytoflex daily QC	B53230	Beckman Coulter
Distilled water	15230-147	Gibco
Dimethyl sulfoxide (DMSO)	D8418	Sigma-Aldrich
EDTA	15575-038	Invitrogen
Escherichia coli Bioparticles Fluorescein conjugate	E2861	Invitrogen
Ethanol	11093.01	SERVA Electrophoresis
Fluorescence-activated cell sorting (FACS) Clean	A64669	Beckman Coulter
FACS sheath fluid	B51503	Beckman Coulter
Fetal calf serum (FCS)	P-30-3302	PAN-Biotech
Seahorse XF Rosewell Park Memorial Institute (RPMI) Medium	103576-100	Agilent
Glutaraldehyde 50% solution in water	23116.01	SERVA Electrophoresis
Glycerol	G5516	Sigma-Aldrich
Glycid Ether	21045.02	SERVA Electrophoresis
Goat serum	31872	Invitrogen
Hank's balanced slat solution (HBSS) with calcium and magnesium without phenol red	10-527F	Lonza
4-(2-hydroxyethyl)-1-piperazineethanesulfonic acid (HEPES)	15630056	Gibco
Histopaque 1.119 g/mL	11191	Sigma-Aldrich
Horse radish peroxidase	P-6782	Sigma-Aldrich
Human AB serum	31876	Sigma-Aldrich
Hydrogen peroxide	H1009	Sigma-Aldrich
Hygromycin	1287.2	Carl Roth
Laminarin from Laminaria Digitata	L9634	Sigma-Aldrich
Lead citrate	15158	SERVA Electrophoresis
L-Glutamine	25030-081	Gibco
Lovastatin, Sodium Salt	438186	Calbiochem
Luminol	A8511	Sigma-Aldrich
Methyl β-Cyclodextrin (MβCD)	C4555	Sigma-Aldrich
Millipore water		Millipore
N-acetyl D-Glucosamine (NADG)	A3286	Sigma-Aldrich
Osmium tetroxide (OsO_4)	31251.04	SERVA Electrophoresis
Paraformaldehyde	335.3	Carl Roth
Percoll 1.130 g/mL	17-0891-01	GE Healthcare Biosciences

Phorbol myristate acetate	P1585	Sigma-Aldrich
Propylene oxide	33715.01	SERVA Electrophoresis
Rat serum	R9759	Sigma-Aldrich
RPMI 1640	31870-025	Gibco
RPMI without phenol red	R7509	Sigma-Aldrich
Sodium bicarbonate ($NaHCO_3$)	6329	Merck & Co.
Sodium cacodylate buffer	15540.01	SERVA Electrophoresis
Streptavidin beads	557812	BD Biosciences
Sulphuric acid (H_2SO_4)	4623.1	Carl Roth
3,3',5,5'-Tetramethylbenzidine (TMB) substrate set	421101	Biozol
Tris buffered saline	T-6664	Sigma-Aldrich
Triton X-100	X100	Sigma-Aldrich
Trypan blue	CN76.2	Carl Roth
Tween 20	P1379	Sigma-Aldrich
Tween 80	P-4780	Sigma-Aldrich
Uranyl acetate	77870.02	SERVA Electrophoresis

Table 2.4: Media composition

Media/Solutiions/Buffers	**Composition**
0.5% triton in PBS	0.5% (V/V) Triton X-100 in PBS
1% triton in PBS	1% (V/V) Triton X-100 in PBS
1x Annexin V binding buffer	25 mL 10x annexin binding buffer + 22.5 mL 10x PBS + 202.5 mL millipore water
7H11 agar	19 g 7H11 agar + 0.2% glycerol + 900 mL Millipore water, autoclaved and then 10% OADC was added
7H9 Broth	2,35 g 7H9 Broth + 0.2% Glycerol + 0.05% Tween80 + 450 mL Millipore water, autoclaved and then 10% ADC was added
Assay medium: RPMI 2% FCS	RPMI 1640 medium supplemented with 2% FCS, 50 µM 2-Mercaptoethanol (2ME), 2 mM L-Glutamine, 10 mM HEPES
Assay medium: RPMI 2% human serum	RPMI 1640 medium supplemented with 2% human serum, 50 µM 2ME, 2 mM L-Glutamine, 10 mM HEPES
BD IMag buffer (P-BSA)	PBS, 0.5% Albumin Fraction V, 2mM EDTA
Blocking solution	PBS, 5% goat serum, Fc Receptor block clone 2.4G2 diluted at 30 µg/mL, and rat serum diluted at 16 µg/mL
Erylysis buffer	156 mM NH_4Cl, 12 mM $NaHCO_3$, 0.8 mM EDTA in Millipore H_2O
Seahorse XF RPMI Medium without glucose	Seahorse XF medium (2.5 mL) + 1 mM pyruvate (25 µL) + 2 mM glutamine (25 µL) + 0.5%BSA
PBS + 0.05% Tween 80	0.05% (V/V) Tween 80 in PBS

PBS + 1% BSA (1% PBSA)	1% (W/V) Albumin Fraction V in PBS
PBS + 1% FCS	1% (V/V) FCS in PBS
PBS + 1% human serum	1% (V/V) human serum in PBS
PBS + 5% goat serum	5% (V/V) goat serum in PBS
RPMI + 0.5% BSA	RPMI 1640 medium supplemented with 0.5% Albumin Fraction V, 50 µM 2ME, 2 mM L-Glutamine, 10 mM HEPES

2.2.3 Readymade kits and consumables

Table 2.5: Overview of readymade kits used

Kit	Reference#	Supplier
Bovine IL-8/ CXCL-8 Basic ELISA kit	3114-1H-20	Mabtech
Bovine TNF-α Duoset ELISA kit	DY2279	R & D Systems
Cell fractionation kit	9038	Cell Signaling technology
Human IL-8/CXCL8 Duoset ELISA kit	DY208	R & D Systems
Human TNF-α Duoset ELISA kit	DY210	R & D Systems
MACSxpress® Whole Blood Neutrophil Isolation Kit, human	130-104-434	Miltenyi Biotec

Table 2.6: Overview of consumables used

Consumables	Reference#	Supplier
5 mL Luer lock omnifix syringe	4616037V	Braun
50 mL soft-Ject Luer lock syringe	8300006682	VWR
15 mL tube	62.554.502	Sarstedt
50 mL tube	62.547.254	Sarstedt
5 mL disposable serological pipette	4487	Corning costar
10 mL disposable serological pipette	4488	Corning costar
25 mL disposable serological pipette	4489	Corning costar
48 well cell culture plate flat bottom	3548	Corning costar
96 Flat non-treated white microwell plate	236105	Thermo Fisher Scientific
96 well black plate	137101	Nunc
96 well cell culture plate flat bottom	3599	Corning costar
Autoclave bag	09.302.0020	Nerbe plus
Bacillol AF	973389	Hartmann
Bacillol AF tissue	13526	Praxisdienst Dieckhoff

BD Plastipak ™ 1 mL Sub-Q 26G syringe	305501	BD Biosciences
BRAND® microplate BRAND plates®, immunoGrade	BR781722-100EA	Sigma-Aldrich
Butterfly syringe	85.1638.205	Sarstedt
Cryo .S™ 2 mL round bottom tube	122263	Greiner bio-one
Cuvette Polystyrene	634-0676	VWR International
Eco nitrile PF250 gloves S	625122	Eco shield
Ethanol 99.8%	140200018	Carl Roth
FACS tube 5 mL	55.1579	Sarstedt
Filter card 76×26 mm	720-2061	VWR International
Flask 100 mL	214-0408	VWR International
Flask 50 mL	214-0407	VWR International
Gigasept FF (neu)	14040027	Schülke
Glass bottle Duran 1000 mL	215-1537	VWR International
Glass bottle Duran 250 mL	215-1535	VWR International
Glass bottle Duran 500 mL	215-1536	VWR International
Glass coverslip	11757414	Thermo Fisher Scientific
Grids 300 mesh, Nickel	7FGN300	Plano
Lids for Rotilabo ®-microtest plate	9297.1	Carl Roth
Melsept	18907	B.Braun
Microscope slides cut edge frosted	631-1551	VWR International
Microtiter plate lid	264122	Thermo Fisher Scientific
Microzid AF wipes	109203	Schülke
Neubauer cell counting chamber	717805	BRAND
Nunc Maxisorp™ ELISA uncoated plate	423501	Biolegend
PETG Square Bottle HDPE Closure 30 mL	382019-0030	Thermo Fisher Scientific
Petri dish	82.1473.001	Sarstedt
Pipette tips: 1000 µL Finntip flex	94060720	Thermo Fisher Scientific
Pipette tip: 200 µL tips	739290	Greiner bio-one
Pipette tip: ART 1000 G	2079G	Molecular bioproducts
Pipette tip: ART 200 G	2069G	Molecular bioproducts
Safe lock tube 1.5 mL	0030 120.086	Eppendorf
Safe lock tube 2 mL	0030.120.094	Eppendorf
S-Monovette® EDTA 9 mL K3E	02.1066.001+EE24:E62	Sarstedt

S-Monovette® EDTA 9 mL Z clot activator	2.1063	Sarstedt
Soft loop 10 µL	612-9357	VWR International
Spin-X centrifuge tube filter	8160	Corning Costar
Stericup millipore plus filtration system 0.22 µm PES 1000 mL	S2GPU10RE-0685	Merck & Co.
Stericup millipore plus filtration system 0.22 µm PES 250 mL	S2GPU02RE-03030	Merck & Co.
Stericup millipore plus filtration system 0.22 µm PES 500 mL	S2GPU05RE-15894	Merck & Co.
Sterile syringe filter 0.2 µm	13336617	VWR International
Steritop 45 mm neck size millipore express plus 0.22 µm 1000 mL	S2GPT10RE-0402	Merck & Co.
Steritop 45 mm neck size millipore express plus 0.22 µm 250 mL	S2GPT02RE-5560	Merck & Co.
Steritop 45 mm neck size millipore express plus 0.22 µm 500 mL	S2GPT05RE-05180	Merck & Co.
U bottom polypropylene 96 well plate	267334	Thermo Fisher Scientific
V bottom polystyrene 96 well plate	9292.1	Carl Roth

2.2.4 Devices and software

Table 2. 7: Devices

Devices	**Supplier**
-20°C freezer	Liebherr
-80°C freezer	Liebherr
BD IMag cell separation magnet	BD Biosciences
Centrifuge 5430R	Eppendorf
Centrifuge 5810R	Eppendorf
Class II biological safety cabinet	Thermo Fisher Scientific
CO2 Incubator MCO-19AIC	Sanyo
CellInsight™ CX7 High Content Analysis Platform	Thermo Fisher Scientific
CytoFLEX S	Beckman Coulter
LSR Fortessa™ X-20	BD Biosciences
Fridge	Liebherr
Incu-line incubator 180-prime	VWR International
MACSmix tube rotator	Miltenyi Biotec
MACSxpress separator	Miltenyi Biotec
Nikon Eclipse TS 100	Nikon

Optical microscope TS2	Nikon
Pipette 100 µL-1000 µL	Thermo Fisher Scientific
Pipette 20 µL-200 µL	Thermo Fisher Scientific
Pipette 2 µL-20 µL	Thermo Fisher Scientific
Pipetteboy	Thermo Fisher Scientific
Plate reader SPARK	TECAN
Shaker incubator KS 4000 I control	IKA
Spectrafuge 16M	Labnet international
T62.2 Cytocentrifuge	MLW electronic
Water bath	Julabo 7A Reutlingen
Weighing balance	Sartorius

Table 2. 8: Software

Software	**Supplier**
BioRender	BioRender
FlowJo V10	Flow Jo LLD
GraphPad Prism 8	Graph Pad Prism Inc
HCS studio	Thermo Fisher Scientific
Microsoft Office 2016	Microsoft
NIS Elements	Nikon
Spark control	Tecan

2.3 Bacterial strains and culture

The following bacterial strains were used: BCG Danish-strain expressing the green fluorescent protein (GFP) (transformed with the plasmid pGFM-11 by electroporation and selected on antibiotics, e.g. hygromycin) (BCG GFP), BCG Danish-1331 wildtype (WT), *M. tb* H37Rv, *M. tb* H37Rv-expressing GFP (Dorhoi, Yeremeev et al. 2014), engineered similarly to BCG GFP, were kindly provided by Stefan H.E. Kaufmann, Max Planck Institute for Infection Biology, Berlin, Germany. *M. bovis* AF 2122/97 WT and *M. bovis* AF 2122/97 GFP, which was derived by electroporation with an integrative plasmid (pNIP) were kindly provided by Aude Remot and Nathalie Winter, INRAE Val de Loire, Nouzilly, France (Abadie, Badell et al. 2005).

BCG and *M. tb* strains were grown in Middlebrook 7H9 broth supplemented with 0.2% (v/v) glycerol and 0.05% (v/v) Tween 80, and 10% (v/v) ADC enrichment medium. *M. bovis* strains were grown in Middlebrook 7H9 broth supplemented with 40 mM sodium pyruvate, 0.05% (v/v) Tween 80, and 10% (v/v) ADC enrichment medium. The GFP reporter strains required addition of 50 µg/millilitre (mL) hygromycin in the cultivation medium. Bacterial cultures were grown and the harvested cultures were stored at -80˚C until use.

Early log phase cultures of optical density (OD_{600}) ranging between 0.4 and 0.6 and up to passage 5 were used for all the experiments. The required amount of bacteria were collected in Eppendorf tubes and spun down at 17,949 x g for 5 minute (min) at 4° C. The supernatant was discarded and the pellet was resuspended in PBS and centrifuged again at 17,949 x g for 5 min. After discarding the supernatant, the pellet was resuspended in PBS, passed through sterile 26G needle minimum 5 times to break the clumps and get a single suspension of bacteria. The OD was measured against PBS and diluted accordingly for infection. The OD of the grown culture was calculated by measuring the $OD_{(600)}$= 0.1 corresponding to 2 x 10^7 bacteria/mL for BCG and *M. bovis* AF2122/97. For *M. tb* calculation was done with $OD_{(600)}$= 0.1 corresponding to 5 x 10^7 bacteria/mL.

For opsonization of the bacteria, on the day of experiment human and bovine blood was collected in vacutainer tubes without anti-coagulant. The tubes were centrifuged at 1,000 x g for 15 min for serum collection. Fresh serum from both species was collected separately. Required amount of BCG GFP or *M. bovis* AF2122/97 GFP or *M. tb* H37Rv GFP was pelleted in an Eppendorf tube by centrifugation at 17,949 x g for 5 min and the supernatant was discarded. The pellet was then resuspended in 700 µL fresh bovine or human serum and the tube was incubated at 37 ˚C for 30 min. After incubation 700 µL PBS was added and tube was spun at 17,949 x g for 5 min. The resulting pellet was resuspended in 1 mL PBS and optical density was measured to determine bacterial density and the opsonized bacteria was used for infection.

2.4 Cellular cytospin and staining

To check the purity of isolated cells, 5 x 10^5 sorted cells were taken in 750 µL PBS and loaded in the cytospin cuvette with the slide and filter assembled in the T62.2 cytocentrifuge. The cytospin was run for 3 min at 900 rounds per min (rpm), disassembled and the slide was air dryed. Kwik-Diff Staining protocol was followed according to manufacturer's instructions. The slides were air dryed before mounting with oil for counting cells.

2.5 Density gradient centrifugation methods

All steps were performed inside a class II biological safety cabinet to maintain sterile environments and avoid sample contamination.

2.5.1 Isolation of bovine and human neutrophils using Histopaque 1.119 g/mL and Percoll

To isolate PMN, blood was collected from healthy donors, humans or cattle, using a butterfly syringe in EDTA tubes. The separating solution Histopaque 1.119 g/mL was allowed to reach room temperature (RT). 5 mL of Histopaque were added to 15 mL tubes and using a sterile pipette 5 mL blood was slowly layered on top of the Histopaque solution. The tube was then centrifuged at 800 x g for 20 min at RT with brakes off. After centrifugation, the upper plasma layer was removed and the cloudy layer of peripheral blood mononuclear cells or monocytes (PBMCs) was discarded. The layer underneath was collected and washed by adding 3x the volume of 1% PBSA. The tubes were then centrifuged at 300 x g for 10 min at RT. The supernatant was discarded and the pellets were pooled together in 2 mL 1% PBSA. Percoll gradient stock was prepared by mixing 36 mL Percoll with 4 mL 10x PBS. This stock could be stored for 2-4 days at 4˚ C. Percoll gradient was prepared for layering as shown in the following table:

Table 2. 9: Percoll gradient

Concentration of gradient	Gradient stock	1x PBS
85%	8.5 mL	1.5 mL
80%	8 mL	2 mL
75%	7.5 mL	2.5 mL
70%	7 mL	3 mL
65%	6.5 mL	3.5 mL

2 mL from each gradient concentration was carefully added to 15 mL falcon tube starting with 85% through 65%. The 2 mL of cell suspension obtained post centrifugation on Histopaque 1.119 g/mL was added on top of the 65% Percoll gradient layer. The tube was centrifuged at 800 x g for 20 min at RT with brakes off. The remaining PBMC layer after centrifugation was removed and the lower cloudy fraction of PMN was collected in a fresh tube. The collected fraction was washed by adding 3x the volume of 1% PBSA and centrifuged at 300 x g for 10 min at RT. The pellet was resuspended in 2 mL 1% PBSA. The isolated cells were counted using Neubauer cell counting chamber by diluting the cells in trypan blue solution.

2.5.2 Isolation of bovine neutrophils using Biocoll 1.077 g/mL and Histopaque 1.119 g/mL

Blood was collected from the jugular vein of healthy cows in 9 mL vacutainer tubes containing 1.6 mg EDTA/mL blood. The Histopaque 1.119 g/mL and Biocoll 1.077 g/mL required for the isolation were brought to RT. 20 mL whole blood was divided in two tubes. One tube was diluted 1:1 and the other tube 1:4, with PBS. 5 mL Histopaque 1.119 g/mL was added to a 15 mL tubes. 5 mL Biocoll 1.077 g/mL was added on top of the Histopaque layer. With sterile pipette, 5 mL washed (1:1) or diluted blood (1:4) was added on top of the layers in corresponding tube. The tubes were then centrifuged at 800 x g for 20 min at RT with brakes off. After centrifugation, the cloudy layer containing PBMCs was removed and the layer at the interface of Histopaque and Biocoll containing PMN plus erythrocytes was taken in a fresh tube. Erylysis was performed by adding 9x the volume erylysis buffer to the collected fraction. The tube was mixed slowly by inversion for 1 min or until the solution was clear and subsequently centrifuged at 450 x g for 10 min at RT. The supernatant was removed and if the pellet looked red, the erylysis step was repeated. The resulting pellet was washed by adding 1% PBSA and centrifuged at 450 x g for 10 min at RT. The supernatant was discarded and the cells were resuspended in 500 µL 1% PBSA and counted in Neubauer cell counting chamber to determine yield and viability and the purity was determined in cytospins using a T62.2 cytocentrifuge.

2.5.3 Isolation of bovine neutrophils by whole blood centrifugation

Blood was collected from the jugular vein of healthy cows in 9 mL vacutainer tubes containing 1.6 mg EDTA/mL blood. 20 mL whole blood was divided in two tubes. One tube contained 10 mL whole blood and in the other tube 10 mL whole blood was diluted 1:4 with PBS. The tubes were centrifuged at 400 x g for 20 min at RT with brakes off. The supernatants were discarded and the pellet was taken up in 45 mL 1% PBSA and centrifuged at 800 x g for 20 min at RT with brakes off. The upper plasma layer as well as one third of the erythrocyte pellet were discarded. The remaining pellet was diluted with 1% PBSA and centrifuged at 1,000 x g for 30 min at RT with brakes off. The remaining plasma and thin buffy coat layer was discarded and erylysis was performed by adding 9x the volume erylysis buffer to the pellet. The tubes were mixed by gentle inversion for 1 min or until the cell suspension was clear. Osmolarity was reconstituted with 1:10 10x sterile PBS and tubes were centrifuged at 300 x g for 10 min at RT. The supernatant was removed and erylysis was repeated until a white cell pellet was obtained, indicating disposal of residual erythrocytes. The PMN enriched pellet was then washed with 45 mL 1% PBSA and centrifuged at 340 x g for 5 min at RT. The supernatant was removed, the pellet was resuspended in 2 mL 1% PBSA and cells were counted in Neubauer cell counting chamber.

2.6 Neutrophil isolation using antibody labelling and fluorescence-activated cell sorting

2.6.1 CD15 labelling and sorting of human neutrophils

Human blood was collected from healthy donors in 9 mL vacutainer tubes containing 1.6 mg EDTA/mL blood. The tubes were centrifuged at 1,500 x g for 10 min at RT. After removing the plasma and the upper one third layer of cells, the remaining fraction was transferred to a 50 mL falcon tube. Erythrocytes were lysed by using 9x the volume erylysis buffer and the tube was inversed slowly until red turbidity dissapeared and the suspension was dark red and clear. The osmolarity was reconstituted with 1:10 10x sterile PBS. The tube was centrifuged at 300 x g for 10 min at RT. The erylysis step was repeated if required. The supernatant was removed and the pellet was washed once with PBS+ 1% human serum to wash off remaining erylysis buffer. The tube was centrifuged at 450 x g for 3 min at RT and the pellet was resuspended in PBS+ 1% human serum. Total leukocytes were counted using Neubauer chamber and the required amount of cells were blocked using human Fc block (20 µL/10^7cells) for 5 min on ice. The cells were labelled with anti-human CD15-APC (dilution 1:1,000) and incubated on ice for 15 min. After incubation, 1 mL PBS+ 1% human serum was added and the tube was centrifuged at 450 x g for 3 min. The pellet was resuspended in 1 mL PBS+ 1% human serum and passed through a nylon mesh cell strainer snap cap tube and cells were sorted using the morphometric gate and further gating on APC positive population. The cells were sorted in tubes containing FCS.

2.6.2 Antibody labelling and sorting of bovine neutrophils

Bovine blood was collected from the jugular vein of healthy cows in 9 mL vacutainer tubes containing 1.6 mg EDTA/mL blood. The vacutainer tubes were then centrifuged at 1,000 x g for 15 min at RT with brakes off. After centrifugation, plasma was removed and the upper one third layer of the pellet was removed with a sterile pipette. The bottom two-third pellet was collected and transferred to 50 mL falcon tubes. Erythrocytes were erylysed by adding 9 x the volume of erylysis buffer to the pellet. The tubes were mixed by inversion for 1 min or until the color in the tube was clear. The osmolarity of the sample was reconstituted with 1:10 10x sterile PBS. The sample was washed by adding 1x PBS and centrifuged at 300 x g for 10 min at RT. In case the RBC lysis was not successful the erylysis step was repeated. The pellet was washed once with PBS to get rid of any remaining erylysis buffer. The cells were taken up in blocking solution, purified leukocytes were counted and cell numbers were adjusted to 2 x 10^7 cells/mL. The required amount of cells was taken in a tube and centrifuged at 450 x g for 3 min at 4˚ C. The supernatant was removed and the pellet was resuspended in 100 µL of blocking solution and mouse anti-bovine G1 antibody clone CH138A antibody

(dilution 1:2,000) and anti-bovine Major histocompatibility complex (MHC II) antibody clone CAT82A (primary MHCII) antibody (dilution 1:500) was added in 100 µL of blocking solution. The tube was incubated for 15 min on ice. After incubation 3 mL blocking solution was added to the tube and centrifuged at 450 x g for 3 min at 4˚ C. The pellet was resuspended in 100 µL of blocking solution and anti-mouse IgM Alexa Fluor 647 (dilution 1:2,000) and anti-mouse IgG1 Alexa Fluor 405 (dilution 1:500) was added in 100 µL of blocking solution. The tube was incubated for 15 min on ice. After incubation 3 mL 1 % PBSA was added to the tube and centrifuged at 450 x g for 3 min at 4˚ C. The pellet was resuspended in 1,000 µL PBS+ 1% FCS and passed through a nylon mesh cell strainer snap cap tube and sorted using a morphometric gate and further gating on CH138A positive population. The cells were sorted in tubes containing FCS using LSR Fortessa™ X-20.

2.7 Magnetic isolation of neutrophils

2.7.1 Negative selection of human neutrophils

The principle of this isolation method is to deplete the non-target cells using magnetically labelled magnetic activated cell sorting (MACS)xpress beads while aggregating erythrocytes settle at the bottom of the tube. The following procedure was followed according to the vendor's protocol.

Preparation of MACSxpress PMN isolation cocktail: the lyophilized bead pellet was reconstituted by adding 2 mL of buffer A. The pellet was mixed gently by pipetting up and down 3-4 times to obtain a homogenous suspension. The final cocktail was prepared by mixing 2 mL of buffer B to the reconstituted pellet. For magnetic labelling, 8 mL of anti-coagulated human whole blood was taken in a 15 mL falcon tube. 4 mL final cocktail was added to the whole blood. The tube was closed tightly and inverted gently for 3 times and incubated at RT using the MACSmix tube rotator on permanent run speed of approximately 12 rpm. After incubation the tube was removed from the rotator, the cap was opened and the tube was placed in the magnetic field of the MACSxpress separator for 15 min. Magnetically labelled cells adhered to the tube wall whereas the erythrocytes settled at the bottom. While the tube was still in the magnet, the non-adherent cell suspension was carefully collected in a fresh falcon tube which contained the target cell fraction. This fraction was then spun down at 300 x g for 10 min at RT. In case the pellet appeared red it was further erylysed using erylysis buffer and spun down at 300 x g for 10 min at RT. The supernatant was removed and the cell pellet was resuspended in PBS + 1% BSA. An aliquot was removed to establish the cell yield after isolation.

2.8 Transmission electron microscopy

To comparatively study the ultrastructure of PMN the cells were isolated and the following procedure was followed. Cell pellets were fixed in 2.5% glutaraldehyde in 0.1 M cacodylate buffer pH 7.2 for 2 h at 4˚C. The cells were further embedded in a low-melting point agarose followed by fixation with 1% aqueous OsO_4 for 2 h at 4˚C. An overnight *en-bloc* staining was performed with 2.5% uranyl acetate in ethanol at 4˚C. A stepwise dehydration was carried out in ethanol 30/50/70/90/95/100% for 25 min each at 4°C. Dehydration of the sample was followed by incubation in propylenoxid for 25 min at RT and embedding in glycidether 100. The polymerization was carried out for 3 days at 60˚C. Ultrathin sections (60-70 nm) were made using an ultramicrotome and the section were collected on grids and contrasted using uranyl acetate and lead citrate staining. Analysis of the grids was done with transmission electron microscopy (TEM) using an acceleration voltage of 80 kiloVolt. The preparation and imaging of PMN was carried out by the electron microscopy facility of the FLI, Insel Riems.

2.9 Viability assays using flow cytometry

Viability of isolated cells was assessed by checking for early apoptotic (EA; Annexin V positive), late apoptotic (LA; Annexin V and propidium iodide (PI) positive and necrotic (PI positive cells). 5 x 10^5 human and bovine PMN were seeded in 100 µL assay medium containing 2% human/bovine serum in U-bottom polypropylene plates in triplicates. At different time point cells were transferred to FACS tubes and 1 mL annexin binding buffer (ABB) was added. The tubes were centrifuged at 340 x g for 5 min at 4 ˚C, supernatant was discarded. 50 µL of prepared staining solution (1 µL from Annexin V BV421 stock and 1 µL from PI stock) was added to the tubes and the tubes were incubated for 15 min in dark protected from light at 4˚C. After 15 min of incubation 15 µL ABB was added and the cells were acquired within 60 min on the CytoFLEX S Cell Analyzer. Single stains were prepared the same way leaving out either annexin V or PI. As positive controls: for annexin V cells were treated with 100 µM camptothecin (CPT) to induce apoptosis, for necrosis, samples were freeze thawed several times.

2.10 Glucose uptake by purified cells

5 x 10^5 PMN were seeded in 100 µL Seahorse XF RPMI Medium without glucose in a U bottom polypropylene 96 well plate in triplicates and incubated for 10 min and 30 min at 37˚C under 5% CO_2 before any treatment to rest the cells. After starving the cells in medium without glucose, 2NBDG a cell-permeable fluorescent glucose uptake probe at 200 µM concentration

was added and cells were further incubated for 30 min at 37˚C and 5% CO_2. Following incubation, the plate was centrifuged at 450 x g for 3 min and pellet was resuspended in PBS and centrifuged again at 450 x g for 3 min. The pellets were resuspended in 200 µL PBS, the cells were transferred to FACS tubes, and were acquired on the CytoFLEX S Cell Analyzer. The PMN were selected using morphometric forward scatter (FSC) and sideward scatter (SSC) gating and 2NBDG PMN were quantified using geometric mean fluorescence intensity (gMFI). The fold change in 2NBDG uptake from 10 min to 30 min was calculated by dividing gMFI values for 30 min by gMFI for 10 min.

2.11 Assessment of neutrophil activation by flow cytometry

To determine whether isolated bovine PMN were activated upon isolation, staining for the cell surface markers CD11b and CD62L was performed. Activated cells upregulate CD11b on their surface and downregulate CD62L (Fortunati, Kazemier et al. 2009).

2.11.1 Staining of purified bovine neutrophils

5 x 10^5 PMN in 100 µL PBS was added per FACS tube, mouse anti-bovine CD62L antibody clone BAQ92A diluted at 5 µg/mL in PBS was added and cells were incubated for 10 min on ice. After a wash in PBS cells were stained with anti-bovine CD11b-FITC diluted at 0.5 µg/mL and anti-mouse IgG1 Dylight 405 diluted at 1 µg/mL and were incubated for 20 min on ice. Excess antibodies were washed away using PBS and spinning down at 450 x g for 3 min at RT. Cells were fixed in 100 µL 4% paraformaldehyde (PFA) at RT for 15 min in dark protected from light. After incubation, cells were washed twice with 200 µL PBS and the pellet was resuspended in 300 µL PBS and the samples were acquired at the CytoFLEX S Cell Analyzer. PMN were selected using morphometric FSC and SSC gating and CD11b CD62L were gated to evaluate the activation of isolated PMN.

2.11.2 Staining of bovine neutrophils in whole blood

500 µL whole blood was added in a FACS tube in triplicates assuming there were approximately 1x 10^6 PMN/mL. A tube for unstained control and a tube for staining with primary anti-bovine G1 (clone CH138A) antibody was also included. The whole blood was blocked with 100 µL blocking solution and the tube was incubated for 5 min at RT. The primary antibody and anti-bovine CD62L antibody were added to the cells accordingly in the respective tubes. The tubes were incubated for 10 min on ice. After incubation 1 mL PBS was

added and the tubes were centrifuged at 450 x g for 3 min at RT. The pellet was resuspended in 100 µL PBS containing anti-mouse IgM AF 647, anti-mouse IgG1 Dylight 405 and anti-bovine CD11b-FITC. The tubes were incubated for additional 15 min on ice. After incubation 1 mL PBS was added and the tubes were centrifuged at 450 x g for 3 min at RT. The supernatant was removed and cells were resuspended in 2 mL of diluted BD fix lyse solution to lyse the red blood cells (RBCs). After RBC lysis the tubes were centrifuged at 450 x g for 3 min at RT. The pellet was resuspended in 300 µL PBS and acquired on the CytoFLEX S Cell Analyzer. Granulocytes were selected using morphometric FSC and SSC gating and doublets were excluded using FSC area (FSC-A) and forward scatter height (FSC-H). The cells which stained for CH138A were gated and the population was further evaluated for CD11b and CD62L expression.

2.12 Flow cytometry for assessment of phagocytosis

2.12.1 *M. bovis* BCG GFP, *M. tb* H37Rv GFP, *M. bovis* AF2122/97 GFP and Fluorescein conjugated *E. coli* bioparticles

5 x 10^5 PMN were seeded in 100 µL assay medium containing human/bovine serum a U-bottom polypropylene 96 well plate in triplicates and incubated for 30 min at 37˚C and 5% CO_2 before infection to rest the cells. Subsequently, cells were infected with BCG GFP, *M. tb* H37Rv GFP, *M. bovis* AF2122/97 GFP at MOI of 10 or MOI 30; or stimulated with fluorescein conjugated *E. coli* at MOI 1. All conditions were incubated for 10 min or 30 min. To synchronize the infection, the plate was centrifuged at 135 x g for 3 min at 4˚C. After incubation the plates were centrifuged at 450 x g for 3 min to remove any extracellular bacteria. The supernatant was removed and the resulting pellet was washed with 100 µL PBS and fixed with 4% PFA and incubated at RT for 30 min at RT and afterwards 2% PFA at 4˚C for the experiments with virulent strains. The plate was centrifuged at 450 x g for 3 min and pellet was resuspended in PBS and centrifuged again at 450 x g for 3 min to remove any remaining PFA. The pellets were resuspended in 200 µL PBS and the cells were transferred to FACS tubes, and acquired at the CytoFLEX S Cell Analyzer. The PMN were selected using morphometric FSC and SSC gating and PMN which phagocytosed mycobacteria were identified as GFP^+ cells and were evaluated as percent phagocytosis (frequencies of cells positive for mycobacteria) and gMFI (relative amounts of internalized bacteria).

2.12.2 Phagocytosis of serum opsonized bacteria

5 x 10^5 PMN were seeded in a U-bottom polypropylene 96 well plate in triplicates and incubated for 30 min at 37˚C and 5% CO_2 before infection to rest the cells. Following

incubation, the PMN were infected with serum opsonized BCG GFP/ *M. bovis* AF2122/97 GFP/ *M. tb* H37Rv GFP at MOI of 30 or fluorescein conjugated *E. coli* at MOI 1 for 30 min. Samples were further processed and analyzed as described under 2.12.1.

2.12.3 Analysis of phagocytic pathways using CD11b neutralizing antibodies and chemical inhibitors

Laminarin (50 µg/mL), a dectin-1 agonist, methyl β-cyclodextrin (MβCD) 5 millimolar (mM) which is a membrane cholesterol depleting agent, N-acetyl D-Glucosamine (NADG) 0.15 M, a glucose polymer found on the cell wall of bacteria which binds to the C-domain of CR3 and Cytochalasin D (10 µM), an actin depolymerizer were used. 5 x 10^5 PMN were seeded in 80 µL RPMI + 0.5% BSA without serum in U-bottom 96 well polypropylene plates in triplicates. Cells were either blocked using neutralizing antibodies, anti-CD11b (CC126 10 µg/mL, anti-CD11b (CC104; 2 µg/mL), isotype control mouse IgG1 for bovine PMN; or anti-CD11b (M1/70; 10 µg/mL) and anti-CD11b (ICRF44 2 µg/mL), isotype control rat IgG2b for human PMN, all delivered in 20 µL/well. Chemical inhibitors, i.e., MβCD 5 mM, NADG 0.15 M or Cytochalasin D 10 µM/20 µM, were preincubated with PMN for 30 min at 37°C, 5% CO_2. Afterwards, the cells were infected with either non-opsonized or opsonized BCG GFP/ *M. tb* H37Rv GFP/ *M. bovis* AF2122/97 GFP at MOI 30 at MOI 30 or *E. coli* at MOI 1. To synchronize the infection, plates were centrifuged at 135 x g for 3 min at 4°C. Finally, cells were transferred to V-bottom plates and centrifuged at 453 x g for 3 min. Cell pellets were washed with 100 µL PBS and fixed in 100 µL 4% PFA in the dark for 30 min in 4% PFA at RT and afterwards 2% at 4°C for the experiments with virulent strains. After fixation, plates were centrifuged at 450 x g for 3 min and the resulting pellets were washed with 100 µL PBS to remove excess PFA. Cells were resuspended in 200 µL PBS and acquired at the CytoFLEX S Cell Analyzer.

2.13 High-content imaging for assessment of phagocytosis

3 x 10^5 PMN were seeded in 100 µL HBSS in a 96 well cell culture treated plate in triplicates. Cells were allowed to adhere to the plate for 60 min at 37 °C, 5% CO_2. After incubation they were infected with non-opsonized or opsonized BCG GFP at MOI 10. The plate was centrifuged at 135 x g for 5 min to synchronize the infection. The plate was further incubated at 37°C, 5% CO_2 and the infection were allowed to proceed for 30 min. After incubation, the infection medium was carefully aspirated with a pipette and cells were washed twice with 200 µL RT PBS to remove extracellular bacteria and then fixed with 4% PFA for 20 min in dark at RT. After washing and removing PFA cells were stained with DAPI (1:10,000) in PBS for 5 min in dark to visualize the nuclei. After staining the cells were washed five times with 100 µL PBS to remove excess DAPI stain. 100 µL PBS was added and the plate was scanned at

the CellInsight™ CX7 High Content Analysis Platform to evaluate infected cells. The nucleus was identified as the primary object with a fixed threshold method and segmentation intensity of 2. The validation of the cells was done by masking on the total intensity of the primary object. The region of interest was defined with a ring around the object by adjusting the width and distance from the nucleus. The bacteria were detected using the spot detection algorithm from which percentage of infected cells per well from the selected primary objects was deduced. The spot count per cell indicating amounts of bacteria per cell was calculated using the spot count per object feature from the available well features in the HCS studio software. A total of 121 fields and totally 50,000 cells were counted for each sample.

2.14 Cholesterol quantification

2.14.1 Total cholesterol: Amplex red assay

5 x 10^5 PMN were seeded in 100 µL HBSS in a 96 well cell culture treated plate in triplicates. Cells were left untreated, treated with MβCD 10 mM or infected with WT BCG at MOI 30. The plate was incubated for 30 min at 37 °C, 5% CO_2. After incubation the culture medium was removed and cells were washed with 200 µL PBS and then 100 µL of 0.5% Triton X 100 was added per well and the plate was further incubated for 30 min at RT.

To determine total cholesterol concentration, amplex red cholesterol assay kit was used. 25 µL supernatant was collected in a 96 flat bottom black well plate and the supernatant was diluted with 25 µL of the reaction buffer provided in the kit. 50 µL of amplex red reagent (prepared according to manufacturer's instructions) was added and the plate was incubated for 30 min at RT in dark and fluorescence intensity was measured at an excitation of 545 nm and emission 590 nm using the TECAN SPARK plate reader. For each point, the background fluorescence was corrected by subtracting the values derived from the no-cholesterol control. A standard curve was plotted and the cholesterol concentration values were extrapolated from the formula obtained from the standard curve.

2.14.2 Free cholesterol: Filipin staining

To determine free cholesterol content in the cell, Filipin was used. It is a naturally fluorescent polyene antibiotic that binds to free cholesterol in the cell but not the sterols. 5 x 10^5 PMN were seeded in 80 µL HBSS in a U-bottom polypropylene 96 well plate in triplicates. The cells were left untreated, treated with MβCD 5 mM or infected with BCG GFP at MOI 30. The plate was incubated for 30 min at 37 °C, 5% CO_2. After incubation, the cells were transferred to V-bottom plate and centrifuged at 450 x g for 3 min. The cell pellets were washed with 100 µL

PBS and centrifuged again. 100 µL 4% PFA was added to fix the cells in the dark for 20 min at RT. After incubation, the plate was centrifuged at 450 x g for 3 min and the resulting pellet was washed with 100 µL PBS and centrifuged again to get rid of remaining PFA. The cells were resuspended in Filipin at a final concentration of 50 µg/mL and the staining was allowed for 60 min in dark at RT. Samples were immediately acquired at LSR Fortessa X-20. Doublets were excluded from all events and BCG infected cells were gated using the GFP channel. From the GFP^+ population, the percentage of cells staining positive for filipin was measured and the gMFI of the filipin positive population was calculated.

2.14.3 Membrane cholesterol: Cell fractionation

2.5×10^6 human or bovine PMN were seeded in a RPMI + 0.5% BSA in duplicates in a U-bottom polypropylene plate. The cells were left untreated or treated with either lovastatin 5 µg/mL, to block the synthesis of cholesterol, or 5 mM MβCD to deplete cholesterol in the membrane. The plate was incubated for 30 min at 37 °C, 5% CO_2 and subsequently cells were infected with WT BCG at MOI 30 and further incubated for 30 min. Subsequently, cells were transferred to 1.5 mL Eppendorf tubes and washed with PBS to remove any extracellular bacteria. The tubes were spun at 453 x g for 3 min. Supernatants were discarded and cell pellets were resuspended in 250 µL cell isolation buffer provided in the cell fractionation kit, vortexed for 5 sec and incubated on ice for 5 min. After centrifugation at 500 x g for 5 min the supernatant, which represented the cytoplasmic fraction, was collected. The pellet was resuspended in 250 µL membrane isolation buffer and the tubes were vortexed for 15 sec and incubated on ice for 5 min. Centrifugation of the tubes at 8,000 x g for 5 min allows for recovery of the membrane fraction in the supernatant. To determine membrane cholesterol concentration, amplex red cholesterol assay kit was used as detailed under 2.14.1.

2.15 Measurement of reactive oxygen species by luminescence

ROS production by isolated human and bovine PMN was measured using luminol and horseradish peroxidase (HRP) based chemiluminescence assay. PMN were diluted in freshly prepared phenol free ROS assay medium containing 2% human or bovine serum, 50 µM luminol and 1.2 U/mL HRP. Cells were seeded in a flat bottom non-treated 96 white well plate and incubated at 37˚C and 5% CO_2 for 30 min. TECAN SPARK plate reader instrument was pre-heated to 37˚C and 5% CO_2. The stimuli (e.g., PMA) were prepared in ROS assay medium. WT BCG was used at MOI 30. The plate was removed from the incubator and placed in TECAN SPARK, to measure 10 cycles of baseline at 1,000 ms/cycle. Afterwards stimuli, BCG and 1 µM PMA (final concentration) were pipetted in 100 µL, the plate was sealed and measured

immediately in continuous rounds for at least 450 cycles. ROS curves and area under the curve (AUC) were calculated.

2.16 Myeloperoxidase release assay

MPO catalyzes the reaction of H_2O_2 with chloride ions (Cl^-) to form HOCl (Nauseef 2014). The activity of MPO can be measured using Tetramethylbenzidine (TMB) substrate which develops a blue colored product which can then be converted into a yellow-colored final product using H_2SO_4. The optical density as a measurement of MPO amounts can be read at 450 nm using a plate reader. Isolated bovine and human PMN were seeded at a density of 5 x 10^5 cells/well in 100 µL in triplicates and allowed to settle for 30 min at 37˚C and 5% CO_2 and then pre-treated for 5 min with 10 µg/mL cytochalasin B. PMN were then stimulated with PMA 1 µM or infected with BCG MOI 10 or 30, *M. bovis* and *M. tb* MOI 30 for 30 min. The plate was then incubated for 30 min at 37˚C and 5% CO_2. After incubation, for quantification of the total MPO release, unstimulated cells in few wells were treated with 0.01% triton for 5 min. After incubation the cells were transferred to a V-bottom plate and centrifuged at 453 x g for 3 min. 50 µL supernatant was collected in ELISA plates and 150 µL TMB solution was added and the plate was incubated for 30 min in dark for colour development. The reaction was stopped using 50 µL 2 M H_2SO_4. The absorbance was read at 450 nm using TECAN SPARK plate reader. The medium control value was subtracted from all the values and the percent of MPO release was calculated based on values obtained for cells lysed with triton by dividing all the values by triton values.

2.17 Colony forming unit assay

Bovine and human PMN were allowed to adhere to a tissue culture treated flat bottom 96 well plate at 5 x 10^5 PMN/well in triplicates in 100 µL HBSS medium containing calcium and magnesium. The plates were incubated for 30 min at 37°C, 5% CO_2 to rest the cells. After resting, PMN were infected with BCG at MOI 10 (delivered in 50 µL), for intracellular and total killing and plates were further incubated for respective time points: 30 min, 90 min, 180 min and 240 min. For intracellular killing, the infection medium was completely removed from all the time points and the wells were washed twice with 100 µL RT PBS and replaced with same amount of HBSS for further incubation if required (i.e. 90-240 min). After removing the supernatant 100 µL 0.5% Triton X 100 was added per well and the plate was incubated at RT for 5 min. Similarly, for total killing, 50 µL of 1% triton X 100 was directly added to the wells without washing the infection medium and the plate was incubated for 5 min at RT. 10-fold serial dilution of lysates were performed in 0.05% tween 80 in PBS and then were plated on

7H11 Middlebrook agar plates. The CFUs were counted after four weeks of incubation at 37°C and countable values were plotted for every time point.

2.18 Enzyme linked immunosorbent assays for cytokine measurement

For measurement of cytokines released after infection, 1x 10^6 PMN per well in 200 µL assay medium with 2% bovine or human serum were seeded in a cell culture treated 24 well plate in triplicates. The plate was incubated for 30 min at 37 °C, 5% CO_2. The cells were left uninfected or were infected with BCG, *M. bovis* AF2122/97, *M. tb* H37Rv at MOI 10 and further incubated for 20 h. After incubation the supernatants were filtered sterile using spin-X tubes with 0.22 µm pore cellulose acetate membrane. The supernatants were stored at -20°C until the ELISA was performed. The release of TNF-α and IL-8 by bovine and human PMN after infection with the bacteria was measured using different ELISA kits: Bovine TNF-α Duoset, Human TNF-α Duoset, Bovine IL-8/ CXCL-8 Basic, Human IL-8/ CXCL8 Duoset according to the manufacturers' protocols. A standard curve was plotted and the cytokine values were extrapolated from the equation obtained from the standard curve.

2.19 Statistical analysis

The software GraphPad Prism 8 was used for the statistical analysis. Analysis of the data was performed using Two-way ANOVA and multiple comparisons using Bonferroni correction method. Data normalization for some experiments was done by considering the maximum release condition as 100% and comparing the test values with the maximum release for each experiment and plotting the normalized values together from all experiments. For grouped data and paired analysis, one-tailed paired t-test was used. The statistical significance was indicated as ns (not significant); $P>0.05$, *$P\leq0.05$, **$P\leq0.01$, ***$P\leq0.001$, ****$P\leq0.0001$.

Results

3 Establishment of a method for isolation of highly pure bovine neutrophils

3.1 Isolation by density gradient centrifugation results in reduced viability and low yields of bovine neutrophils

To comparatively investigate responses of human and bovine PMN to mycobacteria highly pure cell culture systems are required. A well-established isolation method for human PMN (Brinkmann, Laube et al. 2010) using Histopaque and Percoll was tested. The blood was layered on Histopaque to enrich PBMCs and granulocytes. To further fractionate the granulocytes discontinuous Percoll gradient was used. The protocol allowed the isolation of non-stimulated viable PMN with purity greater than 95%. Therefore, it was chosen for human PMN isolation. The method resulted in a clear separation of leukocytes from human blood after the Histopaque centrifugation step. PMN+RBC layer was collected and layered on top of the discontinuous Percoll gradient (85%, 80%, 75%, 70%, 65%) and the PMN layer was purified (Figure 3.1 A).

However, no clear separation between the leukocytes was observed with the bovine blood with Histopaque (Figure 3.1 B). For the fractionation using the discontinuous Percoll gradient, PMN and the eosinophil layer was selected for further PMN separation (Figure 3.1 B). This indicates that the bovine cells have different buoyancy properties compared to human cells (Figure 3.1 A (left panel) and 3.1 B) and the isolation method resulted in reduced cell numbers for the bovine preparation (Figure 3.1 C). Viability assessed by trypan blue exclusion (Figure 3.1 D) and purity assessed by Kwik Diff-stained cytospin was above 95% for human PMN (Figure 3.1 E) which was comparable to published results (Aga, Katschinski et al. 2002). Purity was estimated only for human PMN and not for bovine PMN due to the reduced viability (Figure 3.1 D) and presence of numerous RBCs which made the cell count difficult. According to the literature, the circulating human PMN are 2-8 x 10^6/mL blood (Kuhns, Priel et al. 2015). The cell numbers/mL blood obtained for human PMN was in range with the values reported in literature. However, this did not hold true for the bovine PMN considering their buoyancy properties and the presence of physiologically less bovine PMN in circulation (approximately 25% in comparison to 50-70% in humans). Therefore, this method could not be used for bovine PMN isolation.

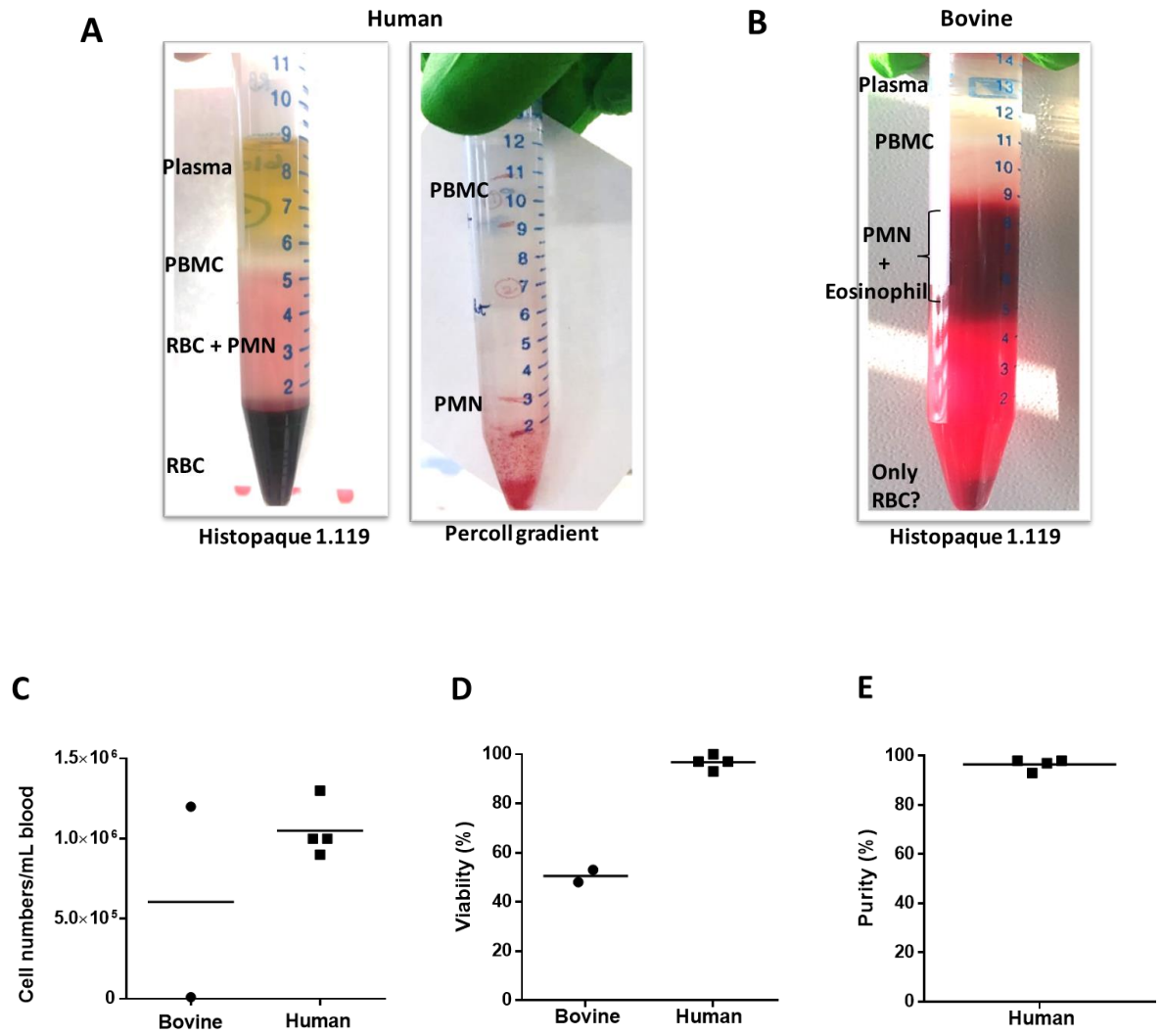

Figure 3.1: Bovine PMN isolation using gradient isolation results in reduced yield and viability. Bovine and human PMN were isolated based on buoyant density using Histopaque 1.119 g/mL and discontinuous Percoll gradient (85%, 80%, 75%, 70%, 65%), n=2 and n=4. **(A)** Representative picture of the isolation outcome with separation layers between the different blood cells in human blood samples after Histopaque centrifugation, followed by Percoll gradient, **(B)** shows no clear separation between the different layers in case of bovine blood after Histopaque centrifugation. **(C)** Cell number/mL blood, **(D)** viability with trypan blue exclusion, and **(E)** purity of isolated PMN, estimated by counting cytospins. Each symbol corresponds to a single donor, shown are mean values from two (bovine), four (human) donors.

Biocoll which has a density of 1.077 g/mL and Histopaque with a density of 1.119 g/mL was used as an alternative gradient isolation method. Histopaque was used to separate PMN and Biocoll was layered on top of Histopaque to facilitate separation of lymphocytes and monocytes (Figure 3.2 A, left panel). The centrifugation resulted in a thick red band of cells at

the interface between Biocoll and Histopaque (PMN + Eosinophils) as represented in Figure 3.2 A (right panel). This layer was chosen for further erylysis and final purification of PMN. The isolation with whole blood (undiluted) and blood diluted 1:4 with PBS resulted in low cell numbers (Figure 3.2 B) and the viability (Figure 3.2 C) was improved when diluted blood was used. Purity varied between 60% and 86% (Figure 3.2 D). Due to extremely low cell recovery and varying outcomes in cell numbers with both whole blood and diluted blood samples and also, given the low purity of the isolated PMN, density gradient centrifugation methods were excluded. The different buoyancy properties of bovine cells resulted in no clear cell separation, thus making the isolation method inaccurate.

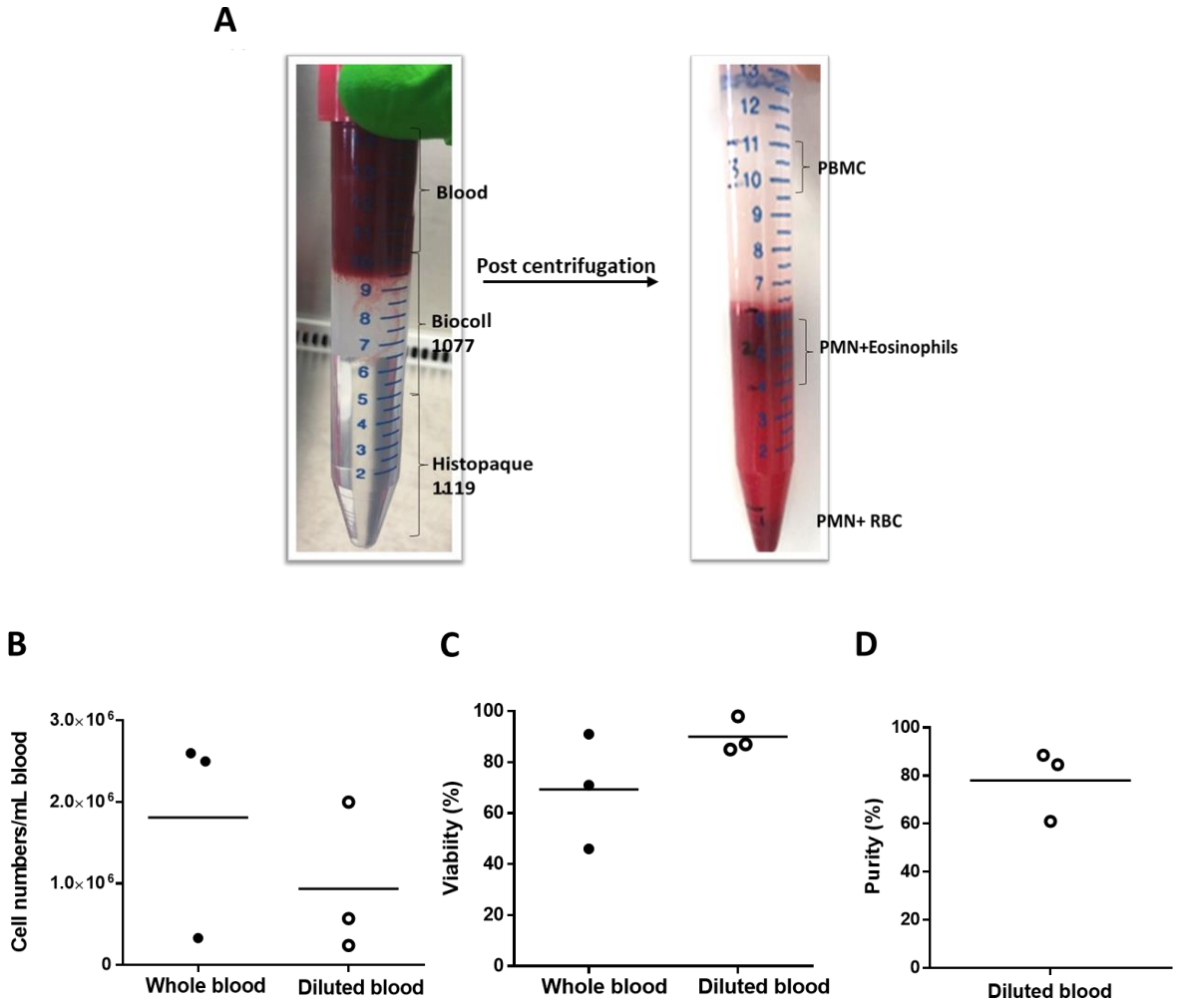

Figure 3.2: Bovine PMN isolation using Biocoll and Histopaque results in low yield and purity. Bovine PMN were isolated based on buoyant density (Biocoll 1.077 g/mL and Histopaque 1.119 g/mL), n=3. **(A)** Representative picture indicating the outcome of the isolation procedure. **(B)** Cell numbers, **(C)** viability by trypan blue exclusion and **(D)** purity of isolated PMN based on analysis of cytospins. Each symbol represents one donor. Shown are mean values.

3.2 Isolation by whole blood centrifugation enriches bovine granulocytes while maintaining mononuclear contaminants

A very crude method for bovine PMN isolation using direct centrifugation of whole blood or dilution of blood 1:4 with PBS before centrifugation was applied. Upper 1/3rd layer of buffy coat was removed and PMN layer was collected for further purification as represented in Figure 3.3 A. The isolation procedure resulted in increased cell numbers (Figure 3.3 C) compared with previously used methods, higher viability (Figure 3.3 D) and purity ranging between 60% and 90% when diluted blood was used (Figure 3.3 E). Nevertheless, the purified cells also contained lymphocytes and eosinophils as contaminants (Figure 3.3 B). The variability of cell number and purity was a considerable limitation of this isolation procedure. Also, the presence of eosinophils in the purified PMN fraction could significantly impact the cytokine measurements as these granulocytes produce cytokines (Driss, Legrand et al. 2009). Therefore, this method had to be dismissed.

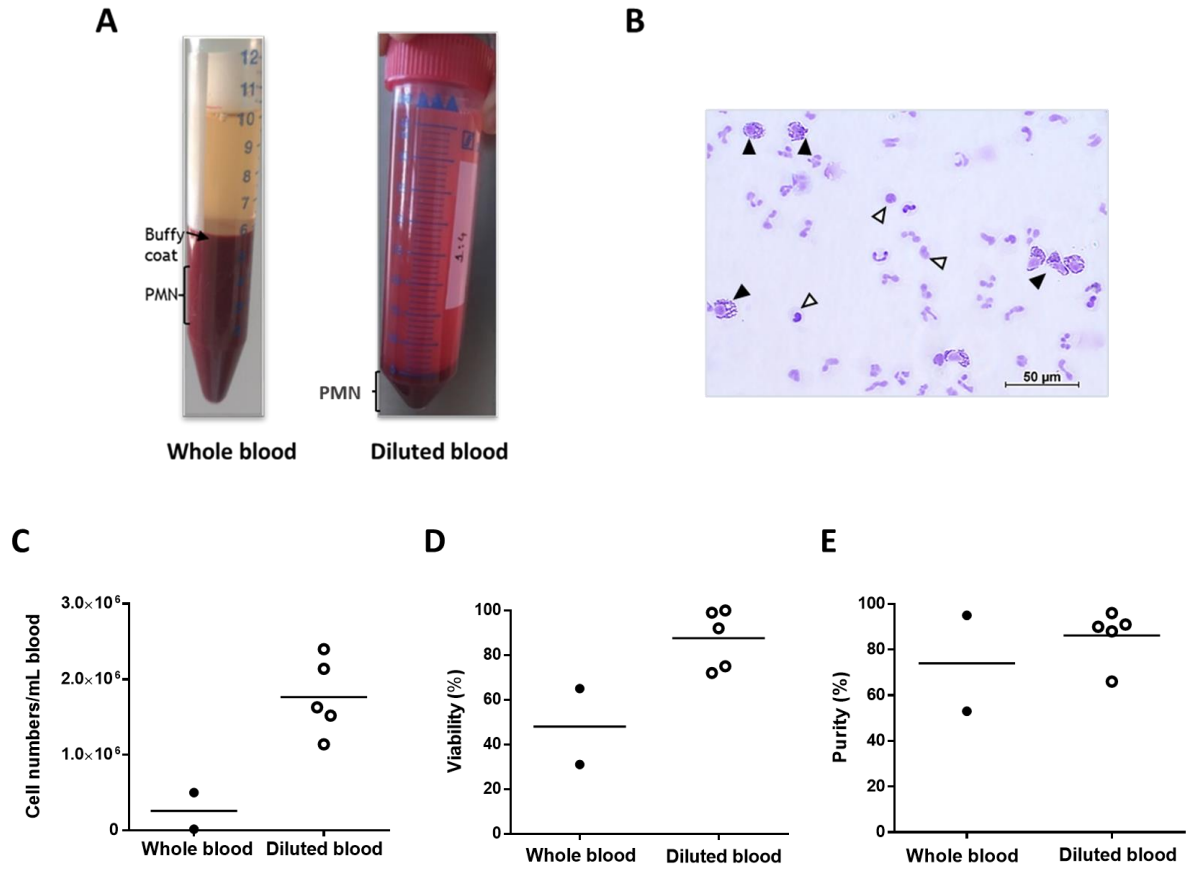

Figure 3.3: Centrifugation of diluted bovine blood results in higher cell number, viability and purity compared to whole blood centrifugation. Bovine PMN were isolated from whole blood by centrifugation only without dilution (n=2), or dilution with PBS with subsequent centrifugation (n=5). **(A)** Representative pictures for the outcome after centrifugation of whole blood and diluted blood are shown. **(B)** Cell purity was evaluated using cytospins, shown is diluted blood sample consisting of PMN and contaminants like eosinophils (black

arrow head) and lymphocytes (white arrow heads). The image was acquired using the Nikon Type 120c microscope with 40X objective. **(C)** Cell numbers, **(D)** viability and **(E)** purity of the isolated PMN was estimated. Each symbol represents one donor. Shown are mean values.

3.3 Isolation of human and bovine neutrophils by fluorescence-activated cell sorting results in reduced yields and contaminants in case of bovine samples

To employ comparable isolation procedures for both species and to improve the purity of the isolated PMN fluorescent labelling followed by cell sorting was established for bovine PMN (Rambault, Borkute et al. 2021). This method was used also for human cells, employing well-established cell markers. For human PMN, the cell surface marker CD15 was used to label circulating PMN (Zhou, Somasundaram et al. 2012). $CD15^+$ cells were sorted using the BD FACS Aria cell sorter (Figure 3.4 A). The sorting resulted in less cell numbers per mL of blood (Figure 3.4 B) compared to the isolation procedure mentioned in 3.1. However, the isolation resulted in 99% pure human PMN (Figure 3.4 F).

Bovine cells were labelled with the granulocyte marker G1, clone CH138A, and MHC II marker, clone CAT82A. $CH138A^+$ cells were selected for the sorting process (Figure 3.4 C). Within the granulocytes, the PMN highly express G1 marker whereas the eosinophils are G1-low or intermediate depending upon the donor (Rambault, Doz-Deblauwe et al. 2021). MHC II marker was used to exclude primarily monocytes. The resulting cell number after sort was low (Figure 3.4 D), sorted cells contained contaminants like eosinophils (indicated with black arrow heads) (Figure 3.4 E) and the cell purity was 94%. The time required for the sorting procedure (>3 h) was critical, considering the short life span of PMN. Therefore, the isolation using sorting was disadvantageous with respect to time, obtained cell numbers for both species and purity for bovine PMN.

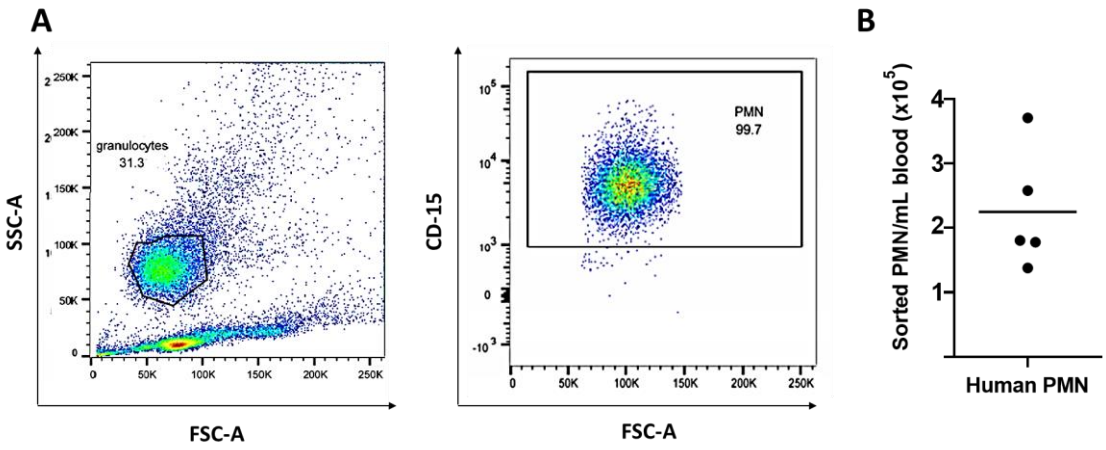

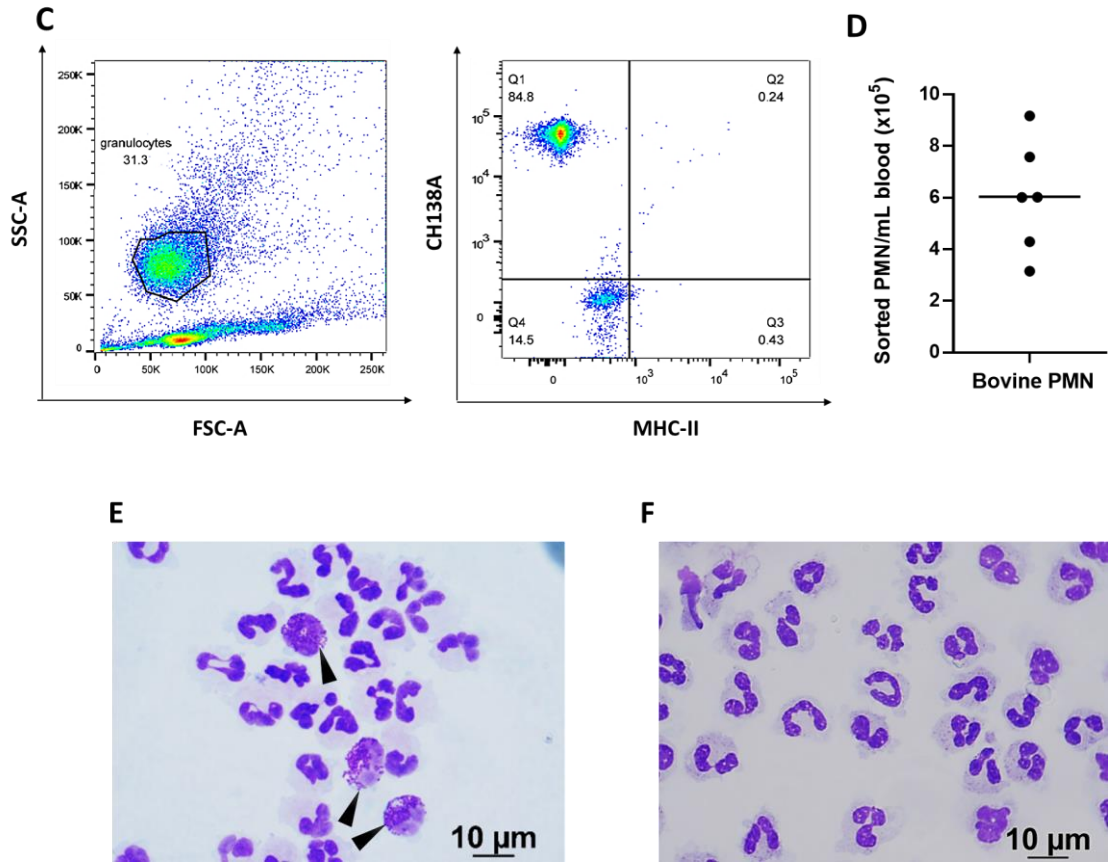

Figure 3.4: FACS sorting of human and bovine PMN results in reduced cell yield. Human cells were labelled with anti-CD15 for sorting **(A)** and PMN numbers recovered post sort were calculated **(B).** Bovine cells were labelled with antibodies against the granulocyte marker CH138A and against MHCII. CH138A^{+} granulocytes were gated and sorted **(C)** and PMN counts per mL blood were calculated **(D)**. The gating strategy illustrated is representative of individual donors. Purity of Kwik Diff-stained cytospins from sorted bovine **(E)** and human PMN **(F)** was evaluated. Images were acquired using the Nikon Type 120c microscope with 100X objective, contaminating eosinophils are indicated by black arrow heads.

3.4 MACSxpress human whole blood neutrophil isolation kit results in high yield of naïve cells

The MACSxpress whole blood PMN isolation kit (Miltenyi) was the fastest isolation procedure to obtain untouched PMN. Cells were purified in 20 min without requirement of any density gradient by using 8 mL of freshly drawn anti-coagulated blood. This procedure resulted in high cell number per mL of blood (Figure 3.5 A) with excellent viability (Figure 3.5 B) and purity reaching 99% (Figure 3.5 B and C). PMN enriched based on various procedures, notably Histopaque and Percoll density gradient isolation method and MACSXpress isolation, were comparatively evaluated for cell activation using immunophenotyping i.e., CD11b and CD62L surface expression. PMN isolated based on buoyancy showed higher expression of CD11b and

downregulation of CD62L compared to MACS PMN (Figure 3.5 D). Therefore, MACS isolation rendered optimal cell number, highest purity and viability and hence, was chosen for all the comparative functional assays between human and bovine PMN.

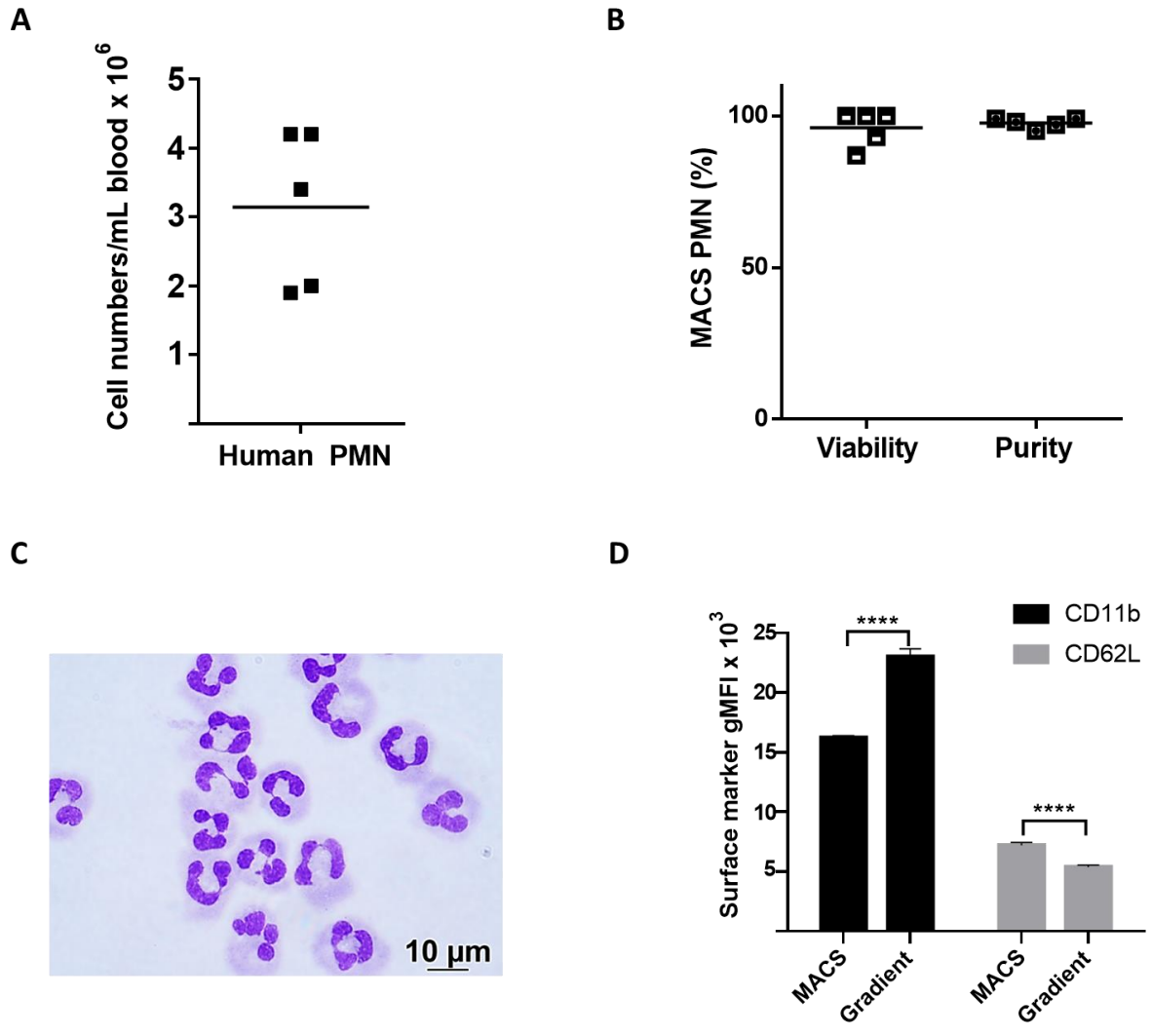

Figure 3.5: Magnetic isolation of human PMN results in higher cell yield, viability and purity. Human PMN were isolated using the MACSxpress PMN isolation kit and the yield **(A)**, viability using trypan blue exclusion and cytospin-based purity **(B)** was estimated (n=5). Each symbol corresponds to a single donor, mean values are indicated by horizontal lines. **(C)** Representative cytospin of Kwik-Diff stained MACS isolated human PMN. Image was aquired using Nikon Type 120c with 100X objective. **(D)** MACS and gradient isolated human PMN were stained with antibodies against CD11b and CD62L to determine cell activation after isolation. Data in **(D)** is representative of one independent experiment performed out of two, each with independent donors **(D)**. The statistical analysis was done using Two-way ANOVA with Bonferroni correction. ****$P \leq 0.0001$.

3.5 MACS cell separation results in high yield and purity of bovine neutrophils

Since no commercial kits are available for the isolation of bovine PMN, a new method based on cell enrichment using antibodies coupled to magnetic-beads was developed (Rambault, Borkute et al. 2021). Bovine blood was collected from jugular vein of healthy cows in 9 mL vacutainer tubes containing 1.6 mg EDTA/mL blood. The vacutainer tubes were centrifuged at 1,000 x g for 15 min with brakes off. After centrifugation, plasma and top 1/3 layer of cells was removed. The lower 2/3 pellet was collected and erylysis was performed by transferring the fractions to 50 mL falcon tubes and adding 9x the volume of erylysis buffer. The tubes were slowly inversed until the solution was clear (approximately 1 min) and the osmolarity was reconstituted using 10x sterile PBS. The tubes were filled with 1x PBS and centrifuged at 300 x g for 10 min at RT. If the RBC lysis was not successful, the erylysis step was repeated. The supernatant was removed and the pellet was washed once with 1x PBS and centrifuged at 300 x g for 5 min to remove any remaining erylysis buffer. The resulting pellet was then resuspended in 1,000 µL blocking solution and leukocytes were counted on Neubauer cell counting chamber using trypan blue solution as a sample diluent. Cells were adjusted to 2 x 10^7 /mL in PBS transferred to a FACS tube and centrifuged at 450 x g for 3 min at RT. The resulting pellet was resuspended in 100 µL P-BSA, stained with the primary anti-bovine MHC II antibody to deplete primarily mononuclear phagocytes and also eosinophils, clone CAT82A at a dilution of 1:2,000 and incubated for 10 min on ice. After incubation 1,000 µL P-BSA was added and the tube was centrifuged at 450 x g for 3 min at RT. Upon centrifugation, cell pellet was re-suspended in 100 µL P-BSA and 10 µL anti-mouse IgG1 magnetic particles were added, following a general recommendation of 10 to 50 µL/ 10^7 cells. The tube was incubated for 15 min on ice, the buffer volume was adjusted to 2 mL and placed in BD IMag cell separation magnet for 10 min. Non-adherent cells were carefully aspirated and were transferred into a new FACS tube (negative selection) which was placed in the magnetic field for 4 min to get rid of any remaining magnetically labelled cells. This step was repeated twice and subsequently the tube was centrifuged at 450 x g for 3 min at RT. The pellet was resuspended in primary anti-bovine G1 antibody, clone CH138A at a dilution of 1:2,000 in 100 µL P-BSA and incubated for 10 min on ice. Afterwards, 1,000 µL P-BSA was added and the tube was centrifuged at 450 x g for 3 min at RT, supernatant was discarded, the pellet was resuspended in anti-mouse IgM biotin antibody at a dilution of 1:500 and incubated on ice for 10 min. After incubation 10 µL streptavidin magnetic particles were added. The tube was further incubated for 15 min on ice, the final volume was adjusted to 2 mL with P-BSA and tube was placed in the magnet for 10 min. The supernatant was carefully discarded (positive selection). Magnetically labelled cells were then washed by adding 1,000 µL P-BSA and left in the magnet for additional 4 min. This step was repeated at least twice for both the pellet and the supernatant fraction. In the last step magnetically labelled cells were resuspended in 1,000 µL P-BSA and the yield was estimated by counting the cells on Neubauer chamber.

Due to expression of the granulocyte G1 marker (stained by clone CH138A) on myeloid cells other than PMN, namely eosinophils, the cells were labelled first with MHC II marker and

eosinophils were excluded at the first magnetic isolation step. To selectively label the PMN, CH138A granulocyte marker was used in the later step. The isolation procedure resulted in a higher cell number (Figure 3.6 A) compared to all the previously applied methods and the cell fraction in the end was highly enriched for PMN (Figure 3.6 B and C). By using this method, the cell yield was improved and the procedure was robust. Therefore, this isolation procedure was chosen for the further comparative assays.

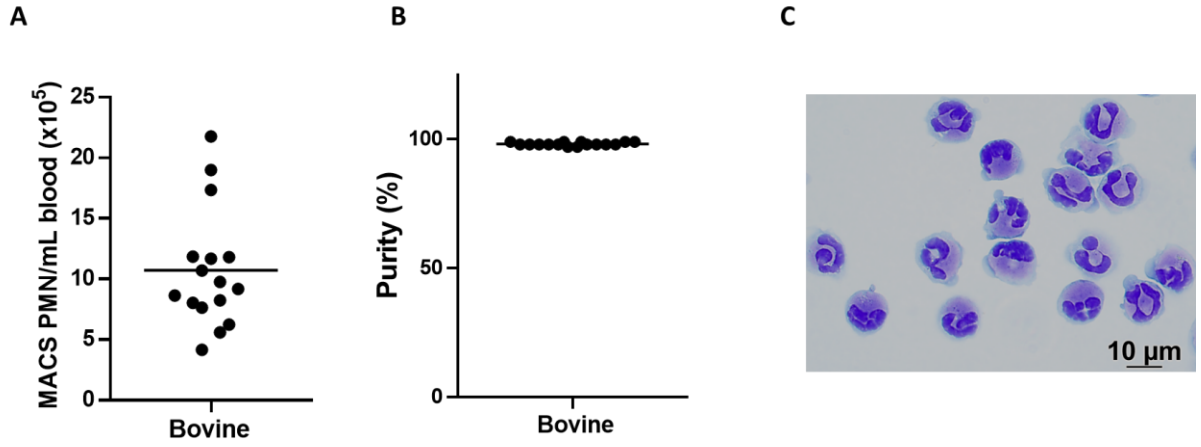

Figure 3.6: Magnetic enrichment of bovine PMN results in high yield and purity. PMN were isolated using magnetic labeling and the yield **(A)** and purity which was evaluated by enumerating PMN and evaluation of the cytospin preparations **(B)**. Each symbol represents a donor, mean values are indicated by horizontal lines. **(C)** Representative picture of Kwik Diff-stained MACS-isolated PMN. The image was acquired using the Nikon Type 120c microscope with 100X objective.

3.5.1 Morphology and ultrastructure of purified neutrophils

TEM of the isolated bovine and human PMN indicated presence of lobulated nucleus (N) and various granules clearly visible in the cytoplasm (Figure 3.7 A and B). The PMN from the two species differ morphologically as reported earlier. Unlike human PMN, the bovine PMN in addition to primary, secondary and tertiary granules also contain numerous peroxidase negative granules in the cytoplasm. However, in this study the differentiation of these granules was not carried out. Quantification of mitochondria was done in order to understand whether bovine and human PMN are metabolically different and considering that mitochondria also regulate viability of these phagocytes. A total of 100 PMN were evaluated from each species and the total number of mitochondria in each cell was counted (Figure 3.7 C). Approximately 56% of human PMN contained between 1 and 4 mitochondria per cell and approximately 30% of bovine PMN contain more than 9 mitochondria per cell (Figure 3.7 C). These findings suggest increased mitochondrial ATP production rate in bovine PMN due to the presence of higher number of mitochondria per cell.

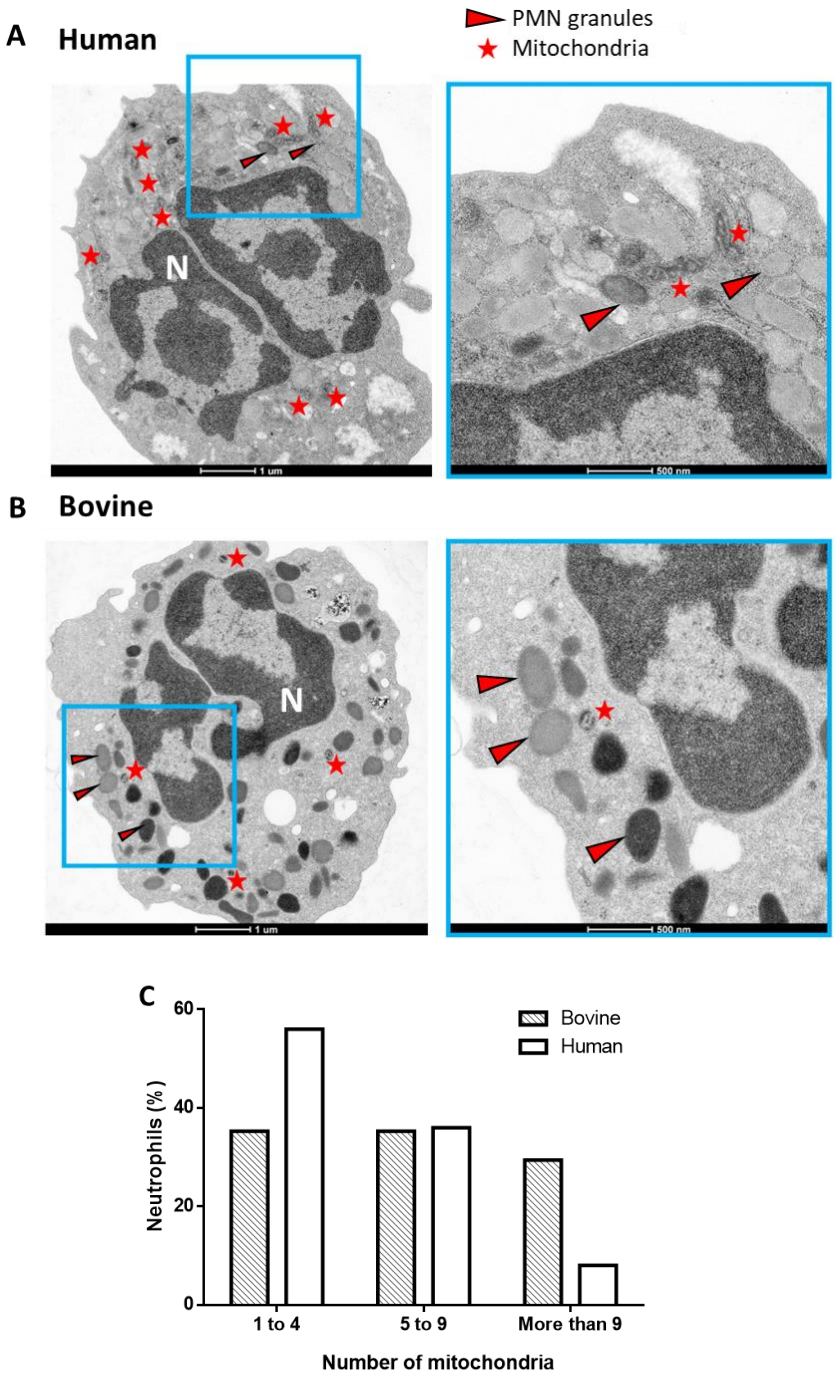

Figure 3.7: PMN ultrastructure. Freshly isolated human **(A)** and bovine PMN **(B)** were analyzed by TEM. PMN show characteristic segmented nucleus (N) and numerous cytoplasmic granules were visible **(B)** particularly in bovine PMN. Quantification of mitochondria per PMN was estimated in a total of 100 cells from each species **(C).** The images were acquired using Tecnai-Spirit TEM at 80 kiloVolt. Scale bar 1 µm; magnified image scale bar 500 nm. The experiment was performed once. Dr. Kati Franzke, coordinator of electron microscopy facility of the FLI, Insel Riems, processed samples and kindly provided the TEM images.

3.5.2 Extended viability of MACS-purified cells

The viability of freshly isolated bovine and human PMN was determined using annexin V and PI staining as a marker for apoptosis and necrosis respectively. The PMN were cultured in assay medium for 0 h, 2 h, 20 h, 27 h and after each time point cells were washed and stained determine EA, LA, necrotic and live cells. At T=0, more than 90% of the PMN were alive in both species. With the incubation time, a gradual increase in apoptotic cells was observed as depicted in Figure 3.8 A. PMN viability in both species was comparable and interestingly the PMN survived longer than 20 h in the normal assay medium with almost 40% of PMN still alive at T=27 h (Figure 3.8 B and C). The findings for human PMN were comparable to published results (Zyntek, Schmitz et al. 2020) where at 3 h over 92% PMN were viable after isolation. Considering the recent data challenging the short lifespan of PMN in circulation and demonstrating a turnover of 5.4 days (and not 7-12 h *in vivo*) (Pillay, den Braber et al. 2010), the results suggest that MACS PMN isolation retains the viability of the cells for a longer time.

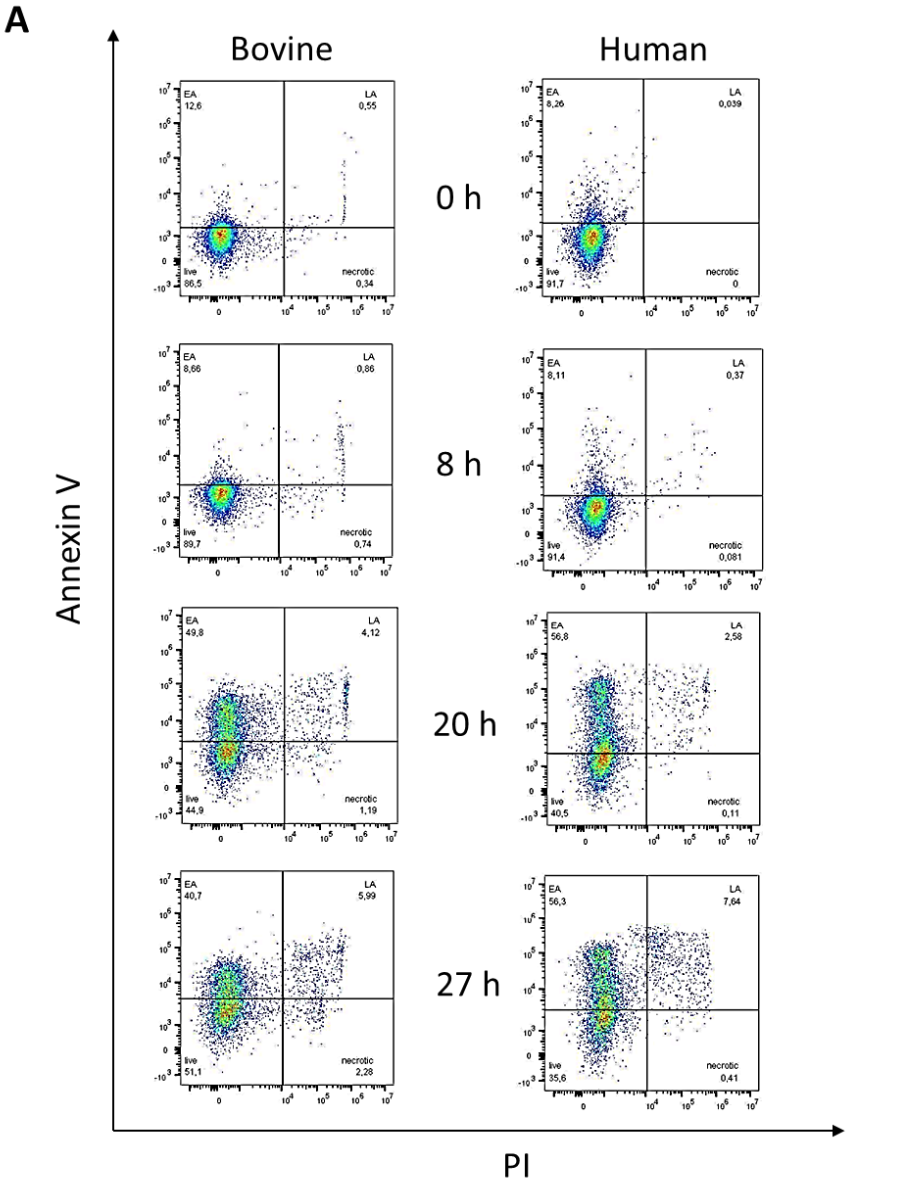
A
Bovine
Human
0 h
8 h
20 h
27 h
Annexin V
PI
EA
LA
live
necrotic

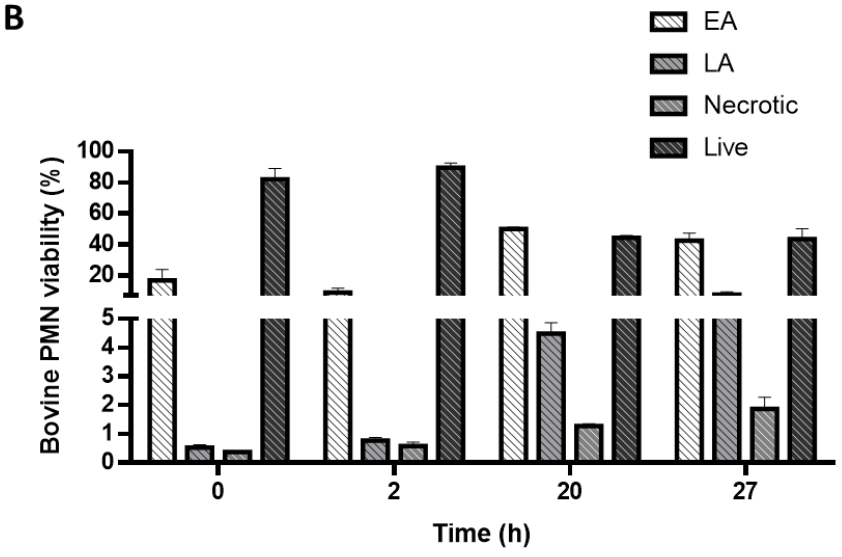
B
EA
LA
Necrotic
Live
Bovine PMN viability (%)
Time (h)

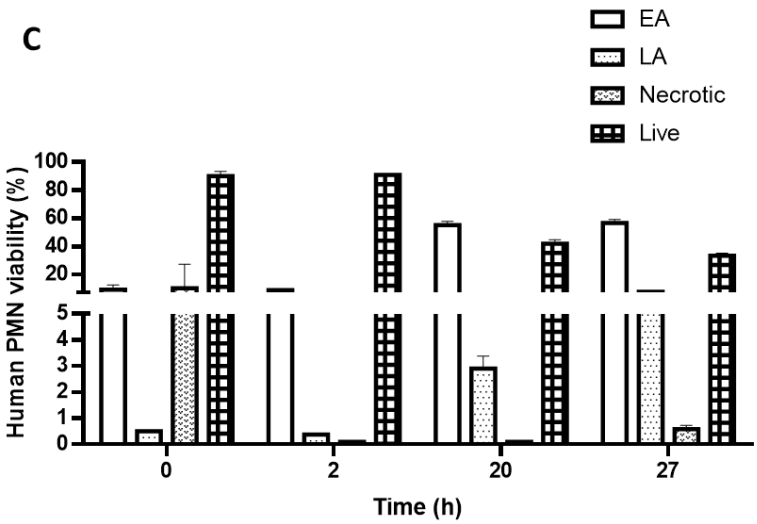

Figure 3.8: Bovine and human PMN show extended viability after isolation. Isolated human and bovine PMN were stained with annexin V and PI to determine their viability. FACS analysis of PMN after staining depicts viable cells negative for annexin V and PI (lower left quadrant). Annexin V^+ cells are indicated as EA (top left quadrant), Annexin V^+ PI^+ PMN are indicated as LA (top right quadrant) and PI^+ as necrotic (bottom right quadrant), **(A)** after isolation T= 0 h, T=2 h, T=20 h, T=27 h for bovine PMN (left column) and human PMN (right column). **(B** and **C)** show cell viability of bovine and human PMN. Bar graphs depict mean +/- SD of triplicate measurements from one experiment out of two, each with individual donors.

3.5.3 Analogous glucose uptake by purified cells

Glucose uptake by cells is a dynamic state and to some extent is a reflection of the cells' metabolic condition. Estimation of 2NBDG, an analogue of glucose was used to monitor the glucose uptake by PMN (Yamamoto, Ueda-Wakagi et al. 2015). Bovine PMN internalized more 2NBDG compared to human counterparts (Figure 3.9 A). The uptake over time (10 min to 30 min) was calculated as fold change indicating that there was a two-fold increase in 2NBDG uptake by bovine PMN compared to a fold change of approximately 1.5 in human cells (Figure 3.9 B). This suggests that due to increased metabolic needs a higher amount of 2NBDG is required by bovine PMN after glucose starvation.

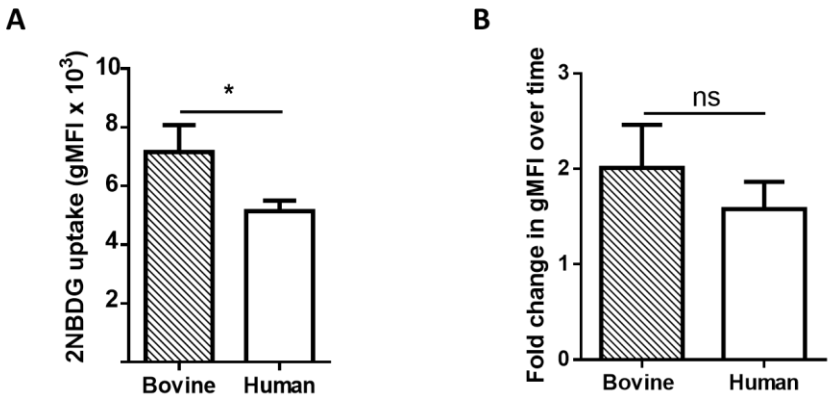

Figure 3.9: Bovine PMN take up higher amounts of 2NBDG. Isolated bovine and human PMN were starved in medium without glucose for 10 min and 30 min. At 10 min or 30 min, 2NBDG was added for next 30 min and, cells were acquired on a flow cytometer. **(A)** gMFI values of 2NBDG taken up by bovine and human PMN at 30 min. **(B)** Fold change in 2NBDG uptake at 30 min compared to 10 min, pooled data from n=2. The data in **(A)** is a representative of one independent experiment performed out of three, each with different donors, shown are mean +/- SD of triplicate measurements. The data was analyzed using unpaired Two-tailed t-test, *$P \leq 0.05$, ns; $P > 0.05$.

3.5.4 Activation patterns of neutrophils in whole blood and subsequent purification

To elucidate differences in expression levels of PMN activation markers in whole blood and purified PMN and to evaluate whether the bovine PMN isolation procedure results in activation of the PMN, samples were stained with antibodies cross-reacting with bovine CD11b and CD62L (Figure 3.10 A and B). The upregulation of CD11b and the downregulation of CD62L in purified PMN compared to whole blood PMN would suggest an activated state of the purified cells. An increase in the expression of CD11b in purified PMN was found. However, no downregulation of the degranulation marker CD62L was observed, but instead an increase in expression. This indicates that although sorted PMN seemed to be activated they did not degranulate (Figure 3.10 C, D and E), suggesting that the $CD62L^{high}$ population in purified PMN could be a subset with segmented nuclei which are found in homeostatic condition also in humans (van Grinsven, Textor et al. 2019) or the isolation method resulted in upregulation of CD62L (Figure 3.10 E). This needs further investigation.

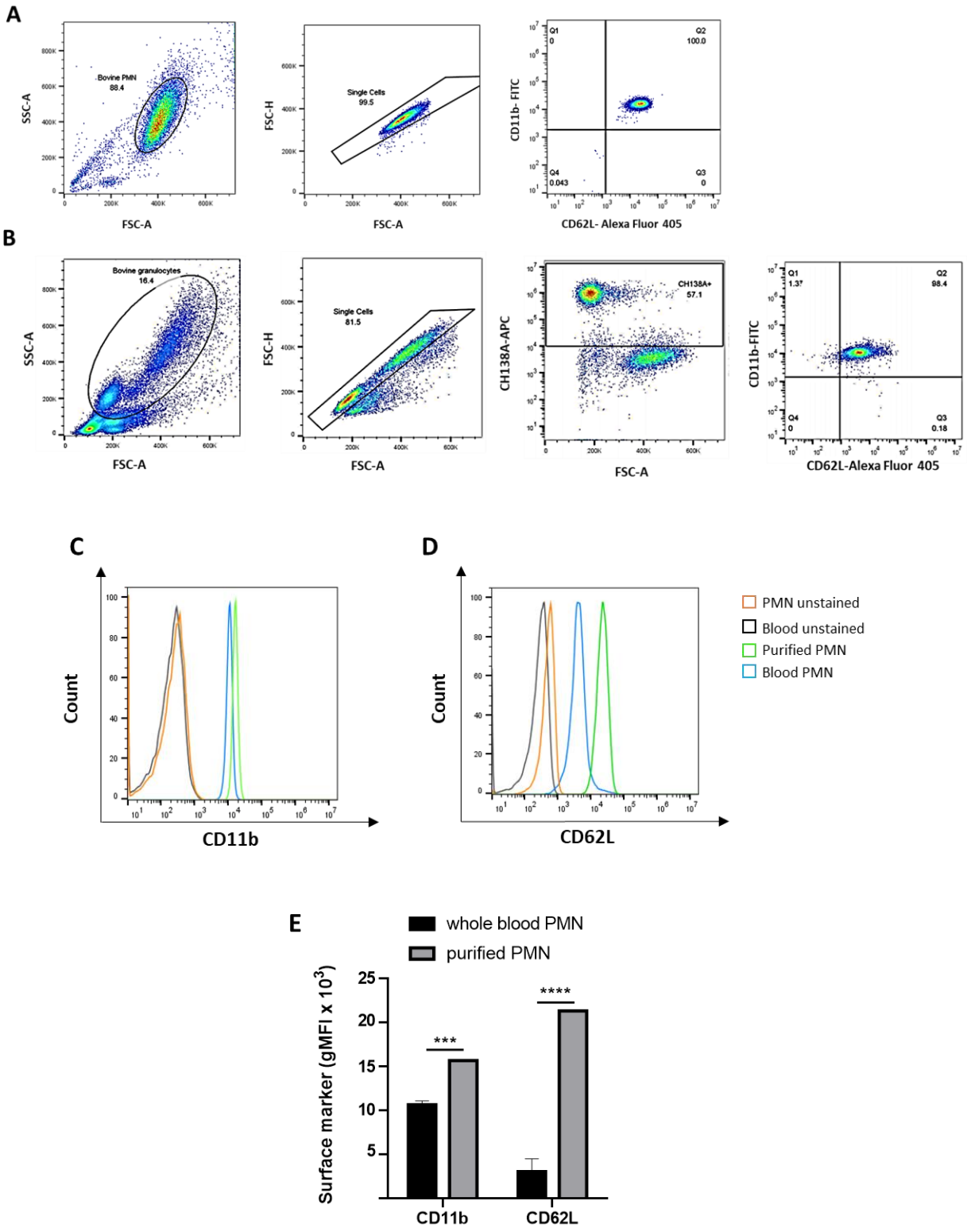

Figure 3.10**:** Purified bovine PMN are not activated compared to whole blood PMN. Purified bovine PMN were labelled with CD11b-FITC and CD62L-Alexa Fluor 405 antibodies. **(A)** Gating strategy displaying FSC and SSC of purified bovine PMN expressing CD11b^{high} and CD62L^{high}. **(B)** Bovine whole blood cells were stained for the granulocyte marker CH138A-APC, CD11b-FITC and CD62L-Alexa Flour 405 and the CH138A-APC^{+} cells expressing CD11b^{high} and

$CD62L^{high}$ are represented. Gating strategy is representative of one individual donor. Representative overlay histograms displaying expression of **(C)** CD11b and **(D)** CD62L are shown. **(E)** gMFI values for the expression of CD11b and CD62L in whole blood and purified PMN. The data represents mean +/- SD of triplicate measurements from one experiment performed out of three, each with independent donors. The statistical analysis was done using Two-way ANOVA with Bonferroni correction ***$P \leq 0.001$, ****$P \leq 0.0001$.

4 Responses of bovine and human neutrophils to *M. bovis* BCG

Human and bovine PMN were isolated from peripheral blood of healthy human and cattle donor resulting in 98-99% pure PMN in both species. To comparatively investigate the ability of these cells to interact with mycobacteria and whether they differentially take up BCG GFP or Ops BCG, or degranulate, release cytokines or produce bactericidal molecules, PMN from both species were left uninfected (naïve) or were infected with reporter bacteria. The phagocytic ability was evaluated as this cell function impacts on downstream functional assays. Furthermore, the receptors (CD11b, dectin-1) and entry pathways (cholesterol, actin cytoskeleton) utilized by PMN to internalize bacteria were investigated. Finally, the ability of PMN from both the species to produce ROS, release MPO, cytokines as well as their capacity to kill mycobacteria was compared.

4.1 Heightened phagocytosis by human neutrophils

Upon incubation with BCG, the frequencies of human PMN which phagocytosed BCG was significantly higher compared to bovine cells. This was observed at both time points, i.e. for early phagocytosis at 10 min and after 30 min incubation (Figure 4.1 A and B). Moreover, mean phagocytosis (reflected by gMFI and indicating amounts of bacteria per cell) was significantly higher for human PMN (Figure 4.1 C). When serum opsonized bacteria were used, there was an enhancement in phagocytosis in both human and bovine PMN. Human PMN more avidly internalized Ops bacteria (Figure 4.1 D, E and F), demonstrating the importance of serum factors for efficacious BCG uptake. Altogether, these findings indicate that BCG is more efficiently engulfed by human PMN and that infection with Ops bacteria increases the uptake in both species suggesting involvement of complement factors in internalization of Ops BCG.

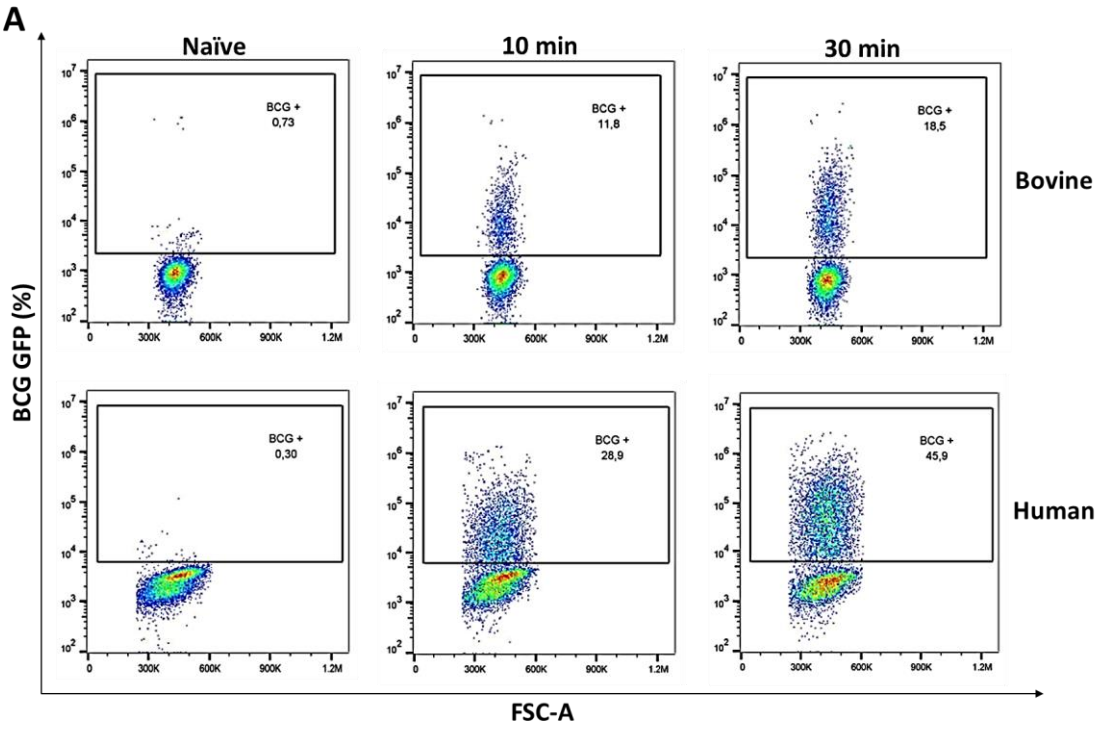
A
Naïve
10 min
30 min
BCG +
0,73
BCG +
11,8
BCG +
18,5
Bovine
BCG +
0,30
BCG +
28,9
BCG +
45,9
Human
BCG GFP (%)
FSC-A

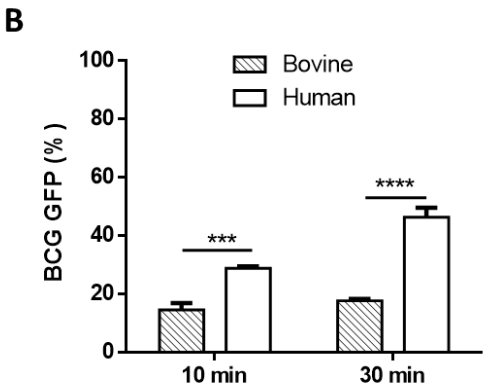
B
Bovine
Human
BCG GFP (%)
***
****
10 min
30 min

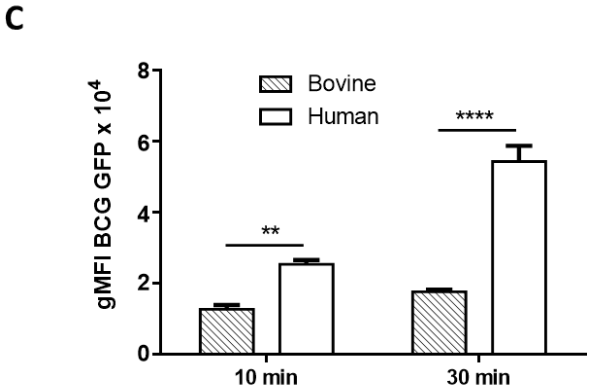
C
Bovine
Human
gMFI BCG GFP x 10^4
**
****
10 min
30 min

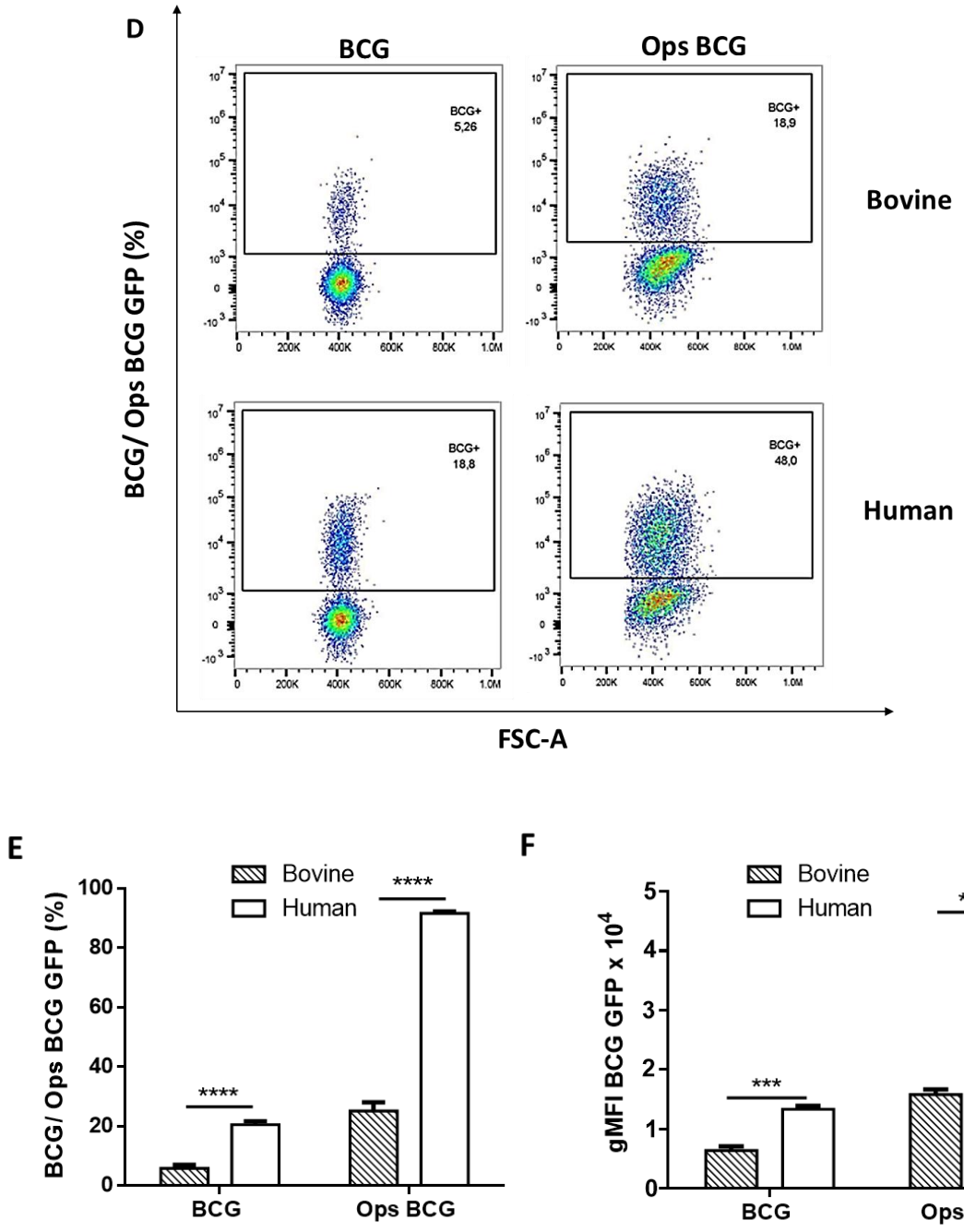

Figure 4.1: Differential phagocytic rates of BCG in bovine and human PMN. Magnetic isolated bovine and human PMN were infected with BCG GFP at MOI 10 for 10min and 30 min. **(A)** FACS plots of naïve and infected PMN, **(B and C)** show percent phagocytosis and gMFI values, respectively. Data is representative of one experiment performed in triplicates out of six experiments, each with independent donors. Data shows mean+/- SD of triplicate values. FACS plots for the comparison of BCG and Ops BCG after 30 min incubation are shown in **(D)** with **(E)** percent phagocytosis and **(F)** gMFI values. Data in **(D, E, F)** is a representative of one independent experiment performed in triplicates, out of four experiments, each with independent donors. The analysis of the data was done using Two-way ANOVA with Bonferroni correction ***P*≤0.01, ****P*≤0.001, *****P*≤0.0001.

As bovine PMN phagocytosed BCG less efficiently compared to human PMN, fluorescein conjugated *E. coli* bioparticles were used and the uptake by PMN from the two species was compared. This elucidated whether the differences observed were specific to BCG. Infection with *E. coli* at MOI 1 for 10 min and 30 min (Figure 4.2 A) resulted in a similar pattern as that observed with the BCG infection. Human PMN showed higher phagocytic capacity for *E. coli* bioparticles (Figure 4.2 B and C). This suggests that the low responsiveness of bovine PMN compared to human PMN is a common phenomenon in context of bacterial phagocytosis.

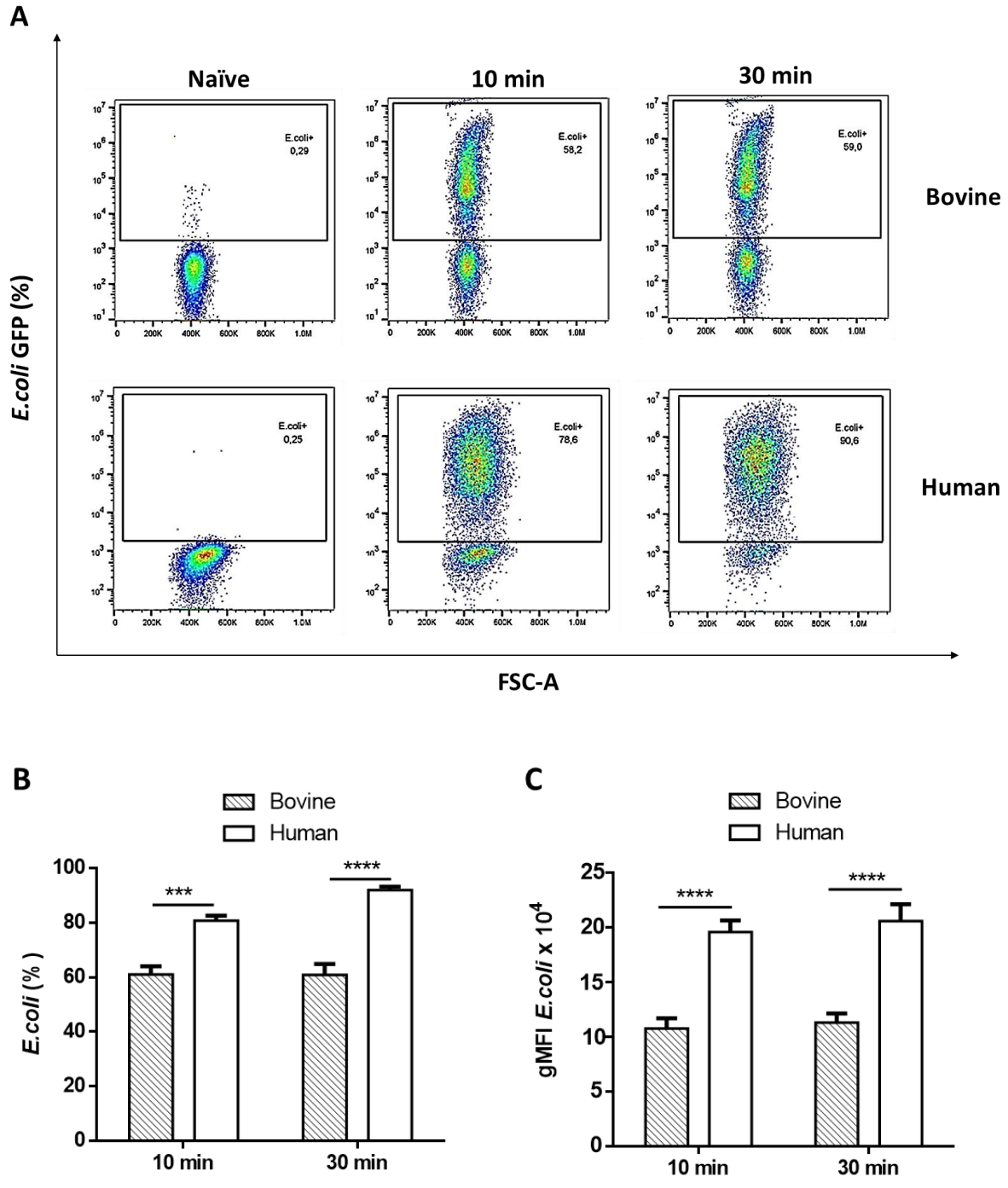

Figure 4.2: Higher phagocytic capacity of *E. coli* by human PMN. Human and bovine PMN were fed with fluorescein conjugated *E. coli* at MOI 1 for 10 min and 30 min. FACS plots depicting naïve and *E. coli* treated PMN are shown in **(A)**, **(B and C)** present percent phagocytosis and gMFI of phagocytosed *E. coli* particles. The data is a representative of one experiment performed in triplicates, out of three with independent donors for each specie. The data obtained was analyzed using Two-way ANOVA with Bonferroni correction. Data are shown as mean +/- SD of triplicate values, ***$P \leq 0.001$, ****$P \leq 0.0001$.

In a parallel approach wide field microscopy was used to comparatively evaluate phagocytosis. PMN were infected with BCG GFP or Ops BCG GFP for 30 min followed by processing and analysis using a high-content microscope (Figure 4.3 A). The percentage of infected cells and the spot count per cell were determined (Figure 4.3 B and C). The microscopy results were comparable to the FACS data and emphasized that human PMN were endowed with higher phagocytic capacity for both BCG and Ops BCG (Figure 4.1). Also, opsonization of the bacteria enhanced the uptake in both species and this effect was also observed with flow cytometry confirming the robustness of the findings.

In summary, PMN engulf BCG in the conditions tested herein and human PMN, in contrast to bovine PMN, are highly phagocytic.

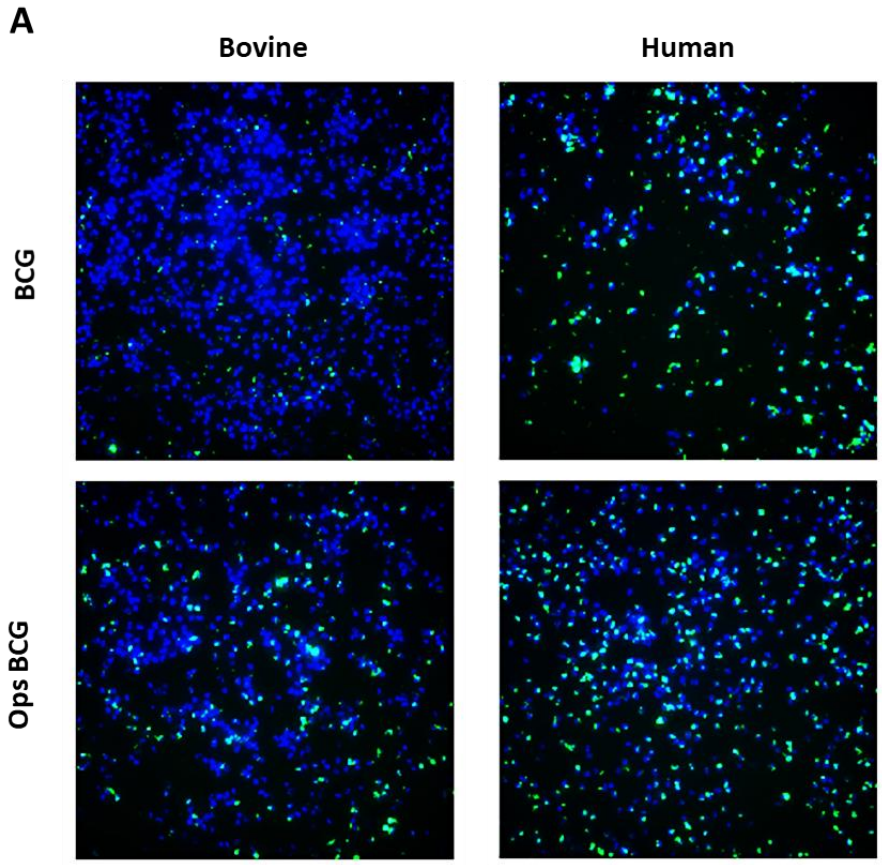

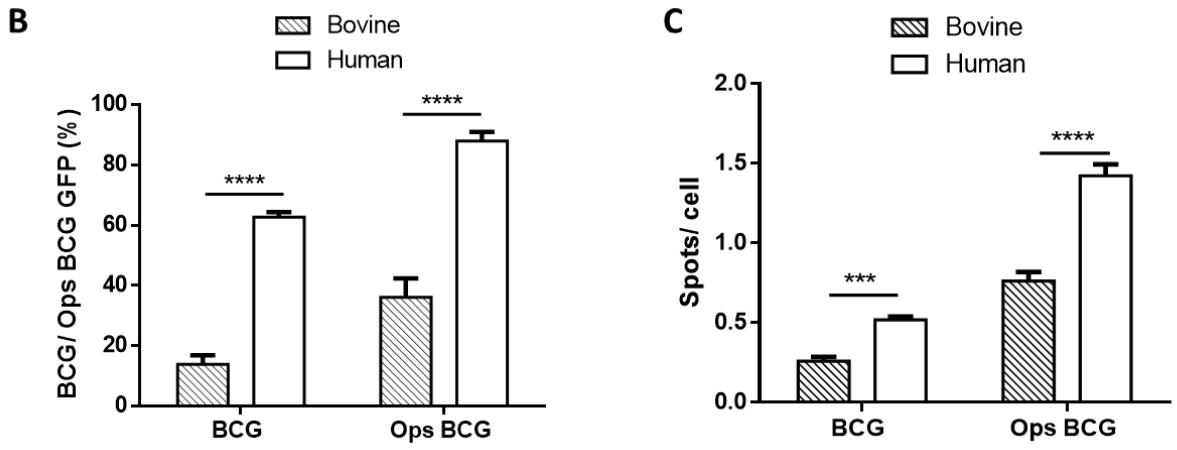

Figure 4.3: Wide field microscopy unveils higher uptake of BCG by human PMN compared to bovine cells. PMN from both the species were infected with BCG GFP or Ops BCG GFP at MOI 10 for 30 min. After infection, the bacteria (Green) were removed and the cells were fixed followed by staining with the nuclear dye DAPI (Blue) **(A)**. Images were obtained with a 20x objective using a high-content microscope. Quantification of the percent phagocytosis **(B)** was done by counting 50,000 cells and a total of 121 fields per well, and **(C)** bacterial fluorescence as spots per cell, a surrogate for mean phagocytosis, was determined. Images and bar graphs are representative of one experiment performed in triplicates, out of three, each with independent donors. Data was analyzed using Two-way ANOVA with Bonferroni correction. Data shown as mean +/- SD of triplicate values; ***$P \leq 0.001$, ****$P \leq 0.0001$.

4.2 Pathways relevant for phagocytosis of mycobacteria for entry into neutrophils

To determine the possible path(s) of mycobacterial entry into the PMN, the CD11b/CD18 receptor which is known to be involved in the non-opsonic and opsonic uptake of mycobacteria was targeted (Peyron, Bordier et al. 2000, Miralda, Klaes et al. 2020). CD11b was blocked by pre-incubating the cells with antibodies cross-reactive with epitopes of each species. No reduction in uptake of BCG was observed for both human and bovine PMN after CD11b blocking as the percentages of phagocytosis were similar to BCG-infected untreated cells. In human PMN a significant increase in BCG uptake after CD11b block as well as upon delivery of the isotype controls was observed (Figure 4.4 A). The gMFI values were unchanged upon CD11b blocking (Figure 4.4 B). Furthermore, when the PMN were infected with Ops BCG and/ or blocked with CD11b, no reduction in the percent phagocytosis was observed for bovine PMN (Figure 4.4 C). However, gMFI values for Ops BCG were significantly reduced following CD11b blocking solely in human PMN (Figure 4.4 D).

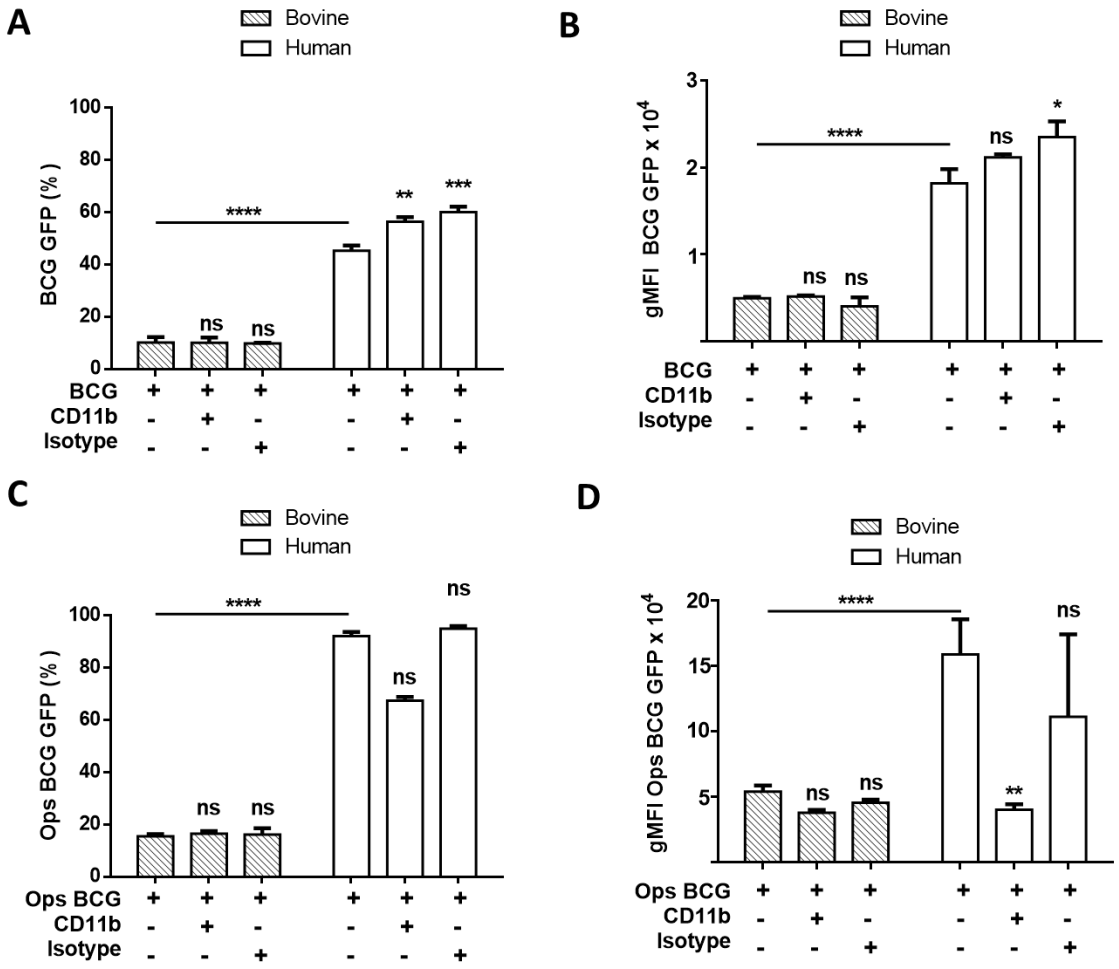

Figure 4.4: Blocking CD11b reduces phagocytosis of Ops BCG solely in human PMN. Bovine and human PMN were pre-treated with anti-CD11b antibody (clone CC126 10 µg/mL + clone CC104 2 µg/mL for bovine cells, clone M1/70 10 µg/mL + clone ICFR44 2 µg/mL for human cells), mouse IgG2b (for bovine PMN) and mouse IgG1 isotype control (for human PMN) for 30 min and subsequently infected with BCG GFP MOI 30 for 30 min. The percent phagocytosis **(A, C)** for BCG and Ops BCG, as well as mean phagocytosis, which was evaluated by gMFI **(B, D)**, were calculated for all conditions. The data is representative of one independent experiment performed in triplicates, out of three experiments each with independent donors. The analysis was done using Two-way ANOVA with Bonferroni correction. Data shows mean +/- SD of triplicate values; ns $P>0.05$, *$P\leq0.05$ **$P\leq0.01$, ***$P\leq0.001$, ****$P\leq0.0001$.

To investigate additional phagocytic pathways used by PMN to internalize non-opsonized mycobacteria various chemical inhibitors were utilized. MβCD depletes cholesterol from the cell membrane thereby potentially impeding on phagocytosis of mycobacteria. Human PMN and MΦ use cholesterol enriched lipid rafts for uptake of mycobacteria (Peyron, Bordier et al. 2000, Astarie-Dequeker, Le Guyader et al. 2009). NADG binds and blocks the C-domain of the CR3 (Peyron, Bordier et al. 2000). Laminarin, a dectin-1 agonist was used to investigate

whether dectin-1 is involved in uptake and cytochalasin D to depolymerize the actin cytoskeleton, which is required for membrane remodeling and internalization of particulate material. Concentrations which did not alter PMN viability were selected in pilot studies. Pre-treating the cells with these reagents for 30 min followed by 30 min infection resulted in a significant reduction in uptake of BCG by human PMN. More precisely, incubation with MβCD, NADG and cytochalasin D, but not with laminarin resulted in decreased internalization of mycobacteria (Figure 4.5 A and B). There was no significant reduction in BCG uptake by bovine PMN with any of these reagents (Figure 4.5 A and B).

Altogether, these results suggest the importance of the cholesterol in interactions of human PMN with BCG. Membrane cholesterol is important for mycobacterial entry in human PMN unlike bovine PMN. Reduction in BCG uptake by human PMN following pre-treatment with NADG signifies BCG uptake via the C-domain of CR3 in these cells. Also, requirement of an intact cytoskeleton for phagocytosis by human PMN could be confirmed. However, the reason for the differential effect of the above-mentioned reagents for bovine PMN still remains to be elucidated.

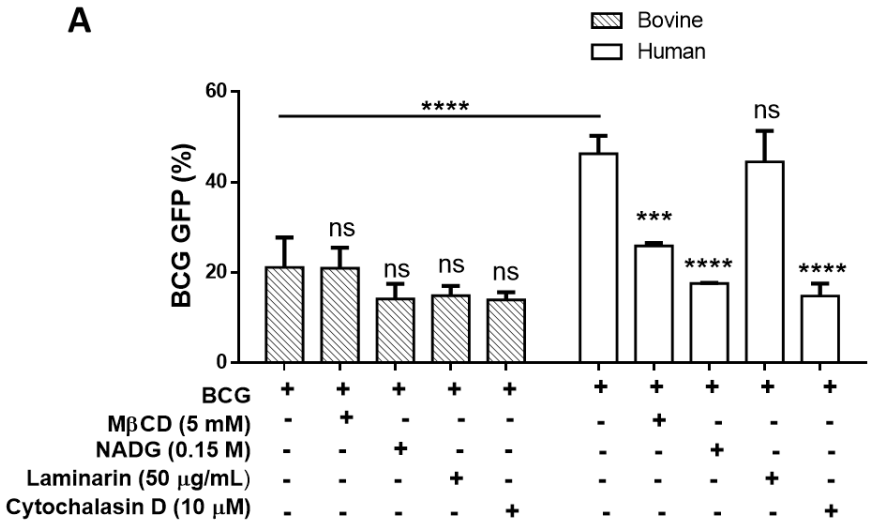

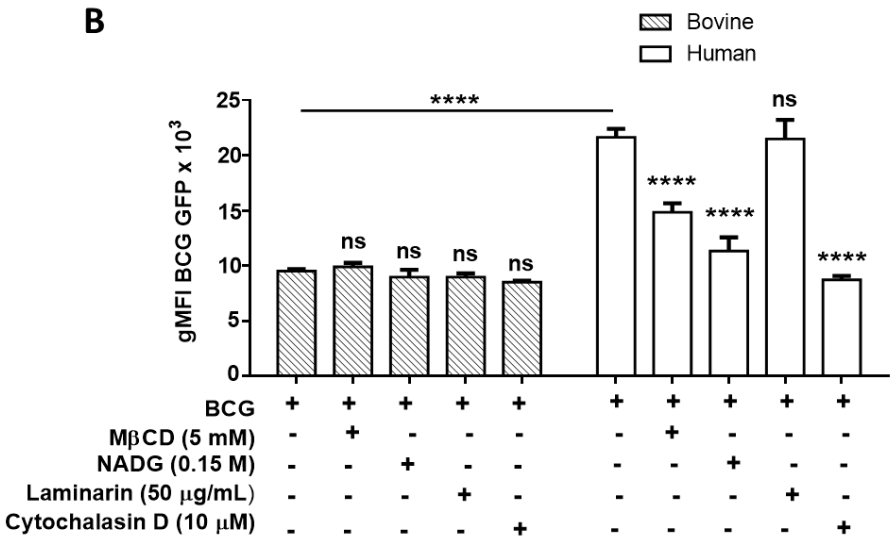

Figure 4.5: Human and bovine PMN differently restrict phagocytosis of BCG upon pre-treatment with chemical inhibitors. Bovine and human PMN were pre-treated with MβCD (5 mM), NADG (0.15 M), Laminarin (50 μg/mL), Cytochalasin D (10 μM) for 30 min at 37° C, 5% CO_2 followed by infection with BCG GFP MOI 30. Percent phagocytosis **(A)** and mean phagocytosis evaluated using gMFI **(B)** were obtained for all tested conditions. Data is representative of one experiment performed in triplicates, out of three, each with independent donors. Data shows mean +/- SD of triplicate values. Data obtained was analyzed using Two-way ANOVA with Bonferroni correction, ns; $P>0.05$, ***$P\leq0.001$ ****$P\leq0.0001$.

To investigate whether differences observed in BCG uptake after treatment with chemical inhibitors were unique to mycobacteria, *E. coli* bioparticles, a G- bacteria with different cell wall composition, were used. Infection with *E. coli* bioparticles resulted in a significant reduction in *E. coli* internalization after treatment with cytochalasin D (10 μM and 20 μM) and NADG (0.1 M), yet phagocytic rates remained unchanged for BCG infected cells. MβCD and laminarin did not affect BCG and *E. coli* uptake by bovine PMN (Figure 4.6 A and B). These experiments indicate possible species specific-human versus bovine and bacteria specific-BCG versus *E. coli* differences in responses.

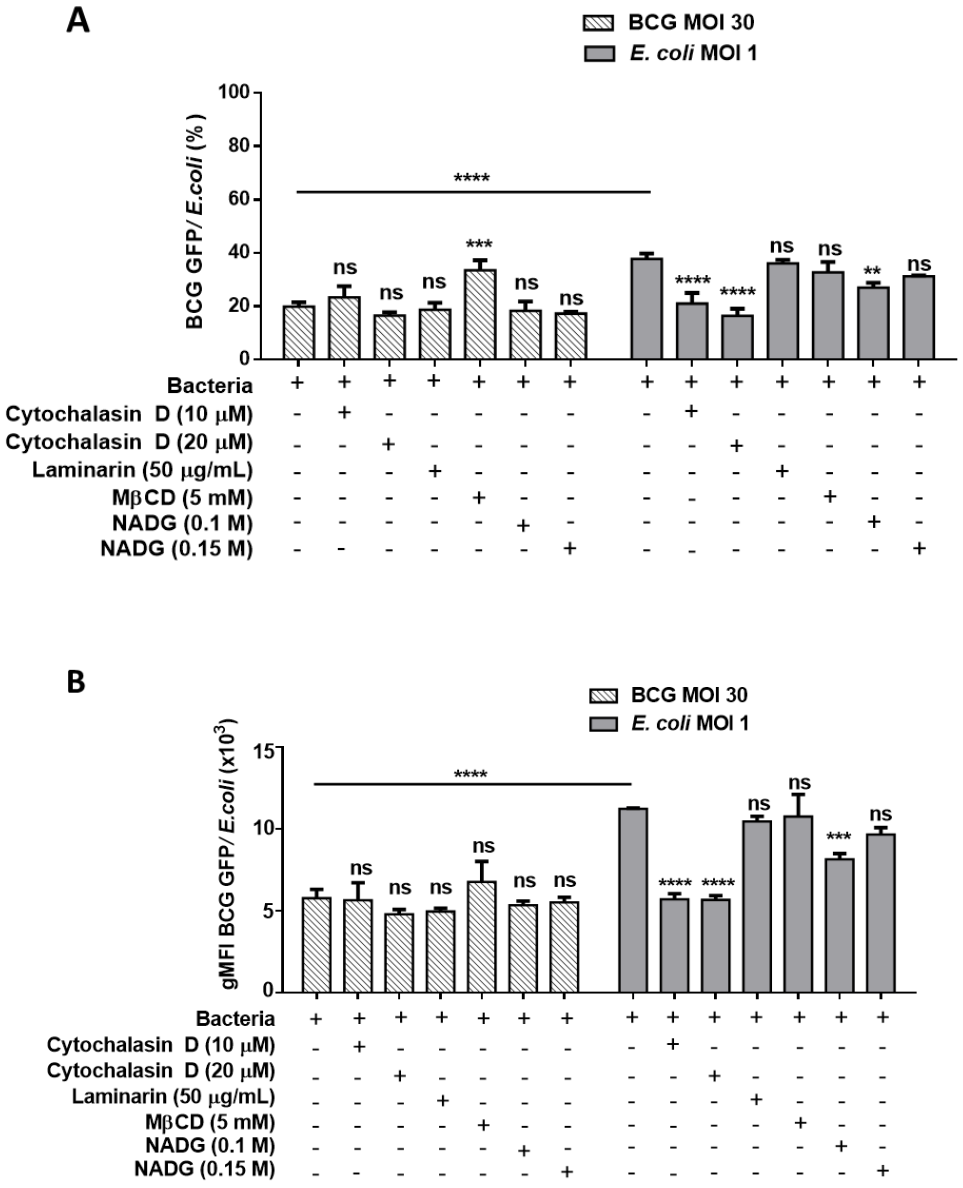

Figure 4.6: Phagocytosis of BCG and *E. coli* by bovine PMN is differentially altered by chemical inhibitors. Bovine PMN were pre-treated with MβCD (5 mM), NADG (0.1 M and 0.15 M), Laminarin (50 µg/mL), Cytochalasin D (10 µM, 20 µM) for 30 min at 37°C, 5 % CO_2 followed by infection with BCG GFP or fluorescein conjugated *E. coli* for 30 min. Percent phagocytosis **(A)** and mean phagocytosis assessed as gMFI **(B)** were acquired for all tested conditions. The data is representative of one experiment performed in triplicates, out of three, each with independent donors. Data shows mean +/- SD of triplicates values. The analysis was done using Two-way ANOVA with Bonferroni correction; ns $P>0.05$, $^{**}P\leq0.01$ $^{***}P\leq 0.001$, $^{****}P\leq0.0001$.

4.3 Cholesterol content is similar in human and bovine neutrophils

Mycobacterium requires cholesterol for entry into MΦ (Gatfield and Pieters 2000) and the cholesterol rich microdomains are used by *M. kansasii* to enter human PMN (Peyron, Bordier et al. 2000). Depletion of cholesterol from the membrane of human and bovine PMN with MβCD (see Figure 4.5 A and B) resulted in reduced internalization of BCG only in human PMN. Therefore, to evaluate potential differences in cholesterol content between the two species, the total cholesterol content in the cell was measured. No difference in the total cholesterol content was found between the two species. MβCD significantly reduced the total cholesterol in human PMN and there was no difference in cholesterol concentration after BCG infection (Figure 4.7) indicating that BCG infection leaves cellular cholesterol content unchanged.

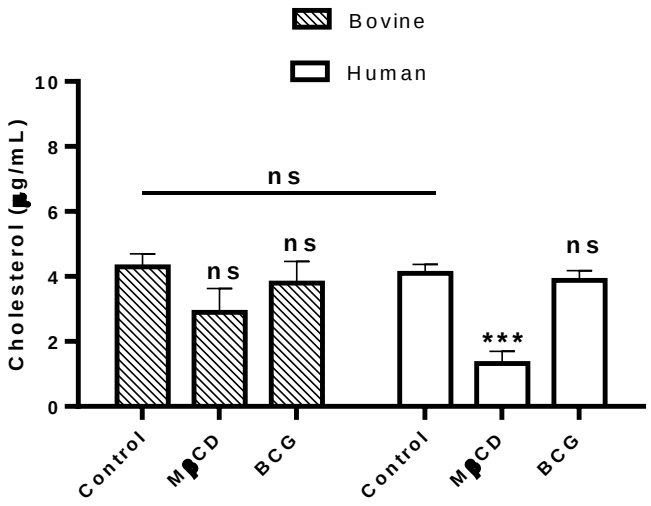

Figure 4.7: Basal levels of cholesterol is similar in bovine and human PMN. Cells were left untreated (control), treated with MβCD (5 mM) or infected with BCG WT (MOI 30) for 30 min and cholesterol concentration was determined using the amplex red cholesterol assay kit. Data is representative of one experiment performed in triplicates, out of four experiments, each with individual donors. Data shown as mean +/- SD of triplicate values, Two-way ANOVA with Bonferroni correction. ns; $P>0.05$, ***$P\leq0.001$.

To further evaluate differences in the free cholesterol content in PMN from distinct species, the polyene macrolide antibiotic filipin, which is isolated as a major component from *Streptomyces fillipinensis* (Whitfield, Brock et al. 1955) and stains free cholesterol but not cholesteryl esters was used. Naïve (control) cells, cells treated with MβCD and cells infected with BCG were stained with filipin. No significant difference in the gMFI for free cholesterol was found between the two species and the different conditions (Figure 4.8 A and B).

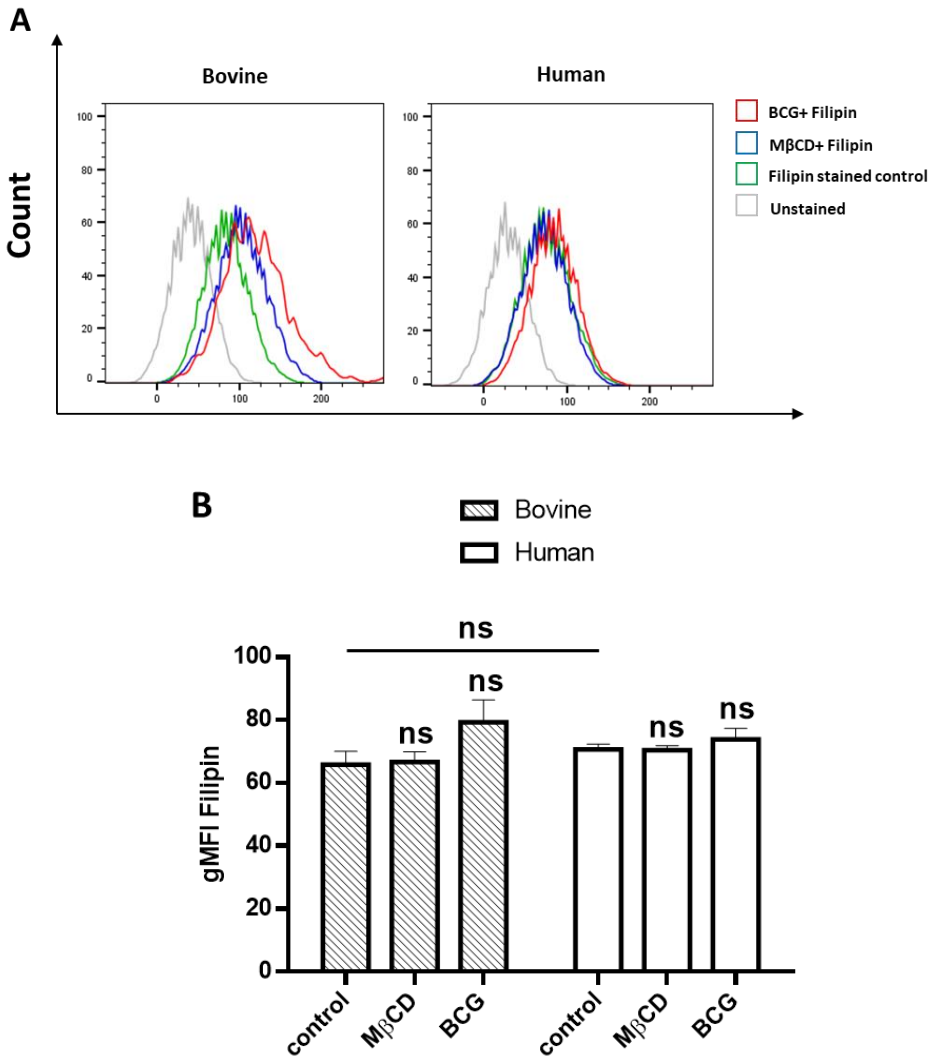

Figure 4.8: Free cholesterol content is similar between human and bovine PMN. Bovine and human PMN were left unstained, stained with filipin (control), treated with MβCD (5 mM) or infected with BCG GFP (MOI 30) for 30 min. After infection cells were fixed with 4% PFA and stained with filipin (50 µg/mL) for 60 min and samples were analyzed by flow cytometry, shown are representative histograms **(A)** and gMFI values **(B)**. Data represents mean +/- SD of triplicate values from one individual experiment out of three, each with independent donors. The data was analyzed using Two-way ANOVA with Bonferroni correction, ns; *P*>0.05.

Due to the similarities observed in the total and free cholesterol concentration for human and bovine PMN, membrane cholesterol concentration in the two species was quantified using a cell fractionation method. There was no difference between the control cells from the two species. Pre-treatment of cells with lovastatin, which blocks the synthesis of cholesterol, did not reduce the membrane cholesterol level at steady state and post BCG infection. These findings ruled out the possibility of an increase in membrane cholesterol caused by mycobacteria or variability in provision of membrane cholesterol via synthesis pathway for

the two species analyzed. The significant reduction in cholesterol with MβCD treatment confirms the effective depletion of membrane cholesterol post MβCD delivery (Figure 4.9). Nevertheless, the cell fractionation performed after the infection needs a validation using western blot to prove that fraction used was indeed the intended membrane fraction.

In summary, the experiments assessing cholesterol abundances indicate that the cholesterol content in cells purified from the two species is similar. The reasoning for the lack of effect observed for MβCD in bovine PMN infected with BCG (see Figure 4.5 A and B) needs further evaluation.

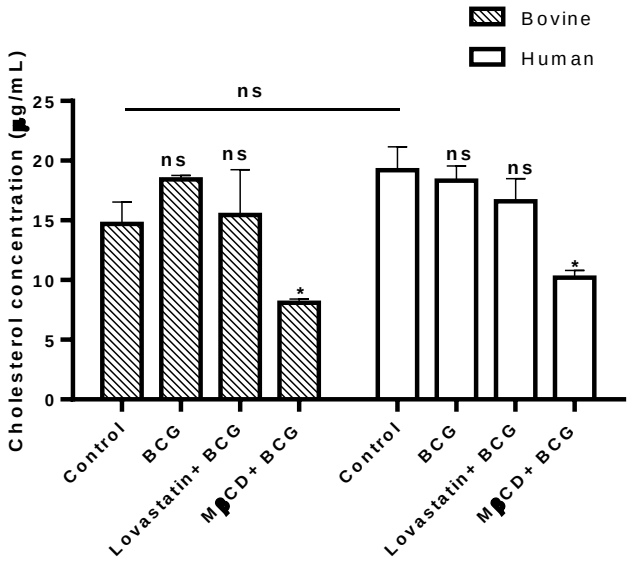

Figure 4.9: Membrane cholesterol concentration is similar in bovine and human PMN. Cells were either left untreated (control) or pre-incubated with Lovastatin (5 µg/mL) or MβCD (5 mM) for 30 min followed by infection with BCG at MOI 30 for 30 min. Cell fractionation was performed prior to quantification of cholesterol levels in the membrane fraction using the amplex red cholesterol assay. The data represents mean +/- SD of triplicate values from one representative experiment out of three independent experiments, each with individual donors. Data was analyzed using Two-way ANOVA with Bonferroni correction, ns; $P>0.05$, $*P\leq0.05$.

4.4 *M. bovis* BCG triggers a robust oxidative burst in human neutrophils

The production of ROS by PMN is essential for killing an invading pathogen. Upon neutrophil activation, the assembly of NADPH complex at the phagosomal site is the key event in ROS generation. Upon PMA stimulation, which is an efficient ROS inducer via the PKC pathway, the human PMN showed higher ROS burst compared to bovine cells (Figure 4.10 A and C) and the peak occurred between 200-400 sec. Similarly, after BCG challenge at MOI 30 there was

a higher ROS response from human PMN with a peak at 10,000 sec. (Figure 4.10 B and D). In summary, human PMN are highly responsive to PMA stimulation and BCG infection, with responses exceeding those recorded for bovine counterparts.

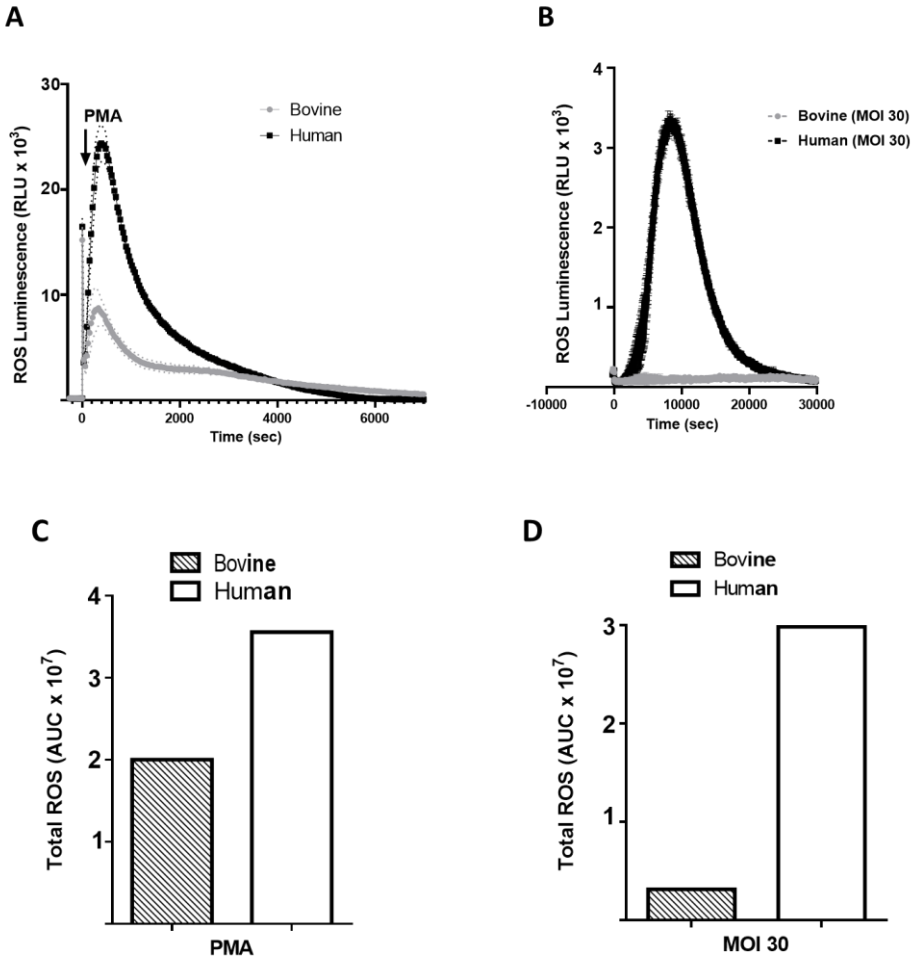

Figure 4.10: Human PMN show a higher ROS burst compared to bovine PMN. PMN were stimulated with **(A)** PMA (1 µM) or were **(B)** infected with BCG MOI 30 and ROS was measured over time using luminol assay. AUC was calculated for PMA stimulated PMN **(C)** and BCG infected PMN **(D)**. Data shown is mean +/- SD of triplicate values from one representative experiment out of four, each with individual donors.

4.5 Human neutrophils contain and release abundant myeloperoxidase upon stimulation

MPO present in the primary azurophilic granules in PMN catalyzes the conversion of H_2O_2 to HOCl and contributes to microbial killing (Nauseef 2014). Whether bovine and human PMN are able to release MPO was investigated in context of the BCG infection and treatment with chemicals which trigger degranulation. The stimulation of PMN with PMA resulted in more abundant MPO release by human PMN compared to bovine PMN. Stimulation with PMA

followed by infection with BCG boosted MPO release in both species and the values were significantly higher for human PMN. When supernatants from BCG infected cells were compared, no significant difference in MPO release was observed (Figure 4.11). These results confirm already reported differences in MPO in cells from humans and cattle (Bassel and Caswell 2018) emphasizing an abundant pool of MPO in human PMN.

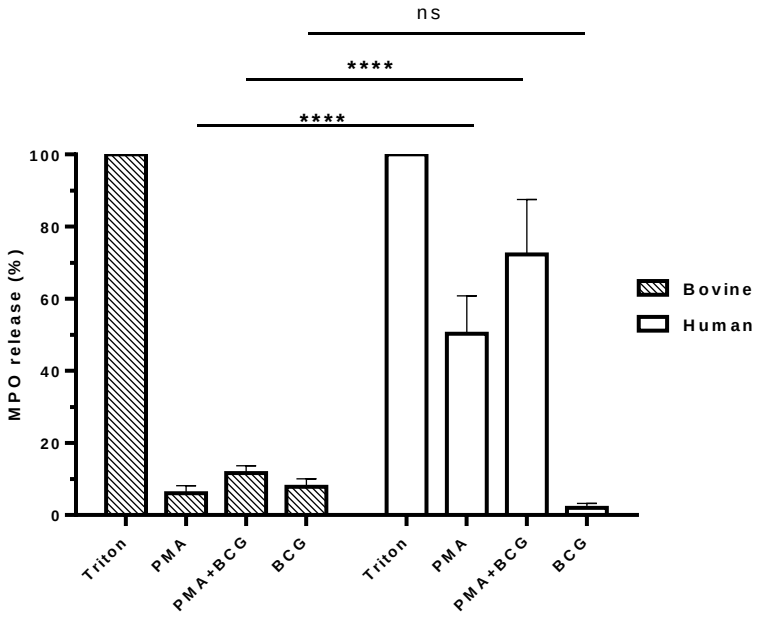

Figure 4.11: Human PMN release higher MPO amounts than bovine PMN. PMN pre-treated with cytochalasin B (10 µg/mL) were stimulated with PMA (1 µM) or stimulated and infected with BCG at MOI 10 for 30 min. The MPO release was calculated by normalizing the data to amounts obtained from lysed cells. Data cumulatively derived from four independent experiments and analyzed using Two-way ANOVA with Bonferroni correction; ns $P>0.05$, ****$P\leq0.0001$.

4.6 *M. bovis* BCG is not killed by human or bovine neutrophils

Whether PMN are able to destroy mycobacteria is controversial as discussed in section 1.5.1. To investigate whether bovine and human PMN were able to kill BCG, the CFU assay was performed for a duration of 240 min post infection. For intracellular killing (Figure 4.12 A, B and C) the infection was allowed for 30 min and the extracellular bacteria were removed. There was no reduction of the CFU over time (30, 90, 180, 240 min) in both human and bovine PMN. The intracellular CFU at 30 min (Figure 4.12 A) was similar to the phagocytosis data, again emphasizing that human PMN take up more BCG compared to bovine counterparts (see Figure 4.1). Also, BCG being a slow growing bacterium with a generation time of 20 h under culture conditions (Cole, Brosch et al. 1998), the presence of similar number of bacterial colonies after 240 min suggested no killing.

For total CFU, bacteria were incubated with the PMN until the time point was reached, PMN did not kill BCG as the CFU remained constant with time (Figure 4.12 B, C). In summary, both human and bovine PMN failed to kill BCG under experimental conditions used herein.

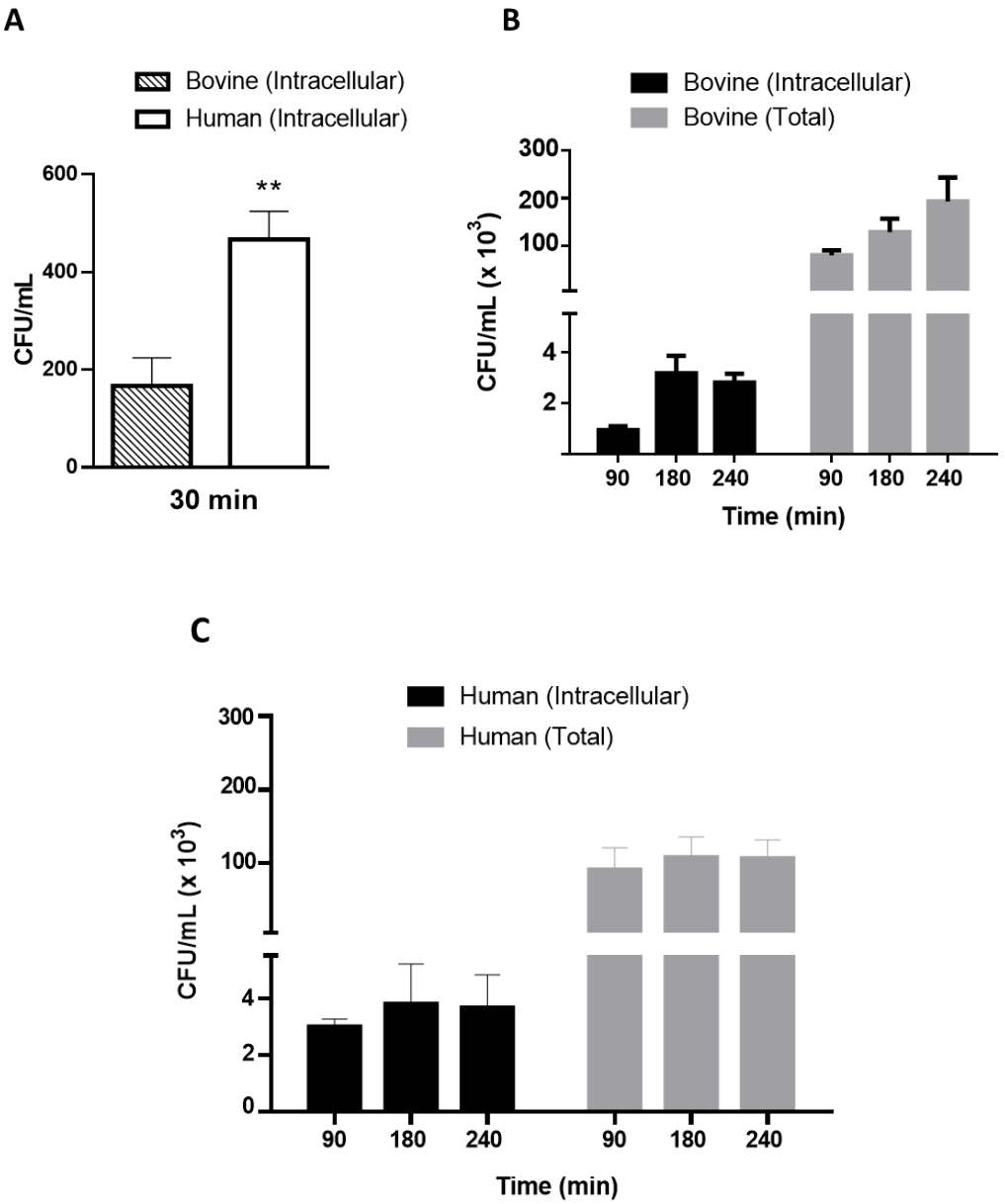

Figure 4.12: Human and bovine PMN fail to kill BCG. Human and bovine PMN were infected with BCG at MOI 10 and infection was allowed to proceed for 30 min for intracellular killing and extracellular bacteria were removed and CFU was monitored for 30 min, 90 min, 180 min and 240 min **(A, B)**. For total CFU bacteria were not removed after 30 min and samples were processed for CFU assay at various time points **(B, C)**. Data represents mean +/-SD of triplicate values from one representative experiment out of two with independent donors from each species. **(A)** Data was analyzed using t-test; ***P*<0.01.

4.7 Bovine and human neutrophils release selective cytokine upon infection

Cytokines act as critical messengers to signal other immune or tissue resident cells thereby resulting in an immune cascade (Hilda and Das 2015). The ability of bovine and human PMN to release TNF-α and IL-8, which are amongst the main pro-inflammatory cytokines released during infection (Sohn, Paape et al. 2007, Krupa, Fol et al. 2015) was investigated. Incubation of PMN from both the species with BCG at MOI 10 for 20 h did not result in significant release of TNF-α unlike PMN from other species (Petrofsky and Bermudez 1999, Gideon, Phuah et al. 2019) (Figure 4.13 A and B). However, they did release IL-8 (Figure 4.13 C and D), albeit showing donor-related variability.

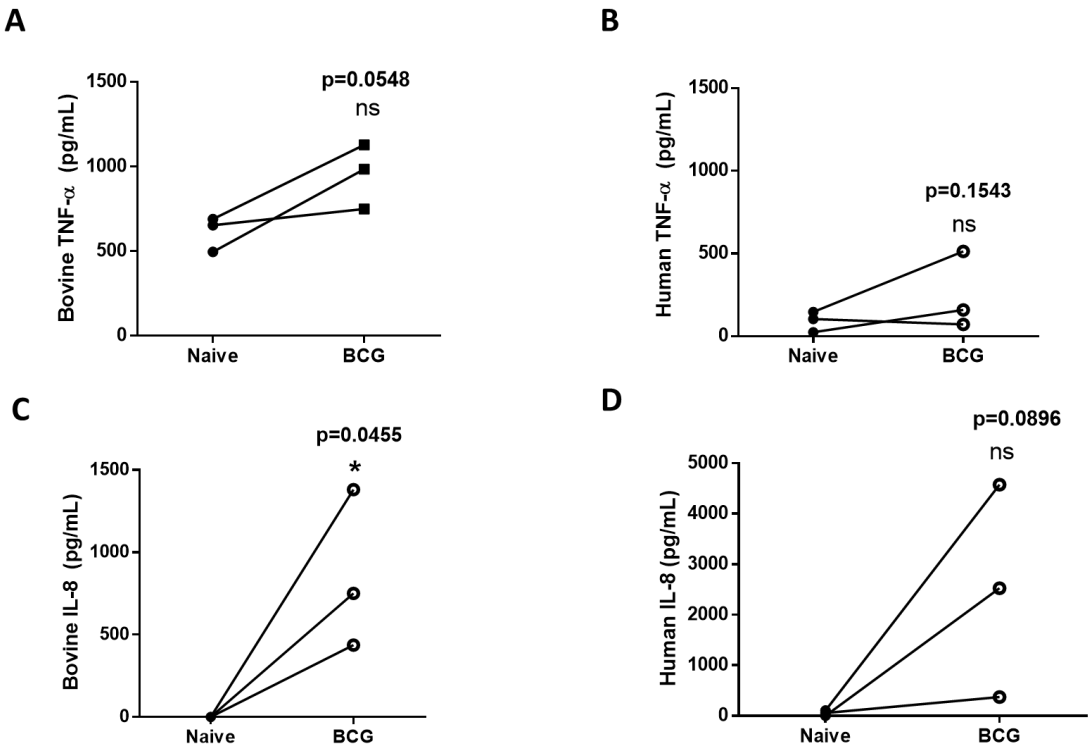

Figure 4.13: Human and bovine PMN release IL-8 upon BCG infection. Bovine and human PMN were left uninfected (naïve) or infected with BCG for 20 h. Cytokine levels in cell culture supernatants were measured using ELISA kits. TNF-α release by bovine **(A)** and human PMN **(B)** as well as IL-8 release for bovine **(C)** and human PMN **(D)** are shown. Each symbol represents an individual donor, shown are mean values for each donor, which was tested in triplicates. Paired human and bovine PMN were infected in independent experiments. This data with three donors was analyzed using One-tailed Paired t-test, ns; $P>0.05$, * $P\leq0.05$.

5 Responses of bovine neutrophils to *M. bovis* BCG, *M. tb* H37Rv and *M. bovis* AF2122/97

5.1 Uptake of *M. bovis* BCG and *M. tb* H37Rv by bovine neutrophils

To evaluate whether the bovine PMN respond differently to distinct members of MTBC, the phagocytic ability of these cells for *M. tb* and BCG was compared. Bovine PMN were infected with BCG GFP and *M. tb* H37Rv GFP at MOI 30 for 30 min. The percent phagocytosis (Figure 5.1 A) and mean phagocytosis calculated as gMFI (Figure 5.1 B) was compared between the two bacterial strains. Between BCG and *M. tb*, no significant uptake was found for either MTC member as depicted using gMFI. No reduction in uptake of BCG and *M. tb* could be seen when CR3 was blocked using antibodies against CD11b (Figure 5.1 A and B).

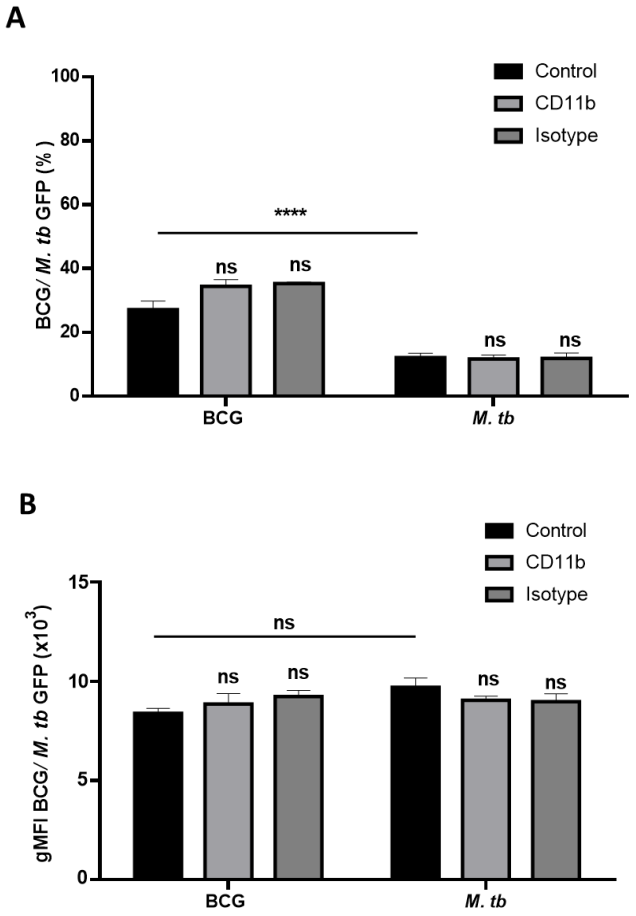

Figure 5.1: Similar uptake of BCG and *M. tb* by bovine PMN. Cells were blocked with anti-CD11b antibody (clone CC126 10 µg/mL + clone CC104 2 µg/mL) or incubated with mouse IgG2b isotype control for 30 min and infected with BCG GFP or *M. tb* GFP at MOI 30 for 30 min. Percent phagocytosis **(A)** and mean phagocytosis calculated as gMFI **(B)** of infected PMN were obtained for all conditions. The data is representative of one experiment performed in

triplicates out of two experiments, each with independent donors. The data was analyzed using Two-way ANOVA with Bonferroni correction, ns; P >0.05.

Additionally, to study the effect of serum opsonization on the uptake of BCG and *M. tb* by bovine PMN, PMN were left uninfected, treated with antibodies against CD11b or isotype control for 30 min before infection. PMN were further infected with Ops BCG GFP or Ops *M. tb* GFP with MOI 30 for 30 min. The infection resulted in higher uptake of Ops BCG compared to Ops *M. tb,* however, there was no significant reduction upon blocking of CD11b with monoclonal antibodies (Figure 5.2 A and B).

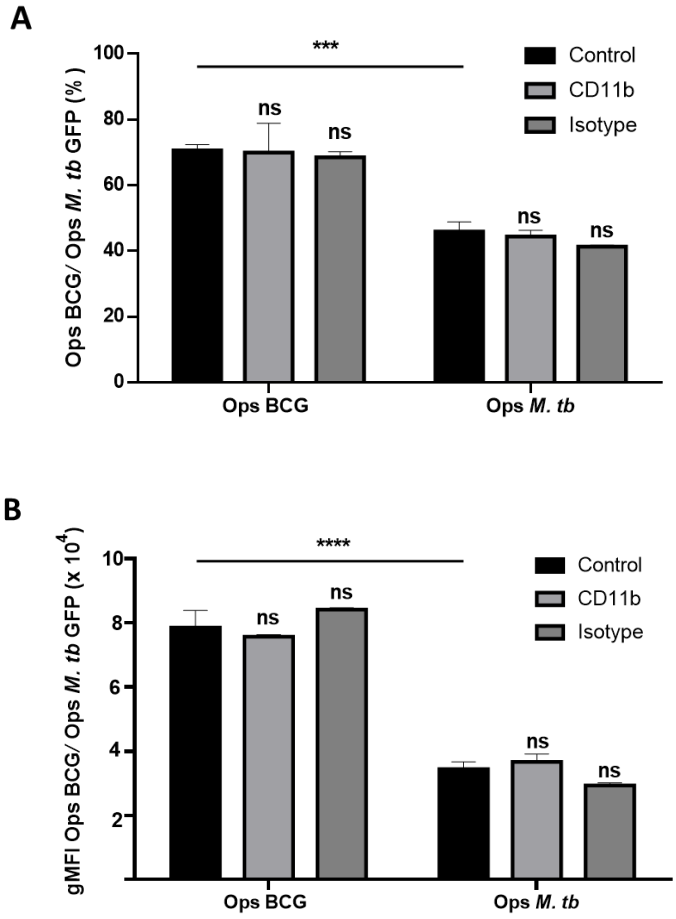

Figure 5.2: Higher uptake of Ops BCG than Ops *M. tb* by bovine PMN. Cells were pre-incubated with anti-CD11b antibody (clone CC126 10 µg/mL + clone CC104 2 µg/mL) or with mouse IgG2b isotype control for 30 min and subsequently infected with Ops BCG GFP or Ops *M. tb* GFP at MOI 30 for 30 min. **(A)** Percent phagocytosis and **(B)** mean phagocytosis quantified as gMFI of infected PMN was assessed. The data shows mean +/- SD of triplicate values from one representative experiment performed in triplicates out of two experiments, each with independent donors. The data was analyzed using Two-way ANOVA with Bonferroni correction, ns; *P* >0.05, ****P* ≤0.001, *****P* ≤0.0001.

5.2 Bovine neutrophils release comparable amounts of myeloperoxidase after infection with *M. bovis* BCG and *M. tb* H37Rv

To explore whether the bovine PMN differently respond to attenuated and virulent mycobacteria, MPO release as a subsequent mobilization of the azurophilic granules was investigated. The PMN were left uninfected or infected with BCG or *M. tb* at MOI 30 for 30 min. No difference in MPO release was seen between the two mycobacterial strains used. Also, the release after infection was relatively low (Figure 5.3). This suggests that bovine PMN are less responsive to mycobacterial infection and they have less MPO reserves in general.

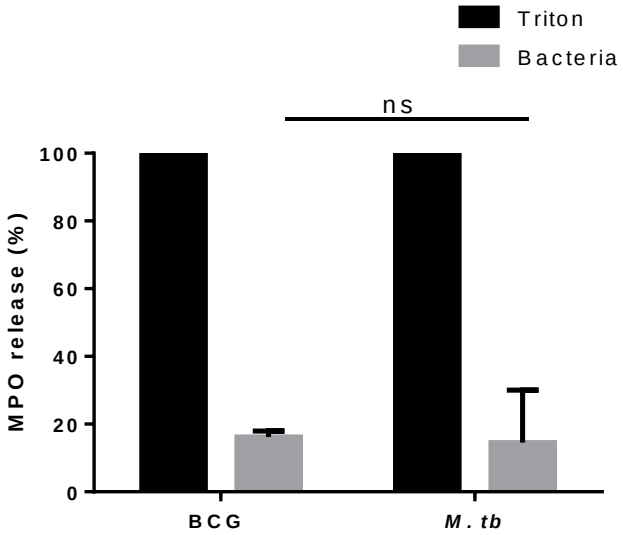

Figure 5.3: MPO release after BCG and *M. tb* infection was similar in bovine PMN. Cells were pre-treated with cytochalasin B (10 µM) for 5 min and infected with BCG or *M. tb* at MOI 30 for 30 min. The total MPO release was normalized to total cell amounts. Data is cumulative from two experiments, each performed in triplicates and analyzed using Two-way ANOVA with Bonferroni correction ns; $P > 0.05$.

5.3 Phagocytosis of *M. bovis* AF2122/97 and *M. tb* H37Rv by bovine neutrophils

Whether bovine PMN would have different responses to the animal-adapted (*M. bovis* AF2122/97) and the human-adapted (*M. tb* H37Rv) mycobacteria is unknown. Therefore, to investigate this, flow cytometry was used to compare phagocytic rates upon challenge with two virulent strains. Infection experiments were performed by leaving the PMN untreated or by pre-treating with monoclonal antibodies against CD11b or isotype control for 30 min. Treatment was followed by infection with *M. bovis* and *M. tb* at MOI 30

for 30 min. Higher uptake of *M. bovis* in contrast to *M. tb* was an outcome in the percent phagocytosis (Figure 5.4 B), however, mean phagocytosis was higher for *M. tb* (Figure 5.4 B). Antibody blocking did not have any effect on phagocytosis of any of the two strains and the levels remained similar to those of the infected controls.

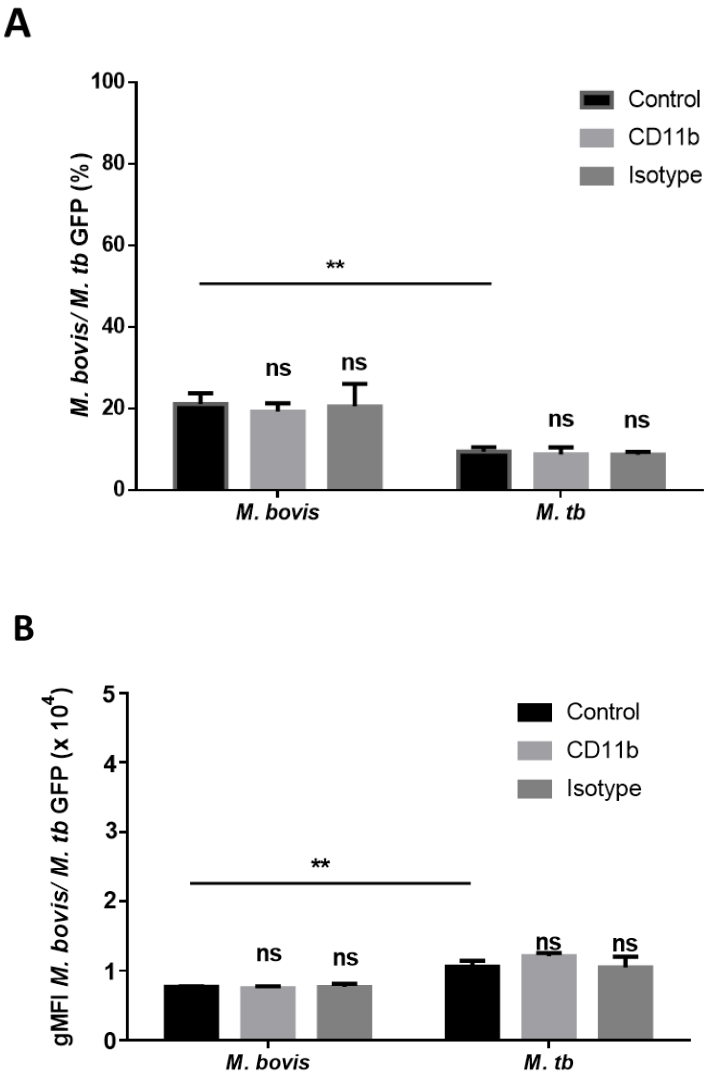

Figure 5.4: Bovine PMN phagocytose more *M. tb* compared to *M. bovis*. Cells were pre-treated with anti-CD11b antibody (clone CC126 10 µg/mL + clone CC104 2 µg/mL) or with mouse IgG1 isotype control and infected with *M. bovis* AF2122/97 and *M. tb* H37Rv at MOI 30 for 30 min. **(A)** percent phagocytosis and **(B)** mean phagocytosis evaluated as gMFI was quantified for all the conditions. Data is representative of one experiment performed in triplicates out of three independent experiments, each with independent donors. Error bars indicate mean +/- SD of triplicate values. Data obtained was analyzed using Two-way ANOVA with Bonferroni correction ns; $P > 0.05$, ** $P \leq 0.01$.

To investigate whether pre-incubation of the virulent strains with fresh bovine serum from the same donor animal enhanced their uptake by PMN and whether pre-incubation with antibodies against CD11b or isotype control reduce the uptake, PMN were subsequently infected with Ops *M. bovis* or Ops *M. tb* and afterwards infection was monitored using flow cytometry. Infection with serum opsonized bacteria showed no significant difference in uptake between the two strains considering the percent phagocytosis (Figure 5.5 A), however, the gMFI values were significantly higher for the *M. bovis* samples (Figure 5.5 B). Also, blocking CD11b using antibodies did not result in reduction in phagocytosis of both pathogens (Figure 5.5 A and B). The significant increase in gMFI signifies that at the cell level the PMN have phagocytosed higher amount of *M. bovis*.

In summary, the data suggest a higher response of bovine PMN towards the host adapted pathogen *M. bovis* in terms of phagocytosis.

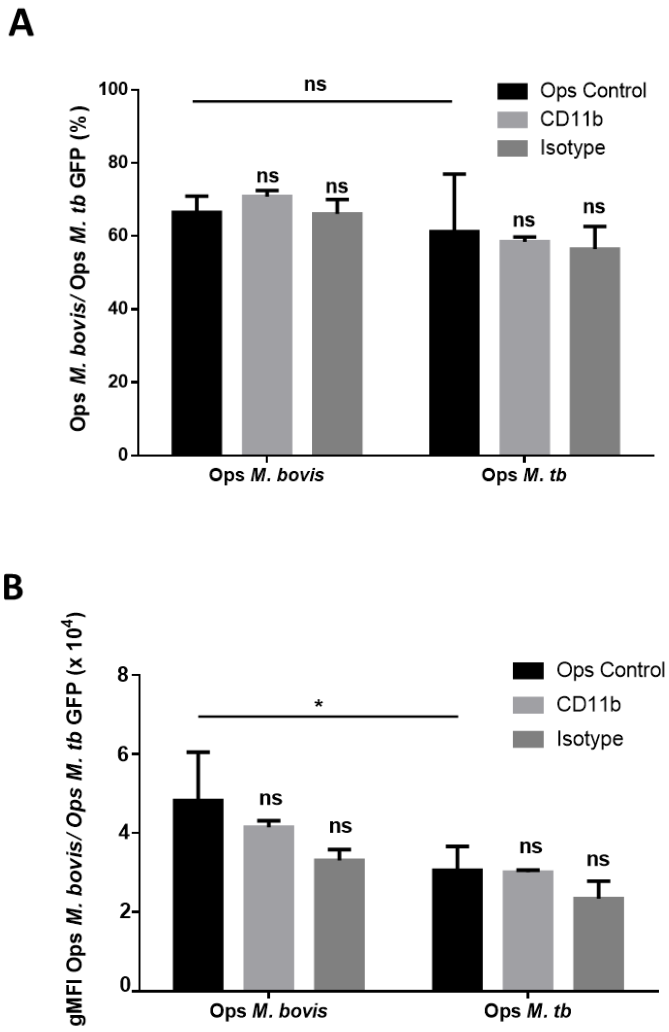

Figure 5.5: Higher uptake of opsonized *M. bovis* by bovine PMN. Bovine PMN were blocked with anti-CD11b antibody (clone CC126 10 µg/mL + clone CC104 2 µg/mL) or with mouse IgG1 isotype control and infected with Ops *M. bovis* AF2122/97 or Ops *M. tb* H37Rv at MOI 30 for 30 min. **(A)** Percent phagocytosis and **(B)** mean phagocytosis calculated as gMFI was

evaluated. The data is a representative of one independent experiment out of three, each experiment was performed in triplicates. Data shown as mean +/- SD of triplicate values analyzed using Two-way ANOVA with Bonferroni correction ns; *P* >0.05, * *P* ≤0.05.

5.4 Blocking selected phagocytic pathways leaves uptake of *M. bovis* AF2122/97 and *M. tb* H37Rv unchanged

To evaluate the role of several phagocytic pathways on the uptake of *M. bovis* and *M. tb*, PMN were pre-treated with MβCD, NADG and cytochalasin D followed by infection with *M. bovis* or *M. tb*. There was no reduction in bacterial uptake upon mentioned treatments for any of the bacterial strain. Engulfment of *M. bovis* remained significantly higher compared to *M. tb* (Figure 5.6 A) considering percent phagocytosis whereas the gMFI (Figure 5.6 B) seemed higher for *M. tb*. Treatment with MβCD significantly increased the gMFI of *M. tb* rather than reducing it. This effect was not observed with *M. bovis* (Figure 5.6 A and B). No significant effect of MβCD could be seen with BCG uptake when bovine and human responses were compared (see Figure 4.5). The samples were fixed with PFA overnight. Therefore, the possibility of extracellular bacteria sticking to the cell after washing cannot be ruled out.

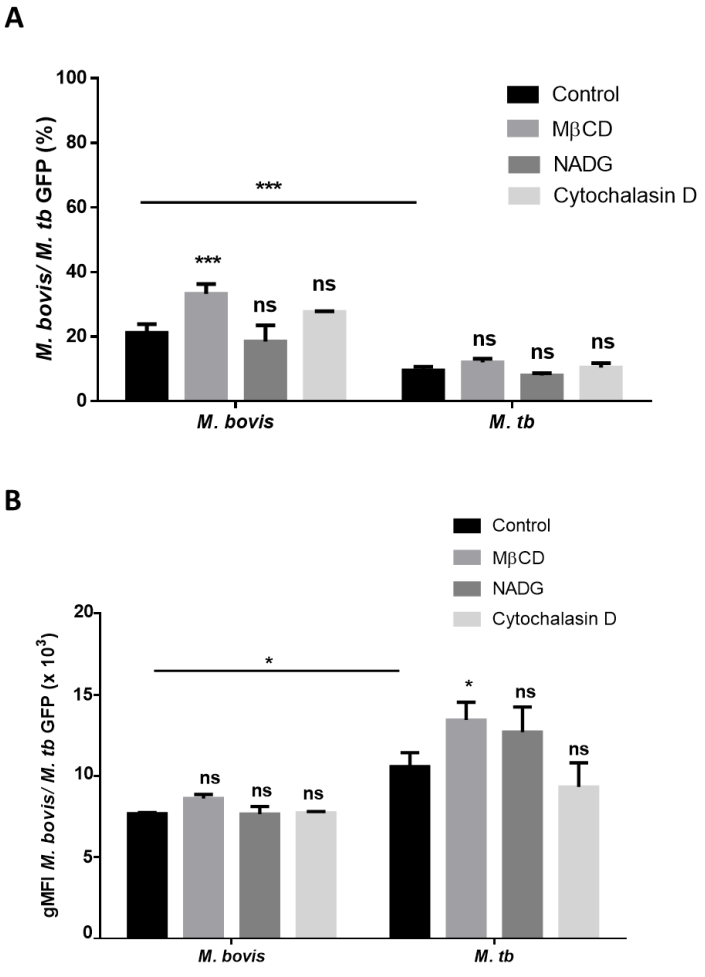

Figure 5.6: Blocking with MβCD, NADG and Cytochalasin D leaves phagocytosis of *M. bovis* and *M. tb* by bovine PMN unchanged. Cells were blocked with MβCD (5 mM), NADG (0.15 M), Cytochalasin D (10 µM) for 30 min at 37°C, 5 % CO_2. Percent phagocytosis **(A)** and gMFI **(B)** was determined for all conditions. Data shown is a representative of one experiment performed in triplicates, out of two, each with independent donors. Data obtained was analyzed using Two-way ANOVA with Bonferroni correction, ns; *P* >0.05, * *P* ≤0.05, *** *P* ≤0.001.

5.5 Bovine neutrophils release similar amounts of myeloperoxidase after infection with *M. bovis* AF2122/97 and *M. tb* H37Rv

To evaluate the MPO release as a proxy for azurophilic granule release after infection, the bovine PMN were infected with *M. bovis* or *M. tb* with MOI 30 for 30 min. A negligibly low level of MPO could be detected in the supernatants with no difference between the two strains (Figure 5.7). This data indicates that infection with *M. bovis* or *M. tb* did not trigger MPO release. The negligible MPO release could be due to low basal levels of this enzyme in bovine PMN.

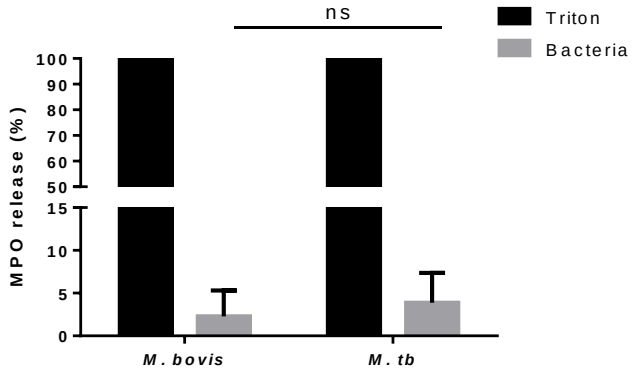

Figure 5.7: Similar MPO release by bovine PMN after infection with *M. bovis* or *M. tb*. Cells were pre-treated with cytochalasin B (10 µM) for 5 min followed by infection with *M. bovis* or *M. tb* for 30 min. The total MPO release was quantified by spectrophotometry. Data was normalized to total MPO cellular content and are pooled from three independent experiments. Data obtained was analyzed using Two-way ANOVA with Bonferroni correction, ns; *P* >0.05.

5.6 Selective cytokine release in bovine neutrophils infected with *M. bovis* AF2122/97 and *M. tb* H37Rv infection

Inflammatory cytokines are crucial for the recruitment of immune cells at the infection site to mount an immune response. Therefore, to explore the ability of bovine PMN to release cytokines after *M. bovis* and *M. tb* infection, PMN were infected with the two pathogens for 20 h and cytokines were measured in cell-free culture supernatant. Infected PMN released TNF-α (Figure 5.8 A and B) however, the fold increase between *M. bovis* and *M. tb* was not significant (Figure 5.8 C). Interestingly, the IL-8 release in infected cells was not significantly different compared to naïve samples, possibly due to inter-individual variability (Figure 5.8 D and E), However, the fold increase in IL-8 releases between *M. bovis* and *M. tb* differed (Figure 5.8 F).

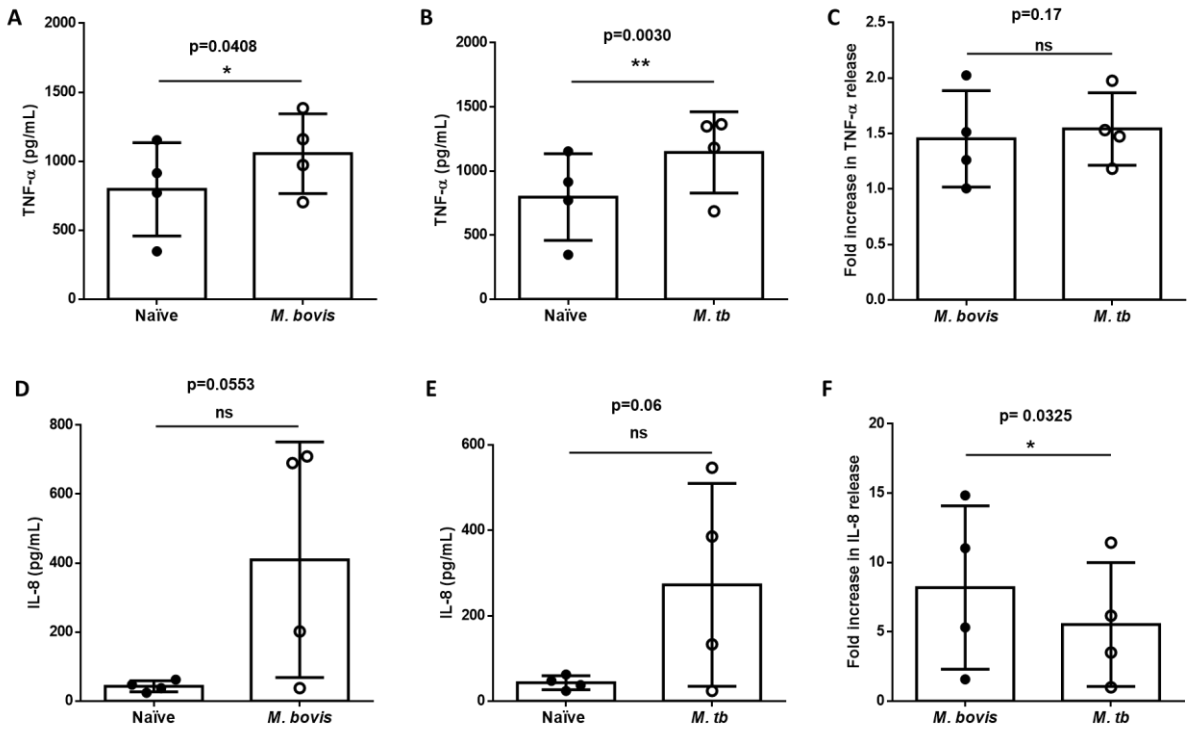

Figure 5.8: Bovine PMN release more abundant IL-8 upon infection with *M. bovis* compared to *M. tb* challenge. Cells were infected with *M. bovis* and *M. tb* at MOI 10 for 20 h at 37°C, 5 %CO_2. **(A)** TNF-α and **(B)** IL-8 release was quantified in the cell-free supernatants by ELISA. Each experiment was performed in duplicates. Shown are mean +/- SD values from pooled experiments, each symbol denoting mean value for individual donor. Data was analyzed using one tailed Paired t-test, ns; $P > 0.05$, * $P \leq 0.05$, ** $P \leq .0.01$.

6 Discussion

6.1 Development of a method for efficient enrichment of bovine neutrophils

PMN are short-lived and highly fragile cells essential for defense against pathogens. Recent findings emphasize that PMN cross-talk with lymphocytes (Costa, Bevilacqua et al. 2019) and other phagocytes and these activities along with their direct antimicrobial capacities modulate host responses to infection (Mantovani, Cassatella et al. 2011). Following pathogen encounter, activation of PMN contributes to the influx of immune cells along the chemotactic gradient, which may disrupt tissue integrity and result in excessive inflammation (Muefong and Sutherland 2020). Although human and bovine PMN utilize common antimicrobial strategies (Braian, Hogea et al. 2013, Ladero-Auñon, Molina et al. 2021) several differences between cells from the two species exist. Lack of fMLP receptors, presence of large peroxidase-negative granules, antimicrobial peptides like bactenectins and little or no lysozyme within granules are unique to bovine PMN (Gennaro, Dewald et al. 1983). Because of these differences it is conceivable that the immune response of bovine PMN to infection may not be similar to that of human counterparts. To accurately evaluate responses of PMN from distinct species to pathogenic bacteria in comparative manner, it is imperative to obtain highly pure cell preparation. Well-established protocols which enable purity exceeding 95% and high cell yields are available for isolation of PMN from human blood (Brinkmann, Laube et al. 2010, Son, Mukherjee et al. 2017). Besides high purity and cell numbers, viability of the isolated cells is also a critical parameter for downstream functional assays. Therefore, a primary aim of this work was to develop an isolation method for bovine PMN that is robust, yields high cell number and enables a cell purity reaching 99%.

There are several methods available for bovine PMN isolation that use density gradient, monoclonal antibodies or blood lysis (Riding and Willadsen 1981, Roth and Kaeberle 1981, Kremer, Noordhuizen-Stassen et al. 1992, Soltys, Swain et al. 1999). First attempts to isolate bovine PMN and eosinophils from blood employed acid citrate dextrose as anticoagulant followed by enrichment using Ficoll-Hypaque density gradient centrifugation (Roth and Kaeberle 1981). In spite of the fact that isolated cells ingested *Staphylococcus aureus*, centrifugation for 45 min could pre-stimulate and activate the cells. In addition, Ficoll-Hypaque markedly impaired the migration of isolated cells, which rendered this isolation method inappropriate for the evaluation of e.g. chemotaxis (Roth and Kaeberle 1981). Bovine PMN isolated using Ficoll-Hypaque followed by hypotonic lysis differed significantly in their membrane CD14 expression, a coreceptor for LPS. Expression levels of this bacterial sensor was reduced in purified PMN and also when anticoagulants such as EDTA, heparin, or sodium citrate were used, with EDTA and citrate rendering lowest membrane abundances of CD14. Therefore, choosing the ideal anticoagulant can be crucial for functional assays (Ibeagha-Awemu, Ibeagha et al. 2012). Another method to enrich PMN from cattle blood used Percoll

as a separation solution and disodium EDTA as an anticoagulant (Riding and Willadsen 1981). The centrifugation parameters used for the separation of granulocytes on the Percoll gradient was 20,000 x g for 20 min, i.e. extremely high speed that would likely activate the cells. Several other methods use hypotonic lysis of the RBCs followed by the Percoll or metrizamide density gradient centrifugation (Hallén-Sandgren and Björk 1988, Kremer, Noordhuizen-Stassen et al. 1992, Sláma, Sládek et al. 2006, Baien, Langer et al. 2018). However, the purity of the isolated cells using these techniques was low, with eosinophils being the most common contaminants. Therefore, other approaches for isolation of bovine PMNs were required in order to obtain reliable results. Several modifications of published methods were tested and refined to develop a new isolation procedure. These experiments were a prerequisite to proceed to the comparative study of human and cattle PMN.

The gradient isolation method for human PMN using Histopaque and Percoll resulted in clear separation of cell populations into distinct layers and resulted in 95% pure PMN. These results are in line with the previously published data (Brinkmann, Laube et al. 2010). However, the same method when used for bovine PMN isolation, did not result in clear separation of myeloid cells. The cell yield was extremely low and only 50% of purified cells were viable. Percoll density gradient at specific gravity of 1.092 was found to yield a PMN purity of 97% (Chambers, Taylor et al. 1983). This exceptional enrichment was however not reproduced. Usage of Percoll density gradient method by other groups reached only 80% pure bovine PMN while lymphocytes and monocytes were major contaminants (Soltys, Swain et al. 1999). This finding suggests that the bovine PMN have different buoyancy than human counterparts and require different centrifugation speed for enrichment. Therefore, in this work the isolation method using Biocoll and Histopaque was modified with the aim to achieve high cell purity. This procedure resulted in increased cell yield compared to the Histopaque and Percoll gradient method. However, even this method did not yield a clear separation between the cell populations; a thick band was observed at the interface of Biocoll and Histopaque, as well as a pellet at the bottom of the tube. The dilution of blood before adding it to the gradient resulted in increased viability after isolation. However, the purity of the diluted cell sample still remained poor and the PMN purity ranged between 50 to 86%. Therefore, considering results obtained using various gradient isolation methods, notably low cell yield, reduced viability and purity hardly reaching 80%, suitability of these methods was questionable. A recently published protocol has used various densities of Histopaque for PMN isolation and reported a purity of 93% with unknown contaminants (Siemsen, Kirpotina et al. 2020). The studies in this thesis confirmed that conventional methods using Percoll density gradients or discontinuous Biocoll and Histopaque gradients result in low yields and purity of the sample remain compromised.

To achieve highly pure bovine PMN samples, whole blood centrifugation without the use of any gradient was tested. This resulted in enhanced cell numbers, viability and purity when the blood was diluted with PBS compared to whole blood centrifugation. However, the purity obtained with this method was maximum 90% and the cell suspension in the end also

contained lymphocytes and eosinophils. Similar findings were reported in the past, notably 88.5% of the isolated cells were pure PMN, with 92.3% of those cells being viable (Garcia, Elsasser et al. 2015). Another study employing similar enrichment techniques reported a cell purity of 92.2% (Carlson and Kaneko 1973). Since lymphocytes and eosinophils release cytokines (Braun, Franchini et al. 1993), both contaminating cell types could cause artifacts if present in the PMN samples. Relevance of contaminants for accurate measurements of PMN functions has been demonstrated recently using cell suspension of variable purity obtained upon cell sorting. Broberg *et al*. used high speed sorting technique after gating for autofluorescence high and low leukocytes to separate eosinophils and PMN respectively (Broberg, Gonzalez-Cano et al. 2021). Responses of PMN and eosinophils to TLR agonists revealed the greater expression of IL-1, IL-6, and TNF-α in PMN than in eosinophils, again demonstrating the importance of pure cell preparation (Broberg, Gonzalez-Cano et al. 2021).

Considering the parameters for obtaining high purity, viability and yield of the PMN, an isolation method using centrifugation followed by antibody labelling and cell sort was carried out for both human and bovine PMN. The human cells were stained with the CD15 granulocyte marker and sorted based on morphometric gating and immunostaining. The isolation method proved promising with 99% pure PMN, however the yield obtained was low. These findings were comparable to the positive selection method using anti-CD15 microbead for PMN enrichment (Zhou, Somasundaram et al. 2012). The sorting procedure for bovine PMN based on labelling the cells with the CH138A granulocyte marker and MHC II to exclude monocytes leaving CH138A+ PMN for purification resulted in 94% purity of bovine PMN. Contaminants in the PMN sample were lymphocytes and eosinophils, unlike the literature which quoted 99% purity of PMN (Rambault, Doz-Deblauwe et al. 2021). Rambault *et al*. could show that a small population of PMN could simultaneously express MHCII+ and CH138A+. The double positive population of PMN was enriched in lymphoid organs, specifically tracheobronchial lymph nodes (Rambault, Doz-Deblauwe et al. 2021). However, in this study only circulating blood was collected for the PMN isolation, hence CH138A+ MHCII+ PMN were not observed. Furthermore, this FACS-sorting technique was time consuming, as the sorting procedure took up to 4 h, which is disadvantageous given the short life time of PMN. Therefore, to reduce the isolation time and increase the yield and purity of both human and bovine PMN magnetic isolation was tested. An isolation kit from Miltenyi Biotec was used for negative selection of human PMN (Miltenyi 2020). The procedure took less than 30 min and resulting PMN were 99% pure. A high yield in the range of 1.9-4.2 x 10^6 PMN/mL was obtained with low amount of blood demonstrating the method is highly reproducible, gives high purity cells and requires less time. The results obtained were comparable to published reports which show the yield of purified PMN as 3 x 10^6 PMN/mL blood and purity in the range of 69.3-98.1% (Son, Mukherjee et al. 2017).

In order to eliminate any differences due to variable enrichment methods for the species under study, a magnetic isolation procedure for bovine PMN was developed, similar to that used for human PMN. Therefore, a modification in the centrifugation and sorting method was

done. This technique resulted in high yield and purity of the PMN and the method required less than 3 h until the final purification step. A further benefit of magnetic isolation over gradient isolation or sorting is that it eliminated the possibility of cell activation and reduced viability caused by gradient solutions. Furthermore, the purity attained was 99%, which was robust in comparison to so far published isolation procedures, restricting the possibility of artifacts in functional studies due to cellular contaminants (Rambault, Borkute et al. 2021).

6.2 Features of the isolated neutrophils

TEM is used to determine the ultrastructural features of the cells by providing detailed observations on subcellular organization. As known from the literature, PMN have multilobulated nuclei lined in a straight line allowing it to easily pass through the endothelium during migration. In humans, two to five lobed nuclei are usually seen in PMN with 40 to 50% PMN containing three lobes (Chan, Tsai et al. 2010). In comparison to humans, murine PMN have hyper-segmented nuclei with more than five lobes due to the presence of numerous grooves (Fingerhut, Dolz et al. 2020). TEM analysis of PMN purified with protocols developed within this thesis revealed that the lobulation of nuclei in human and bovine PMN were comparable. Along with the different granules present in PMN irrespective of species origin, large electron-dense granules were seen in bovine PMN. These organelles are known to have antimicrobial activity as they are rich in highly cationic peptides called bactenectins (Paape, Bannerman et al. 2003). Approximately 35% PMN from both species had 5 to 8 mitochondria/cell and interestingly, 30% of bovine PMN had more than 9 mitochondria per cell in comparison to 8% in human PMN. This finding suggests a potential difference in mitochondrial content in PMN from the two species. For more reliable evaluation of mitochondria, as it is difficult to accurately count them in the dense cytoplasm of PMN, additional investigations are required. For instance, mitochondrial dyes, e.g., Mito Tracker Red, can be used to stain these organelles and quantification can be done using confocal microscopy (Fossati, Moulding et al. 2003, Quiroga, Alarcon et al. 2020). Several metabolic functions are carried out by mitochondria, and they are also known to regulate PMN apoptosis via intrinsic signaling (Maianski, Geissler et al. 2004). PMN use anti-apoptotic proteins such as B cell lymphoma protein 2 related protein A1/Bf1, Myeloid cell leukemia-1 and B cell lymphoma protein 2 family members for their survival (Chuang, Yee et al. 1998, Moulding, Akgul et al. 2001, Vier, Groth et al. 2016). The mRNA expression level of A1 protein is regulated by the Janus kinase pathway while the expression of Myeloid cell leukemia-1 depends on the PI3K pathway during steady state (Vier, Groth et al. 2016). The cell viability measurements from the current work suggest that PMN isolated from both species show extended survival, with minimal death events as indicated by flow cytometry. Thus, the isolation procedure used does not cause cell death and leaves PMN functionally active for extended time. However, the involvement of mitochondria in cell survival could not be explored in this study. Additional investigations employing mitochondria-targeting

compounds will be required to assess their roles in survival of PMN under *ex vivo* conditions. In addition, treating the cells with glucocorticoids to delay spontaneous apoptosis may also inform on potential differences between the two species as well as on viability post enrichment (Madsen-Bouterse, Rosa et al. 2006). It has previously been reported that bovine PMN isolated using Percoll density gradient when cultured for 12 h showed disrupted mitochondria while inclusion of dexamethasone maintained the stability of mitochondrial membrane (Madsen-Bouterse, Rosa et al. 2006). Aside from this, erylysis solution used for cell isolation (Vuorte, Jansson et al. 2001), culture medium (Hannah, Nadra et al. 1998) and temperature play an important role in maintaining PMN viability (Lecchi, Rota et al. 2016).

To meet the energy needs for phagocytosis and respiratory burst, PMN depend on glycolysis (Borregaard and Herlin 1982). Glucose import is regulated by the sodium coupled glucose transporters or by the glucose transporter facilitators (Scheepers, Joost et al. 2004). The mitochondrial membrane potential via the glycerol-3-phosphate shuttle also sustains aerobic glycolysis in PMN (van Raam, Sluiter et al. 2008). Recently, it has been shown that PMN granules contain stores of glycogen which are important for PMN survival during hypoxic conditions (Sadiku, Willson et al. 2021). Deprivation of glucose had a considerable impact on glucose uptake by PMN. In contrast to human PMN, increased 2NBDG uptake by bovine PMN implies a higher need for glucose. Yet, the fold change of 2NBDG uptake over time suggests no significant difference between PMN from the two species. Hence, it remains unclear whether human and cattle PMN have different metabolic needs in the tested experimental conditions. Metabolic flux measurements could be used to quantify the oxygen consumption and proton production rates which can be correlated to mitochondrial function and glycolysis, respectively. This method is currently being identified as a new approach for assessing PMN metabolism (Fossati, Moulding et al. 2003, Quiroga, Alarcon et al. 2020). Along with the above discussed functions, other key functions of the human and bovine PMN such as ROS burst and MPO release as a degranulation marker have been comparatively evaluated in this study in the context of their responses to mycobacteria and will be discussed in the sections 6.3.2 and 6.4.

The activation status of whole blood PMN in comparison to isolated PMN was assessed by flow cytometry. Regarding expression levels of CD11b and CD62L in MACS isolated human PMN it has already been shown that CD11b is slightly increased upon purification, and CD62L showed no downregulation compared to levels detected in blood PMN (Zyntek, Schmitz et al. 2020). In the current study, human PMN isolated using density gradient upregulated CD11b and downregulated CD62L in comparison to magnetically isolated cells, suggesting that the gradient activates PMN. These results are in accordance with the manufacturer's data (Zyntek, Schmitz et al. 2020). MACS sorted bovine PMN showed a slight increase in CD11b expression and interestingly also an increase in CD62L surface levels. During homeostasis, a homogeneous population of circulating human PMN display nuclear segmentation and phenotypically these cells are $CD16^{high}$ (FcγRIII) and $CD62L^{high}$ (L-selectin) (van Grinsven, Textor et al. 2019). Upon LPS stimulation three subsets of PMN have been detected ($CD16^{low}$

banded PMN, CD16^{high} CD62L^{high} segmented nuclei equal to homeostatic PMN and a third subset CD16^{high} and CD62L^{low} PMN) with increased segmentation and lobulation of nucleus (van Grinsven, Textor et al. 2019). The banded and hyper segmented subsets remained undetected in the circulation of healthy humans (van Grinsven, Textor et al. 2019). In bovines, subsets unrelated to CD62L abundances, but categorized on phenotypic profiles of other cell surface markers have recently been described. A new regulatory subset of PMN which express MHCII and suppress T cell proliferation have been identified (Rambault, Doz-Deblauwe et al. 2021). During *Ostertagia ostertagi* parasite infection in cattle, the MHCII+ PMN in circulation and particularly in spleen produce the suppressive IL-10 making the PMN-T cell interaction less effective (Li, Si et al. 2019). The question of whether the CD62L^{high} subset is enriched in bovine at steady state or whether it is related to the isolation process needs further investigation. Moreover, the immune features of a CD62L^{high} PMN population awaits characterization.

6.3 Responses of bovine and human neutrophils to attenuated *M. bovis* BCG

6.3.1 Phagocytosis and early events

Comparative evaluation of BCG internalization in PMN from cattle and humans revealed that human cells more efficiently phagocytosed bacteria compared to bovine counterparts. Differences in phagocytosis was the first major difference observed between PMN from the two species and this was previously unknown. A recent finding comparing responses of human and bovine MΦ to *M. bovis* and *M. tb* revealed that, bovine cells more avidly phagocytosed bacteria, about 10 times more, compared to human MΦ. Therefore, the infection ratios were normalized by using lower MOI for bovine and higher MOI for human MΦ (Queval, Fearns et al. 2021). This suggests that bovine MΦ are highly reactive to mycobacterial infection in comparison to bovine PMN. A head-to-head comparison of distinct bovine myeloid cells was beyond the scope of this thesis and only such an experiment would demonstrate that in cattle PMN are hyporesponsive with regard to BCG internalization. Serum antibodies and complement proteins decorate opsonized bacteria and renders them recognizable by the CR3 or FcR. Fresh serum opsonization enhanced the uptake of BCG by both human and bovine PMN and interestingly human PMN had higher efficiency to phagocytose serum opsonized BCG than bovine cells. The effect of serum opsonization was in line with the previous studies performed with human PMN (Majeed, Perskvist et al. 1998, Persson, Blomgran-Julinder et al. 2009). Enhanced uptake of opsonized bacteria, e.g. *M. smegmatis* and *Staphylococcus aureus,* by human PMN has been already reported (Vandenbroucke-Grauls, Thijssen et al. 1984, Lu, Porter et al. 2014, Miralda, Klaes et al. 2020).

CR3 is a well-known receptor for phagocytosis of non-opsonized and opsonized mycobacteria (Velasco-Velázquez, Barrera et al. 2003). Blocking the CR3 using antibodies against CD11b

followed by infection of human and bovine PMN with non-opsonized BCG did not alter bacterial uptake by both cell types. However, there was a reduction in uptake of opsonized BCG solely by human PMN. The non-opsonic binding region of the CR3 is identified as the lectin like C-domain and it binds to β-glucans such as zymosan, mannose, NADG and glucose. The opsonic binding occurs via the I-domain which binds to the iC3b component of the CR3 (Ross, Cain et al. 1985, Velasco-Velázquez, Barrera et al. 2003). In congruence with these observations, opsonized BCG probably uses the I-domain of the CR3 to gain entry into human PMN. Responses of bovine PMN to CD11b block remains elusive and require further studies. Furthermore, as there was no reduction in uptake of non-opsonized BCG after CD11b block in both human and bovine PMN it could be speculated that either phagocytosis occurs via a distinct outside-in signaling or that different ligands present on the mycobacteria bind differently to the host cell. Using antibody against CD11b, it was found that phagocytosis of non-opsonized *M. gordonae* and *M. avium* was significantly reduced in human PMN (Nakayama, Yoshizaki et al. 2008, Nakayama, Kurihara et al. 2016). Therefore, different uptake mechanism for BCG entry into PMN were explored and these will be discussed below.

NADG was used in phagocytosis assays to block the C-domain of CR3. Significant reduction in uptake of non-opsonized BCG by human PMN suggests internalization of BCG via the C-domain of CR3, while the bovine PMN showed no reduction. The uptake of *E. coli* bioparticle was yet inhibited by NADG treatment in bovine PMN. In human PMN the NADG treatment inhibits the uptake of *M. kansasii* suggesting the importance of the association of GPI-anchored proteins in phagocytosis of mycobacteria (Peyron, Bordier et al. 2000). During *E. coli* uptake by human MΦ, CR3 recognizes bacterial LPS via the lipid A region of the molecule (Wright and Jong 1986). This strongly suggests that the binding sites on CR3 for LPS appears to be distinct from the one that binds the C3bi fragments or different glyco/protein ligands (Wright and Jong 1986, Wright, Levin et al. 1989). NADG effects on bovine PMN, i.e. inhibition of *E. coli* uptake but not BCG, could thus be explained by the molecular determinants related to CR3 specificity. Whether the C-domain of CR3 is used by BCG for internalization by bovine PMN could not be determined. Further investigations of different pathways are needed for going into more mechanistic insights.

Under non-opsonic conditions, the major targets of the pathogen are microdomains enriched in lipid rafts present in the plasma membrane of PMN (Iwabuchi, Nakayama et al. 2012). The major components of these rafts are the glycosphingolipids and cholesterol (Iwabuchi, Nakayama et al. 2012). Mycobacteria use various pathways to gain entry into PMN, including membrane cholesterol (Astarie-Dequeker, Le Guyader et al. 2009). The importance of cholesterol has been shown for phagocytosis of mycobacteria by human MΦ (Gatfield and Pieters 2000, Viswanathan, Jafurulla et al. 2015) and PMN (Pierini, Eddy et al. 2003, Solomkin, Robinson et al. 2007). Depletion of cholesterol using MβCD significantly reduced BCG uptake by human PMN and these results are in conformity with published work regarding the mode of action of MβCD (Pierini, Eddy et al. 2003). Even for an unrelated pathogen, the protozoan *Toxoplasma gondii*, treatment with MβCD inhibited the uptake by human MΦ (Cruz, Cruz et

al. 2014). However, bovine PMN reacted differently to cholesterol depletion. There was no reduction in BCG uptake with the same concentration of MβCD which was used for human PMN and which did not alter cellular viability. Also, the uptake of *E. coli* bioparticles by bovine PMN was not reduced after MβCD treatment suggesting no bacterial species dependency. Therefore, it was hypothesized that bovine PMN have higher pools of membrane cholesterol. *M. tb*, *M. smegmatis* and *M. kansasii* use cholesterol and CR3 to enter human MΦ and PMN (Peyron, Bordier et al. 2000, Cougoule, Constant et al. 2002, Astarie-Dequeker, Le Guyader et al. 2009). Total and free cholesterol content in naïve and BCG infected human and bovine PMN was similar. Thus, cells from these two species do not differ in the cholesterol content. Considering relevance of this lipid for mycobacterial internalization it remains to be established whether its compartmentalization, as well as compartmentalization of other lipids such as glycosphingolipids is similar in cattle and human PMN.

An intact cytoskeleton is required for phagocytosis. Phagocytosis of bacteria by human PMN was reduced by cytochalasin D. However, when bovine PMN were treated with cytochalasin D prior to infection, no significant reduction in uptake was detected. Internalization of *E. coli* was yet restricted after cytochalasin D treatment. This suggests that BCG might not have been completely internalized in bovine PMN. Examination by confocal microscopy, including live cell imaging, would demonstrate whether kinetics of the phagocytosis is variable and also conclusively show the intracellular localization of BCG within cattle PMN. The involvement of dectin-1 in the uptake of BCG was ruled out as blocking dectin-1 using laminarin did not reduce phagocytosis of BCG by both human and bovine PMN. Mycobacteria lack β-glucans on their membrane, which is the bona-fide ligand for dectin-1 and a major component in the cell wall of yeasts. Mycobacteria possess α-glucans instead which are recognized by DC-SIGN (Geurtsen, Chedammi et al. 2009).

In the current study experiments were performed with monoclonal antibodies targeting CD11b, however the involvement of FcR in the uptake cannot be excluded. Isolation of bovine PMN required blocking of the FcR before antibody labelling and therefore these receptors likely could not be targeted during the phagocytosis studies. The studies involving phagocytosis give a basic idea about the differential behavior of the bovine PMN in comparison to the human PMN. The lower phagocytic ability of bovine PMN, lack of inhibitory effects with anti-CD11b monoclonals and distinctive response to chemical inhibitors are the major findings observed in bovine PMN.

6.3.2 Cell activation and microbial killing

Among other PMN functions, the production of ROS (mainly from the NADPH complex) is crucial for bacterial killing. Survival of mycobacteria depends on the levels of ROS produced by the host cells (Esquivel-Solis, Vallecillo et al. 2013). The pathogen survives if the ROS levels are scavenged by the pathogen's antioxidant systems (Jamaati, Mortaz et al. 2017). This study

demonstrated total abundant ROS production by PMN after PMA stimulation and reduced levels upon BCG infection. PMA induces ROS release, exocytosis and NET formation by direct activation of PKC (Saito, Takahashi et al. 2005). PMA is also known as a potent activator of human PMN (Gay and Stitt 1990, Takei, Araki et al. 1996). The kinetics of ROS production by bovine PMN were significantly lower in comparison to human PMN. The magnitude of ROS release by PMA stimulated bovine PMN differs with the donor animal (Salgar, Paape et al. 1991). Unlike PMA, PAF at higher concentrations induces ROS release and azurophilic degranulation in bovine PMN (Swain, Bunger et al. 1998, Larrazabal, Carretta et al. 2017). Bovine PMN express a high affinity PAF receptor coupled to G-protein (Burgos, Hidalgo et al. 2004). Therefore, treatment of cattle PMN with PAF at a higher concentration might be an alternative to PMA stimulation for a robust ROS release. Infection with BCG at a high MOI caused significant ROS release by human PMN, whereas, bovine counterparts released negligible amount of ROS in same conditions. This indicates low responsiveness of bovine PMN towards BCG infection and could correlate with the low phagocytic rate. The ROS burst by human PMN after BCG infection however failed to kill BCG, as demonstrated in the killing assays. No reduction in CFU was observed in PMN over time irrespective of the origin of the cells. Contradictory results have been reported regarding the killing abilities of bovine PMN against BCG and *Mycobacterium avium* subsp*. Paratuberculosis* (Ladero-Auñon, Molina et al. 2021). Of note, the setup and monitoring time largely differed in published reports. Ladero-Auñon *et al*. considered CFU at 0 h as total inoculated bacteria and CFU at 24 h was calculated as total inoculated bacteria minus the CFU obtained from the infection supernatant (non-internalized non-killed bacteria) and the bacteria containing cells (internalized and non-killed bacteria). Since, PMN are short lived it remains unclear how PMN death would impact on such an extended read out. In this thesis, CFU obtained at 30 min was compared to the other timepoints and PMN from both species were inefficient at killing BCG.

The ROS burst and degranulation of the azurophilic granules are important for NET formation (Papayannopoulos, Metzler et al. 2010, Metzler, Fuchs et al. 2011). MPO released by human PMN during NET generation kills *Staphylococcus aureus* in the presence of H_2O_2 (Parker, Albrett et al. 2012). During infection, PMN from CGD patients with lower ROS generation release fewer NETs (Akong-Moore, Chow et al. 2012). Azurophilic granules constitute the major mycobactericidal proteins and restrict the replication of *M. tb* in human MΦ (Jena, Mohanty et al. 2012). Comparison of mycobactericidal activity of azurophilic granules and peroxidase negative granules in PMN suggested that azurophilic granules were more efficient at killing *M. smegmatis* and BCG compared to peroxidase negative granules (Jena, Mohanty et al. 2012). The lack of MPO release after BCG infection, as well as the lack of substantial differences in release between the two species, suggests that BCG failed to promote degranulation. A recent study revealed that human PMN enhance the control of *M. tb* infected MΦ in a ROS- and MPO-dependent manner, thus suggesting importance of degranulation for cooperative killing of virulent mycobacteria (Andersson, Larsson et al. 2020). A potential role of free fatty acid stimulation of bovine PMN in mediating the release of azurophilic granules has been studied in the context of cows suffering from a metabolic

disorder (Song, Jiang et al. 2022). Fatty acids represent an alternative to PMA to induce MPO release in cattle cells and could be used to investigate effects of degranulation in context of bacterial pathogens. Along with the granule contents PMN also release a wide variety of cytokines after mycobacterial infection (Gideon, Phuah et al. 2019). Bovine PMN infected with *Mycoplasma bovis* release TNF-α (Jimbo, Suleman et al. 2017, Gondaira, Nishi et al. 2021). BCG-infected human PMN produce undetectable levels of TNF-α (Morel, Badell et al. 2008). *M. tb* induces significantly higher amount of TNF-α compared to BCG in human PMN (Hilda, Selvaraj et al. 2012) and stimulation of human PMN with TLR ligands leads to increased release of TNF-α subsequent *M. tb* infection (Hilda and Das 2015). In experiments included in this thesis both human and bovine PMN released negligible amounts of TNF-α in response to BCG. These observations are in line with published report (Hilda, Selvaraj et al. 2012). Bovine PMN release IL-8 upon BCG infection (Ladero-Auñon, Molina et al. 2021) and in TB patients IL-8 released by PMN is effective in recruiting T lymphocytes and monocytes (Hilda and Das 2015, Krupa, Fol et al. 2015). In our hands BCG induced IL-8 release by bovine and human PMN. Although due to the small sample size statistical significance was not reached. The data suggests propensity of cells from both the species to produce IL-8, but not TNF-α upon BCG encounter.

Altogether, the current study provides novel insights into the basic biology of cattle and human PMN and offers details on their interaction with BCG. The results advance the knowledge about functions of bovine PMN during mycobacterial infection.

6.4 Responses of bovine neutrophils to BCG, *M. bovis* and *M. tb*

M. bovis, the causative agent for bTB is also causing zoonotic TB in humans (Malama, Johansen et al. 2014, Jiang, Wang et al. 2015, Duffy, Srinivasan et al. 2020, Belete, Tilahun et al. 2021). Not only has *M. bovis* affected human health, it has also resulted in significant challenges to dairy industry causing economic losses (Tschopp, Schelling et al. 2009, Gumi, Schelling et al. 2012). Previous studies with bovine MΦ and virulent as well as attenuated *M. bovis* provided evidence for a differential gene expression in the infected host cell (Wedlock, Kawakami et al. 2006, Blanco, Nunez-Garcia et al. 2009). Bovine MΦ restrict the growth of BCG whereas *M. bovis* grows progressively between different animal species such as cattle, deer, possums, ferrets and mice (Aldwell, Wedlock et al. 2001). *M. bovis* infection of bovine MΦ enhances cytokine production thereby reducing the viability of the cells in comparison to BCG (Aldwell, Wedlock et al. 1996). A comparative omics study with *M. tb* and *M. bovis* infected bovine MΦ has revealed an increased expression of ESX-1 secretion system in *M. bovis* and more activated DNA sensing pathways in MΦ challenged with *M. bovis* (Malone, Rue-Albrecht et al. 2018). Along with this, lipidomic studies have reported a larger variety of lipids that are highly expressed in cells exposed to *M. bovis* in comparison to *M. tb* (Gao, Cai et al. 2022). *M. tb* causes an increase in polyketides and glycerophospholipids

whereas *M. bovis* causes a rise in sterol lipids and glycerophospholipid thereby altering the lipid metabolism in bovine MΦ (Gao, Cai et al. 2022). *M. tb* triggers the formation of foam cells by accumulation of various lipids and likely escapes the bovine MΦ and persist in the host (Singh, Jamwal et al. 2012, Ahluwalia, Pandey et al. 2017). Compared to BCG-infected MΦ, the virulent strains; *M. tb* and *M. bovis* replicate faster in human monocyte-derived MΦ (Mendoza-Coronel and Castanon-Arreola 2016). Such studies have not been done so far with bovine PMN. Also, whether these cells help in resolving or enhance the infection is still unclear.

In comparative studies included in this thesis, infection of bovine PMN with *M. tb* or BCG revealed no difference in uptake and no reduction was observed after blocking with antibodies against CD11b. This suggests that under *ex vivo* conditions receptors on bovine PMN recognize BCG and *M. tb* similarly. In a study investigating bovine MΦ infected with *M. tb* and *M. bovis* both pathogens were phagocytosed at a higher rate compared to human cells (Queval, Fearns et al. 2021). Following infection, *M. tb* and *M. bovis* replicated effectively in bovine MΦ however, only *M. bovis* promoted multinucleated giant cell formation suggesting a unique host-pathogen interaction (Queval, Fearns et al. 2021). Besides this, in case of PMN, following phagocytosis, the microbes reside in a phagosome which fuses with the PMN granules (Jena, Mohanty et al. 2012) and in addition, PMN may release granular contents in response to the encountered pathogen (Miralda, Klaes et al. 2020). MPO release as a marker for azurophilic granules revealed no difference in release between BCG or *M. tb* infection. Whether other functions such as ROS release, cytokines and other granule contents such as MMP9 which are abundantly found in bovine PMN differ upon challenge with BCG and *M. tb* needs to be clarified in future investigations. Comparison of the phagocytic ability of bovine PMN for virulent strains *M. bovis* and *M. tb* unveiled an interesting outcome: the percent phagocytosis was higher for *M. bovis* while the mean phagocytosis was higher for *M. tb* infected bovine PMN. This could indicate that bovine PMN may just take up more *M. tb*. To confirm this hypothesis, confocal microscopic studies will be required. The capsular polysaccharide in different mycobacterial strains may differ and this could relate to their interaction with the CR3 (Cywes, Hoppe et al. 1997).The uptake of Ops *M. bovis* was also higher in comparison to Ops *M. tb,* akin to increased internalization of Ops BCG compared to Ops *M. tb*. As BCG is also an *M. bovis* strain, this might be a species-specific difference. *In vitro* studies with *M. tb* infected human PMN suggest an association between PMN and *M. tb*, which increases when the bacteria is opsonized with fresh human serum (Romero, Basile et al. 2014). Complement mediated uptake of *M. tb* in human PMN is reduced by blocking CD11b with antibodies (Romero, Basile et al. 2014). However, such information in context of bovine PMN is missing. It also remains unanswered how the virulent mycobacterial strains are phagocytosed by bovine PMN as CD11b blocking had no significant impact bacilli engulfment. It could only be speculated that the strain-dependent thickness or composition of capsular polysaccharides could affect the binding of the distinct mycobacteria to the PMN. The differences observed with the virulent strains are preliminary and need an experimental revisit to confirm the observations. Pre-treatment of bovine PMN with blocking reagents did

not reduce the uptake of *M. bovis* and *M. tb*. According to the literature, cytochalasin D treatment reduced phagocytosis of *E. coli* and *Staphylococcus aureus* by bovine granulocytes (Jerjomiceva, Seri et al. 2014). However, in the current study contrasting results were obtained for bovine PMN with BCG, *M. bovis* and *M. tb* suggesting uniqueness of mycobacteria in comparison to other bacteria, or prolonged attachment at the cell wall without involvement of the actin cytoskeleton. Previous studies with human monocyte-derived MΦ have shown that treating the cells with MβCD for 30 min, inhibits the uptake of *M. tb* in a dose-dependent manner (Astarie-Dequeker, Le Guyader et al. 2009). The effect of MβCD treatment on the depletion of cholesterol from the membrane and successive reduction in phagocytosis of mycobacteria by bovine PMN has not been previously addressed. MβCD did not affect phagocytosis of virulent mycobacteria by bovine PMN. Therefore, a thorough analysis of the bovine PMN cell membrane is required in order to understand the potential reason for the effect which probably might be due to distinct membrane cholesterol patterns. NADG block seemed to have no effect in the reduction in uptake of the virulent strains. It can be speculated that mycobacteria might interfere with the lectin-binding site of bovine PMN.

Following mycobacterial uptake, the ability of bovine PMN to release granular contents such as MPO suggests an activated state of the PMN. However, for both MTBC virulent strains, very low MPO release was recorded which indicates lack of degranulation of azurophilic granules. *M. bovis* may boost MPO levels as its mRNA levels were increased post infection in bovine PMN (Wang, Zhou et al. 2013). It can be speculated that azurophilic granules might not be released within the incubation time of 30 min used in the current study. Therefore, other granule release markers such as MMP9 which are also abundantly present in bovine PMN would be an alternative to investigate degranulation early after infection. Previous studies have shown that IFN-γ stimulation of bovine MΦ induces the release of TNF-α. Also, *M. bovis* infected cells released higher amount of TNF-α in comparison to BCG infected cells (Denis, Wedlock et al. 2005). In the current study, no difference in TNF-α release by bovine PMN between the two virulent mycobacterial strains was found. This is in line with observations from bovine blood-derived MΦ infected with BCG, *M. tb* and *M. bovis* (Piercy, Werling et al. 2007). Whether observed changes in the TNF-α release by bovine PMN is due to the different receptor usage by BCG, *M. tb* and *M. bovis* remains to be investigated. It is possible that *M. tb* and *M. bovis* reside in different intracellular compartment leaving *M. tb* accessible to PMN killing mechanism. MΦ from two different cattle breeds had no significant differences in the cytokine release post *M. tb* or *M. bovis* infection (Vordermeier, Ameni et al. 2012). IL-8 has been found in the bronchoalveolar lavage of *M. tb* infected TB patients and the concentration of IL-8 could be corelated to the leukocyte number (Kurashima, Mukaida et al. 1997, Ameixa and Friedland 2001). Increased levels of IL-8 after *M. bovis* infection suggests increased accumulation of bovine PMN at the infection site *in vivo* which may result in pathology instead of resolution of infection.

This study identified differences in responses of bovine PMN to BCG, *M. bovis* and *M. tb*. While no differences in uptake and MPO release were found between BCG and *M. tb,* the bovine cells took up higher amount of *M. tb* in comparison to *M. bovis*. Whether PMN are involved in the clearance of bacteria during *M. tb* infection in cattle remains to be investigated. Heightened phagocytosis of *M. tb* may play a role in this process. These studies shed new light on species-specific host pathogen interaction during TB.

7 Summary and Outlook

PMN are one of the most important cells of the innate immune system and are responsible for fast clearance of invading pathogens in most circumstances. The role of human PMN during mycobacterial infection have been widely studied. Nevertheless, there are contradicting results regarding their role in protection or pathology during TB. Similar studies focusing on bovine PMN and their role in *M. bovis* infection remain understudied. Also, not much is known about attenuation of *M. tb* in cattle and responses of PMN to this MTBC member.

The major aims of this study were to i) gain insights into bovine PMN biology and the cellular processes triggered by challenge with virulent mycobacteria and to ii) find out whether interspecies differences result in different outcomes upon *in vitro* challenge. In the first part of the work, a new isolation method for bovine PMN from whole blood was developed. Human and bovine PMN have different buoyant properties and hence need to be isolated using different procedures. The magnetic isolation method developed within this thesis is robust and results in very good yields of highly pure, viable bovine PMN populations. This is extremely advantageous and indispensable for downstream functional assays that are required to be performed on a single day.

The second goal of this study was to compare and contrast the functional differences between bovine and human PMN upon BCG infection. The findings reveal for the first time that human PMN phagocytose more BCG in comparison to bovine counterparts. Non-opsonized bacteria were internalized via the lectin-like C-domain, require cholesterol and an active cytoskeleton in human PMN, whereas opsonized bacteria entered cells via the CR3 and, in particular, CD11b. It remains unresolved why bovine PMN reacted differently, notably phagocytosis remained unaltered, to various treatments, including blocking monoclonal antibodies to CD11b and chemical inhibitors altering the cell membrane. Nonetheless, the increased uptake of BCG by human PMN correlates to more potent response of these cells in functional assays in comparison to bovine PMN. No PMN intrinsic differences were found in the basal cholesterol content. Comparative assays with the virulent strains would be essential in order to generalize these observations.

The third aim was to investigate the responses of bovine PMN to BCG, *M. tb* and *M. bovis*. While there was no difference in uptake between BCG and *M. tb,* serum opsonized BCG was taken up at a higher amount. This finding suggests differential binding of bacterial epitopes to host cell receptors which modulates mycobacteria uptake. However, between the virulent strains *M. tb* and *M. bovis*, the human-adapted bacillus was phagocytosed at a higher rate which hints towards the possibility of rapid recognition and clearance of *M. tb* in bovine host thereby possibly preventing pathology. The release of selective cytokines by PMN post infection with the virulent strains offers baseline information relevant for processes that probably occur *in vivo*. This work for the first time provides insights into responses of bovine

PMN to mycobacteria in a two-tier approach: by cross-species analysis of PMN responses to selected mycobacterium and by head-to-head analysis of bovine PMN to animal-adapted and human-adapted mycobacteria.

As a prospect for future research in bovine PMN biology in the context of mycobacterial infection, it would be highly advantageous to compare the subcellular localization of *M. tb* and *M. bovis* in bovine PMN using confocal and/or electron microscopy. This analysis would confer proof on attachment or internalization of mycobacteria by PMN and identify the features of the mycobacteria-containing compartments. Also, in-depth investigations of additional entry pathways for the pathogen in bovine cells would be informative for unlocking downstream cell signaling events. In addition, PMN viability studies will be meaningful particularly in bovine PMN challenged with *M. bovis* and *M. tb,* given the impact of death patterns on tissue pathology. Current results and follow up studies will contribute to the understanding of the roles of PMN in controlling elimination or growth of *M. bovis* and *M. tb* in cattle.

8 References

Abadie, V., E. Badell, P. Douillard, D. Ensergueix, P. J. Leenen, M. Tanguy, L. Fiette, S. Saeland, B. Gicquel and N. Winter (2005). "Neutrophils rapidly migrate via lymphatics after *Mycobacterium bovis* BCG intradermal vaccination and shuttle live bacilli to the draining lymph nodes." Blood **106**(5): 1843-1850.

Abrahams, K. A. and G. S. Besra (2018). "Mycobacterial cell wall biosynthesis: a multifaceted antibiotic target." Parasitology **145**(2): 116-133.

Achkar, J. M., S. D. Lawn, M. Y. Moosa, C. A. Wright and V. O. Kasprowicz (2011). "Adjunctive tests for diagnosis of tuberculosis: serology, ELISPOT for site-specific lymphocytes, urinary lipoarabinomannan, string test, and fine needle aspiration." Journal of Infectious Diseases **204 Suppl 4**: S1130-1141.

Aga, E., D. M. Katschinski, G. van Zandbergen, H. Laufs, B. Hansen, K. Muller, W. Solbach and T. Laskay (2002). "Inhibition of the spontaneous apoptosis of neutrophil granulocytes by the intracellular parasite *Leishmania major*." Journal of Immunology **169**(2): 898-905.

Aga, E., A. Mukherjee, D. Rane, V. More, T. Patil, G. van Zandbergen, W. Solbach, J. Dandapat, H. Tackenberg, M. Ohms, A. Sarkar and T. Laskay (2018). "Type-1 interferons prolong the lifespan of neutrophils by interfering with members of the apoptotic cascade." Cytokine **112**: 21-26.

Agier, J., M. Efenberger and E. Brzezinska-Blaszczyk (2015). "Cathelicidin impact on inflammatory cells." Central European Journal of Immunology **40**(2): 225-235.

Ahluwalia, P. K., R. K. Pandey, P. K. Sehajpal and V. K. Prajapati (2017). "Perturbed microRNA Expression by *Mycobacterium tuberculosis* Promotes Macrophage Polarization Leading to Pro-survival Foam Cell." Frontiers in Immunology **8**: 107.

Akong-Moore, K., O. A. Chow, M. von Kockritz-Blickwede and V. Nizet (2012). "Influences of chloride and hypochlorite on neutrophil extracellular trap formation." PLoS One **7**(8): e42984.

Aldwell, F. E., D. N. Wedlock and B. M. Buddle (1996). "Bacterial metabolism, cytokine mRNA transcription and viability of bovine alveolar macrophages infected with *Mycobacterium bovis* BCG or virulent M. bovis." Immunology and Cell Biology **74**(1): 45-51.

Aldwell, F. E., D. N. Wedlock, L. J. Slobbe, J. F. Griffin, B. M. Buddle and G. S. Buchan (2001). "In vitro control of *Mycobacterium bovis* by macrophages." Tuberculosis (Edinb) **81**(1-2): 115-123.

Alexander, K. A., P. N. Laver, A. L. Michel, M. Williams, P. D. van Helden, R. M. Warren and N. C. Gey van Pittius (2010). "Novel *Mycobacterium tuberculosis* complex pathogen, *M. mungi*." Emerging Infectious Diseases **16**(8): 1296-1299.

Alvarado-Kristensson, M., F. Melander, K. Leandersson, L. Ronnstrand, C. Wernstedt and T. Andersson (2004). "p38-MAPK signals survival by phosphorylation of caspase-8 and caspase-3 in human neutrophils." Journal of Experimental Medicine **199**(4): 449-458.

Ameixa, C. and J. S. Friedland (2001). "Down-regulation of interleukin-8 secretion from Mycobacterium tuberculosis-infected monocytes by interleukin-4 and -10 but not by interleukin-13." Infection and Immunity **69**(4): 2470-2476.

Anand, P. K. and D. Kaul (2005). "Downregulation of TACO gene transcription restricts mycobacterial entry/survival within human macrophages." FEMS Microbiology Letters **250**(1): 137-144.

Andersson, A. M., M. Larsson, O. Stendahl and R. Blomgran (2020). "Efferocytosis of apoptotic neutrophils enhances control of *Mycobacterium tuberculosis* in HIV-coinfected macrophages in a myeloperoxidase-dependent manner." Journal of Innate Immunity **12**(3): 235-247.

Anjani, G., P. Vignesh, V. Joshi, J. K. Shandilya, D. Bhattarai, J. Sharma and A. Rawat (2020). "Recent advances in chronic granulomatous disease." Genes & Diseases **7**(1): 84-92.

Aparna, M., L. Rao, V. Kunhikatta and R. Radhakrishnan (2015). "The role of MMP-2 and MMP-9 as prognostic markers in the early stages of tongue squamous cell carcinoma." Journal of Oral Pathology Medicine **44**(5): 345-352.

Ardain, A., R. Domingo-Gonzalez, S. Das, S. W. Kazer, N. C. Howard, A. Singh, M. Ahmed, S. Nhamoyebonde, J. Rangel-Moreno, P. Ogongo, L. Lu, D. Ramsuran, M. de la Luz Garcia-Hernandez, K. U. T, M. Darby, E. Park, F. Karim, L. Melocchi, R. Madansein, K. J. Dullabh, M. Dunlap, N. Marin-Agudelo, T. Ebihara, T. Ndung'u, D. Kaushal, A. S. Pym, J. K. Kolls, A. Steyn, J. Zuniga, W. Horsnell, W. M. Yokoyama, A. K. Shalek, H. N. Kloverpris, M. Colonna, A. Leslie and S. A. Khader (2019). "Group 3 innate lymphoid cells mediate early protective immunity against tuberculosis." Nature **570**(7762): 528-532.

Areda, D. B., A. Muwonge and A. B. Dibaba (2019). Status of Bovine Tuberculosis in Ethiopia: Challenges and Opportunities for Future Control and Prevention. Tuberculosis in Animals: An African Perspective**:** 317-337.

Astarie-Dequeker, C., L. Le Guyader, W. Malaga, F. K. Seaphanh, C. Chalut, A. Lopez and C. Guilhot (2009). "Phthiocerol dimycocerosates of *M. tuberculosis* participate in macrophage invasion by inducing changes in the organization of plasma membrane lipids." PLoS Pathogens **5**(2): e1000289.

Augenstreich, J., A. Arbues, R. Simeone, E. Haanappel, A. Wegener, F. Sayes, F. Le Chevalier, C. Chalut, W. Malaga, C. Guilhot, R. Brosch and C. Astarie-Dequeker (2017). "ESX-1 and phthiocerol dimycocerosates of *Mycobacterium tuberculosis* act in concert to cause phagosomal rupture and host cell apoptosis." Cellular Microbiology **19**(7).

Awah-Ndukum, J., J. Temwa, V. N. Ngwa, M. M. Mouiche, D. Iyawa and P. A. Zoli (2016). "Interpretation criteria for comparative intradermal tuberculin test for diagnosis of bovine tuberculosis in cattle in maroua area of cameroon." Veterinary Medicine International **2016**: 4834851.

Axelrod, S., H. Oschkinat, J. Enders, B. Schlegel, V. Brinkmann, S. H. Kaufmann, A. Haas and U. E. Schaible (2008). "Delay of phagosome maturation by a mycobacterial lipid is reversed by nitric oxide." Cellular Microbiology **10**(7): 1530-1545.

Babior, B. M., R. S. Kipnes and J. T. Curnutte (1973). "The production by leukocytes of superoxide, a potential bactericidal agent." The Journal of clinical investigation **52**(3): 741-744.

Baien, S. H., M. N. Langer, M. Heppelmann, M. von Kockritz-Blickwede and N. de Buhr (2018). "Comparison between K3EDTA and lithium heparin as anticoagulant to isolate bovine granulocytes from blood." Frontiers in Immunology **9**: 1570.

Bainton, D. F., J. L. Ullyot and M. G. Farquhar (1971). "The development of neutrophilic polymorphonuclear leukocytes in human bone marrow." Journal of Experimental Medicine **134**(4): 907-934.

Barbosa, L. A., P. P. Fiuza, L. J. Borges, F. A. Rolim, M. B. Andrade, N. F. Luz, G. Quintela-Carvalho, J. B. Lima, R. P. Almeida, F. K. Chan, M. T. Bozza, V. M. Borges and D. B. Prates (2018). "RIPK1-RIPK3-MLKL-associated necroptosis drives *Leishmania infantum* killing in neutrophils." Frontiers in Immunology **9**: 1818.

Barlow, N. D., J. M. Kean, G. Hickling, P. G. Livingstone and A. B. Robson (1997). "A simulation model for the spread of bovine tuberculosis within New Zealand cattle herds " Preventive veterinary medicine **32**: 57-75.

Bartlomiejczyk, M. A., A. S. Swierzko, A. Brzostek, J. Dziadek and M. Cedzynski (2014). "Interaction of lectin pathway of complement-activating pattern recognition molecules with mycobacteria." Clinical and Experimental Immunology **178**(2): 310-319.

Bassel, L. L. and J. L. Caswell (2018). "Bovine neutrophils in health and disease." Cell Tissue Research **371**(3): 617-637.

Bayissa, B., A. Sirak, A. Zewude, A. Worku, B. Gumi, S. Berg, R. G. Hewinson, J. L. N. Wood, G. J. Jones, E. consortium, H. M. Vordermeier and G. Ameni (2021). "Field evaluation of specific mycobacterial protein-based skin test for the differentiation of *Mycobacterium bovis*-infected and Bacillus Calmette Guerin-vaccinated crossbred cattle in Ethiopia." Transboundary Emerging Diseases.

Beckwith, K. S., M. S. Beckwith, S. Ullmann, R. S. Saetra, H. Kim, A. Marstad, S. E. Asberg, T. A. Strand, M. Haug, M. Niederweis, H. A. Stenmark and T. H. Flo (2020). "Plasma membrane damage causes NLRP3 activation and pyroptosis during *Mycobacterium tuberculosis* infection." Nature Communications **11**(1): 2270.

Belaaouaj, A., R. McCarthy, M. Baumann, Z. Gao, T. J. Ley, S. N. Abraham and S. D. Shapiro (1998). "Mice lacking neutrophil elastase reveal impaired host defense against gram negative bacterial sepsis." Nature Medicine **4**(5): 615-618.

Belaaouaj, A. a., K. S. Kim and S. D. Shapiro (2000). "Degradation of Outer Membrane Protein A in *Escherichia coli* Killing by Neutrophil Elastase." Science **289**(5482): 1185-1187.

Belete, A., S. Tilahun, B. Haile, Y. Demessie, S. Nigatu, A. Getachew, G. Getaneh, E. Kebede and M. Ejo (2021). "Prevalence of bovine tuberculosis and distribution of tuberculous lesions in cattle slaughtered at Gondar, Northwest Ethiopia." Infection Ecology and Epidemiology **11**(1): 1986919.

Belton, M., S. Brilha, R. Manavaki, F. Mauri, K. Nijran, Y. T. Hong, N. H. Patel, M. Dembek, L. Tezera, J. Green, R. Moores, F. Aigbirhio, A. Al-Nahhas, T. D. Fryer, P. T. Elkington and J. S. Friedland (2016). "Hypoxia and tissue destruction in pulmonary TB." Thorax **71**(12): 1145-1153.

Berg, S., D. Kaur, M. Jackson and P. J. Brennan (2007). "The glycosyltransferases of *Mycobacterium tuberculosis* - roles in the synthesis of arabinogalactan, lipoarabinomannan, and other glycoconjugates." Glycobiology **17**(6): 35-56R.

Berry, M. P., C. M. Graham, F. W. McNab, Z. Xu, S. A. Bloch, T. Oni, K. A. Wilkinson, R. Banchereau, J. Skinner, R. J. Wilkinson, C. Quinn, D. Blankenship, R. Dhawan, J. J. Cush, A. Mejias, O. Ramilo, O. M. Kon, V. Pascual, J. Banchereau, D. Chaussabel and A. O'Garra (2010). "An interferon-inducible neutrophil-driven blood transcriptional signature in human tuberculosis." Nature **466**(7309): 973-977.

Bertoni, G., A. Minuti and E. Trevisi (2015). "Immune system, inflammation and nutrition in dairy cattle." Animal Production Science **55**(7).

Bian, Z., Y. Guo, B. Ha, K. Zen and Y. Liu (2012). "Regulation of the inflammatory response: Enhancing neutrophil infiltration under chronic inflammatory conditions." The Journal of Immunology **188**(2): 844-853.

Bianco, M. V., F. C. Blanco, B. Imperiale, M. A. Forrellad, R. V. Roch, L. I. Klepp, A. A. Cataldi, N. Morcillo and F. Bigi (2011). "Role of P27 -P55 operon from *Mycobacterium tuberculosis* in the resistance to toxic compounds." BMC infectious diseases **11**: 195.

Blanco, F. C., J. Nunez-Garcia, C. Garcia-Pelayo, M. Soria, M. V. Bianco, M. Zumarraga, P. Golby, A. A. Cataldi, S. V. Gordon and F. Bigi (2009). "Differential transcriptome profiles of attenuated and hypervirulent strains of *Mycobacterium bovis*." Microbes Infection **11**(12): 956-963.

Blomgran, R., L. Desvignes, V. Briken and J. D. Ernst (2012). "*Mycobacterium tuberculosis* inhibits neutrophil apoptosis, leading to delayed activation of naive CD4 T cells." Cell Host Microbe **11**(1): 81-90.

Blomgran, R. and J. D. Ernst (2011). "Lung neutrophils facilitate activation of naive antigen-specific CD4+ T cells during *Mycobacterium tuberculosis* infection." The Journal of Immunology **186**(12): 7110-7119.

Bonilla, F. A. and H. C. Oettgen (2010). "Adaptive immunity." The Journal of Allergy and Clinical Immunology **125**(2 Suppl 2): S33-40.

Bonsall, M. a. (2013). "Stem cell biology is population biology: differentiation of hematopoietic multipotent progenitors to common lymphoid and myeloid progenitors." Theorotical biology and medical modelling **10**.

Borkute, R. R., S. Woelke, G. Pei and A. Dorhoi (2021). "Neutrophils in Tuberculosis: Cell Biology, Cellular Networking and Multitasking in Host Defense." International Journal of Molecular Sciences **22**(9).

Borregaard, N. and J. B. Cowland (1997). "Granules of human neutrophils polymorphonuclear leukocytes." Blood **89**: 3503-3521.

Borregaard, N. and T. Herlin (1982). "Energy metabolism of human neutrophils during phagocytosis." Journal of clinical investigaton **70**(3): 550-557.

Borregaard, N., M. Sehested, B. S. Nielsen, H. SengelØv and K. Lars (1995). "Biosynthesis of granule proteins in normal human bone marrow cells. Gelatinase is a marker of terminal neutrophil differentiation." Blood **85 (3)**: 812-817.

Braian, C., V. Hogea and O. Stendahl (2013). "*Mycobacterium tuberculosis*- induced neutrophil extracellular traps activate human macrophages." The Journal of Innate Immunity **5**(6): 591-602.

Branzk, N., A. Lubojemska, S. E. Hardison, Q. Wang, M. G. Gutierrez, G. D. Brown and V. Papayannopoulos (2014). "Neutrophils sense microbe size and selectively release neutrophil extracellular traps in response to large pathogens." Nature Immunology **15**(11): 1017-1025.

Braun, R. K., M. Franchini, F. Erard, S. Rihs, I. J. M. De Vries, K. Blaser, T. T. Hansel and C. Walker (1993). "Human peripheral blood eosinophils produce and release interleukin-8 on stimulation with calcium ionophore. ." European Journal of Immunology **24**(4): 956–960.

Brinkmann, V., B. Laube, U. Abu Abed, C. Goosmann and A. Zychlinsky (2010). "Neutrophil extracellular traps: how to generate and visualize them." Journal of Visualized Experiments(36).

Brinkmann, V., U. Reichard, C. Goosmann, B. Fauler, Y. Uhlemann, D. S. Weiss, Y. Weinrauch and A. Zychlinsky (2004). "Neutrophil Extracellular Traps Kill Bacteria." Science **303**(5663): 1532-1535.

Brites, D., C. Loiseau, F. Menardo, S. Borrell, M. B. Boniotti, R. Warren, A. Dippenaar, S. D. C. Parsons, C. Beisel, M. A. Behr, J. A. Fyfe, M. Coscolla and S. Gagneux (2018). "A new phylogenetic framework for the animal-adapted *Mycobacterium tuberculosis* complex." Frontiers in Microbiology **9**: 2820.

Broberg, L., P. Gonzalez-Cano, N. Arsic, Y. Popowych and P. J. Griebel (2021). "Isolation and characterization of eosinophils in bovine blood and small intestine." Veterinary Immunology and Immunopathology **242**: 110352.

Brodin, P., Y. Poquet, F. Levillain, I. Peguillet, G. Larrouy-Maumus, M. Gilleron, F. Ewann, T. Christophe, D. Fenistein, J. Jang, M. S. Jang, S. J. Park, J. Rauzier, J. P. Carralot, R. Shrimpton, A. Genovesio, J. A. Gonzalo-Asensio, G. Puzo, C. Martin, R. Brosch, G. R. Stewart, B. Gicquel and O. Neyrolles (2010). "High content phenotypic cell-based visual screen identifies *Mycobacterium tuberculosis* acyltrehalose-containing glycolipids involved in phagosome remodeling." PLoS Pathogens **6**(9): e1001100.

Brook, M., G. H. Tomlinson, K. Miles, R. W. Smith, A. G. Rossi, P. S. Hiemstra, E. F. van 't Wout, J. L. Dean, N. K. Gray, W. Lu and M. Gray (2016). "Neutrophil-derived alpha defensins control inflammation by inhibiting macrophage mRNA translation." PNAS **113**(16): 4350-4355.

Brosch, R., S. V. Gordon, M. Marmiesse, P. Brodin, C. Buchrieser, K. Eiglmeier, T. Garnier, C. Gutierrez, G. Hewinson, K. Kremer, L. M. Parsons, A. S. Pym, S. Samper, D. van Soolingen and S. T. Cole (2002). "A new evolutionary scenario for the *Mycobacterium tuberculosis* complex." PNAS **99 (6)**: 3684–3689.

Broset, E., C. Martin and J. Gonzalo-Asensio (2015). "Evolutionary landscape of the *Mycobacterium tuberculosis* complex from the viewpoint of PhoPR: implications for virulence regulation and application to vaccine development." mBio **6**(5): e01289-01215.

Broughan, J. M., J. Judge, E. Ely, R. J. Delahay, G. Wilson, R. S. Clifton-Hadley, A. V. Goodchild, H. Bishop, J. E. Parry and S. H. Downs (2016). "A review of risk factors for bovine tuberculosis infection in cattle in the UK and Ireland." Epidemiology and Infection **144**(14): 2899-2926.

Brown, G. B. and J. A. Roth (1991). "Comparison of the response of bovine and human neutrophils to various stimuli." Veterinary immunology and Immunopathology **28**(3-4): 201-218.

Buddle, B. M., F. E. Aldwell, A. Pfeffer, G. W. de Lisle and L. A. Corner (1994). "Experimental *Mycobacterium bovis* infection of cattle: effect of dose of *M. bovis* and pregnancy on immune responses and distribution of lesions." New Zealand Veterinary Journal **42**(5): 167-172.

Bulut, Y., K. S. Michelsen, L. Hayrapetian, Y. Naiki, R. Spallek, M. Singh and M. Arditi (2005). "*Mycobacterium tuberculosis* heat shock proteins use diverse Toll-like receptor pathways to activate pro-inflammatory signals." Journal of Biological Chemistry **280**(22): 20961-20967.

Burgos, R. A., M. A. Hidalgo, S. M. Matthei, R. Hermosilla, H. Folch and J. L. Hancke (2004). "Determination of specific receptor sites for platelet activating factor in bovine neutrophils." Veterinary Research **65**(5): 628-636.

Bussi, C. and M. G. Gutierrez (2019). "*Mycobacterium tuberculosis* infection of host cells in space and time." FEMS Microbiology Review **43**(4): 341-361.

Calmette, A. (1931). "Preventive vaccination against tuberculosis with BCG." Proceedings of the royal society of medicine **24**(11): 11481-11490.

Cambier, C. J., S. Falkow and L. Ramakrishnan (2014). "Host evasion and exploitation schemes of *Mycobacterium tuberculosis*." Cell **159**(7): 1497-1509.

Carlson, G. P. and J. J. Kaneko (1973). "Isolation of leukocytes from bovine peripheral blood." Proceedings of the society for Experimental biology and medicine **142**(3): 853-856.

Carrisoza-Urbina, J., E. Morales-Salinas, M. A. Bedolla-Alva, R. Hernandez-Pando and J. A. Gutierrez-Pabello (2019). "Atypical granuloma formation in *Mycobacterium bovis*-infected calves." PLoS One **14**(7): e0218547.

Carvalho, A. C. C., G. Amorim, M. G. M. Melo, A. K. A. Silveira, P. H. L. Vargas, A. S. R. Moreira, M. S. Rocha, A. B. Souza, M. B. Arriaga, M. Araujo-Pereira, M. C. Figueiredo, B. Durovni, E. S. J. R. Lapa, S. Cavalcante, V. C. Rolla, T. R. Sterling, M. Cordeiro-Santos, B. B. Andrade, E. C. Silva, A. L. Kritski and P. B. c. Re (2021). "Pre-treatment neutrophil count as a predictor of antituberculosis therapy outcomes: A multicenter prospective cohort study." Frontiers in Immunology **12**: 661934.

Casanova-Acebes, M., C. Pitaval, L. A. Weiss, C. Nombela-Arrieta, R. Chevre, A. G. N, Y. Kunisaki, D. Zhang, N. van Rooijen, L. E. Silberstein, C. Weber, T. Nagasawa, P. S. Frenette, A. Castrillo and A. Hidalgo (2013). "Rhythmic modulation of the hematopoietic niche through neutrophil clearance." Cell **153**(5): 1025-1035.

Cassetta, L., E. S. Baekkevold, S. Brandau, A. Bujko, M. A. Cassatella, A. Dorhoi, C. Krieg, A. Lin, K. Lore, O. Marini, J. W. Pollard, M. Roussel, P. Scapini, V. Umansky and G. J. Adema (2019). "Deciphering myeloid-derived suppressor cells: isolation and markers in humans, mice and non-human primates." Cancer Immunology Immunotherapy **68**(4): 687-697.

Cassidy, J. P., D. G. Bryson, J. M. Pollock, R. T. Evans, F. Forster and S. D. Neill (1998). "Early lesion formation in cattle experimentally infected with *Mycobacterium bovis*." Journal of Comparative Pathology **119**(1): 27-44.

Chambers, W. H., J. R. Taylor and P. H. Klesius (1983). "Isolation of bovine polymorphonuclear leukocytes by density gradient centrifugation." Veterinary Immunology and Immunopathology **5**(2): 197-202.

Chan, Y.-K., M.-H. Tsai, D.-C. Huang, Z.-H. Zheng and K.-D. Hung (2010). "Leukocyte nucleus segmentation and nucleus lobe counting." BMC Bioinformatics **11**(558): 1471-2105.

Chauhan, A. S., M. S. George, J. Lindahl, D. Grace and M. Kakkar (2019). "Community, system and policy level drivers of bovine tuberculosis in smallholder periurban dairy farms in India: a qualitative enquiry." BMC Public Health **19**(1): 301.

Cheng, Y. and J. S. Schorey (2018). "*Mycobacterium tuberculosis*-induced IFN-beta production requires cytosolic DNA and RNA sensing pathways." Journal of Experimental Medicine **215**(11): 2919-2935.

Christoffersson, G. and M. Phillipson (2018). "The neutrophil: one cell on many missions or many cells with different agendas?" Cell Tissue Research **371**(3): 415-423.

Chuang, P. I., E. Yee, A. Karsan, R. K. Winn and J. M. Harlan (1998). "A1 Is a Constitutive and Inducible Bcl-2 Homologue in Mature Human Neutrophils." Biophysical and Biochemical Research Communications **249**(2): 361-365.

Clay, H., J. M. Davis, D. Beery, A. Huttenlocher, S. E. Lyons and L. Ramakrishnan (2007). "Dichotomous role of the macrophage in early *Mycobacterium marinum* infection of the zebrafish." Cell Host Microbe **2**(1): 29-39.

Clemens, D. L. and M. A. Horwitz (1995). "Characterization of the *Mycobacterium tuberculosis* phagosome and evidence that phagosomal maturation is inhibited " Journal of Experimental Medicine **181**: 257-270.

Cockle, P. J., S. V. Gordon, R. G. Hewinson and H. M. Vordermeier (2006). "Field evaluation of a novel differential diagnostic reagent for detection of *Mycobacterium bovis* in cattle." Clinical and Vaccine Immunology **13**(10): 1119-1124.

Colangeli, R., A. Haq, V. L. Arcus, E. Summers, R. S. Magliozzo, A. McBride, A. K. Mitra, M. Radjainia, A. Khajo, W. R. Jacobs, P. Salgame and D. Alland (2009). "The multifunctional histone-like protein Lsr2 protects mycobacteria against reactive oxygen intermediates." PNAS **106**(11): 4414-4418.

Cole, A. M., J. Shi, A. Ceccarelli, Y.-H. Kim, A. Park and T. Ganz (2001). "Inhibition of neutrophil elastase prevents cathelicidin activation and impairs clearance of bacteria from wounds." Blood **97**(1): 297-304.

Cole, S. T., R. Brosch, J. Parkhill, T. Garnier, C. Churcher, D. Harris, S. V. Gordon, K. Eiglmeier, S. Gas, C. E. Barry III, F. Tekaia, K. Badcock, D. Basham, D. Brown, T. Chillingworth, R. Connor, R. Davies, K. Devlin, T. Feltwell, S. Gentles, N. Hamlin, S. Holroyd, T. Hornsby, K. Jagels, A. Krogh and J. McLean (1998). "Deciphering the biology of *Mycobacterium tuberculosis* from the complete genome sequence." Nature **393**(6685): 537-544.

Collins, A. C., H. Cai, T. Li, L. H. Franco, X. D. Li, V. R. Nair, C. R. Scharn, C. E. Stamm, B. Levine, Z. J. Chen and M. U. Shiloh (2015). "Cyclic GMP-AMP Synthase Is an Innate Immune DNA Sensor for *Mycobacterium tuberculosis*." Cell Host Microbe **17**(6): 820-828.

Corleis, B., D. Korbel, R. Wilson, J. Bylund, R. Chee and U. E. Schaible (2012). "Escape of *Mycobacterium tuberculosis* from oxidative killing by neutrophils." Cellular Microbiology **14**(7): 1109-1121.

Coscolla, M., S. Gagneux, F. Menardo, C. Loiseau, P. Ruiz-Rodriguez, S. Borrell, I. D. Otchere, A. Asante-Poku, P. Asare, L. Sanchez-Buso, F. Gehre, C. N. Sanoussi, M. Antonio, D. Affolabi, J. Fyfe, P. Beckert, S. Niemann, A. S. Alabi, M. P. Grobusch, R. Kobbe, J. Parkhill, C. Beisel, L. Fenner, E. C. Bottger, C. J. Meehan, S. R. Harris, B. C. de Jong, D. Yeboah-Manu and D. Brites (2021). "Phylogenomics of *Mycobacterium africanum* reveals a new lineage and a complex evolutionary history." Microbial Genomics **7**(2).

Costa, S., D. Bevilacqua, M. A. Cassatella and P. Scapini (2019). "Recent advances on the crosstalk between neutrophils and B or T lymphocytes." Immunology **156**(1): 23-32.

Cougoule, C., P. Constant, G. Etienne, M. Daffe and I. Maridonneau-Parini (2002). "Lack of fusion of azurophil granules with phagosomes during phagocytosis of *Mycobacterium smegmatis* by human neutrophils is not actively controlled by the bacterium." Infection and Immunity **70**(3): 1591-1598.

Crick, D. C., L. Quadri and P. J. Brennan (2017). "Biochemistry of the cell envelop of *Mycobacterium tuberculosis*." Handbook of Tuberculosis.

Cronan, M. R., E. J. Hughes, W. J. Brewer, G. Viswanathan, E. G. Hunt, B. Singh, S. Mehra, S. H. Oehlers, S. G. Gregory, D. Kaushal and D. M. Tobin (2021). "A non-canonical type 2 immune response coordinates tuberculous granuloma formation and epithelialization." Cell **184**(7): 1757-1774.e1714.

Cruz, K. D., T. A. Cruz, G. Veras de Moraes, T. C. Paredes-Santos, M. Attias and W. de Souza (2014). "Disruption of lipid rafts interferes with the interaction of *Toxoplasma gondii* with macrophages and epithelial cells." Biomed Research International **2014**: 687835.

Cywes, C., H. Hoppe, M. Daffe and M. R. W. Ehlers (1997). "Nonopsonic binding of *Mycobacterium tuberculosis* to complement receptor type 3 is mediated by capsular polysaccharides and is strain dependent." Infection and Immunity **65**(10): 4258-4266.

Dąbrowska, D., E. Jabłońska, A. Iwaniuk and M. Garley (2019). "Many ways-one destination: Different types of neutrophils death." International Reviews of Immunology **38**(1): 18-32.

Dale, D. C., L. Boxer and W. C. Liles (2008). "The phagocytes: neutrophils and monocytes." Blood **112**(4): 935-945.

Dallenga, T., U. Repnik, B. Corleis, J. Eich, R. Reimer, G. W. Griffiths and U. E. Schaible (2017). "*Mycobacterium tuberculosis*-induced necrosis of infected neutrophils promotes bacterial growth following phagocytosis by macrophages." Cell Host Microbe **22**(4): 519-530 e513.

Davids, M., A. Pooran, L. Smith, M. Tomasicchio and K. Dheda (2021). "The Frequency and effect of Granulocytic Myeloid-Derived Suppressor Cells on mycobacterial survival in patients With tuberculosis: A preliminary report." Frontiers in Immunology **12**: 676679.

Davies, P. D. O. (2006). "Tuberculosis in humans and animals: are we a threat to each other?" Journal of the royal society of medicine **99(10)**: 539-540.

Davis, J. M. and L. Ramakrishnan (2009). "The role of the granuloma in expansion and dissemination of early tuberculous infection." Cell **136**(1): 37-49.

De Jong, B. C., M. Antonio and S. Gagneux (2010). "*Mycobacterium africanum*-review of an important cause of human tuberculosis in West Africa." PLoS Neglected Tropical Diseases **4**(9): e744.

Dean, G. S., S. G. Rhodes, M. Coad, A. O. Whelan, P. J. Cockle, D. J. Clifford, R. G. Hewinson and H. M. Vordermeier (2005). "Minimum infective dose of *Mycobacterium bovis* in cattle." Infection and Immunity **73**(10): 6467-6471.

Decout, A., S. Silva-Gomes, D. Drocourt, E. Blattes, M. Riviere, J. Prandi, G. Larrouy-Maumus, A. M. Caminade, B. Hamasur, G. Kallenius, D. Kaur, K. M. Dobos, M. Lucas, I. C. Sutcliffe, G. S. Besra, B. J. Appelmelk, M. Gilleron, M. Jackson, A. Vercellone, G. Tiraby and J. Nigou (2018). "Deciphering the molecular basis of mycobacteria and lipoglycan recognition by the C-type lectin Dectin-2." Scientific Reports **8**(1): 16840.

Denis, M., D. N. Wedlock and B. M. Buddle (2005). "IFN-gamma enhances bovine macrophage responsiveness to *Mycobacterium bovis*: Impact on bacterial replication, cytokine release and macrophage apoptosis." Immunology and Cell Biology **83**(6): 643-650.

Diel, R., J. Vandeputte, G. de Vries, J. Stillo, M. Wanlin and A. Nienhaus (2014). "Costs of tuberculosis disease in the European Union: a systematic analysis and cost calculation." European Respiratory Journal **43**(2): 554-565.

Dockrell, H. M. and S. G. Smith (2017). "What Have We Learnt about BCG Vaccination in the Last 20 Years?" Frontiers in Immunology **8**: 1134.

Domingo, M., E. Vidal and A. Marco (2014). "Pathology of bovine tuberculosis." Research in Veterinary Science **97 Suppl**: S20-29.

Dorhoi, A., C. Desel, V. Yeremeev, L. Pradl, V. Brinkmann, H. J. Mollenkopf, K. Hanke, O. Gross, J. Ruland and S. H. Kaufmann (2010). "The adaptor molecule CARD9 is essential for tuberculosis control." Journal of Experimental Medicine **207**(4): 777-792.

Dorhoi, A. and S. H. Kaufmann (2014). "Perspectives on host adaptation in response to *Mycobacterium tuberculosis*: modulation of inflammation." Seminars in Immunology **26**(6): 533-542.

Dorhoi, A., G. Nouailles, S. Jorg, K. Hagens, E. Heinemann, L. Pradl, D. Oberbeck-Muller, M. A. Duque-Correa, S. T. Reece, J. Ruland, R. Brosch, J. Tschopp, O. Gross and S. H. Kaufmann (2012). "Activation of the NLRP3 inflammasome by *Mycobacterium tuberculosis* is uncoupled from susceptibility to active tuberculosis." European Journal of Immunology **42**(2): 374-384.

Dorhoi, A., V. Yeremeev, G. Nouailles, J. Weiner, 3rd, S. Jorg, E. Heinemann, D. Oberbeck-Muller, J. K. Knaul, A. Vogelzang, S. T. Reece, K. Hahnke, H. J. Mollenkopf, V. Brinkmann and S. H. Kaufmann (2014). "Type I IFN signaling triggers immunopathology in tuberculosis-susceptible mice by modulating lung phagocyte dynamics." European Journal of Immunology **44**(8): 2380-2393.

Dostal, S., E. Richter and D. Harmsen (2003). Concise guide to mycobacteria and their molecular differentiation, Ridom Press.

Doz-Deblauwe, E., F. Carreras, A. Arbues, A. Remot, M. Epardaud, W. Malaga, V. Mayau, J. Prandi, C. Astarie-Dequeker, C. Guilhot, C. Demangel and N. Winter (2019). "CR3 engaged by PGL-I Triggers Syk-Calcineurin-NFATc to rewire the innate immune response in leprosy." Frontiers in Immunology **10**: 2913.

Driss, V., F. Legrand, E. Hermann, S. Loiseau, Y. Guerardel, L. Kremer, E. Adam, G. Woerly, D. Dombrowicz and M. Capron (2009). "TLR2-dependent eosinophil interactions with mycobacteria: role of alpha-defensins." Blood **113**(14): 3235-3244.

du Plessis, N., L. A. Kotze, V. Leukes and G. Walzl (2018). "Translational potential of therapeutics targeting regulatory myeloid cells in tuberculosis." Frontiers in Cellular and Infection Microbiology **8**: 332.

du Plessis, N., L. Loebenberg, M. Kriel, F. von Groote-Bidlingmaier, E. Ribechini, A. G. Loxton, P. D. van Helden, M. B. Lutz and G. Walzl (2013). "Increased frequency of myeloid-derived suppressor cells during active tuberculosis and after recent mycobacterium tuberculosis infection suppresses T-cell function." Americal Journal of Respiratory and Critical Care Medicine **188**(6): 724-732.

Duffy, S. C., S. Srinivasan, M. A. Schilling, T. Stuber, S. N. Danchuk, J. S. Michael, M. Venkatesan, N. Bansal, S. Maan, N. Jindal, D. Chaudhary, P. Dandapat, R. Katani, S. Chothe, M. Veerasami, S. Robbe-Austerman, N. Juleff, V. Kapur and M. A. Behr (2020). "Reconsidering *Mycobacterium bovis* as a proxy for zoonotic tuberculosis: a molecular epidemiological surveillance study." The Lancet Microbe **1**(2): e66-e73.

Dupuy, A. G. and E. Caron (2008). "Integrin-dependent phagocytosis: spreading from microadhesion to new concepts." Journal of Cell Science **121**(11): 1773-1783.

Durr, S., B. Muller, S. Alonso, J. Hattendorf, C. J. Laisse, P. D. van Helden and J. Zinsstag (2013). "Differences in primary sites of infection between zoonotic and human tuberculosis: results from a worldwide systematic review." PLoS Neglected Tropical Diseases **7**(8): e2399.

Durr, U. H., U. S. Sudheendra and A. Ramamoorthy (2006). "LL-37, the only human member of the cathelicidin family of antimicrobial peptides." Biochimica et Biophysica Acta (BBA) - Biomembranes **1758**(9): 1408-1425.

Ehrt, S. and D. Schnappinger (2009). "Mycobacterial survival strategies in the phagosome: defence against host stresses." Cellular Microbiology **11**(8): 1170-1178.

Eisenberg, T., A. Nesseler, C. Sauerwald, U. Kling, K. Risse, U. Kaim, G. Althoff, N. Fiege, K. Schlez, H. P. Hamann, A. Fawzy, I. Moser, R. Risse, G. Kraft, M. Zschock and C. Menge (2016). "*Mycobacterium tuberculosis* exposure of livestock in a German dairy farm: implications for intra vitam diagnosis of bovine tuberculosis in an officially tuberculosis-free country." Epidemiology and Infection **144**(4): 724-731.

Ekman, A. K. and L. O. Cardell (2010). "The expression and function of Nod-like receptors in neutrophils." Immunology **130**(1): 55-63.

El Daker, S., A. Sacchi, M. Tempestilli, C. Carducci, D. Goletti, V. Vanini, V. Colizzi, F. N. Lauria, F. Martini and A. Martino (2015). "Granulocytic myeloid derived suppressor cells expansion during active pulmonary tuberculosis is associated with high nitric oxide plasma level." PLoS One **10**(4): e0123772.

Elstak, E. D., M. Neeft, N. T. Nehme, J. Voortman, M. Cheung, M. Goodarzifard, H. C. Gerritsen, P. M. van Bergen En Henegouwen, I. Callebaut, G. de Saint Basile and P. van der Sluijs (2011). "The munc13-4-rab27 complex is specifically required for tethering secretory lysosomes at the plasma membrane." Blood **118**(6): 1570-1578.

Eruslanov, E. B., I. V. Lyadova, T. K. Kondratieva, K. B. Majorov, I. V. Scheglov, M. O. Orlova and A. S. Apt (2005). "Neutrophil responses to *Mycobacterium tuberculosis* infection in genetically susceptible and resistant mice." Infection and Immunity **73**(3): 1744-1753.

Escobar, L. E., A. Molina-Cruz and C. Barillas-Mury (2020). "BCG vaccine protection from severe coronavirus disease 2019 (COVID-19)." PNAS **117**(44): 27741-27742.

Esquivel-Solis, H., A. J. Vallecillo, A. Benitez-Guzman, L. G. Adams, Y. Lopez-Vidal and J. A. Gutierrez-Pabello (2013). "Nitric oxide not apoptosis mediates differential killing of *Mycobacterium bovis* in bovine macrophages." PLoS One **8**(5): e63464.

Eum, S. Y., J. H. Kong, M. S. Hong, Y. J. Lee, J. H. Kim, S. H. Hwang, S. N. Cho, L. E. Via and C. E. Barry, 3rd (2010). "Neutrophils are the predominant infected phagocytic cells in the airways of patients with active pulmonary TB." Chest **137**(1): 122-128.

Faurschou, M. and N. Borregaard (2003). "Neutrophil granules and secretory vesicles in inflammation." Microbes and Infection **5**(14): 1317-1327.

Feinberg, H., S. A. Jegouzo, T. J. Rowntree, Y. Guan, M. A. Brash, M. E. Taylor, W. I. Weis and K. Drickamer (2013). "Mechanism for recognition of an unusual mycobacterial glycolipid by the macrophage receptor mincle." Journal of Biological Chemistry **288**(40): 28457-28465.

Ferguson, J. S., D. R. Voelker, F. X. McCormack and L. S. Schlesinger (1999). "Surfactant Protein D binds to *Mycobacterium tuberculosis* bacilli and lipoarabinomannan via carbohydrate-lectin interactions resulting in reduced phagocytosis of the bacteria by macrophages." Journal of Immunology **163**(1): 312-321.

Ferrari, G., H. Langen, M. Naito and J. Pieters (1999). "A coat protein on phagosomes involved in the intracellular survival of mycobacteria." Cell **97**: 435-447.

Filio-Rodriguez, G., I. Estrada-Garcia, P. Arce-Paredes, M. M. Moreno-Altamirano, S. Islas-Trujillo, M. D. Ponce-Regalado and O. Rojas-Espinosa (2017). "*In vivo* induction of neutrophil extracellular traps by *Mycobacterium tuberculosis* in a guinea pig model." Innate Immunity **23**(7): 625-637.

Fingerhut, L., G. Dolz and N. de Buhr (2020). "What Is the evolutionary fingerprint in neutrophil granulocytes?" International Journal of Molecular Sciences **21**(12).

Firdessa, R., R. Tschopp, A. Wubete, M. Sombo, E. Hailu, G. Erenso, T. Kiros, L. Yamuah, M. Vordermeier, R. G. Hewinson, D. Young, S. V. Gordon, M. Sahile, A. Aseffa and S. Berg (2012). "High prevalence of bovine tuberculosis in dairy cattle in central ethiopia: implications for the dairy industry and public health." PLoS One **7**(12): e52851.

Fitzgerald, L. E., N. Abendano, R. A. Juste and M. Alonso-Hearn (2014). "Three-dimensional in vitro models of granuloma to study bacteria-host interactions, drug-susceptibility, and resuscitation of dormant mycobacteria." Biomed Research International **2014**: 623856.

Flynn, J. L., J. Chan and P. L. Lin (2011). "Macrophages and control of granulomatous inflammation in tuberculosis." Mucosal Immunology **4**(3): 271-278.

Flynn, J. L., M. M. Goldstein, J. Chan, K. J. Triebold, K. Pfeffer, C. J. Lowenstein, R. Schreiber, T. W. Mak and B. R. Bloom (1995). "Tumor necrosis factor-alpha is required in the protective immune response against *Mycobacterium tuberculosis* in mice." Immunity **2**(6): 561-572.

Fortunati, E., K. M. Kazemier, J. C. Grutters, L. Koenderman and J. Van den Bosch v (2009). "Human neutrophils switch to an activated phenotype after homing to the lung irrespective of inflammatory disease." Clinical and Experimental Immunology **155**(3): 559-566.

Fossati, G., D. A. Moulding, D. G. Spiller, R. J. Moots, M. R. White and S. W. Edwards (2003). "The mitochondrial network of human neutrophils: role in chemotaxis, phagocytosis, respiratory burst activation, and commitment to apoptosis." Journal of Immunology **170**(4): 1964-1972.

Fox, S., A. E. Leitch, R. Duffin, C. Haslett and A. G. Rossi (2010). "Neutrophil apoptosis: relevance to the innate immune response and inflammatory disease." The Journal of Innate Immunity **2**(3): 216-227.

Francois, M., V. r. Le Cabec, M.-A. Dupont, P. J. Sansonetti and I. Maridonneau-Parini (2000). "Induction of necrosis in human neutrophils by *Shigella flexneri* requires Type III secretion, IpaB and IpaC invasins, and actin polymerization." Infection and Immunity **68**(3): 1289-1296.

Frigui, W., D. Bottai, L. Majlessi, M. Monot, E. Josselin, P. Brodin, T. Garnier, B. Gicquel, C. Martin, C. Leclerc, S. T. Cole and R. Brosch (2008). "Control of *Mycobacterium tuberculosis* ESAT-6 secretion and specific T cell recognition by PhoP." PLoS Pathogens **4**(2): e33.

Futosi, K., S. Fodor and A. Mocsai (2013). "Neutrophil cell surface receptors and their intracellular signal transduction pathways." International Immunopharmacology **17**(3): 638-650.

Gao, W., Y. Cai, G. Zhang, X. Wang, J. Wang, Y. Li and Y. Wang (2022). "Lipidomics revealed the global lipid responses of primary bovine alveolar macrophages to infections of *Mycobacterium tuberculosis* and *Mycobacterium bovis*." International Immunopharmacology **104**: 108407.

Gao, X., X. Guo, M. Li, H. Jia, W. Lin, L. Fang, Y. Jiang, H. Zhu, Z. Zhang, J. Ding and T. Xin (2019). "Interleukin 8 and Pentaxin (C-Reactive Protein) as potential new biomarkers of bovine tuberculosis." Journal of Clinical Microbiology **57**(10).

Garcia, M., T. H. Elsasser, D. Biswas and K. M. Moyes (2015). "The effect of citrus-derived oil on bovine blood neutrophil function and gene expression *in vitro*." Journal of Dairy Science **98**(2): 918-926.

Garnier, T., K. Eiglmeier, J.-C. Camus, N. Medina, H. Mansoor, M. Pryor, S. Duthoy, S. Grondin, C. Lacroix, C. Monsempe, S. Simon, B. Harris, R. Atkin, J. Doggett, R. Mayes, L. Keating, P. R. Wheeler, J. Parkhill, B. G. Barrell, S. T. Cole, S. V. Gordon and R. G. Hewinson (2003). "The complete genome sequence of *Mycobacterium bovis*." PNAS **100 (13)**: 7877-7882.

Gatfield, J. and J. Pieters (2000). "Essential role of cholesterol in the entry of mycobacteria into macrophages." Science **288**(5471): 1647-1650.

Gay, J. C. and E. S. Stitt (1990). "Chemotactic peptide enhancement of phorbol ester-induced protein kinase C activity in human neutrophils." Journal of Leukocyte Biology **47**(1): 49-59.

Gennaro, R., B. Dewald, U. Horisberger, H. U. Gubler and M. Baggiolini (1983). "A novel type of cytoplasmic granule in bovine neutrophils." Journal of cell biology **96**: 1651-1661.

Geurtsen, J., S. Chedammi, J. Mesters, M. Cot, N. N. Driessen, T. Sambou, R. Kakutani, R. Ummels, J. Maaskant, H. Takata, O. Baba, T. Terashima, N. Bovin, C. M. Vandenbroucke-Grauls, J. Nigou, G. Puzo, A. Lemassu, M. Daffe and B. J. Appelmelk (2009). "Identification of mycobacterial alpha-glucan as a novel ligand for DC-SIGN: involvement of mycobacterial capsular polysaccharides in host immune modulation." Journal of Immunology **183**(8): 5221-5231.

Giamarellos-Bourboulis, E. J., M. Tsilika, S. Moorlag, N. Antonakos, A. Kotsaki, J. Dominguez-Andres, E. Kyriazopoulou, T. Gkavogianni, M. E. Adami, G. Damoraki, P. Koufargyris, A. Karageorgos, A. Bolanou, H. Koenen, R. van Crevel, D. I. Droggiti, G. Renieris, A. Papadopoulos and M. G. Netea (2020). "Activate: Randomized Clinical Trial of BCG Vaccination against Infection in the Elderly." Cell **183**(2): 315-323 e319.

Gideon, H. P., J. Phuah, B. A. Junecko and J. T. Mattila (2019). "Neutrophils express pro- and anti-inflammatory cytokines in granulomas from *Mycobacterium tuberculosis*-infected cynomolgus macaques." Mucosal Immunology **12**(6): 1370-1381.

Golby, P., K. A. Hatch, J. Bacon, R. Cooney, P. Riley, J. Allnutt, J. Hinds, J. Nunez, P. D. Marsh, R. G. Hewinson and S. V. Gordon (2007). "Comparative transcriptomics reveals key gene expression differences between the human and bovine pathogens of the *Mycobacterium tuberculosis* complex." Microbiology **153**(Pt 10): 3323-3336.

Gondaira, S., K. Nishi, J. Fujiki, H. Iwano, R. Watanabe, A. Eguchi, Y. Hirano, H. Higuchi and H. Nagahata (2021). "Innate immune response in bovine neutrophils stimulated with *Mycoplasma bovis*." Veterinary Research **52**(1): 58.

Gong, Q. L., Y. Chen, T. Tian, X. Wen, D. Li, Y. H. Song, Q. Wang, R. Du and X. X. Zhang (2021). "Prevalence of bovine tuberculosis in dairy cattle in China during 2010-2019: A systematic review and meta-analysis." PLoS Neglected Tropical Diseases **15**(6): e0009502.

Gonzalo-Asensio, J., W. Malaga, A. Pawlik, C. Astarie-Dequeker, C. Passemar, F. Moreau, F. Laval, M. Daffe, C. Martin, R. Brosch and C. Guilhot (2014). "Evolutionary history of tuberculosis shaped by conserved mutations in the PhoPR virulence regulator." PNAS **111**(31): 11491-11496.

Good, M. and A. Duignan (2011). "Perspectives on the history of bovine TB and the role of tuberculin in bovine TB eradication." Veterinary Medicine International **2011**: 410470.

Gopal, R., L. Monin, D. Torres, S. Slight, S. Mehra, K. C. McKenna, B. A. Fallert Junecko, T. A. Reinhart, J. Kolls, R. Baez-Saldana, A. Cruz-Lagunas, T. S. Rodriguez-Reyna, N. P. Kumar, P. Tessier, J. Roth, M. Selman, E. Becerril-Villanueva, J. Baquera-Heredia, B. Cumming, V. O. Kasprowicz, A. J. Steyn, S. Babu, D. Kaushal, J. Zuniga, T. Vogl, J. Rangel-Moreno and S. A. Khader (2013). "S100A8/A9 proteins mediate neutrophilic inflammation and lung pathology during tuberculosis." American Journal of Respiratory Critical Care Medicine **188**(9): 1137-1146.

Goren, M. B., A. P. D. Hart, M. R. Young and J. A. Armstrong (1976). "Prevention of phagosome-lysosome fusion in cultured macrophages by sulfatides of *Mycobacterium tuberculosis*." PNAS **73**(7): 2510-2514.

Grange, J. M. (2001). "*Mycobacterium bovis* infection in human beings." Tuberculosis (Edinb) **81**(1-2): 71-77.

Grassi, G., V. Vanini, F. De Santis, A. Romagnoli, A. Aiello, R. Casetti, E. Cimini, V. Bordoni, S. Notari, G. Cuzzi, S. Mosti, G. Gualano, F. Palmieri, M. Fraziano, D. Goletti, C. Agrati and A. Sacchi (2021). "PMN-MDSC frequency discriminates active versus latent tuberculosis and could play a role in counteracting the immune-mediated lung damage in active disease." Frontiers in Immunology **12**: 594376.

Groschel, M. I., F. Sayes, R. Simeone, L. Majlessi and R. Brosch (2016). "ESX secretion systems: mycobacterial evolution to counter host immunity." Nature Reviews Microbiology **14**(11): 677-691.

Guimaraes, A. M. S. and C. K. Zimpel (2020). "*Mycobacterium bovis*: From genotyping to genome sequencing." Microorganisms **8**(5).

Guirado, E., L. S. Schlesinger and G. Kaplan (2013). "Macrophages in tuberculosis: friend or foe." Seminars in Immunopathology **35**(5): 563-583.

Gumi, B., E. Schelling, S. Berg, R. Firdessa, G. Erenso, W. Mekonnen, E. Hailu, E. Melese, J. Hussein, A. Aseffa and J. Zinsstag (2012). "Zoonotic transmission of tuberculosis between pastoralists and their livestock in South-East Ethiopia." Ecohealth **9**(2): 139-149.

Hallén-Sandgren, C. and I. Björk (1988). "A rapid technique for the isolation of highly purified, functionally intact bovine neutrophilic granulocytes." Veterinary Immunology and Immunopathology **18**(1): 81-94.

Hannah, S., I. Nadra, I. Dransfield, J. G. Pryde, A. G. Rossi and C. Haslett (1998). "Constitutive neutrophil apoptosis in culture is modulated by cell density independently of β2 integrin-mediated adhesion." FEBS Letters **421**(2): 141-146.

Harding, J. S., A. Rayasam, H. A. Schreiber, Z. Fabry and M. Sandor (2015). "Mycobacterium-infected dendritic cells disseminate granulomatous inflammation." Scientific Reports **5**: 15248.

Herrero-Turrion, M. J., J. Calafat, H. Janssen, M. Fukuda and F. Mollinedo (2008). "Rab27a regulates exocytosis of tertiary and specific granules in human neutrophils." Journal of Immunology **181**(6): 3793-3803.

Hett, E. C. and E. J. Rubin (2008). "Bacterial growth and cell division: a mycobacterial perspective." Microbiology and Molecular Biology Reviews **72**(1): 126-156.

Hilda, J. N. and S. D. Das (2015). "TLR stimulation of human neutrophils lead to increased release of MCP-1, MIP-1alpha, IL-1beta, IL-8 and TNF during tuberculosis." Human Immunology **77**(1): 63-67.

Hilda, J. N., A. Selvaraj and S. D. Das (2012). "*Mycobacterium tuberculosis* H37Rv is more effective compared to vaccine strains in modulating neutrophil functions: an *in vitro* study." FEMS immunology and medical microbiology **66**(3): 372-381.

Hook, J. S., M. Cao, K. Weng, N. Kinnare and J. G. Moreland (2020). "*Mycobacterium tuberculosis* lipoarabinomannan activates human neutrophils via a TLR2/1 mechanism distinct from Pam3CSK4." Journal of Immunology **204**(3): 671-681.

Ibeagha-Awemu, E. M., A. E. Ibeagha and X. Zhao (2012). "The influence of different anticoagulants and sample preparation methods on measurement of mCD14 on bovine monocytes and polymorphonuclear neutrophil leukocytes." BMC Research Notes **5**: 93.

Iwabuchi, K., H. Nakayama, H. Masuda, K. Kina, H. Ogawa and K. Takamori (2012). "Membrane microdomains in immunity: Glycosphingolipid-enriched domain-mediated innate immune responses." BioFactors **38**(4): 275-283.

Jackson, M. (2014). "The mycobacterial cell envelope-lipids." Cold Spring Harbour Perspectives in Medicine **4**(10).

Jamaati, H., E. Mortaz, Z. Pajouhi, G. Folkerts, M. Movassaghi, M. Moloudizargari, I. M. Adcock and J. Garssen (2017). "Nitric oxide in the pathogenesis and treatment of tuberculosis." Frontiers in Microbiology **8**: 2008.

Jayachandran, R., V. Sundaramurthy, B. Combaluzier, P. Mueller, H. Korf, K. Huygen, T. Miyazaki, I. Albrecht, J. Massner and J. Pieters (2007). "Survival of mycobacteria in macrophages is mediated by coronin 1-dependent activation of calcineurin." Cell **130**(1): 37-50.

Jena, P., S. Mohanty, T. Mohanty, S. Kallert, M. Morgelin, T. Lindstrom, N. Borregaard, S. Stenger, A. Sonawane and O. E. Sorensen (2012). "Azurophil granule proteins constitute the major mycobactericidal proteins in human neutrophils and enhance the killing of mycobacteria in macrophages." PLoS One **7**(12): e50345.

Jerjomiceva, N., H. Seri, L. Vollger, Y. Wang, N. Zeitouni, H. Y. Naim and M. von Kockritz-Blickwede (2014). "Enrofloxacin enhances the formation of neutrophil extracellular traps in bovine granulocytes." The Journal of Innate Immunity **6**(5): 706-712.

Jia, X., L. Yang, M. Dong, S. Chen, L. Lv, D. Cao, J. Fu, T. Yang, J. Zhang, X. Zhang, Y. Shang, G. Wang, Y. Sheng, H. Huang and F. Chen (2017). "The bioinformatics analysis of comparative genomics of *Mycobacterium tuberculosis* Complex (MTBC) provides insight into dissimilarities between intraspecific groups differing in host association, virulence, and epitope diversity." Frontiers in Cellular and Infection Microbiology **7**: 88.

Jiang, G., G. Wang, S. Chen, X. Yu, X. Wang, L. Zhao, Y. Ma, L. Dong and H. Huang (2015). "Pulmonary tuberculosis caused by *Mycobacterium bovis* in China." Scientific Reports **5**: 8538.

Jimbo, S., M. Suleman, T. Maina, T. Prysliak, M. Mulongo and J. Perez-Casal (2017). "Effect of *Mycoplasma bovis* on bovine neutrophils." Veterinary Immunology and Immunopathology **188**: 27-33.

Johnson, J. L., A. A. Brzezinska, T. Tolmachova, D. B. Munafo, B. A. Ellis, M. C. Seabra, H. Hong and S. D. Catz (2010). "Rab27a and Rab27b regulate neutrophil azurophilic granule exocytosis and NADPH oxidase activity by independent mechanisms." Traffic **11**(4): 533-547.

Jones, B. W., T. K. Means, K. A. Heldwein, M. A. Keen, P. J. Hill, J. T. Belisle and M. J. Fenton (2001). "Different Toll-like receptor agonists induce distinct macrophage responses." Journal of Leukocyte Biology **69**(6): 1036-1044.

Jones, G. S., H. J. Amirault and B. R. Andersen (1990). "Killing of *Mycobacterium tuberculosis* by Neutrophils: A Nonoxidative Process." Journal of infectious diseases **162**(3): 700-704.

Jones, T. P. W., S. Dabbaj, I. Mandal, J. Cleverley, C. Cash, M. C. I. Lipman and D. M. Lowe (2021). "The blood neutrophil count after 1 month of treatment predicts the radiologic severity of lung disease at treatment end." Chest **160**(6): 2030-2041.

Kalscheuer, R., A. Palacios, I. Anso, J. Cifuente, J. Anguita, W. R. Jacobs, Jr., M. E. Guerin and R. Prados-Rosales (2019). "The *Mycobacterium tuberculosis* capsule: a cell structure with key implications in pathogenesis." Biochemical Journal **476**(14): 1995-2016.

Kan-Sutton, C., C. Jagannath and R. L. Hunter, Jr. (2009). "Trehalose 6,6'-dimycolate on the surface of *Mycobacterium tuberculosis* modulates surface marker expression for antigen presentation and costimulation in murine macrophages." Microbes Infection **11**(1): 40-48.

Kang, Y. A., S. Y. Kwon, H. I. Yoon, J. H. Lee and C. T. Lee (2009). "Role of C-reactive protein and procalcitonin in differentiation of tuberculosis from bacterial community acquired pneumonia." The Korean Journal of Internal Medicine **24**(4): 337-342.

Kaplan, M. J. and M. Radic (2012). "Neutrophil extracellular traps: double-edged swords of innate immunity." Journal of Immunology **189**(6): 2689-2695.

Kato, Y. (2016). "Neutrophil myeloperoxidase and its substrates: formation of specific markers and reactive compounds during inflammation." Journal of clinical biochemistry and nutrition **58**(2): 99-104.

Kaul, D., P. K. Anand and I. Verma (2004). "Cholesterol-sensor initiates *Mycobacterium tuberculosis* entry into human macrophages." Molecular and Cellular Biochemistry **258**(1-2): 219-222.

Keane, J., H. G. Remold and H. Kornfeld (2000). "Virulent *Mycobacterium tuberculosis* strains evade apoptosis of infected alveolar macrophages." Journal of Immunology **164**(4): 2016-2020.

Keller, C., R. Hoffmann, R. Lang, S. Brandau, C. Hermann and S. Ehlers (2006). "Genetically determined susceptibility to tuberculosis in mice causally involves accelerated and enhanced recruitment of granulocytes." Infection and Immunity **74**(7): 4295-4309.

Kelley, V. A. and J. S. Schorey (2003). "Mycobacterium's arrest of phagosome maturation in macrophages requires Rab5 activity and accessibility to iron." Molecular Biology of the Cell **14**(8): 3366-3377.

Kennedy, A. D. and F. R. DeLeo (2009). "Neutrophil apoptosis and the resolution of infection." Immunologic Research **43**(1-3): 25-61.

Kerkhoff, A. D., R. Wood, D. M. Lowe, M. Vogt and S. D. Lawn (2013). "Blood neutrophil counts in HIV-infected patients with pulmonary tuberculosis: association with sputum mycobacterial load." PLoS One **8**(7): e67956.

Kim, C. and M. C. Dinauer (2001). "Rac2 is an essential regulator of neutrophil nicotinamide adenine dinucleotide phosphate oxidase activation in response to specific signaling pathways." Journal of Immunology **166**(2): 1222-1232.

Kim, M. H., W. Liu, D. L. Borjesson, F. R. Curry, L. S. Miller, A. L. Cheung, F. T. Liu, R. R. Isseroff and S. I. Simon (2008). "Dynamics of neutrophil infiltration during cutaneous wound healing and infection using fluorescence imaging." Journal of Investigative Dermatology **128**(7): 1812-1820.

Kim, M. J., H. C. Wainwright, M. Locketz, L. G. Bekker, G. B. Walther, C. Dittrich, A. Visser, W. Wang, F. F. Hsu, U. Wiehart, L. Tsenova, G. Kaplan and D. G. Russell (2010). "Caseation of human tuberculosis granulomas correlates with elevated host lipid metabolism." EMBO Molecular Medicine **2**(7): 258-274.

Kisich, K. O., M. Higgins, G. Diamond and L. Heifets (2002). "Tumor necrosis factor alpha stimulates killing of *Mycobacterium tuberculosis* by human neutrophils." Infection and Immunity **70**(8): 4591-4599.

Knaul, J. K., S. Jorg, D. Oberbeck-Mueller, E. Heinemann, L. Scheuermann, V. Brinkmann, H. J. Mollenkopf, V. Yeremeev, S. H. Kaufmann and A. Dorhoi (2014). "Lung-residing myeloid-derived suppressors display dual functionality in murine pulmonary tuberculosis." American Journal of Respiratory Critical Care Medicine **190**(9): 1053-1066.

Kobayashi, S. D., J. M. Voyich, C. Burlak and F. R. DeLeo (2005). "Neutrophils in the innate immune response." Archivum immunologiae et therapiae experimentalis (Warsz) **53**(6): 505-517.

Koch, A. and V. Mizrahi (2018). "*Mycobacterium tuberculosis*." Trends in Microbiology **26**(6): 555-556.

Kondo, M. (2010). "Lymphoid and myeloid lineage commitment in multipotent hematopoietic progenitors." Immunological Reviews **238**(1): 37-46.

Kremer, W. D. J., E. N. Noordhuizen-Stassen, P. A. J. Henricks and H. van der Vlieta (1992). "A procedure for parallel isolation of white blood cells, granulocyte and purified neutrophil suspensions from the peripheral blood of cattle " Veterinary immunology and immunopathology **31**: 189-193.

Kroon, E. E., A. K. Coussens, C. Kinnear, M. Orlova, M. Möller, A. Seeger, R. J. Wilkinson, E. G. Hoal and E. Schurr (2018). "Neutrophils: Innate Effectors of TB Resistance?" Frontiers in Immunology **9**.

Kruger, P., M. Saffarzadeh, A. N. Weber, N. Rieber, M. Radsak, H. von Bernuth, C. Benarafa, D. Roos, J. Skokowa and D. Hartl (2015). "Neutrophils: Between host defence, immune modulation, and tissue injury." PLoS Pathogens **11**(3): e1004651.

Krupa, A., M. Fol, B. R. Dziadek, E. Kepka, D. Wojciechowska, A. Brzostek, A. Torzewska, J. Dziadek, R. P. Baughman, D. Griffith and A. K. Kurdowska (2015). "Binding of CXCL8/IL-8 to *Mycobacterium tuberculosis* modulates the innate immune response." Mediators of Inflammation **2015**: 124762.

Kuhns, D. B., D. A. L. Priel, J. Chu and K. A. Zarember (2015). "Isolation and functional analysis of human neutrophils." Current Protocols in Immunology **111**: 7 23 21-27 23 16.

Kunz, P., H. Sahr, B. Lehner, C. Fischer, E. Seebach and J. Fellenberg (2016). "Elevated ratio of MMP2/MMP9 activity is associated with poor response to chemotherapy in osteosarcoma." BMC Cancer **16**: 223.

Kurashima, K., N. Mukaida, M. Fujimura, M. Yasui, Y. Nakazumi, T. Matsuda and K. Matsushima (1997). "Elevated chemokine levels in bronchoalveolar lavage fluid of tuberculosis patients." Americal Journal of Respiratory and Critical Care Medicine **155**(4): 1474-1477.

Lacy, P. (2006). "Mechanisms of degranulation in neutrophils." Allergy, Asthma and Clinical Immuonlogy **2**(3): 98-108.

Ladero-Auñon, I., E. Molina, A. Holder, J. Kolakowski, H. Harris, A. Urkitza, J. Anguita, D. Werling and N. Elguezabal (2021). "Bovine neutrophils release extracellular traps and cooperate with macrophages in *Mycobacterium avium* subsp. Paratuberculosis clearance *in vitro*." Frontiers in Immunology **12**.

Lahoz-Beneytez, J., M. Elemans, Y. Zhang, R. Ahmed, A. Salam, M. Block, C. Niederalt, B. Asquith and D. Macallan (2016). "Human neutrophil kinetics: modeling of stable isotope labeling data supports short blood neutrophil half-lives." Blood **127**(26): 3431-3438.

Lahuerta-Marin, A., M. Gallagher, S. McBride, R. Skuce, F. Menzies, J. McNair, S. W. McDowell and A. W. Byrne (2015). "Should they stay, or should they go? Relative future risk of bovine tuberculosis for interferon-gamma test-positive cattle left on farms." Veterinary Research **46**: 90.

Lao, W., H. Kang, G. Jin, L. Chen, Y. Chu, J. Sun and B. Sun (2017). "Evaluation of the relationship between MARCO and CD36 single-nucleotide polymorphisms and susceptibility to pulmonary tuberculosis in a Chinese Han population." BMC Infectious Diseases **17**(1): 488.

Larrazabal, C. S., M. D. Carretta, M. A. Hidalgo and R. A. Burgos (2017). "Amiloride interferes with platelet- activating factor-induced respiratory burst and MMP-9 release in bovine neutrophils independent of Na(+)/H(+) exchanger 1." Veterinary Immunology and Immunopathology **191**: 68-73.

Lawrence, S. M., R. Corriden and V. Nizet (2018). "The ontogeny of a neutrophil: Mechanisms of granulopoiesis and homeostasis." Microbiology and Molecular Biology Reviews **82**(1).

Le'Negrate, G., P. Rostagno, P. Auberger, B. Rossi and P. Hofman (2003). "Downregulation of caspases and Fas ligand expression, and increased lifespan of neutrophils after transmigration across intestinal epithelium." Cell Death and Differentiation **10**(2): 153-162.

Le Cabec, V., S. Carreno, A. Moisand, C. Bordier and I. Maridonneau-Parini (2002). "Complement receptor 3 (CD11b/CD18) mediates type I and type II phagocytosis during nonopsonic and opsonic phagocytosis, respectively." Journal of Immunology **169**(4): 2003-2009.

Lecchi, C., N. Rota, A. Vitali, F. Ceciliani and N. Lacetera (2016). "*In vitro* assessment of the effects of temperature on phagocytosis, reactive oxygen species production and apoptosis in bovine polymorphonuclear cells." Veterinary Immunology and Immunopathology **182**: 89-94.

Lee, W. B., J. S. Kang, J. J. Yan, M. S. Lee, B. Y. Jeon, S. N. Cho and Y. J. Kim (2012). "Neutrophils promote mycobacterial trehalose dimycolate-induced lung inflammation via the mincle pathway." PLoS Pathogens **8**(4): e1002614.

Lee, W. L., R. E. Harrison and S. Grinstein (2003). "Phagocytosis by neutrophils." Microbes Infection **5**(14): 1299-1306.

Lemassu, A., F. Bardou, G. Silve and M.-A. L. l. M. Daffe (1996). "Extracellular and surface-exposed polysaccharides of non-tuberculous mycobacteria." Microbiology **142**: 1515-1520.

Lenaerts, A., C. E. Barry and V. Dartois (2015). "Heterogeneity in tuberculosis pathology, microenvironments and therapeutic responses." Immunological Reviews **264**(1): 288-307.

Lewis, K. N., R. Liao, K. M. Guinn, M. J. Hickey, S. Smith, M. A. Behr and D. R. Sherman (2003). "Deletion of RD1 from *Mycobacterium tuberculosis* Mimics *Bacille Calmette-Guérin* Attenuation." The Journal of Infectious Diseases **187**(1): 117-123.

Ley, K., H. M. Hoffman, P. Kube, M. A. Cassatella, A. Zychlinsky, C. C. Hedrick and S. D. Catz (2018). "Neutrophils: New insights and open questions " Science Immunology **3**(30).

Li, L., H. Si, S. W. Wu, J. O. Mendez, D. Zarlenga, W. Tuo and Z. Xiao (2019). "Characterization of IL-10-producing neutrophils in cattle infected with Ostertagia ostertagi." Scientific Reports **9**(1): 20292.

Lim, J. J., S. Grinstein and Z. Roth (2017). "Diversity and versatility of phagocytosis: Roles in innate immunity, tissue remodeling, and homeostasis." Frontiers in Cellular and Infection Microbiology **7**.

Lizasa, E., Y. Chuma, T. Uematsu, M. Kubota, H. Kawaguchi, M. Umemura, K. Toyonaga, H. Kiyohara, I. Yano, M. Colonna, M. Sugita, G. Matsuzaki, S. Yamasaki, H. Yoshida and H. Hara (2021). "TREM2 is a receptor for non-glycosylated mycolic acids of mycobacteria that limits anti-mycobacterial macrophage activation." Nature Communications **12**(1): 2299.

Lombard, R., E. Doz, F. Carreras, M. Epardaud, Y. Le Vern, D. Buzoni-Gatel and N. Winter (2016). "Il-17ra in non-hematopoietic cells controls cxcl-1 and 5 critical to recruit neutrophils to the lung of mycobacteria-infected mice during the adaptive immune response." PLoS One **11**(2): e0149455.

Lu, J., K. D. Marjon, L. L. Marnell, R. Wang, C. Mold, T. W. Du Clos and P. Sun (2011). "Recognition and functional activation of the human IgA receptor (FcalphaRI) by C-reactive protein." PNAS **108**(12): 4974-4979.

Lu, T., A. R. Porter, A. D. Kennedy, S. D. Kobayashi and F. R. DeLeo (2014). "Phagocytosis and killing of *Staphylococcus aureus* by human neutrophils." The Journal of Innate Immunity **6**(5): 639-649.

Madsen-Bouterse, S. A., G. J. Rosa and J. L. Burton (2006). "Glucocorticoid modulation of Bcl-2 family members A1 and Bak during delayed spontaneous apoptosis of bovine blood neutrophils." Endocrinology **147**(8): 3826-3834.

Mahairas, G. G., P. J. Sabo, M. J. Hickey, D. C. Singh and C. K. Stover (1996). "Molecular analysis of genetic differences between *Mycobacterium bovis* BCG and virulent *M. bovis*." Journal of bacteriology **178**(5): 1274-1282.

Maianski, N. A., J. Geissler, S. M. Srinivasula, E. S. Alnemri, D. Roos and T. W. Kuijpers (2004). "Functional characterization of mitochondria in neutrophils: a role restricted to apoptosis." Cell Death and Differentiation **11**(2): 143-153.

Majeed, M., N. Perskvist, J. D. Ernst, K. Orselius and O. Stendahl (1998). "Roles of calcium and annexins in phagocytosis and elimination of an attenuated strain of *Mycobacterium tuberculosis* in human neutrophils." Microbial Pathogenesis **24**: 309-320.

Majlessi, L. and R. Brosch (2015). "*Mycobacterium tuberculosis* meets the cytosol: The role of cGAS in anti-mycobacterial immunity." Cell Host Microbe **17**(6): 733-735.

Malama, S., T. B. Johansen, J. B. Muma, M. Munyeme, G. Mbulo, A. Muwonge, B. Djonne and J. Godfroid (2014). "Characterization of *Mycobacterium bovis* from humans and cattle in Namwala District, Zambia." Veterinary Medicine International **2014**: 187842.

Malone, K. M., K. Rue-Albrecht, D. A. Magee, K. Conlon, O. T. Schubert, N. C. Nalpas, J. A. Browne, A. Smyth, E. Gormley, R. Aebersold, D. E. MacHugh and S. V. Gordon (2018). "Comparative 'omics analyses differentiate *Mycobacterium tuberculosis* and *Mycobacterium bovis* and reveal distinct macrophage responses to infection with the human and bovine tubercle bacilli." Microbial Genomics **4**(3).

Mantovani, A., M. A. Cassatella, C. Costantini and S. Jaillon (2011). "Neutrophils in the activation and regulation of innate and adaptive immunity." Nature Reviews Immunology **11**(8): 519-531.

Manzanillo, P. S., M. U. Shiloh, D. A. Portnoy and J. S. Cox (2012). "*Mycobacterium tuberculosis* activates the DNA-dependent cytosolic surveillance pathway within macrophages." Cell Host Microbe **11**(5): 469-480.

Martineau, A. R., S. M. Newton, K. A. Wilkinson, B. Kampmann, B. M. Hall, N. Nawroly, G. E. Packe, R. N. Davidson, C. J. Griffiths and R. J. Wilkinson (2007). "Neutrophil-mediated innate immune resistance to mycobacteria." Journal of Clinical Investigation **117**(7): 1988-1994.

Mattila, J. T., P. Maiello, T. Sun, L. E. Via and J. L. Flynn (2015). "Granzyme B-expressing neutrophils correlate with bacterial load in granulomas from *Mycobacterium tuberculosis*-infected cynomolgus macaques." Cellular Microbiology **17**(8): 1085-1097.

Means, T. K., B. W. Jones, A. B. Schromm, B. A. Shurtleff, J. A. Smith, J. Keane, D. T. Golenbock, S. N. Vogel and M. J. Fenton (2001). "Differential effects of a Toll-like receptor antagonist on *Mycobacterium tuberculosis*-induced macrophage responses." Journal of Immunology **166**(6): 4074-4082.

Medzhitov, R. (2008). "Origin and physiological roles of inflammation." Nature **454**(7203): 428-435.

Mendoza-Coronel, E. and M. Castanon-Arreola (2016). "Comparative evaluation of in vitro human macrophage models for mycobacterial infection study." Pathogens and Disease **74**(6).

Menin, A., R. Fleith, C. Reck, M. Marlow, P. Fernandes, C. Pilati and A. Bafica (2013). "Asymptomatic cattle naturally infected with *Mycobacterium bovis* present exacerbated tissue pathology and bacterial dissemination." PLoS One **8**(1): e53884.

Metzler, K. D., T. A. Fuchs, W. M. Nauseef, D. Reumaux, J. Roesler, I. Schulze, V. Wahn, V. Papayannopoulos and A. Zychlinsky (2011). "Myeloperoxidase is required for neutrophil extracellular trap formation: implications for innate immunity." Blood **117**(3): 953-959.

Metzler, K. D., C. Goosmann, A. Lubojemska, A. Zychlinsky and V. Papayannopoulos (2014). "A myeloperoxidase-containing complex regulates neutrophil elastase release and actin dynamics during NETosis." Cell Reports **8**(3): 883-896.

Miltenyi (2020). "MACSxpress whole blood neutrophil isolation kit, human."

Miralda, I., C. K. Klaes, J. E. Graham and S. M. Uriarte (2020). "Human neutrophil granule exocytosis in response to *Mycobacterium smegmatis*." Pathogens **9**(2).

Miyake, Y., K. Toyonaga, D. Mori, S. Kakuta, Y. Hoshino, A. Oyamada, H. Yamada, K. Ono, M. Suyama, Y. Iwakura, Y. Yoshikai and S. Yamasaki (2013). "C-type lectin MCL is an FcRgamma-coupled receptor that mediates the adjuvanticity of mycobacterial cord factor." Immunity **38**(5): 1050-1062.

Moorlag, S., Y. A. Rodriguez-Rosales, J. Gillard, S. Fanucchi, K. Theunissen, B. Novakovic, C. M. de Bont, Y. Negishi, E. T. Fok, L. Kalafati, P. Verginis, V. P. Mourits, V. Koeken, L. C. J. de Bree, G. J. M. Pruijn, C. Fenwick, R. van Crevel, L. A. B. Joosten, I. Joosten, H. Koenen, M. M. Mhlanga, D. A. Diavatopoulos, T. Chavakis and M. G. Netea (2020). "BCG vaccination induces long-term functional reprogramming of human neutrophils." Cell Reports **33**(7): 108387.

Moreira-Teixeira, L., P. J. Stimpson, E. Stavropoulos, S. Hadebe, P. Chakravarty, M. Ioannou, I. V. Aramburu, E. Herbert, S. L. Priestnall, A. Suarez-Bonnet, J. Sousa, K. L. Fonseca, Q. Wang, S. Vashakidze, P. Rodriguez-Martinez, C. Vilaplana, M. Saraiva, V. Papayannopoulos and A. O'Garra (2020). "Type I IFN exacerbates disease in tuberculosis-susceptible mice by inducing neutrophil-mediated lung inflammation and NETosis." Nature Communications **11**(1): 5566.

Morel, C., E. Badell, V. Abadie, M. Robledo, N. Setterblad, J. C. Gluckman, B. Gicquel, S. Boudaly and N. Winter (2008). "*Mycobacterium bovis* BCG-infected neutrophils and dendritic cells cooperate to induce specific T cell responses in humans and mice." European Journal of Immunology **38**(2): 437-447.

Mortaz, E., S. D. Alipoor, I. M. Adcock, S. Mumby and L. Koenderman (2018). "Update on neutrophil function in severe inflammation." Frontiers in Immunology **9**: 2171.

Moulding, D. A., C. Akgul, M. Derouet, M. R. H. White and S. W. Edwards (2001). "BCL-2 family expression in human neutrophils during delayed and accelerated apoptosis." Journal of Leukocyte Biology **70**(5): 783-792.

Moura-Alves, P., K. Fae, E. Houthuys, A. Dorhoi, A. Kreuchwig, J. Furkert, N. Barison, A. Diehl, A. Munder, P. Constant, T. Skrahina, U. Guhlich-Bornhof, M. Klemm, A. B. Koehler, S. Bandermann, C. Goosmann, H. J. Mollenkopf, R. Hurwitz, V. Brinkmann, S. Fillatreau, M. Daffe, B. Tummler, M. Kolbe, H. Oschkinat, G. Krause and S. H. Kaufmann (2014). "AhR sensing of bacterial pigments regulates antibacterial defence." Nature **512**(7515): 387-392.

Muefong, C., O. Owolabi, S. Donkor, S. Charalambous, A. Bakuli, A. Rachow, C. Geldmacher and J. S. Sutherland (2021). "Neutrophils contribute to severity of tuberculosis pathology and recovery from lung damage pre- and post-treatment." Clinical Infectius Diseases: ciab729.

Muefong, C. N., O. Owolabi, S. Donkor, S. Charalambous, J. Mendy, I. C. M. Sey, A. Bakuli, A. Rachow, C. Geldmacher and J. S. Sutherland (2021). "Major neutrophil-derived soluble mediators associate with baseline lung pathology and post-treatment recovery in tuberculosis patients." Frontiers in Immunology **12**: 740933.

Muefong, C. N. and J. S. Sutherland (2020). "Neutrophils in tuberculosis-associated inflammation and lung pathology." Frontiers in Immunology **11**: 962.

Murphy, D., E. Gormley, E. Costello, D. O'Meara and L. A. Corner (2010). "The prevalence and distribution of *Mycobacterium bovis* infection in European badgers (Meles meles) as determined by enhanced post mortem examination and bacteriological culture." Research in Veterinary Science **88**(1): 1-5.

Nakaya, Y., J. Lilue, S. Stavrou, E. A. Moran and S. R. Ross (2017). "AIM2-like receptors positively and negatively regulate the interferon response induced by cytosolic DNA." mBio **8**(4).

Nakayama, H., H. Kurihara, Y. S. Morita, T. Kinoshita, L. Mauri, A. Prinetti, S. Sonnino, N. Yokoyama, H. Ogawa, K. Takamori and K. Iwabuchi (2016). "Lipoarabinomannan binding to lactosylceramide in lipid rafts is essential for the phagocytosis of mycobacteria by human neutrophils." Science Signalling **9**(449): ra101.

Nakayama, H., F. Yoshizaki, A. Prinetti, S. Sonnino, L. Mauri, K. Takamori, H. Ogawa and K. Iwabuchi (2008). "Lyn-coupled LacCer-enriched lipid rafts are required for CD11b/CD18-mediated neutrophil phagocytosis of nonopsonized microorganisms." Journal of Leukocyte Biology **83**(3): 728-741.

Naranjo, V., C. Gortazar, J. Vicente and J. de la Fuente (2008). "Evidence of the role of European wild boar as a reservoir of *Mycobacterium tuberculosis* complex." Veterinary Microbiology **127**(1-2): 1-9.

Nauseef, W. M. (2014). "Myeloperoxidase in human neutrophil host defence." Cellular Microbiology **16**(8): 1146-1155.

Ndlovu, H. and M. J. Marakalala (2016). "Granulomas and inflammation: Host-directed therapies for tuberculosis." Frontiers in Immunology **7**: 434.

Ndlovu, L. N., L. Peetluk, S. Moodley, S. Nhamoyebonde, A. T. Ngoepe, M. Mazibuko, K. Khan, F. Karim, A. S. Pym, F. Maruri, M. S. Moosa, Y. F. van der Heijden, T. R. Sterling and A. Leslie (2020). "Increased neutrophil count and decreased neutrophil CD15 expression correlate with tb disease severity and treatment response irrespective of HIV Co-infection." Frontiers in Immunology **11**: 1872.

Neeli, I., S. N. Khan and M. Radic (2008). "Histone deimination as a response to inflammatory stimuli in neutrophils." Journal of Immunology **180**(3): 1895-1902.

Neill, S. D., D. G. Bryson and J. M. Pollock (2001). "Pathogenesis of tuberculosis in cattle." Tuberculosis (Edinb) **81**(1-2): 79-86.

Neill, S. D., J. M. Pollock, D. B. Bryson and J. Hanna (1994). "Pathogenesis of *Mycobacterium bovis* infection in cattle " Veterinary Microbiology **40**: 41-52.

Neufert, C., R. K. Pai, E. H. Noss, M. Berger, W. H. Boom and C. V. Harding (2001). "*Mycobacterium tuberculosis* 19-kDa lipoprotein promotes neutrophil activation." Journal of Immunology **167**(3): 1542-1549.

Neumann, A., L. Vollger, E. T. Berends, E. M. Molhoek, D. A. Stapels, M. Midon, A. Friaes, A. Pingoud, S. H. Rooijakkers, R. L. Gallo, M. Morgelin, V. Nizet, H. Y. Naim and M. von Kockritz-Blickwede (2014). "Novel role of the antimicrobial peptide LL-37 in the protection of neutrophil extracellular traps against degradation by bacterial nucleases." The Journal of Innate Immunity **6**(6): 860-868.

Neyrolles, O. and C. Guilhot (2011). "Recent advances in deciphering the contribution of *Mycobacterium tuberculosis* lipids to pathogenesis." Tuberculosis (Edinb) **91**(3): 187-195.

Ng, V. H., J. S. Cox, A. O. Sousa, J. D. MacMicking and J. D. McKinney (2004). "Role of KatG catalase-peroxidase in mycobacterial pathogenesis: countering the phagocyte oxidative burst." Molecular Microbiology **52**(5): 1291-1302.

Nordenfelt, P. and H. Tapper (2011). "Phagosome dynamics during phagocytosis by neutrophils." Journal of Leukocyte Biology **90**(2): 271-284.

Oettinger, T., M. Jørgensen, A. Ladefoged, K. Hasløv and P. Andersen (1999). "Development of the *Mycobacterium bovis* BCG vaccine: review of the historical and biochemical evidence for a genealogical tree." Tubercle and lung disease **79**(4): 243-250.

OIE (2017). "Zoonotic TB factsheet."

OIE (2018). "Manual of Diagnostic Tests and Vaccines for Terrestrial Animals, OIE Terrestrial manual."

OIE (2019). Controlling bovine tuberculosis: A One health challenge

Olea-Popelka, F., A. Muwonge, A. Perera, A. S. Dean, E. Mumford, E. Erlacher-Vindel, S. Forcella, B. J. Silk, L. Ditiu, A. El Idrissi, M. Raviglione, O. Cosivi, P. LoBue and P. I. Fujiwara (2016). "Zoonotic tuberculosis in human beings caused by *Mycobacterium bovis* —a call for action." The Lancet Infectious Diseases **17**(1): e21-e25.

Ong, C. W., P. T. Elkington, S. Brilha, C. Ugarte-Gil, M. T. Tome-Esteban, L. B. Tezera, P. J. Pabisiak, R. C. Moores, T. Sathyamoorthy, V. Patel, R. H. Gilman, J. C. Porter and J. S. Friedland (2015). "Neutrophil-derived MMP-8 drives AMPK-dependent matrix destruction in human pulmonary tuberculosis." PLoS Pathogens **11**(5): e1004917.

Ong, C. W. M., K. Fox, A. Ettorre, P. T. Elkington and J. S. Friedland (2018). "Hypoxia increases neutrophil-driven matrix destruction after exposure to *Mycobacterium tuberculosis*." Scientific Reports **8**(1): 11475.

Ortalo-Magne, A., M.-A. Laneelles, F. Bardou, G. Silve, P. Gounon, G. Marchal and M. Daffe (1996). "Identification of the surface-exposed lipids on the cell envelopes of *Mycobacterium tuberculosis* and other mycobacterial species." Journal of bacteriology **178 (2)**: 456-461.

Paape, M. J., D. D. Bannerman, X. Zhao and J. W. Lee (2003). "The bovine neutrophil: Structure and function in blood and milk." Veterinary Research **34**(5): 597-627.

Pai, M., M. A. Behr, D. Dowdy, K. Dheda, M. Divangahi, C. C. Boehme, A. Ginsberg, S. Swaminathan, M. Spigelman, H. Getahun, D. Menzies and M. Raviglione (2016). "Tuberculosis." Nature Reviews Disease Primers **2**: 16076.

Palmer, M. V., T. C. Thacker, C. Kanipe and P. M. Boggiatto (2021). "Heterogeneity of pulmonary granulomas in cattle experimentally infected with *Mycobacterium bovis*." Frontiers in Veterinary Science **8**: 671460.

Palmer, M. V., T. C. Thacker, W. R. Waters, C. Gortazar and L. A. Corner (2012). "*Mycobacterium bovis*: A model pathogen at the interface of livestock, wildlife, and humans." Veterinary Medicine International **2012**: 236205.

Palmer, M. V., J. Wiarda, C. Kanipe and T. C. Thacker (2019). "Early pulmonary lesions in cattle infected via aerosolized *Mycobacterium bovis*." Veterinary Pathology **56**(4): 544-554.

Panteleev, A. V., I. Y. Nikitina, I. A. Burmistrova, G. A. Kosmiadi, T. V. Radaeva, R. B. Amansahedov, P. V. Sadikov, Y. V. Serdyuk, E. E. Larionova, T. R. Bagdasarian, L. N. Chernousova, V. V. Ganusov and I. V. Lyadova (2017). "Severe tuberculosis in humans correlates best with neutrophil abundance and lymphocyte deficiency and does not correlate with antigen-specific CD4 T-cell response." Frontiers in Immunology **8**: 963.

Papayannopoulos, V., K. D. Metzler, A. Hakkim and A. Zychlinsky (2010). "Neutrophil elastase and myeloperoxidase regulate the formation of neutrophil extracellular traps." Journal of Cell Biology **191**(3): 677-691.

Park, S. A. and Y. M. Hyun (2016). "Neutrophil extravasation cascade: What can we learn from two-photon intravital imaging?" Immune Network **16**(6): 317-321.

Parker, H., A. M. Albrett, A. J. Kettle and C. C. Winterbourn (2012). "Myeloperoxidase associated with neutrophil extracellular traps is active and mediates bacterial killing in the presence of hydrogen peroxide." Journal of Leukocyte Biology **91**(3): 369-376.

Patin, E. C., A. C. Geffken, S. Willcocks, C. Leschczyk, A. Haas, F. Nimmerjahn, R. Lang, T. H. Ward and U. E. Schaible (2017). "Trehalose dimycolate interferes with FcgammaR-mediated phagosome maturation through Mincle, SHP-1 and FcgammaRIIB signalling." PLoS One **12**(4): e0174973.

Pauwels, A. M., M. Trost, R. Beyaert and E. Hoffmann (2017). "Patterns, receptors, and signals: Regulation of phagosome maturation." Trends in Immunology **38**(6): 407-422.

Pedrosa, J., B. M. Saunders, R. Appelberg, I. M. Orme, M. T. Silva and A. M. Cooper (2000). "Neutrophils play a protective nonphagocytic role in systemic *Mycobacterium tuberculosis* infection of mice." Infection and Immunity **68**(2).

Pellegrini, J. M., F. Sabbione, M. P. Morelli, N. L. Tateosian, F. A. Castello, N. O. Amiano, D. Palmero, A. Levi, L. Ciallella, M. I. Colombo, A. S. Trevani and V. E. Garcia (2020). "Neutrophil autophagy during human active tuberculosis is modulated by SLAMF1." Autophagy: 1-10.

Penn-Nicholson, A., S. K. Mbandi, E. Thompson, S. C. Mendelsohn, S. Suliman, N. N. Chegou, S. T. Malherbe, F. Darboe, M. Erasmus, W. A. Hanekom, N. Bilek, M. Fisher, S. H. E. Kaufmann, J. Winter, M. Murphy, R. Wood, C. Morrow, I. Van Rhijn, B. Moody, M. Murray, B. B. Andrade, T. R. Sterling, J. Sutherland, K. Naidoo, N. Padayatchi, G. Walzl, M. Hatherill, D. Zak, T. J. Scriba, t. Adolescent Cohort Study, G. C. Consortium, S. Clinical, T. Laboratory, T. B. C. Screen, A.-T. Consortium, P. B. T. Re, T. Peruvian Household Contacts Cohort and C. I. team (2020). "RISK6, a 6-gene transcriptomic signature of TB disease risk, diagnosis and treatment response." Scientific Reports **10**(1): 8629.

Perobelli, S. M., R. G. Galvani, T. Goncalves-Silva, C. R. Xavier, A. Nobrega and A. Bonomo (2015). "Plasticity of neutrophils reveals modulatory capacity." Brazilian Journal of Medical and Biological Research **48**(8): 665-675.

Perskvist, N., K. Roberg, A. Kulyté and O. Stendahl (2002). "ab5a GTPase regulates fusion between pathogen containing phagosomes and cytoplasmic organelles in human neutrophils." Journal of cell science **115**(6): 1321-1330.

Persson, A., R. Blomgran-Julinder, D. Eklund, C. Lundstrom and O. Stendahl (2009). "Induction of apoptosis in human neutrophils by *Mycobacterium tuberculosis* is dependent on mature bacterial lipoproteins." Microbial Pathogens **47**(3): 143-150.

Petrofsky, M. and L. E. Bermudez (1999). "Neutrophils from *Mycobacterium avium*-infected mice produce TNF-a, IL-12, and IL-1b and have a putative role in early host response." Clinical Immunology **91**(3): 354-358.

Peyron, P., C. Bordier, E. N. N'Diaye and I. Maridonneau-Parini (2000). "Nonopsonic phagocytosis of *Mycobacterium kansasii* by human neutrophils depends on cholesterol and is mediated by CR3

associated with glycosylphosphatidylinositol-anchored proteins." Journal of Immunology **165**(9): 5186-5191.

Peyron, P., J. Vaubourgeix, Y. Poquet, F. Levillain, C. Botanch, F. Bardou, M. Daffe, J. F. Emile, B. Marchou, P. J. Cardona, C. de Chastellier and F. Altare (2008). "Foamy macrophages from tuberculous patients' granulomas constitute a nutrient-rich reservoir for *Mycobacterium tuberculosis* persistence." PLoS Pathogens **4**(11): e1000204.

Phillips, C. J. C., C. R. W. Fosterb, P. A. Morrisc and R. Teversond (2003). "The transmission of *Mycobacterium bovis* infection to cattle." Research in Veterinary science **74**: 1-15.

Phuah, J. Y., B. Junecko and J. T. Mattila (2018). "Neutrophil responses to acute *Mycobacterium tuberculosis* infection in non-human primates." Journal of Immunology **200**(1 Supplement): 114.110.

Picasso, C., J. Alvarez, K. L. VanderWaal, F. Fernandez, A. Gil, S. J. Wells and A. Perez (2017). "Epidemiological investigation of bovine tuberculosis outbreaks in Uruguay (2011-2013)." Preventive Veterinary Medicine **138**: 156-161.

Piercy, J., D. Werling and T. J. Coffey (2007). "Differential responses of bovine macrophages to infection with bovine-specific and non-bovine specific mycobacteria." Tuberculosis (Edinb) **87**(5): 415-420.

Piergallini, T. J., J. M. Scordo, P. A. Pino, L. S. Schlesinger, J. B. Torrelles and J. Turner (2021). "Acute inflammation confers enhanced protection against *Mycobacterium tuberculosis* infection in mice." Microbiology Spectrum **9**(1): e0001621.

Pierini, L. M., R. J. Eddy, M. Fuortes, S. Seveau, C. Casulo and F. R. Maxfield (2003). "Membrane lipid organization is critical for human neutrophil polarization." Journal of Biological Chemistry **278**(12): 10831-10841.

Pillay, J., I. den Braber, N. Vrisekoop, L. M. Kwast, R. J. de Boer, J. A. Borghans, K. Tesselaar and L. Koenderman (2010). "In vivo labeling with 2H2O reveals a human neutrophil lifespan of 5.4 days." Blood **116**(4): 625-627.

Pivot-Pajot, C., F. Varoqueaux, G. de Saint Basile and S. G. Bourgoin (2008). "Munc13-4 regulates granule secretion in human neutrophils." Journal of Immunology **180**(10): 6786-6797.

Pokkali, S. and S. D. Das (2009). "Augmented chemokine levels and chemokine receptor expression on immune cells during pulmonary tuberculosis." Human Immunology **70**(2): 110-115.

Pollock, J. M. and S. D. Neill (2002). "*Mycobacterium bovis* infection and tuberculosis in cattle." The Veterinary Journal **163**(2): 115-127.

Prentice, S., B. Nassanga, E. L. Webb, F. Akello, F. Kiwudhu, H. Akurut, A. M. Elliott, R. J. W. Arts, M. G. Netea, H. M. Dockrell, S. Cose, S. Prentice, B. Nassanga, H. Akurut, F. Akello, F. Kiwudhu, S. Cose, H. Dockrell, E. Webb, A. Elliott, I. Nabaweesi, C. Zziwa, M. Namutebi, B. Namarra, F. Akello, E. Nakazibwe, S. Amongi, G. Kamukama, S. Iwala, C. Ninsiima, J. Tumusiime, F. Kiwanuka, S. Nsubuga, J. Akello, S. Owilla, J. Levin, S. Nash, P. Kabuubi Nakawungu, E. Abayo, G. Nabakooza, Z. Kaushaaga and M. Akello (2021). "BCG-induced non-specific effects on heterologous infectious disease in Ugandan neonates: an investigator-blind randomised controlled trial." The Lancet Infectious Diseases **21**(7): 993-1003.

Prisic, S., R. N. Husson, G. F. Hatfull and W. R. Jacobs Jr. (2014). "*Mycobacterium tuberculosis* Serine/Threonine Protein Kinases." Microbiology Spectrum **2**(5): 2.5.08.

Probst, C., C. Freuling, I. Moser, L. Geue, H. Kohler, F. J. Conraths, H. Hotzel, E. M. Liebler-Tenorio and M. Kramer (2011). "Bovine tuberculosis: making a case for effective surveillance." Epidemiology Infection **139**(1): 105-112.

Pugin, J., M. C. Widmer, S. Kossodo, C. M. Liang, P. HL2nd and S. A. F (1999). " Human neutrophils secrete gelatinase B *in vitro* and *in vivo* in response to endotoxin and proinflammatory mediators." American Journal Of Respiratory Cell and Molecular Biology **20**(3): 458-464.

Quesniaux, V. J., D. M. Nicolle, D. Torres, L. Kremer, Y. Guerardel, J. Nigou, G. Puzo, F. Erard and B. Ryffel (2004). "Toll-like receptor 2 (TLR2)-dependent-positive and TLR2-independent-negative regulation of proinflammatory cytokines by mycobacterial lipomannans." Journal of Immunology **172**(7): 4425-4434.

Queval, C. J., R. Brosch and R. Simeone (2017). "The macrophage: A disputed fortress in the battle against *Mycobacterium tuberculosis*." Frontiers in Microbiology **8**: 2284.

Queval, C. J., A. Fearns, L. Botella, A. Smyth, L. Schnettger, M. Mitermite, E. Wooff, B. Villarreal-Ramos, W. Garcia-Jimenez, T. Heunis, M. Trost, D. Werling, F. J. Salguero, S. V. Gordon and M. G. Gutierrez (2021). "Macrophage-specific responses to human- and animal-adapted tubercle bacilli reveal pathogen and host factors driving multinucleated cell formation." PLoS Pathogens **17**(3): e1009410.

Quie, P. G., J. G. White, B. Holmes and R. A. Good (1967). "*In vitro* bactericidal capacity of human polymorphonuclear leukocytes: diminished activity in chronic granulomatous disease of childhood." Journal of Clinical Investigation **46**(4): 668-679.

Quigley, J., V. K. Hughitt, C. A. Velikovsky, R. A. Mariuzza, N. M. El-Sayed and V. Briken (2017). "The Cell Wall Lipid PDIM contributes to phagosomal escape and host cell exit of mycobacterium tuberculosis." mBio **8**(2).

Quiroga, J., P. Alarcon, C. Manosalva, A. Taubert, C. Hermosilla, M. A. Hidalgo, M. D. Carretta and R. A. Burgos (2020). "Glycolysis and mitochondrial function regulate the radical oxygen species production induced by platelet-activating factor in bovine polymorphonuclear leukocytes." Veterinary Immunology and Immunopathology **226**: 110074.

Rahman, A., P. Sobia, N. Gupta, L. V. Kaer and G. Das (2014). "*Mycobacterium tuberculosis* subverts the TLR-2-MyD88 pathway to facilitate its translocation into the cytosol." PLoS One **9**(1): e86886.

Rajaram, M. V. S., E. Arnett, A. K. Azad, E. Guirado, B. Ni, A. D. Gerberick, L. Z. He, T. Keler, L. J. Thomas, W. P. Lafuse and L. S. Schlesinger (2017). "*Mycobacterium tuberculosis*-Initiated human mannose receptor signaling regulates macrophage recognition and vesicle trafficking by FcRgamma-Chain, Grb2, and SHP-1." Cell Reports **21**(1): 126-140.

Ramachandra, L., J. L. Smialek, S. S. Shank, M. Convery, W. H. Boom and C. V. Harding (2005). "Phagosomal processing of *Mycobacterium tuberculosis* antigen 85B is modulated independently of mycobacterial viability and phagosome maturation." Infection and Immunity **73**(2): 1097-1105.

Rambault, M., R. Borkute, E. Doz-Deblauwe, Y. Le-Vern, N. Winter, A. Dorhoi and A. Remot (2021). "Isolation of bovine neutrophils by fluorescence- and magnetic-activated cell sorting." Methods in Molecular Biology **2236**: 203-217.

Rambault, M., E. Doz-Deblauwe, Y. Le Vern, F. Carreras, P. Cunha, P. Germon, P. Rainard, N. Winter and A. Remot (2021). "Neutrophils encompass a regulatory subset suppressing T cells in apparently healthy cattle and mice." Frontiers in Immunology **12**: 625244.

Ramos-Kichik, V., R. Mondragón-Flores, M. Mondragón-Castelán, S. Gonzalez-Pozos, S. Muñiz-Hernandez, O. Rojas-Espinosa, R. Chacón-Salinas, S. Estrada-Parra and I. Estrada-García (2009). "Neutrophil extracellular traps are induced by *Mycobacterium tuberculosis*." Tuberculosis (Edinb) **89**(1): 29-37.

Ramos, D. F., P. E. Silva and O. A. Dellagostin (2015). "Diagnosis of bovine tuberculosis: review of main techniques." Brazilian Journal of Biology **75**(4): 830-837.

Refaya, A. K., G. Bhargavi, N. C. Mathew, A. Rajendran, R. Krishnamoorthy, S. Swaminathan and K. Palaniyandi (2020). "A review on bovine tuberculosis in India." Tuberculosis (Edinb) **122**: 101923.

Renwick, A. R., P. C. White and R. G. Bengis (2007). "Bovine tuberculosis in southern African wildlife: a multi-species host-pathogen system." Epidemiology and Infection **135**(4): 529-540.

Riding, G. A. and P. Willadsen (1981). "Simultaneous isolation of bovine eosinophils and neutrophils on gradients of Percoll." Journal of Immunological methods **46**(1): 113-119.

Rodriguez-Campos, S., N. H. Smith, M. B. Boniotti and A. Aranaz (2014). "Overview and phylogeny of *Mycobacterium tuberculosis* complex organisms: implications for diagnostics and legislation of bovine tuberculosis." Respiratory Veterinary Science **97 Suppl**: S5-S19.

Romagnoli, A., M. P. Etna, E. Giacomini, M. Pardini, M. E. Remoli, M. Corazzari, L. Falasca, D. Goletti, V. Gafa, R. Simeone, G. Delogu, M. Piacentini, R. Brosch, G. M. Fimia and E. M. Coccia (2012). "ESX-1 dependent impairment of autophagic flux by *Mycobacterium tuberculosis* in human dendritic cells." Autophagy **8**(9): 1357-1370.

Romero, M. M., J. I. Basile, B. López, V. Ritacco, L. Barrera, M. d. C. Sasiain and M. Alemán (2014). "Outbreaks of *Mycobacterium tuberculosis* MDR strains differentially induce neutrophil respiratory burst involving lipid rafts, p38 MAPK and Syk." BMC Infectious diseases **14**(262).

Rosen, H. and S. J. Klebanoff (1979). "Bactericidal activity of a superoxide anion-generating system. A model for the polymorphonuclear leukocyte." Journal of experimental medicine **149**(1): 27-39.

Ross, G. D., J. A. Cain and P. J. Lachmann (1985). "Membrane complement receptor type three (CR3) has lectin-like properties analogous to bovine conglutinin and functions as a receptor fro zymosan and rabbit erythrocytes as well as a receptor for iC3b." Journal of Immunology **134**(5): 3307-3315.

Roth, J. and M. Kaeberle (1981). "Isolation of neutrophils and eosinophils from the peripheral blood of cattle and comparison of their functional activities." Journal of Immunological methods **45**(2): 153-164.

Rothfuchs, A. G., A. Bafica, C. G. Feng, J. G. Egen, D. L. Williams, G. D. Brown and A. Sher (2007). "Dectin-1 interaction with Mycobacterium tuberculosis leads to enhanced IL-12p40 production by splenic dendritic cells." Journal of Immunology **179**(6): 3463-3471.

Ryu, J. C., M. J. Kim, Y. Kwon, J. H. Oh, S. S. Yoon, S. J. Shin, J. H. Yoon and J. H. Ryu (2017). "Neutrophil pyroptosis mediates pathology of *Pseudomonas aeruginosa* lung infection in the absence of the NADPH oxidase NOX2." Mucosal Immunology **10**(3): 757-774.

Sada-Ovalle, I., A. Chiba, A. Gonzales, M. B. Brenner and S. M. Behar (2008). "Innate invariant NKT cells recognize *Mycobacterium tuberculosis*-infected macrophages, produce interferon-gamma, and kill intracellular bacteria." PLoS Pathogens **4**(12): e1000239.

Sadiku, P., J. A. Willson, E. M. Ryan, D. Sammut, P. Coelho, E. R. Watts, R. Grecian, J. M. Young, M. Bewley, S. Arienti, A. S. Mirchandani, M. A. Sanchez Garcia, T. Morrison, A. Zhang, L. Reyes, T. Griessler, P. Jheeta, G. G. Paterson, C. J. Graham, J. P. Thomson, K. Baillie, A. A. R. Thompson, J. M. Morgan, A. Acosta-Sanchez, V. M. Darde, J. Duran, J. J. Guinovart, G. Rodriguez-Blanco, A. Von Kriegsheim, R. R. Meehan, M. Mazzone, D. H. Dockrell, B. Ghesquiere, P. Carmeliet, M. K. B. Whyte and S. R. Walmsley (2021). "Neutrophils fuel effective immune responses through gluconeogenesis and glycogenesis." Cell Metabolism **33**(2): 411-423 e414.

Saiga, H., S. Kitada, Y. Shimada, N. Kamiyama, M. Okuyama, M. Makino, M. Yamamoto and K. Takeda (2012). "Critical role of AIM2 in *Mycobacterium tuberculosis* infection." International Immunology **24**(10): 637-644.

Saito, T., H. Takahashi, H. Doken, H. Koyama and Y. Aratani (2005). "Phorbol myristate acetate induces neutrophil death through activation of p38 Mitogen-Activated Protein Kinase that requires endogenous reactive oxygen species other than HOCl." Bioscience, Biotechnology, and Biochemistry **69**(11): 2207-2212.

Salgar, S., M. Paape, B. Alston-Mills and R. Miller (1991). "Flow cytometric study of oxidative burst activity in bovine neutrophils." American Journal of veterinary research **52**(8): 1201-1207.

Savill, J. S., A. H. Wyllie, J. E. Henson, M. J. Walport, P. M. Henson and C. Haslett (1989). "Macrophage phagocytosis of aging neutrophils in inflammation. Programmed cell death in the neutrophil leads to its recognition by macrophages." Journal of Clinical Investigation.

Scheepers, A., H. Joost and A. Schurmann (2004). "The glucose transporter families SGLT and GLUT: molecular basis of normal and aberrant function." Journal of Parenteral and Enteral Nutrition **28**(5): 364-371.

Schlesinger, L., A. K. Azad, J. B. Torrelles, E. Roberts, I. Vergne and V. Deretic (2017). "Determinants of phagocytosis, phagosome biogenesis and autophagy for *Mycobacterium tuberculosis*." Handbook of Tuberculosis: Immunology and Cell biology.

Scott, N. R., R. V. Swanson, N. Al-Hammadi, R. Domingo-Gonzalez, J. Rangel-Moreno, B. A. Kriel, A. N. Bucsan, S. Das, M. Ahmed, S. Mehra, P. Treerat, A. Cruz-Lagunas, L. Jimenez-Alvarez, M. Munoz-Torrico, K. Bobadilla-Lozoya, T. Vogl, G. Walzl, N. du Plessis, D. Kaushal, T. J. Scriba, J. Zuniga and S. A. Khader (2020). "S100A8/A9 regulates CD11b expression and neutrophil recruitment during chronic tuberculosis." Journal of Clinical Investigation **130**(6): 3098-3112.

Segal, A. W. (2005). "How neutrophils kill microbes." Annual Reviews Immunology **23**: 197-223.

Seiler, P., P. Aichele, S. Bandermann, A. E. Hauser, B. Lu, N. P. Gerard, C. Gerard, S. Ehlers, H. J. Mollenkopf and S. H. Kaufmann (2003). "Early granuloma formation after aerosol *Mycobacterium tuberculosis* infection is regulated by neutrophils via CXCR3-signaling chemokines." European Journal of Immunology **33**(10): 2676-2686.

Selsted, M. E., Y. Q. Tang, W. L. Morris, P. A. McGuire, M. J. Novotny, W. Smith, A. H. Henschen and J. S. Cullor (1996). "Purification, primary structures, and antibacterial activities of beta-defensins, a new family of antimicrobial peptides from bovine neutrophils." Journal of Biological Chemistry **271**(27): 16430.

Shenderov, K., D. L. Barber, K. D. Mayer-Barber, S. S. Gurcha, D. Jankovic, C. G. Feng, S. Oland, S. Hieny, P. Caspar, S. Yamasaki, X. Lin, J. P. Ting, G. Trinchieri, G. S. Besra, V. Cerundolo and A. Sher (2013).

"Cord factor and peptidoglycan recapitulate the Th17-promoting adjuvant activity of mycobacteria through mincle/CARD9 signaling and the inflammasome." Journal of Immunology **190**(11): 5722-5730.

Sheppard, F. R., M. R. Kelher, E. E. Moore, N. J. McLaughlin, A. Banerjee and C. C. Silliman (2005). "Structural organization of the neutrophil NADPH oxidase: phosphorylation and translocation during priming and activation." Journal of Leukocyte Biology **78**(5): 1025-1042.

Sheshachalam, A., N. Srivastava, T. Mitchell, P. Lacy and G. Eitzen (2014). "Granule protein processing and regulated secretion in neutrophils." Frontiers in Immunology **5**: 448.

Sia, J. K. and J. Rengarajan (2019). "Immunology of *Mycobacterium tuberculosis* Infections." Microbiol Spectrum **7**(4).

Siemsen, D. W., L. N. Kirpotina, N. Malachowa, I. A. Schepetkin, A. R. Porter, B. Lei, F. R. DeLeo and M. T. Quin (2020). "Isolation of Neutrophils from Nonhuman Species." Methods in Molecular biology.

Simon, H. U. (2003). "Neutrophil apoptosis pathways and their modifications in inflammation." Immunological Reviews **193**: 101-110.

Singh, B., D. K. Singh, S. R. Ganatra, R. A. Escobedo, S. Khader, L. S. Schlesinger, D. Kaushal and S. Mehraa (2021). "Myeloid-derived suppressor cells mediate T cell dysfunction in nonhuman primate tb granulomas." mBio **12**(6): e03189-03121.

Singh, V., S. Jamwal, R. Jain, P. Verma, R. Gokhale and K. V. Rao (2012). "Mycobacterium tuberculosis-driven targeted recalibration of macrophage lipid homeostasis promotes the foamy phenotype." Cell Host Microbe **12**(5): 669-681.

Sláma, P., Z. Sládek and D. Ryšánek (2006). "Effect of isolation techniques on viability of bovine blood neutrophils." Acta Veterinaria Brno **75**(3): 343-353.

Sohn, E. J., M. J. Paape, E. E. Connor, D. D. Bannerman, R. H. Fetterer and R. R. Peters (2007). "Bacterial lipopolysaccharide stimulates bovine neutrophil production of TNF-alpha, IL-1beta, IL-12 and IFN-gamma." Veterinary Research **38**(6): 809-818.

Solomkin, J. S., C. T. Robinson, C. M. Cave, B. Ehmer and A. B. Lentsch (2007). "Alterations in membrane cholesterol cause mobilization of lipid rafts from specific granules and prime human neutrophils for enhanced adherence-dependent oxidant production." Shock **28**(3): 334-338.

Soltys, J., S. D. Swain, K. M. Sipes, L. K. Nelson, A. J. Hanson, J. M. Kantele, M. A. Jutila and M. T. Quinn (1999). "Isolation of bovine neutrophils with magnetic beads: comparison with standard percoll demsity gradient isolation methods." Journal of immunological methods **226**(1-2): 71-84.

Son, K., M. Mukherjee, B. A. S. McIntyre, J. C. Eguez, K. Radford, N. LaVigne, C. Ethier, F. Davoine, L. Janssen, P. Lacy and P. Nair (2017). "Improved recovery of functionally active eosinophils and neutrophils using novel immunomagnetic technology." Journal of Immunological Methods **449**: 44-55.

Song, Y., X. Ge, Y. Chen, T. Hussain, Z. Liang, Y. Dong, Y. Wang, C. Tang and X. Zhou (2022). "Mycobacterium bovis induces mitophagy to suppress host xenophagy for its intracellular survival." Autophagy **18**(6): 1401-1415.

Song, Y., S. Jiang, C. Li, J. J. Loor, Q. Jiang, Y. Yang, X. Feng, S. Liu, J. He, K. Wang, Y. Li, C. Zhang, X. Du, Z. Wang, X. Li and G. Liu (2022). "Free fatty acids promote degranulation of azurophil granules in

neutrophils by inducing production of NADPH oxidase-derived reactive oxygen species in cows with subclinical ketosis." Journal of Dairy Science **105**(3): 2473-2486.

Spickler, A. R. (2019). "Zoonotic tuberculosis in mammals, including bovine and caprine tuberculosis." Retreived from http://www.cfsph.iastate.edu/DiseaseInfo/factsheets.php.

Srinivasan, S., L. Easterling, B. Rimal, X. M. Niu, A. J. K. Conlan, P. Dudas and V. Kapur (2018). "Prevalence of bovine tuberculosis in india: A systematic review and meta-analysis." Transboundary Emerging Diseases **65**(6): 1627-1640.

Srinivasan, S., G. Jones, M. Veerasami, S. Steinbach, T. Holder, A. Zewude, A. Fromsa, G. Ameni, L. Easterling, D. Bakker, N. Juleff, G. Gifford, R. G. Hewinson, H. M. Vordermeier and V. Kapur (2019). "A defined antigen skin test for the diagnosis of bovine tuberculosis." Science Advances **5**(7): eaax4899.

Stamm, C. E., A. C. Collins and M. U. Shiloh (2015). "Sensing of *Mycobacterium tuberculosis* and consequences to both host and bacillus." Immunological Reviews **264**(1): 204-219.

Stanski, K., S. Lycett, T. Porphyre and B. M. C. Bronsvoort (2021). "Using machine learning improves predictions of herd-level bovine tuberculosis breakdowns in Great Britain." Scientific Reports **11**(1): 2208.

Strydom, N. and S. M. Rankin (2013). "Regulation of circulating neutrophil numbers under homeostasis and in disease." Journal of Innate Immunity **5**(4): 304-314.

Stutz, M. D., C. C. Allison, S. Ojaimi, S. P. Preston, M. Doerflinger, P. Arandjelovic, L. Whitehead, S. M. Bader, D. Batey, M. L. Asselin-Labat, M. J. Herold, A. Strasser, N. P. West and M. Pellegrini (2021). "Macrophage and neutrophil death programs differentially confer resistance to tuberculosis." Immunity **54**(8): 1758-1771 e1757.

Styrt, B. (1989). "Species variation in neutrophil biochemistry and function." Journal of leukocyte biology **46**: 63-74.

Swaim, L. E., L. E. Connolly, H. E. Volkman, O. Humbert, D. E. Born and L. Ramakrishnan (2006). "*Mycobacterium marinum* infection of adult zebrafish causes caseating granulomatous tuberculosis and is moderated by adaptive immunity." Infection and Immunity **74**(11): 6108-6117.

Swain, S. D., P. L. Bunger, K. M. Sipes, L. K. Nelson, K. L. Jutila, S. M. Boylan and M. T. Quinn (1998). "Platelet-activating factor induces a concentration-dependent spectrum of functional responses in bovine neutrophils." Journal of Leukocyte Biology **64**(6): 817-827.

Sweet, L., P. P. Singh, A. K. Azad, M. V. Rajaram, L. S. Schlesinger and J. S. Schorey (2010). "Mannose receptor-dependent delay in phagosome maturation by Mycobacterium avium glycopeptidolipids." Infection and Immunity **78**(1): 518-526.

Tailleux, L., O. Schwartz, J. L. Herrmann, E. Pivert, M. Jackson, A. Amara, L. Legres, D. Dreher, L. P. Nicod, J. C. Gluckman, P. H. Lagrange, B. Gicquel and O. Neyrolles (2003). "DC-SIGN is the major *Mycobacterium tuberculosis* receptor on human dendritic cells." Journal of Experimental Medicine **197**(1): 121-127.

Takei, H., A. Araki, H. Watanabe, A. Ichinose and F. Sendo (1996). "Rapid killing of human neutrophils by the potent activator phorbol 12-myristate 13-acetate (PMA) accompanied by changes different from typical apoptosis or necrosis." Journal of Leukocyte Biology **59**(2): 229-240.

Theander, S., D. P. Lew and O. Nüsse (2002). "Granule-specific ATP requirements for Ca2+-induced exocytosis in human neutrophils. Evidence for substantial ATP-independent release." Journal of Cell Science **115**(Pt 14): 2975-2983.

Thoma-Uszynski, S., S. Stenger, O. Takeuchi, M. T. Ochoa, M. Engele, P. A. Sieling, P. F. Barnes, M. Röllinghoff, P. L. Bölcskei, M. Wagner, S. Akira, M. V. Norgard, P. J. Godowski, B. R. Bloom and R. L. Modlin (2001). "Induction of direct antimicrobial activity through mammalian toll-like receptors." Science **291**(5508): 1544-1547.

Tintinger, G. R., J. J. van der Merwe, H. Fickl, P. Rheeder, C. Feldman and R. Anderson (2012). "Soluble triggering receptor expressed on myeloid cells in sputum of patients with community-acquired pneumonia or pulmonary tuberculosis: a pilot study." European Journal of Clinical Microbiology and Infectious Diseases **31**(1): 73-76.

Tsai, M. C., S. Chakravarty, G. Zhu, J. Xu, K. Tanaka, C. Koch, J. Tufariello, J. Flynn and J. Chan (2006). "Characterization of the tuberculous granuloma in murine and human lungs: cellular composition and relative tissue oxygen tension." Cellular Microbiology **8**(2): 218-232.

Tsairidou, S., S. Brotherstone, M. Coffey, S. C. Bishop and J. A. Woolliams (2016). "Quantitative genetic analysis of the bTB diagnostic single intradermal comparative cervical test (SICCT)." Genetics Selection Evolution **48**(1): 90.

Tschopp, R., E. Schelling, J. Hattendorf, A. Aseffa and J. Zinsstag (2009). "Risk factors of bovine tuberculosis in cattle in rural livestock production systems of Ethiopia." Preventive Veterinary Medicine **89**(3-4): 205-211.

Ugajin, M., S. Miwa, M. Shirai, H. Ohba, T. Eifuku, H. Nakamura, T. Suda, H. Hayakawa and K. Chida (2011). "Usefulness of serum procalcitonin levels in pulmonary tuberculosis." European Respiratory Journal **37**(2): 371-375.

Ulrichs, T. and S. H. Kaufmann (2006). "New insights into the function of granulomas in human tuberculosis." Journal of Pathology **208**(2): 261-269.

Upadhyay, S., E. Mittal and J. A. Philips (2018). "Tuberculosis and the art of macrophage manipulation." Pathogens and Disease **76**(4).

Van Acker, H. and T. Coenye (2017). "The Role of Reactive Oxygen Species in Antibiotic-Mediated Killing of Bacteria." Trends in Microbiology **25**(6): 456-466.

van der Wel, N., D. Hava, D. Houben, D. Fluitsma, M. van Zon, J. Pierson, M. Brenner and P. J. Peters (2007). "*Mycobacterium tuberculosis* and *Mycobacterium leprae* translocate from the phagolysosome to the cytosol in myeloid cells." Cell **129**(7): 1287-1298.

van der Woude, A. D., E. J. Stoop, M. Stiess, S. Wang, R. Ummels, G. van Stempvoort, S. R. Piersma, A. Cascioferro, C. R. Jimenez, E. N. Houben, J. Luirink, J. Pieters, A. M. van der Sar and W. Bitter (2014). "Analysis of SecA2-dependent substrates in *Mycobacterium marinum* identifies protein kinase G (PknG) as a virulence effector." Cellular Microbiology **16**(2): 280-295.

van Grinsven, E., J. Textor, L. S. P. Hustin, K. Wolf, L. Koenderman and N. Vrisekoop (2019). "Immature neutrophils released in acute inflammation exhibit efficient migration despite incomplete segmentation of the nucleus." Journal of Immunology **202**(1): 207-217.

van Raam, B. J., W. Sluiter, E. de Wit, D. Roos, A. J. Verhoeven and T. W. Kuijpers (2008). "Mitochondrial membrane potential in human neutrophils is maintained by complex III activity in the absence of supercomplex organisation." PLoS One **3**(4): e2013.

Vandenbroucke-Grauls, C. M., H. M. Thijssen and J. Verhoef (1984). "Interaction between human polymorphonuclear leucocytes and *Staphylococcus aureus* in the presence and absence of opsonins." Immunology **52**(3): 427-435.

Vazquez, C. L., M. V. Bianco, F. C. Blanco, M. A. Forrellad, M. G. Gutierrez and F. Bigi (2017). "*Mycobacterium bovis* Requires P27 (LprG) to arrest phagosome maturation and replicate within bovine macrophages." Infection and Immunity **85**(3).

Velasco-Velázquez, M. A., D. Barrera, A. González-Arenas, C. Rosales and J. Agramonte-Hevia (2003). "Macrophage—*Mycobacterium tuberculosis* interactions: role of complement receptor 3." Microbial Pathogenesis **35**(3): 125-131.

Vergne, I., J. Chua and V. Deretic (2003). "Tuberculosis toxin blocking phagosome maturation inhibits a novel Ca2+/calmodulin-PI3K hVPS34 cascade." Journal of Experimental Medicine **198**(4): 653-659.

Vermeulen, I., M. Baird, J. Al-Dulayymi, M. Smet, J. Verschoor and J. Grooten (2017). "Mycolates of *Mycobacterium tuberculosis* modulate the flow of cholesterol for bacillary proliferation in murine macrophages." Journal of Lipid Research **58**(4): 709-718.

Vier, J., M. Groth, M. Sochalska and S. Kirschnek (2016). "The anti-apoptotic Bcl-2 family protein A1/Bfl-1 regulates neutrophil survival and homeostasis and is controlled via PI3K and JAK/STAT signaling." Cell Death and Disease **7**: e2103.

Villarreal-Ramos, B., S. Berg, A. Whelan, S. Holbert, F. Carreras, F. J. Salguero, B. L. Khatri, K. Malone, K. Rue-Albrecht, R. Shaughnessy, A. Smyth, G. Ameni, A. Aseffa, P. Sarradin, N. Winter, M. Vordermeier and S. V. Gordon (2018). "Experimental infection of cattle with *Mycobacterium tuberculosis* isolates shows the attenuation of the human tubercle bacillus for cattle." Scientific Reports **8**(1): 894.

Viswanathan, G., M. Jafurulla, G. A. Kumar, T. R. Raghunand and A. Chattopadhyay (2015). "Dissecting the membrane cholesterol requirement for mycobacterial entry into host cells." Chemistry and Physics of Lipids **189**: 19-27.

Volkman, H. E., H. Clay, D. Beery, J. C. Chang, D. R. Sherman and L. Ramakrishnan (2004). "Tuberculous granuloma formation is enhanced by a mycobacterium virulence determinant." PLoS Biology **2**(11): e367.

Volkman, H. E., T. C. Pozos, J. Zheng, J. M. Davis, J. F. Rawls and L. Ramakrishnan (2010). "Tuberculous granuloma induction via interaction of a bacterial secreted protein with host epithelium." Science **327**(5964): 466-469.

Vordermeier, H. M., G. J. Jones, B. M. Buddle and R. G. Hewinson (2016). "Development of immune-diagnostic reagents to diagnose bovine tuberculosis in cattle." Veterinary Immunology and Immunopathology **181**: 10-14.

Vordermeier, H. M., A. Whelan, P. J. Cockle, L. Farrant, N. Palmer and R. G. Hewinson (2001). "Use of synthetic peptides derived from the antigens ESAT-6 and CFP-10 for differential diagnosis of bovine tuberculosis in cattle." Clinical and Diagnostic Laboratory Immunology **8**(3): 571-578.

Vordermeier, M., G. Ameni and E. J. Glass (2012). "Cytokine responses of Holstein and Sahiwal zebu derived monocytes after mycobacterial infection." Tropical Animal Health Production **44**(3): 651-655.

Vuorte, J., S. E. Jansson and H. Repo (2001). "Evaluation of red blood cell lysing solutions in the study of neutrophil oxidative burst by the DCFH assay." Cytometry **43**(4): 290-296.

Walters, S. B., E. Dubnau, I. Kolesnikova, F. Laval, M. Daffe and I. Smith (2006). "The *Mycobacterium tuberculosis* PhoPR two-component system regulates genes essential for virulence and complex lipid biosynthesis." Molecular Microbiology **60**(2): 312-330.

Wang, J., X. Zhou, B. Pan, H. Wang, F. Shi, W. Gan, L. Yang, X. Yin, B. Xu and D. Zhao (2013). "Expression pattern of interferon-inducible transcriptional genes in neutrophils during bovine tuberculosis infection." DNA and Cell Biology **32**(8): 480-486.

Wang, J., X. Zhou, B. Pan, L. Yang, X. Yin, B. Xu and D. Zhao (2013). "Investigation of the effect of *Mycobacterium bovis* infection on bovine neutrophils functions." Tuberculosis (Edinb) **93**(6): 675-687.

Warrington, R., W. Watson, H. L. Kim and F. R. Antonetti (2011). "An introduction to immunology and immunopathology." Allergy, Asthma and Clinical Immunology **7**.

Wassermann, R., M. F. Gulen, C. Sala, S. G. Perin, Y. Lou, J. Rybniker, J. L. Schmid-Burgk, T. Schmidt, V. Hornung, S. T. Cole and A. Ablasser (2015). "*Mycobacterium tuberculosis* differentially activates cGAS- and inflammasome-dependent intracellular immune responses through ESX-1." Cell Host Microbe **17**(6): 799-810.

Waters, W. R., M. F. Maggioli, J. L. McGill, K. P. Lyashchenko and M. V. Palmer (2014). "Relevance of bovine tuberculosis research to the understanding of human disease: historical perspectives, approaches, and immunologic mechanisms." Veterinary Immunology and Immunopathology **159**(3-4): 113-132.

Waters, W. R., M. V. Palmer, B. M. Buddle and H. M. Vordermeier (2012). "Bovine tuberculosis vaccine research: historical perspectives and recent advances." Vaccine **30**(16): 2611-2622.

Watson, R. O., S. L. Bell, D. A. MacDuff, J. M. Kimmey, E. J. Diner, J. Olivas, R. E. Vance, C. L. Stallings, H. W. Virgin and J. S. Cox (2015). "The Cytosolic Sensor cGAS detects *Mycobacterium tuberculosis* DNA to induce type i interferons and activate autophagy." Cell Host Microbe **17**(6): 811-819.

Watson, R. O., P. S. Manzanillo and J. S. Cox (2012). "Extracellular *Mycobacterium tuberculosis* DNA targets bacteria for autophagy by activating the host DNA-sensing pathway." Cell **150**(4): 803-815.

Wedlock, D. N., R. P. Kawakami, J. Koach, B. M. Buddle and D. M. Collins (2006). "Differences of gene expression in bovine alveolar macrophages infected with virulent and attenuated isogenic strains of *Mycobacterium bovis*." International Immunopharmacology **6**(6): 957-961.

Welin, A. and M. Lerm (2012). "Inside or outside the phagosome? The controversy of the intracellular localization of *Mycobacterium tuberculosis*." Tuberculosis (Edinb) **92**(2): 113-120.

Whelan, A. O., M. Coad, P. J. Cockle, G. Hewinson, M. Vordermeier and S. V. Gordon (2010). "Revisiting host preference in the *Mycobacterium tuberculosis* complex: experimental infection shows *Mycobacterium tuberculosis* H37Rv to be avirulent in cattle." PLoS One **5**(1): e8527.

Whitfield, G. B., T. D. Brock, A. Ammann, D. Gottlieb and H. E. Carter (1955). "Filipin, an antifungal antibiotic: Isolation and properties." Journal of the American Chemical Society **77**(18): 4799-4801.

WHO (2017). "Roadmap of Zoonotic TB ".

WHO (2019). "Global tuberculosis report ".

Witko-Sarsat, V. r., P. Rieu, B. a. Descamps-Latscha, P. Lesavre and L. Halbwachs-Mecarelli (2000). "Neutrophils: Molecules, functions and pathophysiological aspects." Laboratory Investigations **80**(5): 617-653.

Wong, D., W. Li, J. D. Chao, P. Zhou, G. Narula, C. Tsui, M. Ko, J. Xie, C. Martinez-Frailes and Y. Av-Gay (2018). "Protein tyrosine kinase, PtkA, is required for *Mycobacterium tuberculosis* growth in macrophages." Scientific Reports **8**(1): 155.

Wood, P. R. and J. S. Rothel (1994). "*In vitro* immunodiagnostic assays for bovine tuberculosis." Veterinary Microbiology **40**(1-2): 125-135.

Wright, S. D. and M. T. Jong (1986). "Adhesion-promoting receptors on human macrophages recognize *Escherichia coli* by binding to lipopolysaccharide." Journal of experimental medicine **164**(6): 1876-1888.

Wright, S. D., S. M. Levin, M. T. Jong, Z. Chad and L. G. Kabbash (1989). "CR3 (CD11b/CD18) expresses one binding site for Arg-Gly-Asp-containing peptides and a second site for bacterial lipopolysaccharide." Journal of Experimental medicine **a69**(1): 175-183.

Xin, T., H. Jia, J. Ding, P. Li, H. Yang, S. Hou, W. Yuan, X. Guo, H. Wang, Q. Liang, M. Li, B. Wang and H. Zhu (2013). "Assessment of a protein cocktail-based skin test for bovine tuberculosis in a double-blind field test in cattle." Clinical Vaccine Immunology **20**(4): 482-490.

Xu, S., S. E. Webb, T. C. K. Lau and S. H. Cheng (2018). "Matrix metalloproteinases (MMPs) mediate leukocyte recruitment during the inflammatory phase of zebrafish heart regeneration." Scientific Reports **8**(1): 7199.

Yamamoto, N., M. Ueda-Wakagi, T. Sato, K. Kawasaki, K. Sawada, K. Kawabata, M. Akagawa and H. Ashida (2015). "Measurement of glucose uptake in cultured cells." Current Protocols in Pharmacology **71**: 12 14 11-12 14 26.

Yamashiro, L. H., S. C. Oliveira and A. Bafica (2014). "Innate immune sensing of nucleic acids from mycobacteria." Microbes Infection **16**(12): 991-997.

Yeboah-Manu, D., B. C. de Jong and F. Gehre (2017). "The Biology and Epidemiology of *Mycobacterium africanum*." Advances in Experimental Medicine and Biology **1019**: 117-133.

Yin, C. and B. Heit (2018). "Armed for destruction: formation, function and trafficking of neutrophil granules." Cell Tissue Research **371**(3): 455-471.

Yoshioka, Y., T. Mizutani, S. Mizuta, A. Miyamoto, S. Murata, T. Ano, H. Ichise, D. Morita, H. Yamada, Y. Hoshino, T. Tsuruyama and M. Sugita (2016). "Neutrophils and the S100A9 protein critically regulate granuloma formation." Blood Advances **1**(3): 184-192.

Yvan-Charvet, L. and L. G. Ng (2019). "Granulopoiesis and neutrophil homeostasis: A metabolic, daily balancing act." Trends in Immunology **40**(7): 598-612.

Zhang, B., J. Hirahashi, X. Cullere and T. N. Mayadas (2003). "Elucidation of molecular events leading to neutrophil apoptosis following phagocytosis: cross-talk between caspase 8, reactive oxygen species, and MAPK/ERK activation." Journal of Biological Chemistry **278**(31): 28443-28454.

Zhang, L., H. W. Ru, F. Z. Chen, C. Y. Jin, R. F. Sun, X. Y. Fan, M. Guo, J. T. Mai, W. X. Xu, Q. X. Lin and J. Liu (2016). "variable virulence and efficacy of BCG vaccine strains in mice and correlation with genome polymorphisms." Molecular Therapy **24**(2): 398-405.

Zhang, X., L. Majlessi, E. Deriaud, C. Leclerc and R. Lo-Man (2009). "Coactivation of Syk kinase and MyD88 adaptor protein pathways by bacteria promotes regulatory properties of neutrophils." Immunity **31**(5): 761-771.

Zhou, L., R. Somasundaram, R. F. Nederhof, G. Dijkstra, K. N. Faber, M. P. Peppelenbosch and G. M. Fuhler (2012). "Impact of human granulocyte and monocyte isolation procedures on functional studies." Clinical and Vaccine Immunology **19**(7): 1065-1074.

Zhu, Y. P., L. Padgett, H. Q. Dinh, P. Marcovecchio, A. Blatchley, R. Wu, E. Ehinger, C. Kim, Z. Mikulski, G. Seumois, A. Madrigal, P. Vijayanand and C. C. Hedrick (2018). "Identification of an early unipotent neutrophil progenitor with pro-tumoral activity in mouse and human bone marrow." Cell Reports **24**(9): 2329-2341 e2328.

Zuber, B., M. Chami, C. Houssin, J. Dubochet, G. Griffiths and M. Daffe (2008). "Direct visualization of the outer membrane of mycobacteria and corynebacteria in their native state." Journal of Bacteriology **190**(16): 5672-5680.

Zulauf, K. E., J. T. Sullivan and M. Braunstein (2018). "The SecA2 pathway of *Mycobacterium tuberculosis* exports effectors that work in concert to arrest phagosome and autophagosome maturation." PLoS Pathogens **14**(4): e1007011.

Zyntek, C., J. Schmitz and G. Winkels (2020). Untouched isolation of functionally unaffected neutrophils from whole blood within 20 minutes, Miltenyi Biotec.

Zysk, G., L. Bejo, B. K. Schneider-Wald, R. Nau and H.-P. Heinz (2000). "Induction of necrosis and apoptosis of neutrophil granulocytes by *Streptococcus pneumoniae*." Clinical and experimental immunology **122**(1): 61-66.

List of figures

List of tables

Publications

Publications included in this thesis

2021

- **Rachana R. Borkute**, Sören Woelke, Gang Pei and Anca Dorhoi
  Neutrophils in Tuberculosis: Cell Biology, Cellular Networking and Multitasking in Host Defense
  International Journal of molecular sciences. doi: 10.3390/ijms22094801

- Marion Rambault*, **Rachana Borkute***, Emilie Doz-Deblauwe*, Yves Le-Vern, Nathalie Winter, Anca Dorhoi, Aude Remot. *, joint first authors
  Isolation of Bovine Neutrophils by Fluorescence- and Magnetic-Activated Cell Sorting. Myeloid-Derived Suppressor Cells.
  Methods in Molecular Biology, doi: 10.1007/978-1-0716-1060-2_16

Publications not included in this thesis

2018

- Yogesh Patil, Ramesh Shingare, Shakti Chakraborty, **Rachana Borkute**, Dhiman Sarkar and Balaji Madje
  Synthesis and biological evaluation of some bicyclic[2-(2,4-dimethylphenylthio) phenyl] aniline and its amide derivatives as potential antitubercular agents.
  Journal of chemical sciences. doi: 10.1007/s12039-018-1424-5

- Mahendra A. Wagh, Sachin B. Baravkar, Ganesh S. Jedhe, **Rachna Borkute**, Amit S. Choudhari, Dhiman Sarkar, Gangadhar J. Sanjayan
  Design and synthesis of 2-Amino-thiophene-tethered ureidopenicillin analogs with potent antibacterial and antitubercular activity.
  Chemistry Select. doi: 10.1002/slct.201800027

- Yogesh Patil, Ramesh Shingare, Amit Choudhari, **Rachana Borkute**, Dhiman Sarkar, Balaji R. Madje
  Synthesis and biological evaluation of some new tricyclic pyrrolo[3,2 *e*]tetrazolo[1,5 *c*]pyrimidine derivatives as potential antitubercular agents
  Archiv der Pharmazie. doi: 10.1002/ardp.201800040

- Urja D Nimbalkar , Julio A Seijas , **Rachna Borkute**, Manoj G Damale , Jaiprakash N Sangshetti , Dhiman Sarkar, Anna Pratima G Nikalje
  Ultrasound Assisted Synthesis of 4-(Benzyloxy)- *N*-(3-chloro-2-(substitutedphenyl)-oxoazetidin-1-yl) Benzamide as Challenging Anti-Tubercular Scaffold.
  Molecules. doi: 10.3390/molecules23081945

Scientific presentations

2019

- Poster: **Rachana Borkute**, Valesca Lindenberg, Anca Dorhoi
  Responses of human and bovine neutrophils to mycobacteria
  8th Junior scientist symposium, Friedrich Loeffler Institute, Jena
- Talk: **Rachana Borkute**
  Responses of human and bovine neutrophils to *Mycobacterium tuberculosis* Complex members.
  TB-BBR Retreat, Friedrich Loeffler Institute, Insel-Riems
- Talk: **Rachana Borkute**
  An accurate method for isolation and functional analysis of bovine neutrophils.
  23rd DGFI-Symposium "*Infection and Immune Defence*", Castle Rothenfels

2018

- Poster: **Rachana Borkute**, Valesca Lindenberg, Anca Dorhoi
  Comparative analysis of neutrophil responses to virulent mycobacteria in mammalian species.
  10th Autumn School *Current Concepts in Immunology*, Merseburg

Acknowledgement

My PhD would not have been possible without the help of numerous people, whom I would like to acknowledge here.

First and foremost, I want to express my gratitude to **Prof. Dr. Anca Dorhoi**, my PhD adviser, for her steadfast support, patience, prompt assistance, and depth of knowledge throughout my PhD studies. Her guidance has been quite helpful to me in my scientific progress over the years, and I am grateful for it.

I also want to express my appreciation to **Dr. Valesca Lindenberg** for her co-supervision during the early phase of my PhD. Though for a short time but learning and working with her in the lab was so much fun.

I want to thank **Ulrike Zedler** for being an incredible technician and a "lab mom" to me. Through her experience, I was able to brush up on some of my lacking practical skills, and it was enjoyable to share the work space with her.

Dr. Robert Golinski, for his great organizational abilities and for assisting me in dealing with German bureaucracy as well as for being a consistent cheerleader throughout this journey, deserves my heartfelt gratitude.

I would especially like to thank **Dr. Bärbel Hammerschmidt, Dr. Björn Corleis, Dr. Claudia Drabent, Dr. Alexander Schäfer** and all the animal caretakers for their effort in organizing blood for my experiments. It was a delight to work with you all.

I sincerely like to thank **Dr. Kati franzke** and the electron microscopy facility for processing the experimental samples and generating wonderful neutrophil pictures.

Special thanks to **Dr. Aude Remot**, **Dr. Nathalie Winter**, INRAE, France and **Prof. Dr. Stefan H. E. Kaufmann**, MPI Berlin for kindly providing me with mycobacterial strains. Without their support my PhD would not have been possible.

I am deeply touched by the care and co-operation of all the colleagues not only from my institute but also from other institutes. I specially would like to thank **Dr. Ulrike Blohm, Dr. Max Bastian, Dr. Gang Pei, Alex, Sören, Gini, Svea, Emmelie, Claudia, Silke, Lisa, Stefanie, Franziska, Björn Zessin** for being there for me when I needed it the most. Thanks for all the encouragement, and support.

I thank the FLI for funding my project.

I would like to thank **Aishwarya, Rokshana, Kunal** and **Nisarg** for being fantastic friends and for sharing my highs and lows. **Prachi** and **Harshu**, thanks for always being there for me.

Finally, I want to thank my **mom**, **dad**, and **brother** for being my strength in this journey. Without your love and support, I would not have been able to stay miles away for so long to

fulfill my dream. Without you, I am nothing. We've been through a lot together, and I can't express how much your words meant to me!